Investigating the role of bisphosphonates on bone cells and the potential of ionic therapy to restore bone regeneration in osteonecrosis of the jaw

Weijia Huang



A dissertation submitted in partial fulfilment of the requirements for the degree of

Doctor of Philosophy

of

Division of Surgery and Interventional Science
University College London

Declaration

'I, Weijia Huang confirm that the work presented in	this thesis is my own. Where
information has been derived from other sources,	I confirm that this has been
indicated in the thesis.'	
	Signature:
	Date:
	Date.

Acknowledgement

I would like to express my deepest gratitude to my three supervisors, without whose dedicated effort and guidance, this thesis would not have had the opportunity to begin or be completed. Firstly, my primary supervisor, Pof. Gavin Jell, a pure scientist, whose wisdom and patience allowed me to expand the boundaries of knowledge during these four years. Through him, I caught a glimpse of the scientific realm and learned how to approach clinical problems using a scientific perspective, and reflecting on my experiences as a clinician. My second supervisor, Prof. Kaveh Shakib, whose intellect and openmindedness gave me the courage to venture into a new field, and continuously provided essential guidance and encouragement. And my tertiary supervisor, Dr. Azadeh Rezaei, an incredibly keen and rigorous researcher who has been supervising me from the first day till the completion of study. I also want to extend my sincere thanks to all the partners inJell's group. I'm grateful for the guidance from Dr. Amy Yutong Li, especially in osteoclastogenesis, as well as for her remote teaching and countless discussions during the pandemic. Thanks to Dr. Joel Turner for guiding me in systematic review and electron microscopy. I also appreciate Dr. Carolina Ramus and Dr. Medina Guliyeva for discussing experiment plans with me multiple times and providing inspiration. Many thanks to PhD students Adriana Radu, Mohammad Aghamir and Maria Florez Martin, your constructive ideas and critical feedback have greatly helped me.

I also want to extend my heartfelt gratitude to Prof. Song Wenhui and her research group members: Dr. Chang Jinke, Dr. Wu Lei, Dr. Chen Jishizhan, Dr.

Wang Jingyou, and Dr. Naheem Yaqub. They have consistently offered various timely and effective solutions whenever I encountered challenges in my experiments, significantly enhancing my efficiency. Special thanks to Dr. Elena Zattera, Dr. Ebrahim Abdal, and Dr. Patricia Santos for sharing their opinions, offering support, and enjoying life besides research.

As my PhD research comes to an end, I am returning to my role as a clinician. My deepest thanks go to Dr. Wang Jianan for his years of guidance and support, opening up international perspectives for clinicians. I would also like to thank my supervisor, Dr. Ping Feiyun, for her years of imparting wisdom and skills. I also appreciate the department leader, Dr. Liu Yanming, for providing opportunity to disseminate what I've learned. My great thanks also extend to every colleague for their support.

The pandemic has changed many aspects of life and severely affect the study. However, I was fortunate to persevere, for which I have to thank the people from the Institute of Basic Medicine and Cancer, Chinese Academy of Sciences. I am grateful to Dr. Li Juan and Dr. Fu Ting for guiding my project, to Dr. Zhou Wei and Dr. Wang Wenxi for bringing me into their cancer research initiatives, and to the following colleagues for their guidance on my experiments: Dr. Xie Sitao, Dr. Zhang Hui, Dr. Zhang Dailiang, Dr. Xiao Yating, and PhD student Hou Peidong. I want to thank my best friends, Alina Zhang and Chen Yan, for supporting everything I do, no matter where they are. I am also grateful to my family members Dr. Li, Dr. Qian, and Dr. Ying for their support and advice at every stage of my PhD journey. I owe much to my family for their support. Deepest thanks to my wise in-laws, my parents, my baby girl Yue and love of life, Hui.

Abstract

Bisphosphonate-related osteonecrosis of the jaw (BRONJ) is a severe side effect of antiresorptive bisphosphonates (BPs) used to treat patients with cancer and osteoporosis. The mechanism underlying BRONJ remains unclear, and there are no effective therapies, making it a significant clinical challenge. Surgical removal of necrotic bone is often the only available option, a similar approach to that used in the Victorian era. Novel therapies, such as tissue engineering strategies, have emerged as a promising approach. Here, we investigate the use of therapeutic ions (silicate (Si) and cobalt (Co) ions that can be released from bioactive glasses), as a possible method to either prevent or restore bone regeneration in patients with BRONJ.

A systematic review of existing literature (123 papers investigating the *in vitro* role of BPs were included for quantitative analysis) revealed a concentration-dependent effect of BPs on cells regardless of cell type or experimental conditions. Increasing BP concentrations had an increased frequency of undesirable outcomes. The mean BP concentration reported to have undesirable effects (50 μM) was higher than the concentration reported to have desirable outcomes (20 μM) (P<0.01). Furthermore, nitrogen-containing BPs caused undesirable cellular outcomes at lower concentrations than non-nitrogen containing BPs. The main cellular pathways studied in response to BPs *in vitro* include inflammation, oxidative stress, apoptosis and angiogenesis.

Based on the literature review, the effect of Zoledronate (ZA) and Alendronate (AL) on both osteoblasts (OBs) and osteoclasts (OCs) behavior was investigated. ZA and AL had concentration-dependent effects. ZA at concentrations below 1.8 μ M

did not inhibit OB metabolic activity or proliferation but it did inhibit ALP production. ZA also inhibited bone nodule formation at all concentrations (from 0.067 to 1.8 μ M), except the lowest dose of 0.067 μ M ZA which increased bone nodule formation (P<0.01). In addition, both ZA and AL above 0.067 μ M inhibited OC differentiation (P<0.05). This is the first study to investigate BPs using a bone nodule formation assay for up to 21 days and the OC subclone.

In the context of ionic therapy, Si inhibited ROS availability caused by ZA treatment, and this may account for the partially restored bone formation (at D7) observed in Si-treated OBs exposed to ZA. Whilst the addition of Co ions, to BP-treated (ZA and AL) OCs, restored OC differentiation as determined by the expression of the OC-specific marker TRAP5b and OC number. The hypoxia mimetic and iron chelator DFO also restored OC formation in treated cells, suggesting that Co restoration may be via the HIF-1 α pathway or iron chelation and inhibition of iron-dependent enzymes involved in metabolism and OC differentiation.

Based on our findings, Si and Co released from materials (e.g. from bioceramic coated dental implants or bioactive glass [BG] particles used for bone fillers) may provide a novel approach for managing BP-induced inhibition of bone regeneration by modulating both OB and OC behavior. Currently, this approach is not applying in clinical practice. Our findings provide evidence for the potential repurposed use of these materials in treating BRONJ or patients at risk. Furthermore, new BGs containing Co ions can be tailored according to this evidence.

Impact Statement

Scientific impact

This thesis investigates the cellular response to BPs through both quantitative literature review and experimental studies. The systematic review of the literature revealed concentration-dependent BP effects on various cells, and highlighted the cellular pathways most studied in response to BPs. The quantitative approach used to evaluate the concentration effects of BPs in previously published research is novel, and demonstrated the variance in approaches used by research groups.

The thesis also explored the potential of therapeutic ions in managing BRONJ-induced bone cell inhibition, and demonstrated, for the first time, that Si can partially restore early bone formation in BP-inhibited bone cultures, whilst Co can restore BP-inhibited osteoclastogenesis. Furthermore, we suggest that the potential mechanism for both Si and Co restoration is via the reactive oxygen species (ROS) pathway and HIF- 1α stabilisation.

Commercial impact

There are several potential commercial outcomes from the research conducted during this thesis. Firstly, this thesis used a custom-made TRAP-5b quantitative assay, developed within our group [1]. This assay was designed to determine OCspecific generation, unlike commercially available TRAP assays that measure all types of TRAP. The thesis successfully demonstrated the feasibility of using this assay in testing pharmaceuticals such as BPs. Secondly, the thesis demonstrated that therapeutic ions (Co and Si) may hold promise in the treatment and prevention of BRONJ. It was demonstrated that Si (0.5 mM) may help restore BP-inhibited bone formation and Co (25 µM) and DFO (2 µM) were found to restore the inhibitory effects of BP on osteoclasts. The controlled release of these ions from bone substitute materials (e.g. BGs) offers new therapeutic options and the development of new materials with optimised release profiles for specific subgroups of patients with BRONJ or those at risk. For patients at risk of bone loss after dental extraction, BG powder could be applied directly into the extraction socket or used as dental coating. For patients with stages 1-3 of a specific condition, combining BG powder with surgical interventions is a supplementary therapy.

Patients impact

The management of BRONJ is currently an urgent need among patients, with incidences ranging from 0.01-0.06% in patients taking oral BPs and 0.8-12% in

patients receiving IV BPs [2-4]. No preventive or therapeutic interventions have been confirmed to be effective. As the disease progresses, patients experience both bone loss and impairment of oral function, severely impacting their quality of life. This study systematically assessed the potential of ionic therapy for managing BRONJ, focusing on cellular responses to BP and ions. The findings demonstrate the possibility of using ionic therapy to counteract BP-induced inhibition of bone cells and pave the way for developing biomaterials or tissue scaffolds specifically designed for BRONJ patients or those at risk.

Acknowledgement	ii
Impact Statement	v
List of Figs	xvi
List of Tables	хх
Abbreviations	xxi
Chapter 1 General Introduction	1
1.1 BRONJ	1
1.1.1 History evolution: From the mystery of 'phossy jaw' to medication	related
osteonecrosis of the jaw	1
1.1.2 BP structure, classification and mechanisms of action	4
1.1.3 BRONJ and medication-related osteonecrosis of the jaw (MRONJ)	6
1.1.4 Pathophysiology	8
1.1.5 Risk factors	12
1.2 Current management of BRONJ	13
1.2.1 Prevention	14
1.2.2 Conservative treatment	15
1.2.3 Surgical interventions	16
1.2.4 Drug holiday	16
1.2.5 Clinical trials	17
1.3 Tissue Engineering (TE) strategies for MRONJ prevention and treatment	22
1.3.1 Bone TE	22
1.3.2 Tissue Engineering for oral and maxillofacial (OMF) region	24
1.3.3 Tissue engineering for medication-related osteonecrosis of the jaw	25

1.3.3.1 <i>In vitro</i> studies	
1.3.3.2 <i>In vivo</i> studies	
1.3.3.3 Clinical studies34	
1.3.4 Bioactive glass (BG)35	
1.3.5 Therapeutic ions released from BG38	
1.4 Genetic factors associated with MRONJ42	
1.4.1 Findings from GWAS, WES and single PCRs44	
1.4.1.1 Findings from GWAS and WES44	
1.4.1.2 Findings from candidate gene studies46	
1.4.2 Findings from microbiota47	
1.4.3 Differently Expressed Gene (DEG) identification from Gene expression omni bus	
(GEO)47	
1.4.4 Limitations of current findings48	
Chapter 2 Cellular response to BP: A literature review49	
2.1 Search strategies and exclusion criteria49	
2.2 Data extraction and statistical analysis50	
2.3 Results	
2.3.1 Descriptive comparison of BPs analysed with the wider field52	
2.3.2 Quantification of the studies53	
2.3.3 Influence of BP concentration on cellular response53	
2.3.4 Methodology used to analyse in vitro response to BPs54	
2.3.5 Effect of BP concentration on cell metabolic activity and proliferation55	
2.3.6 Does BP concentration influence cell response?57	

2.3.7 Impact of varying concentrations of ZA and AL on cell proliferation rates59	
2.3.8 How do other BPs affect cell proliferation?60	
2.3.9 The effect of BP Concentration on OB differentiation factors61	
2.3.10 The effect of BP concentration on VEGF, oxidative stress markers and Mmp963	
2.3.11 BP concentration affects metabolic activity and cell proliferation in different cell	
types63	
2.4 Discussion66	
2.4.1 BP affects cell behaviour in a concentration-dependent manner67	
2.4.2 Overview of cell response to BP and possible pathways67	
Chapter 3 General Methods and Materials70	
3.1 Cell culture models70	
3.1.1 SaOs-2 cell culture70	
3.1.2 Enzymatic primary rat osteoblasts isolation71	
3.1.3 <i>In vitro</i> bone nodule formation72	
3.2 Macrophage73	
3.3 Osteoclast74	
3.3.1 Osteoclastic sub-clone generation74	
3.3.2 Sub-clone culture and osteoclastic differentiation74	
3.4 Preparation of conditioned mediums75	
3.4.1 Sodium Metasilicate (Na ₂ SiO3)75	
3.4.2 Cobalt Chloride (CoCl ₂)	
3.4.3 Deferoxamine mesylate salt (DFO)	
3.4.4 BP medium	

3.5 Metabolic Activity of Osteoblasts: AlamarBlue ^(T) Assay	76
3.6 Cell number and Proliferation Rate: Total DNA Assay	76
3.7 Alkaline Phosphatase Activity	77
3.8 VEGF ELISA	78
3.9 Alizarin Red Calcium Staining Assay	79
3.10 Measurement of reactive oxygen species (ROS)	80
3.11 Quantification of osteoclast formation	80
3.11.1 TRAP staining	80
3.11.2 TRAP 5b activity	81
3.12 Bone nodule morphological study	81
3.12.1 Measuring Nodule Dimensions Using Interferometry	81
3.13 Statistical analysis	81
Chapter 4 Osteoblast response to BP	83
4.1 Introduction	83
4.2 Investigating OBs responses to BPs: Methodological approaches	86
4.3 Chapter aims	87
4.4 Testable null hypothese	88
4.5 Methods and materials	88
4.6 Results	88
4.6.1 The effect of ZA on SaOs-2 cells metabolic activity and proliferation	88
4.6.2 The effect of AL on Saos-2 cell metabolic activity and proliferation	89
4.6.3 The effect of ZA on SaOs-2 cells ROS production	90
4.6.4 The effect of AL on SaOs-2 cells ROS production	91

4.6.5 The effect of ZA on OB ALP production	92
4.6.6 The effect of ZA on OB VEGF production	93
4.6.7 ZA effect on bone nodule formation	94
4.6.8 ZA 1.8 uM inhibited Alizarin red staining areas and maximum he	ight of bone
nodules	95
4.7 Discussion	96
4.7.1 How does ZA affect OB metabolic activity and proliferation	96
4.7.2 How AL affects OB metabolic activity and proliferation	97
4.7.3 How ZA affects OB ROS production	97
4.7.4 How AL affects OB ROS production	98
4.7.5 How does ZA affects OB ALP production	99
4.7.6 How ZA affects OB angiogenic response	99
4.7.7 How ZA affects OB bone nodule formation	100
4.7.8 How do ZA and AL potentially affect other types of cells?	101
Chapter 5 Osteoclast response to BP	102
5.1 Introduction	102
5.2 Chapter Aims	107
5.3 Testable hypotheses	107
5.4 Methods and Materials	107
5.5 Results	107
5.5.1 The effect of ZA on the metabolic activity and proliferation of Raw264	.7 cells108
5.5.2 The effect of AL on the metabolic activity and proliferation of undiffere	entiated
Raw264.7 cells	108

5.5.3 The effect of ZA on the metabolic activity and proliferation of differentiated
Raw264.7 cells
5.5.4 The effect of AL on the metabolic activity and proliferation of differentiated
Raw264.7 cells
5.5.5 The effect of ZA on ROS production on undifferentiated C10 Raw264.7 cells111
5.5.6 The effect of AL on ROS production in undifferentiated C10 Raw264.7 cells112
5.5.7 The effect of ZA on ROS production in differentiated C10 Raw264.7 cells112
5.5.8 The effect of AL on ROS production in differentiated C10 Raw264.7 cells113
5.5.9 The effect of ZA on differentiated C10 Raw264.7 cells114
5.5.10 The effect of AL on differentiated C10 Raw264.7 cells115
5.6 Discussion116
5.6.1 How does ZA and AL affect the metabolic activity and proliferation of the Raw264.7
macrophage?116
5.6.2 How does ZA and AL affect the metabolic activity and proliferation of differentiated
Raw264.7 C10 subclones?
5.6.3 How does ZA and AL affect the ROS production of Raw264.7 macrophages?118
5.6.4 How does ZA and AL affect the ROS production of differentiated Raw264.7 C10
subclones?
5.6.5 How does ZA and AL affect TRAP 5b activity and OC formation of differentiated
Raw264.7 C10 subclones?
5.6.6 The protocol of Raw264.7 cells differentiation to OC and sub clone screening120
5.6.7 How do BPs affect OB-OC cross-talk?120
Chapter 6 Can Si restore BP induced inhibition of OB?122

6.1 Introduction	122
6.2 Chapter Aims	123
6.3 Testable null hypotheses	123
6.4 Methods and materials	123
6.5 Results	124
6.5.1 Effect of Si on the metabolic activity, DNA concentration, and proliferation	on of
SaOs-2 cells	124
6.5.2 Si -ROS on SaOs-2 cells	125
6.5.3 Effect of Si on the ROS in BP-treated Saos-2 cells	126
6.5.4 Si effect on ZA treated OB DNA concentration and proliferation	127
6.5.5 Si treated OB VEGF	128
6.5.6 Si + ZA treated OB VEGF	129
6.5.7 Si-treated OB bone nodule formation	130
6.5.8 Si + ZA treated OB bone nodule formation	131
6.6 Discussion	132
6.6.1 How does Si affect SaOs-2 cell metabolic activity and proliferation?	133
6.6.2 How does Si affect primary OB bone nodule formation?	133
6.6.3 How does Si affect SaOs-2 cell ROS production	133
6.6.4 How does Si reverse BP inhibited early bone nodule formation	134
6.6.5 How does Si affect primary OB angiogenesis	134
Chapter 7 Can HIF mimetics restore BP induced inhibition of OC?	135
7.1 Introduction	135
7.1.1 The role of HIF in bone regeneration and remodelling	135

7.1.2 HIF-1 α and BRONJ138
7.2 Chapter aims139
7.3 Testable hypotheses139
7.4 Methods and Materials140
7.5 Results140
7.5.1 DFO and Cobalt on ZA and AL treated OC ROS production140
7.5.2 Effect of DFO and Co on TRAP 5b activity in ZA- and AL-treated OCs141
7.5.3 Effect of Co on ZA-treated OC TRAP staining142
7.5.4 Effect of Co on AL-treated OC TRAP staining143
7.5.5 Effect of DFO on ZA-treated OC TRAP staining143
7.5.6 Effect of DFO on AL-treated OC TRAP staining144
7.6 Discussion
7.6.1 Mechanism through which Co affects OC ROS145
7.6.2 Mechanism through which Co affects OC TRAP 5b activity and OC formation145
7.6.3 Mechanism through which Co reverses BP-induced ROS increase in OCs145
7.6.4 Mechanism through which Co reverses the inhibition of TRAP 5b activity and OC
formation by BP146
7.6.5 Mechanism through which DFO affects OC ROS146
7.6.6 Mechanism through which DFO affects OC TRAP 5b activity and OC formation.147
7.6.7 Mechanism through which DFO reverses BP-induced ROS increase in OCs147
7.6.8 Correlation between TRAP 5b activity and OC cell number147
Chapter 8 Overall discussion149
8.1 Limitations of the methodological approaches149

8.1.1 Validity of the <i>in vitro</i> bone models	150
8.1.2 Two dimensional (2D) or Three dimensional (3D)?	151
8.1.3 Characterisation approaches	151
8.1.4 Lack of in vivo data	152
8.1.5 Lack of mechanistic studies	153
8.2 Therapeutic ions	154
8.2.1 Regulation of OB and OC	154
8.2.2 Concerns and toxicity of using ions in clinical settings	155
8.3 Potential confounding factors of this thesis	156
8.4 Future work	156
8.4.1 Experiments to confirm findings	156
8.4.2 Application of ionic therapy to prevention and treatment	159
8.5 Conclusion	160
Appendix	
Reference	

List of Figs

Fig 1.1—Historical album of 'phossy jaw'	.2
Fig 1.2—Medications resulting in osteonecrosis of the jaw	6
Fig 1.3—Staging and treatment of MRONJ	8
Fig 1.4—Pathophysiology and risk factors of BRONJ1	.1
Fig 1.5—Current management for MRONJ and clinical trial strategies 1	L 4
Fig 1.6—Transcriptional factors of bone cells in differentiation, maturation and remo	delling
phases2	3
Fig 1.7—TE strategies for MRONJ: From <i>in vitro</i> to clinical studies2	:8
Fig 1.8—Characterization of TE studies for MRONJ3	30
Fig 1.9—Characterization of <i>in vitro</i> studies3	2
Fig 1.10—Characterization of <i>in vivo</i> studies3	34
Fig 1.11—Overview of the clinical application of genome diagnostic approach	nes to
MRONJ	45
Fig 1.12—Summary of findings from genetic studies of BRONJ	17
Fig 2.1—PRISMA flowchart of the article selection process5	52
Fig 2.2—The effect of [BP] on cellular behaviour5	54
Fig 2.3—Effect of [BP] on cell metabolic activity and proliferation5	6
Fig 2.4—Effect of ZA, AL, IBAN, PAMI, and CLO on cell metabolic activity5	8
Fig 2.5—The effect of ZA and AL on cell proliferation6	iO
Fig 2.6—Comparison of the influence of different BPs on cell proliferation6	51
Fig 2.7—Influence of BP concentration on OB differentiation factors6	52

Fig 2.8—Influence of BP on VEGF, oxidative stress and Mmp963	
Fig 2.9—The influence of BP concentration on metabolic activity and cell proliferation	า in
different cell types65	
Fig 2.10—Overview of cell response to BPs68	
Fig 2.11—A summary of the possible pathways involved in OB response to BPs69	
Fig 3.1—A schematic diagram of experimental set up70	
Fig 3.2—The process of enzymatic rat calvaria osteoblast isolation72	
Fig 3.3—Osteoclastic sub-clone generation from Raw264.7 cells74	
Fig 3.4—R&D VEGF ELISA protocol steps	
Fig 4.1—Quantity of research papers on the topic of BP, osteonecrosis of the jaw (O	NJ)
and cells83	
Fig 4.2—The effect of BPs on OBs metabolic activity and proliferation85	
Fig 4.3—The effect of ZA on metabolic activity and proliferation of SaOs-2 cells89	
Fig 4.4—The effect of ZA on metabolic activity and proliferation of SaOs-2 cells90	
Fig 4.5—The effect of ZA on ROS production of SaOs-2cells91	
Fig 4.6—The effect of AL on ROS production of SaOs-2 cells92	
Fig 4.7—ALP production of ZA treated primary OB92	
Fig 4.8—VEGF production of ZA treated primary OB93	
Fig 4.9—Images of bone nodules formed after 21 days' culture95	
Fig 4.10—Quantitatively analysis of bone nodules96	
Fig 5.1—The process of OC formation	
Fig 5.2—OCs respond to BP via two pathways105	
Fig 5.3—Proliferation and metabolic activity of OC response to BP106	

Fig 5.4—The effect of ZA on the metabolic activity and proliferation of Raw264.7
cells
Fig 5.5—The effect of AL on the metabolic activity and proliferation of Raw264.7
cells
Fig 5.6—The effect of ZA on the metabolic activity and proliferation of differentiated
Raw264.7 cells
Fig 5.7—The effect of AL on the metabolic activity and proliferation of differentiated
Raw264.7 cells
Fig 5.8—The effect of ZA on ROS production on undifferentiated RawC10 cells112
Fig 5.9—The effect of AL on ROS production in undifferentiated RawC10 cells112
Fig 5.10—ROS production of the ZA treated differentiated Raw C10 cells113
Fig 5.11—ROS production of the AL treated differentiated Raw C10 cells114
Fig 5.12—The effect of ZA on TRAP differentiation results of differentiated C10 Raw264.7
cells
Fig 5.13—The effect of AL on TRAP differentiation results of differentiated C10 Raw264.7
cells116
Fig 6.1—The effect of Si on the metabolic activity and proliferation of SaOs-2
cells
Fig 6.2—The effect of Si on ROS production by Saos-2 cells126
Fig 6.3—Si effect on the ROS in BP-treated Saos-2 cells
Fig 6.4—Si effect on the DNA concentration in ZA-treated primary OB127
Fig 6.5—VEGF production of Si treated primary OB129
Fig 6.6—VEGF production of ZA and ZA + Si treated primary OB129

Fig	6.7—Day21	image,	ARS	and	interferome	try of	primary	ОВ	bone	nodule
forn	nation									130
Fig (5.8—Quantita	tive anal	ysis of	the b	one nodule f	ormatio	on			131
Fig (6.9—Day 21 a	nd day 7	micro	scopi	c image of ZA	and ZA	+Si treate	d OB.		132
Fig (5.10—Quantit	ative and	alysis o	of the	bone nodule	format	ion			132
Fig 7	7.1—Hypoxia	inducible	facto	r (HIF) pathway and	d HIF m	imetics			136
Fig 7	7.2—Hypothe	sis of HIF	mime	etics r	estoring BP-ir	duced	OC inhibit	ion		138
Fig	7.3—The effe	ct of DFO	and C	co on i	ZA and AL ind	uced R	OS produc	tion		141
Fig 7	7.4—Effect of	DFO and	Co or	TRA	P-5b activity in	n ZA- a	nd AL-trea	ted O	Cs	142
Fig 7	7.5—TRAP sta	ining of (OCs tr	eated	with ZA and 0	Co+ZA				142
Fig 7	7.6—TRAP sta	ining of A	AL- an	d Co-t	treated OCs					143
Fig 7	7.7—TRAP sta	ining of (OCs tr	eated	with ZA and Z	ZA+DFC)			144
Fig	7.8—TRAP sta	ining of (OCs tr	eated	with AL and A	\L+DFC)			144
Fig 8	3.1— Future r	esearch	plan o	f this	study					158

List of Tables

Table 1.1—Dosage of BPs for different conditions12	
Table 1.2—Completed Randomized Clinical Trials (RCTs)18	
Table 1.3—List of <i>in vitro</i> TE studies31	
Table 1.4—Approved commercial BG products38	
Table 1.5—Formulation (wt%) of 45S, S53P4, 13-93B3, A-W glass-ceramic and Stronbor	ıe
TM39	
Table 2.1—Cell metabolic activity and proliferation assays used to determine cell	
response to BPs55	
Table 2.2—Median of [BP] induced cell response (positive/increase, no change and negative/decrease)	
Table 3.1—List of reagents of conditioned mediums, stock and working	
concentrations75	
Table 3.2—Star symbols for specific statistical meanings	
Table 4.1—Median concentration (μM) of BPs reported to cause significant changes in	
OB differentiation factor expression86	

Abbreviations

α-MEM Alpha modified minimum essential medium alpha

β-GP β-glycerophosphateALP Alkaline phosphatase

AL Alendronate
BG Bioactive glass

BMP Bone morphogenic protein

BMSCs Bone marrow-derived mesenchymal stem cell

BP Bisphosphonate

BRONJ Bisphosphonate related osteonecrosis of the jaw

Ca Calcium
CLO Clodronate
Co Cobalt

DFO Desferrioxamine **DMB** Denosumab

ECM Extracellular matrix

ELISA Enzyme-Linked Immunosorbent Assay

FBS Fetal bovine serum Hydroxyapatite

HIF Hypoxia-inducible factor
HRE Hypoxia responsive element

IBAN Ibandronate IL- Interleukin

iNOS Inducible nitric oxide synthase gene

L Liter

M-CSF Macrophage colony-stimulating factor

MMP Matrix metalloproteinases

MRONJ Medication related osteonecrosis of the jaw

MSC Mesenchymal stem cell
Na₂SiO₃ Sodium metasilicate

NF-kB Nuclear factor kappa-light-chain-enhancer of activated B

OCN Osteocalcin

OPN Osteopontin **OPG** Osteoprotegerin

Osx Osterix
P Phosphate
PAMI Pamidronate

PBS Phosphate-buffered saline
PDGF Platelet derived growth factor

RANK Receptor activator of nuclear factor kappa-B

RANKL Receptor activator of nuclear factor kappa-B ligand

RISE Risedronate

ROS Reactive oxygen species

RUNX2 Runt-related transcription factor 2

Si Silicate

TGF-β Transforming growth factor-beta

TPTD Teriparatide

TNF-α Tumor necrosis factor-alpha
 TRAP Tartrate resistant acid phosphate
 VEGF Vascular endothelial growth factor

ZA Zoledronate

Chapter 1 General introduction

1.1 Bisphosphonate related osteonecrosis of the jaw (BRONJ)

1.1.1 Historical evolution: From the mystery of 'phossy jaw' to medication related osteonecrosis of the jaw

In the summer of 1888, female matchstick workers in East London initiated a strike against the use of 'white phosphorus', a lethal chemical that enriched wealthy shareholders, while threatening workers' health and lives [5]. These women toiled for approximately 14 hours daily, applying phosphorus to match tips to create a 'strike anywhere effect' (Fig 1.1 A and B) [6]. However, exposure to the toxic substance causes 'phossy jaw', a fatal disease [7, 8] that primarily affects the jaw-bone and surrounding areas, leading to an exposed necrotic jaw-bone. The number of patients affected by phossy jaw remained unknown, and very few documentaries have recorded the treatments administered to the patients.

In 1857, surgeon James Rushmore Wood published a case study on Cornelia S, a 16-year-old girl who had worked in a match factory for 2.5 years and was diagnosed with a phossy jaw [9, 10]. The case study described the damaged jaw-bone and the surgical removal of the entire lower jaw. Historical images reveal that the jaw-bone was extensively affected by necrosis, and the patient had lost almost all her teeth. Despite this, the patient showed only mild swelling on the right side of her face (Fig 1.1 C and D). The incidence of phossy jaw and other toxic reactions subsided quickly after The Berne Convention of 1906, which prohibited the use of yellow (white) phosphorus in matchstick paste [9]. Subsequently, European countries, including the UK, began banning white phosphorus [11].



Fig 1.1. Historical album of 'phossy jaw'. A) 'Strike anywhere' matchbox. B) Young workers adding 'white phosphorous' to the tip of matchsticks. C) Corrosive jaw-bone removed from the patient (text on the Fig: PLATE 1 LOWER JAW AFTER REMOVAL). D) Swollen face of Cornelia S after radical surgery (text on the page: PLATE 2 APPEARANCE OF PATIENT AFTER THE OPERATION) [9, 10].

At the same time, Dr Von Baeyer, a German chemist renowned for synthesizing indigo (a commonly used industrial dye), was awarded the Nobel Prize in Chemistry in 1905 [12]. His collaboration with Dr Hofmann KS in 1897 for synthesising 1-hydroxy-1,1-ethylidene bisphosphonate disodium (etidronate), the first germinal bisphosphonate (BP) product, did not gain attention at that time [13, 14]. People of that era did not imagine that one century later, etidronate would become a frontline treatment for bone diseases, and a new form of 'phossy jaw' induced by etidronate would emerge.

Sixty years later, in 1960, Blazer and Worms reported that etidronate could chelate calcium and magnesium, making it a potential detergent solution for preventing soil

redeposition in water during washing [15]. At the same time, scientists at Procter & Gamble (P&G) investigated the mechanism of action of fluoride on enamel and dentin to prevent dental caries. Pyrophosphate was found to effectively inhibit the crystal growth of surface calcium fluoride (CaF₂), which is responsible for the destructive etching of enamel [16]. It has been demonstrated that etidronate is an effective calcium chelator that did not damage the highly polished enamel surface [17].

~In 1969, studies revealed that BPs can inhibit hydroxyapatite (HA) dissolution *in vitro* and *in vivo* [18], and began to be used to treat patients with myositis ossificans [19]. Additionally, BPs can be utilized in emission computed tomography bone scanning to detect bone metastases and other lesions. This is due to their affinity for bone minerals, particularly at sites of high turnover, combined with their capability to bind with a gamma-emitting technetium isotope [20, 21].

The antiresorptive properties of BPs led to their widespread use in treating metabolic bone diseases, such as Paget's disease, osteogenesis imperfecta, and osteoporosis. Development of BPs for osteoporosis became prominent in the 1990s, initially with the introduction of etidronate in the USA [22, 23] and followed by the global acceptance of alendronate [24-27]. Subsequently, risedronate (Rise), ibandronate (Iban), pamidronate (Pami), tiludronate (Tilu) and zoledronate (ZA) were introduced [28-32]. New BPs have been continuously developed to meet the increasing market demand (summarised in Fig 1.2).

Furthermore, BPs are used to manage skeletal-related events (SREs) in cancer patients owing to their antiresorptive properties. Cancers, particularly those originating from the breast, prostate, lung, kidney, or thyroid gland, often metastasise to the highly vascular bone [33, 34]. A study of 21,562 cancer patients showed that the cumulative incidence of SREs was approximately 45.1% in all bone metastasis patients, including bone fracture (10.9%) and spinal cord compression (3.4%) [35]. Additionally, it has been estimated that between 3% and 30% of patients with cancer experience hypercalcaemia at some point, and up to 5% develop spinal cord compression, as reviewed by Gastanaga VM et al. [36] and Boussios, S [37]. Similarly, cancers like multiple myeloma, that predominantly develop within the bone marrow, can lead to

complications, including severe bone pain, hypercalcaemia, skeletal damage, and pathological fractures [38, 39]. BPs have significantly improved the quality of life in patients with metastasis cancers and multiple myeloma [40-42].

Meanwhile, studies on phosphorus related toxicicity to jaw-bone were ongoing, in 1957, Hunter D described a male patient who was administered strychnine and phosphorus pills. The patient returned 27 years later with advanced jaw necrosis [43]. In 1972, Miles AEW reported 10 cases of phosphorus exposure with delayed healing or residual sepsis after dental extraction [44]. These studies revealed the relationship between necrotic jaw-bone and phosphorus and discussed their possible aetiologies, providing early insights into bisphosphonate (BP)-related osteonecrosis of the jaw (BRONJ). Following the widespread use of BP, the first report of BRONJ cases occurred in 2003. Marx et al. reported 36 cases of painful bone exposure in the mandible, maxilla, or both that did not respond to surgical or medical treatments. All patients were treated with pamidronate or ZA [45]. Several researchers have questioned whether BRONJ is a resurgence of phossy jaw [46-49]. Marx (1906) suggested that the phossy jaw was BRONJ, as the chemical originating from yellow phosphorous is structurally similar to that of modern N-BPs, such as pamidronate and alendronate [8].

The speculation that phossy jaw and BRONJ are the same disease is plausible but difficult to verify. However, the following have been confirmed: (1) phosphorus is toxic to jaw-bone, and (2) treatments for jaw-bone necrosis caused by phosphorus (or BP) have been ineffective for nearly 2 centuries. Just as James Rushmore Wood did in 1857, modern-day surgeons can either remove the entire jaw-bone or a large part of it.

1.1.2 BP structure, classification and mechanisms of action

Structurally, BPs are analogues of inorganic pyrophosphates, with the oxygen atom in the central backbone replaced by a carbon atom (Fig 1.2). The P-C-P backbone structure is linked to two side chains (R₁ and R₂). R₁ is usually a hydroxyl (-OH) group, whereas the R₂ chain is typically a bulky group, with or without nitrogen. In the presence or absence of nitrogen groups in the R₂ chain, BPs can be classified into

nitrogen-containing BPs (N-BPs) or non-N-BPs. N-BPs, including Pami, AL, Tilu, Rise, Iban, and ZA, have a nitrogen atom on R₂ side chain, which inhibit the mevalonate pathway. Non-N-BPs, including etidronate and clodronate, lack a nitrogen group and are metabolised to non-hydrolysable ATP analogues, resulting in osteoclast (OC) apoptosis.

The close binding of BPs to the HA surface in the bone tissue and the rapid clearance of BPs from the circulation [50]. Resorptive OCs active on the bone surface dissolve the surrounding tissue and release BPs from HA, thereby taking up BPs by endocytosis through the ruffled border [51]. As the two BP types have different molecular mechanisms of action, they exhibit different potencies. N-BPs specifically target OC in bone and are used at very low doses (5–10 mg clinically) [52]. The structure, classification, and clinical use of BPs are presented in Fig 1.2.

The strength of these interactions depends on BP structure, type of ions and PH condition. N-BPs showing higher binding affinities compared to their non-nitrogen counterparts, due to the formation of robust coordination bonds between nitrogen atoms and metal ions. This interaction surpasses the strength of electrostatic interactions, making N-BPs more likely to deposit in bone tissues. The binding strength follows the order of calcium > magnesium > zinc. Calcium ions present the strongest binding to BP, followed by magnesium ions, which are approximately 1/5 as strong as calcium ions. Zinc ions, on the other hand, exhibit weaker binding, at approximately 1/50 of the strength of calcium ions [53, 54]. In addition, the affinity (binding constant) of calcium for each BP binding site is pH dependent, especially in the case of the ZA(Ca)² complex, where the affinity (binding constant) at pH 7 is 1.55^10³/M compared to 3.09 ^10³/M at pH 9.5 [55]. On the contrary, When OC releases hydrochloric acid, the low pH conditions, may cause BPs to be released more rapidly from bone, leading to increased local concentrations, further enhancing the calcium chelation and the associated biological effects discussed above [56].

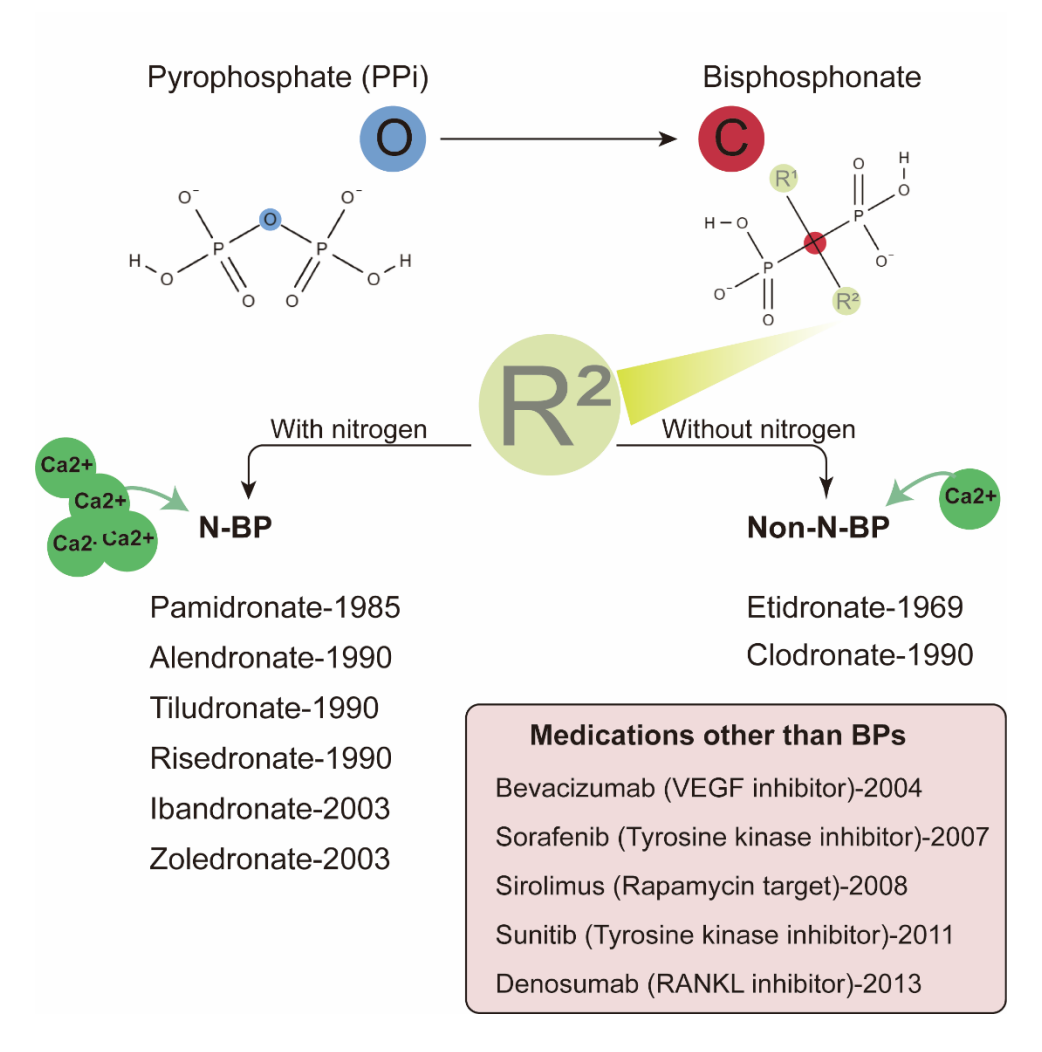


Fig 1.2 Medications resulting in osteonecrosis of the jaw. Bisphosphonates (BPs) are analogues of pyrophosphate (PPi), with the oxygen atom replaced by a carbon atom. BPs can be classified into two types according to the R² side chain composition: N-BP and non-N-BP. Both N-BP and non-N-BP are capable of chelating calcium ions, with N-BP has a stronger chelation capacity compared to non-N-BP. Other medications are also related to osteonecrosis of the jaw.

1.1.3 BRONJ and medication-related osteonecrosis of the jaw (MRONJ)

The American Society for Bone and Mineral Research defined BRONJ in 2007 as an area of exposed bone in the maxillofacial region that does not heal within 8 weeks of diagnosis in a patient who is receiving or has received BP but has not undergone radiation therapy to the craniofacial region [1].

Before the cause of BP-related issues was understood, other medications besides BP were found to be associated with ONJ. There have been continuous reports of patients with necrotic jaw-bone, which can also occur as a side effect of certain medications

used to treat cancer and osteoporosis [57-60], including denosumab (a receptor activator of nuclear factor kappa-B ligand [RANKL] inhibitor, DMB), bevacizumab (a monoclonal antibody targeting vascular endothelial growth factor [VEGF]), sirolimus (a target of rapamycin inhibitor), and sunitinib (a tyrosine kinase inhibitor) (Fig 1. 2). These medications are prescribed to treat osteoporosis and Paget's disease, and prevent cancer metastasis [61].

In 2014, the American Association of Oral and Maxillofacial Surgeons (AAOMS) updated their position papers on BRONJ, approving the use of the term medication-related osteonecrosis of the jaw (MRONJ) [62]. In this thesis, we focus solely on MRONJ induced by BPs. Therefore, the term 'BRONJ' will be used consistently to refer to BP-induced MRONJ.

In their 2014 and 2022 position papers, the AAOMS defined MRONJ, which includes the following criteria [3]: (1) current or previous treatment with antiresorptive or antiangiogenic agents; (2) exposed bone or bone that can be probed through an intraoral or extraoral fistula(e) in the maxillofacial region that has persisted for more than eight weeks; (3) no history of radiation therapy to the jaws or obvious metastatic disease to the jaws [63, 64].

Depending on the disease severity, AAOMS stratified MRONJ into five stages: at risk, 0, 1, 2, and 3 [63]. Patients considered at risk are those who have undergone intravenous (IV) or oral antiresorptive therapy but do not exhibit any visible necrotic bone or other symptoms. Stage 0 is characterized by the absence of visible signs of necrotic bone but may include nonspecific symptoms or abnormalities in clinical or radiographic findings. Stage 1 patients exhibit exposed necrotic bone or a bone-deep fistula without infection. Stage 2 patients experience symptoms related to exposed necrotic bone or a bone-deep fistula, accompanied by infection. Stage 3 is the most severe form of ONJ and includes exposed necrotic bone, infection, and potentially a range of other clinical features such as bone loss extending beyond the alveolar bone region (Fig 1.3).

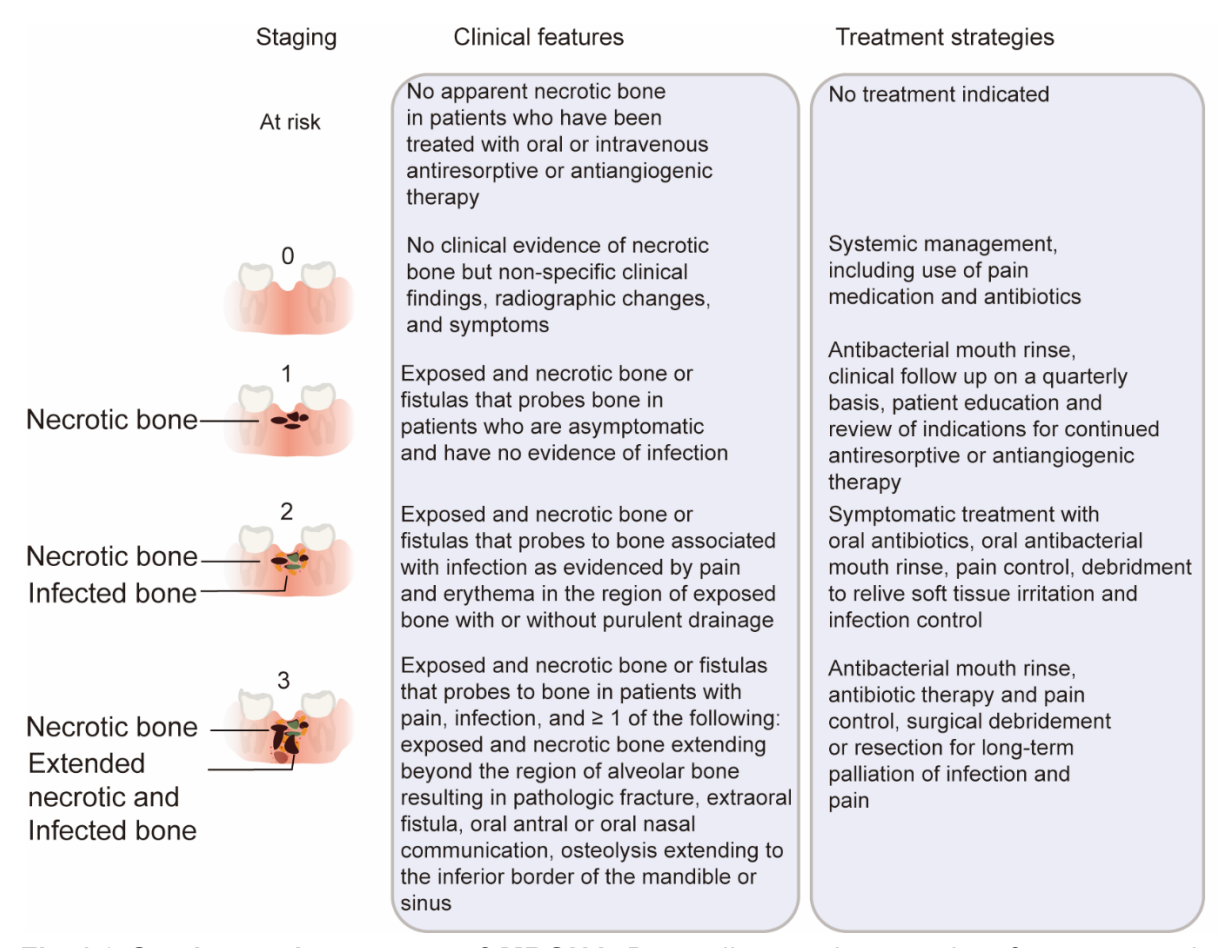


Fig 1.3 Staging and treatment of MRONJ. Depending on the severity of symptoms, the staging is defined as at risk, 0, 1, 2 and 3. The treatment strategies are defined according to the staging.

1.1.4 Pathophysiology

Clinical and preclinical animal studies have helped acquire substantial knowledge regarding the pathophysiology of BRONJ. However, the exact mechanism is not fully understood. Currently, the main causes include direct BP toxicity, inhibition of bone turnover and remodelling, avascular changes, trauma, infection, and immune suppression [61].

Direct toxicity to tissue

In vitro studies have demonstrated that BPs can cause direct toxicity to both bone and soft tissue cells. BPs can have a negative effect on cell metabolic activity and proliferation. This effect is influenced by factors such as BP exposure, type, dosage, and duration. As mentioned in section 1.1.2, BPs are capable of chelating calcium ions.

The decreased serum calcium level can trigger a series of cellular responses, including decrease OB and OC activity [65, 66]. In addition, the reduction in calcium (caused by BP chelation) can inhibit calcium dependent enzymatic reactions, such as protein phosphorylation [67], membrane stability and permeability, potentially leading to membrane instability, ion channel dysregulation, and alterations in the intra- and extracellular environments [68, 69]. These effects lead to the general toxicity of BPs.

Reduced bone turnover

BP's direct effect on OCs function leading to a low rate of bone turnover, (discussed in chapter 3, OC response to BP). Despite the direct toxicity of BP, dysfunctional OCs also play a role in the pathophysiology of BRONJ [70-73]. Human bone specimens from BP-treated patients exhibit an elevated presence of nonfunctional (anti-nuclear factor of activated T-cells, cytoplasmic 1 [NFATc1] positive) OCs surrounding necrotic bone [74]. This finding further supports the hypothesis that the inhibition of bone remodelling plays a crucial role in the pathophysiology of MRONJ. As MRONJ emerges in patients treated with DMB, a human RANKL monoclonal antibody, it becomes evident that the underlying pathophysiology may be associated with dysfunctional OCs [75].

Vascularity

Bone is one of the most vascular tissues in the body due to its high metabolic demand, and vascularisation is vital for bone formation and remodelling [76, 77], osteonecrotic bone can also be associated with the absence or lack of blood supply (e.g. avascular necrosis) [78]. BPs have been found to inhibit angiogenesis *in vitro* [79, 80] and in vivo [81, 82] leading to decreased vascularity and impaired healing. These may caused by BPs' chelation of calcium, which leads to a series of signalling pathway reactions, including the inhibition of endothelial cell proliferation, migration, and vessel stabilization, thereby inhibit angiogenesis [83, 84]. Studies have shown that calcium signalling is essential for VEGF-A-induced proliferation [85], and inhibition of calcium signalling prevents proliferation driven by MAP kinase activation [86, 87]. BPs have been reported to reduce arterial and venous areas as well as overall periodontal vascularity in rat models [88, 89]. As mentioned in section 1.1.3, antiangiogenic

medications, such as VEGF inhibitors, tyrosine kinase receptor inhibitors, and immunomodulatory drugs, have been linked to MRONJ. Studies have shown that the prevalence of MRONJ is higher in patients with multiple myeloma who receive both antiresorptive and antiangiogenic medications [32, 90, 91]. In agreement with this, a crucial aspect of MRONJ treatment is determining disease margins, which can be challenging owing to the presence of microvascular mucosal abnormalities near the MRONJ lesions [92].

Trauma and infection

Trauma and infection can complicate BRONJ predisposition. This is because altered wound healing can lead to delayed epithelial closure of the mucosal opening in the mouth, which can result in chronic infection and necrosis of the bone tissue [93]. The relationship between BRONJ and infection remains unclear. However, research has shown that bacterial microfilms and polymorphonuclear aggregates in the surrounding tissue may be associated with bone resorption and necrosis [94]. Additionally, BPs can impair the proliferation and viability of oral keratinocytes, thereby increasing the risk of infection and damaging the integrity of the oral mucosa [95, 96].

Impaired immune response and jaw-bone specific

Patients with comorbidities, including diabetes and rheumatoid arthritis, or those in immunocompromised states, are notably predisposed to MRONJ, irrespective of their exposure to antiresorptive agents. Individuals with primary or metastatic bone malignancies exhibit compromised immune responses [32, 97]. Studies showed immunity dysfunction is highly involved in the development of MRONJ [98-100]. BPs may compromise the immune response to infection by activating gamma and delta T cells, stimulating proinflammatory cytokine production, and eventually depleting T-cells [101, 102]. Besides, BRONJ mainly occurs in the jaw-bone, possibly because of the increased bone remodelling in this part of the skeleton [103]. Gong et al. found that ZA-treated bone marrow stromal cells derived from jaw and peripheral bones showed differential cell proliferation, alkaline phosphatase activity, osteogenic and chondrogenic marker gene expression, and in vivo bone-formation capacity compare to long bone cells [104].

Genetic factors

Genetic predisposition is a potential risk factor of BRONJ [105, 106]. Studies have identified polymorphisms in farnesyl pyrophosphate synthase or CYP2C8, which codes for a cytochrome P450 enzyme, as predisposing factors for BRONJ in patients with multiple myeloma [105, 107]. Other genes, such as vascular endothelia growth factor (*VEGF*) [108], collagen Type 1 A 1 (*COLIAI*) [106], Matrix metalloproteinase-9 (*MMP9*) [109], and peroxisome proliferator-activated receptor gamma (*PPARG*) [110] have also been linked to an increased risk of BRONJ. A comprehensive description of genetic factors of BRONJ is listed in section 1.4 (Genetic factors of BRONJ). In conclusion, the pathophysiology of BRONJ is a complex condition involving multiple factors. These include BP toxicity, the inhibition of bone remodelling and angiogenesis, trauma, infection, impaired immune response, and genetic factors. (Fig 1.4).

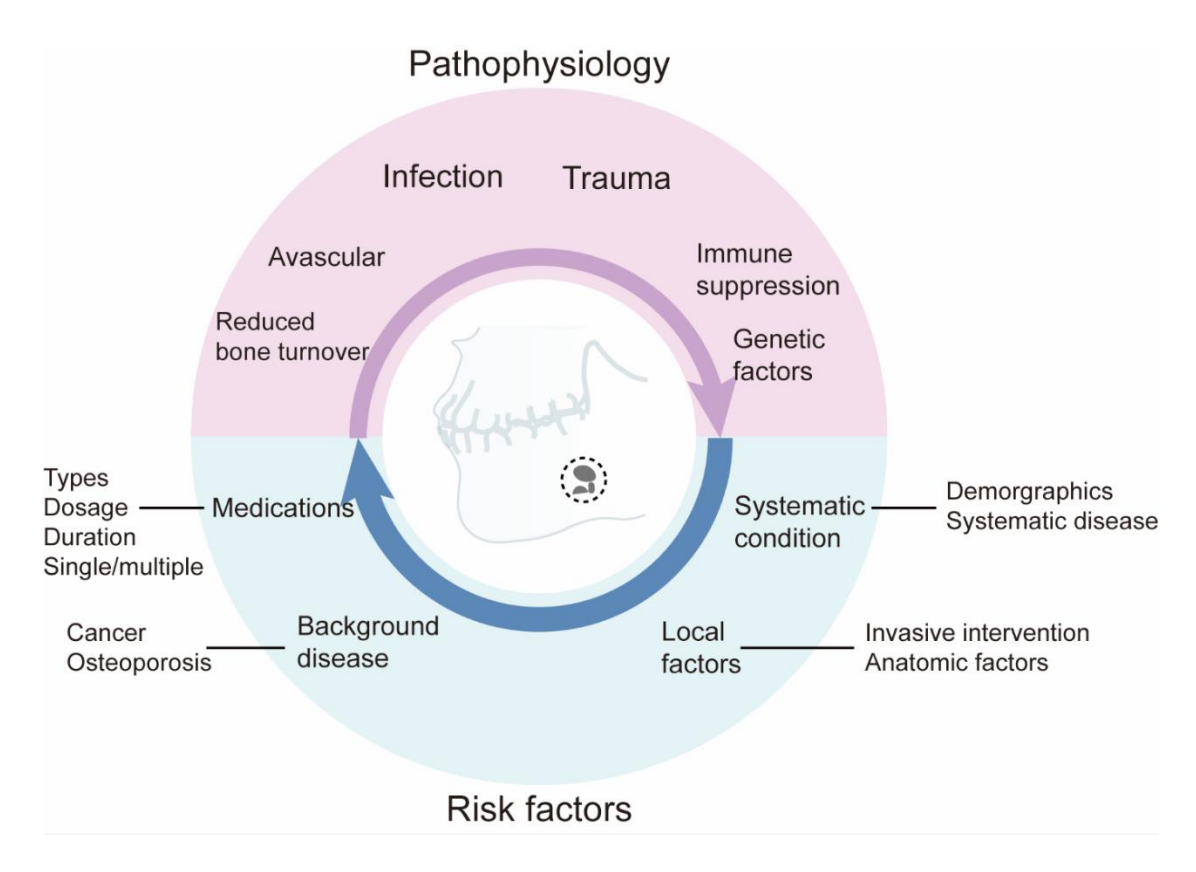


Fig 1.4 Pathophysiology and risk factors of BRONJ. Inhibited bone turnover and angiogenesis, infection, trauma, immune suppression, and genetic factors are considered the pathophysiologic pathways of BRONJ. Medications, underlying disease, trauma and local factors are linked to the development of BRONJ. There are various risk factors associated with the development of BRONJ. These include the effects of bisphosphonates, host factors, and triggers such as trauma and oral infections.

1.1.5 Risk factors

When assessing the risk of developing MRONJ, the key factor to consider is the therapeutic indication for treatment, such as malignancy, osteoporosis, or osteopenia. According to the literature, the incidence of BRONJ in patients receiving oral BPs ranges from 0.01-0.06% and 0.8-12% in patients receiving IV BPs [2-4]. The risk of developing MRONJ is notably higher in patients receiving treatment for malignancy (<5%) compared to that of those being treated for osteoporosis (<0.05%) [111]. This may be induced by the higher dosage of medications for malignancy patients compared to osteoporosis patients, as well as the different conditions of immune system. According to the NICE guideline, the recommended dosages of BPs for various conditions are listed in Table 1.1. It can be observed that patients with malignancies are prescribed BPs more frequently than those with osteoporosis. For example, malignancy patients receive 4 mg ZA per month (48 mg per year), while osteoporosis patients receive 5 mg per year. The current evidence for other medications, except BPs, is insufficient to generate significant risk factors for MRONJ. Compared with intravenous BPs, oral BPs accumulate less, resulting in a lower risk of BRONJ [112, 113].

Table 1.1. Dosage of BPs for different conditions (according to NICE guidelines [114])

	ZA (IV)	AL (Oral)	Iban (IV)	Pami (IV)	Clo (Oral)
Prevention of skeletal related events in advanced malignancies involving bone	4 mg every 3-4 weeks	N/A	6 mg every 3–4 weeks	90 mg every 4 weeks	1.6 g daily
Tumour induced hypercalcaemia	4 mg for 1 dose	N/A	2–4 mg for 1 dose	15–60 mg for 1 dose	N/A
Paget's disease of bone	5 mg for 1 dose	N/A	N/A	30 mg every week for a 6- week course	N/A
Osteoporosis	5 mg once yearly as a single dose	10 mg once daily	3 mg every 3 months	N/A	N/A
Fracture prevention in osteopenia	5 mg once every 18 months for 1 dose	N/A	N/A	N/A	N/A

Several other factors have been associated with an increased risk of developing

BRONJ. These include advanced age, alcohol and tobacco use, and poor oral health [115, 116]. In addition, anatomical factors have also been reported as a risk factor. According to studies by Saad et al. [117] and Hallmer et al. [118], MRONJ is more likely to occur in the mandible (75%) than in the maxilla (25%), but it can affect both jaws (4.5%). This may be attributed to the differential blood supply between the maxilla and mandible. The maxilla receives a rich blood supply from numerous major arteries that are extensively interconnected [119]. In contrast, the mandible is primarily supplied by a single large inferior alveolar artery and a network of smaller extraosseous arteries that nourish the bone, masticatory muscles, and facial tissues [120]. Consequently, the maxilla has a more extensive and higher flow rate [121] of blood supply through its arteries than the mandible.

The risk of developing BRONJ, increases with higher dose of BPs, frequency and duration of administration [63]. The incidence and severity of osteonecrotic events, has been reported to increase with each additional year of BP use, and patients who use BPs for more than 4 years are at particularly high risk [63]. N-BP is more likely to induce BRONJ than Non-N-BP owing to its higher calcium chelation capacity [122, 123]. Further clinical studies have demonstrated that other medications, such as steroids (e.g., prednisone, thalidomide) or antiangiogenic agents (VEGF inhibitors-Bevacizumab), in conjunction with BP therapy, increases the risk of BRONJ compared to the use of BPs alone [124, 125]. Additionally, systemic conditions, such as diabetes, rheumatoid arthritis, and immunosuppression, may also increase the risk of developing BRONJ, which may be association with steroid or immunosuppressant medication[126-128]. Although the underlying mechanism is unknown, the microenvironment (characterized by high glucose, high oxidative stress, and inhibited immune response) caused by these diseases and related medications (such as steroids) might be the cause.

1.2 Current management strategies

The principle treatment strategy is to eliminate pain, control infection of the soft tissue

and bone, and minimise the progression or occurrence of bone necrosis. Depending on the stage and progression of the lesion, treatment measures include prevention, conservative therapy, and surgical intervention. In addition, the concept of drug holiday (cessation of at-risk medication therapy prior to tooth extraction or other procedures involving osseous injury, such as dental implant placement, periodontal or apical endodontic treatment) remains controversial due to insufficient evidence of efficacy [63]. Similarly, clinical trials have not provided enough knowledge to make significant contributions to the protocol. An overview of current management and experimental interventions are summarized in Fig 1.5.

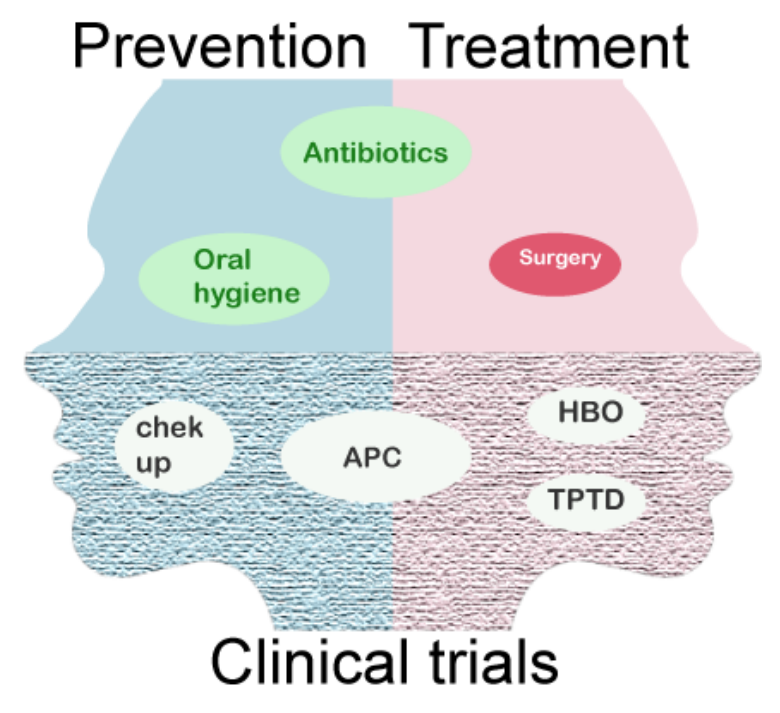


Fig 1.5 Current management for MRONJ and clinical trial strategies. Maintaining oral hygiene is essential for prevention, and the use of antibiotics is suitable for both prevention and treatment. Surgery is an option to remove necrotic tissue and adding implant to support biomechanical function. Clinical trials have shown that regular dental check-ups may be beneficial for prevention, and the application of APC (autograft plasma coagulation) is effective for both prevention [129, 130] and treatment [131-133]. The use of HBO (hyperbaric oxygen) and TPTD (teriparatide) have also involved in experimental treatments.

1.2.1 Prevention

Several studies have identified factors that can effectively decrease the risk of developing BRONJ. One is to perform high-risk surgical procedures, such as dental extraction before initiating BP therapy [134, 135]. Additionally, the use of preoperative

and postoperative antibiotics and antimicrobial mouth rinses has also been highlighted as a BRONJ preventive measure [136, 137]. Another essential factor is ensuring proper closure after tooth extractions, which aids the healing process and reduces the chance of developing BRONJ [138, 139]. Maintaining good oral hygiene is crucial in decreasing the risk of developing BRONJ. Regular brushing, flossing, and dental checkups help keep the oral cavity clean and healthy, reducing the chances of complications arising from BP therapy [140]. By implementing these measures, individuals undergoing BP therapy can significantly reduce their susceptibility to BRONJ.

Recognising that patients receiving antiresorptive therapies may have compromised (gingival) wound healing capacity is also important for BRONJ prevention [141-143]. Similar to other medical and dental preventive practices, coordinated dental care and pre-treatment management are needed to reduce the risk of developing BRONJ. The continuous education of patients, dentists, and medical professionals regarding the risks of these therapies and effective prevention strategies is vital.

1.2.2 Conservative treatment

Conservative treatment has been demonstrated to be effective in managing BRONJ and can be used at all stages of the disease. These strategies focus on patient education, pain control, and control of secondary infections to allow sequestration of the exposed necrotic bone [62, 63]. The decision on whether to use operative or nonoperative therapy should be tailored to the individual patient, considering the risk-versus-benefit ratio and the ability to perform good wound care. The goals of both operative and nonoperative therapies for BRONJ remain the same: curative therapy and improvement in quality of life. Radiographic imaging is important in evaluating BRONJ lesions, and three-dimensional imaging can decrease the invasiveness of surgical procedures [63, 144]. Nonoperative therapy may be indicated for patients who would have a high risk of complications from surgical interventions or those who cannot maintain adequate hygiene. Adjunctive therapies such as HBO or ozone therapy are yet to be proven effective, and a randomised, prospective, placebo-

controlled trial of vitamin E and pentoxifylline is underway to provide more information on this treatment modality [145-147]. Evidence to support the use of adjunctive therapies is limited; however, TPTD is promising as an adjunct for treating BRONJ in patients with osteoporosis [148].

For patients with stage 1 BRONJ, chlorhexidine wound care and improved oral hygiene can be effective, and surgery may not be necessary [63, 149]. For patients with stage 2 BRONJ who struggle with local wound care or cannot maintain adequate hygiene, antibiotics may be needed, and nonoperative therapy may be indicated to allow for sequestrectomy [62, 63, 149].

1.2.3 Surgical interventions

Although lacking of large scale studies, several case reports/series claimed that surgical interventions (such as segmental resection and marginal resection) are effective and may be viable options for managing BRONJ. However, there remain substantial drawbacks, including damage to the surrounding structures and risks of infection, therefore may not be tolerated by all patients, and the reconstruction after resection remained difficult [150, 151]. Maintaining maxillary or mandibular integrity is desirable, as the reconstruction of surgical defects can be challenging. Segmental or marginal resection of the mandible and partial maxillectomy are effective methods of controlling BRONJ, and surgical resection can be performed by experienced surgeons to ensure success [152, 153]. However, physiologically compromised patients may not respond favourably to resection, and active clinical and radiographic surveillance is critical in nonoperative management to monitor disease progression [63, 149]. While controversy exists between operative and nonoperative therapies for BRONJ, operative treatment has demonstrated maintenance of mucosal coverage, improved quality of life, and expedient resumption of antiresorptive therapy for all stages of BRONJ [154].

1.2.4 Drug holiday

The clinical practice of using drug holidays to mitigate the risk of MRONJ in patients

undergoing dentoalveolar surgery remains controversial. Animal studies have demonstrated that the discontinuation of BP for more than 1 week can significantly reduce BP-induced bone resorption in a rat model [155]. However, no prospective clinical data support the benefits of drug holidays. Nevertheless, it has been accepted and recommended by international professional societies [63, 156, 157].

In addition, while discontinuing medication with a higher risk of developing BRONJ may reduce the risk of new BRONJ site [158, 159] and control symptoms, stopping treatment can also result in the recurrence of bone pain or an increase in SRE in patients with bone metastases who are receiving bone resorption inhibitors. To make decisions, the potential benefits and risks to the patient must be weighed on a case-by-case basis.

1.2.5 Clinical trials

Although effective and safe management of BRONJ is lacking, various experimental studies are underway. The safety and efficacy of potential therapies must be evaluated and confirmed in clinical phase studies. The US National Institutes of Health (NIH) defines clinical trials as research studies involving human volunteers assigned to protocol-based interventions and assessed for their effects on biomedical or health outcomes[160].

For MRONJ, information on clinical trials is limited. Tasdogan et al. reviewed 1047 studies focused on MRONJ management, including 13 Randomised clinical trials (RCTs) for the final analysis, other studies were excluded due to the high risks of bias [161]. Among the completed studies, 5 investigated preventive strategies, and 8 focused on treatment. The characteristics of these interventions are listed in Table 1.2.

Table 1.2 Completed Randomised Clinical Trials (RCTs)

YEAR	N. OF PATIENTS	MEDICATIONS	DISEASES	PREVENTION (P) OR TREATMENT (T)	INTERVENTIONS
2005- 2009	500	BP (AL, Clo, Rise, Iban, Eti)	Osteoporosis (92.8%), Rheumatoid arthritis (3.6%), Paget disease (3.6%)	Р	Surgical extractions carried out via an intrasulcular incision and mobilisation of a mucoperiosteal [162]
2008- 2014	253	BP (ZA)	Prostate cancer	Р	Dental checkup per three months [163]
2017- 2019	77	BP (AL, Iban, Pami, Rise, ZA), DMB	Osteoporosis	Р	Application of platelet-rich fibrin (PRF) without subsequent primary closure (Poxleitner 2020) [129]
2016- 2018	160	BP, DMB, BP+DMB	Osteoporosis (45.6%), Breast cancer (28.7%), Multiple myeloma (14.3%), Prostate cancer (7.5%), Other (3.7%)	Р	Subperiosteal wound closure versus epiperiosteal wound closure after tooth extraction (Ristow 2020) [164]
2005- 2007	100	BP (ZA, AL)	Breast Carcinoma (41%), Prostatic, Multiple myeloma (35%), carcinoma (21%), Lung Carcinoma (1%), Ovarian Carcinoma (1%)	Р	Application plasma rich in growth factors (PRGF) into the postextraction alveolus (Mozzati 2012) [130]
2006- 2010	46	BP (ZA, AL, Pami)	Multiple myeloma (39.6%), Breast cancer (25%), Osteoporosis (14.6%), Other (20.4%)	Т	Hyperbaric oxygen (HBO) (Freiberger 2012) [146]
N/A	40	BP (80%), BP+DMD (20%)	Breast cancer (45%), Prostate cancer (25%), Osteoporosis (15%), Multiple myeloma (10%), Kidney cancer (2.5%), Liver cancer (2.5%)	Т	Autofluorescence of vital bone label for surgery (Ristow 2016) [165]
2012- 2015	55	BP (AL, Rise, Pami, ZA, Iban)	Osteoporosis (87.3%), Bone metastasis (12.7%)	Т	Application of leukocyte rich and platelet-rich fibrin (L-PRF group), L-PRF and recombinant human bone morphogenetic protein 2 (rhBMP-2) + bone sequestra (Park 2017) [131]

2015- 2016	36	BP (AL, ZA, Rise, Clo), DMB, BP+DMB	Prostate cancer (25%), Breast cancer (19.4%), Multiple myeloma (11.1%), Chondroblastoma (2.8%), cholangiocarcinoma (2.8%), non-Hodgkin lymphoma (2.8%)	Т	Autofluorescence-guided surgery (Giudice 2018a) [166]
2015- 2016	47	BP (ZA, AL), DMB	Prostate cancer (31.9%), Breast cancer (23.4%), Renal cancer (10.6%), Lung cancer (4.7%), multiple myeloma (2.1%), Osteoporosis (25.5%)	Т	Application of PRF+necrotic bone removal (Giudice 2018b) [132]
2012- 2015	34	BP, DMB	Malignant bone disease (41.2%), Myeloma (29.4%), Breast cancer (5.9%), Prostate cancer (5.9%), Osteoporosis (14.7%)	Т	Eight weeks of subcutaneous teriparatide (TPTD) (Sim 2020) [167]
2016- 2018	28	BP (AL, Rise)	Osteoporosis	Т	Application of concentrated growth factor (CGF) (Yüce 2021) [133]
2011- 2017	13	BP (Rise, AL)	Osteoporosis	Т	Injections of 1x/week 56.5-µg TPTD for six months versus 20-µg TPTD injections daily for six months (Ohbayashi 2020) [168]

Among the listed trials, 4 out of 13 studies utilized products rich in growth factors, including PRGF, PRF, and CGF, to prevent or treat MRONJ. These products are derived from a patient's own blood through specific centrifugation processes and are endowed with the capacity to enhance tissue regeneration and repair. They find applications in fields such as oral surgery, orthopedics, and dermatological regenerative therapies [169, 170]. Mozzati et al. applied PRGF to the alveolar socket after dental extraction in patients prescribed BP and observed a reduced incidence of BRONJ compared to those who did not receive PRGF [130]. By promoting angiogenesis [171, 172], bone regeneration [173], and gingival tissue repair [174], PRGF supports the wound healing after surgical dental procedures, thereby reducing the incidence of BRONJ. Similarly, Park et. al [131] and Giudice et. al [132] applied CGF after bone sequestration to treat MRONJ and observed that it led to the complete and early resolution of MRONJ. In addition to CGF, Park's protocol also incorporated BMP2. It has been demonstrated that there was a 44% decrease in the risk of failure among open tibial fracture patients receiving BMP2 (1.50 mg/ml) compared to those who did not receive BMP2 [175].

Surgical modifications have been suggested of 13 studies, 2 employed the autofluorescence technique to guide jaw-bone resection, while one study compared different surgical protocols for wound closure post-dental extraction. Regardless of the chosen approach (minimally invasive or resective), distinguishing between necrotic and viable bone remains a pivotal and challenging step in surgery. Before the advent of tetracycline fluorescence-guided bone removal, surgical experience and the surgeon's subjective impression, bolstered by various imprecise imaging methods, were the sole indicators for differentiating healthy from diseased bone tissue. The tetracycline method requires a 10-day doxycycline regimen [176], introducing potential drug side effects. Recently, it was discovered that bone exhibits auto-fluorescence when imaged with appropriate wavenumbers, eliminating the need for additional medication. Studies by Ristow et al. [165] and Giudice et. al [166] indicated that auto-fluorescence guided protocols yielded similar wound healing results in MRONJ patients as the tetracycline-guided methods and reliance on surgical experience.

Mozzati et al. compared intrasulcular incisions and the mobilization of mucoperiosteal tissue following tooth extraction in patients prescribed with BP. They found that the incidence of MRONJ did not differ significantly and concluded that the mobilization of mucoperiosteal tissue is preferred due to its lesser invasiveness [162]. The findings from the aforementioned studies suggest that current advances in surgical techniques primarily aim to reduce pharmacological risks and trauma to both the patient and the surgical site. However, there has been no notable improvement in the outcomes related to MRONJ itself.

Furthermore, 2 out of 13 studies used teriparatide (TPTD) injections to treat MRONJ and showcased encouraging results. TPTD, also known as recombinant human parathyroid hormone 1-34, is an osteoanabolic medication used for osteoporosis treatment [154]. Sim et al. administered subcutaneous TPTD injections (20 mg/day) or placebos, in conjunction with calcium and vitamin D supplementation and standard clinical care, to MRONJ patients over 8 weeks. They discovered that TPTD was associated with a higher rate of MRONJ lesion resolution compared to the placebo group [167]. Ohbayashi et al. compared daily and weekly 6-month TPTD administration in osteoporosis patients and observed a notable improvement in MRONJ staging for both the entire patient cohort and the daily group [168]. Yet, the limited sample sizes (34 and 13, respectively) of these two studies and the distinct background diseases in Sim's cohort (with 85.3% being cancer patients and 14.7% osteoporosis patients) affect their reliability. Additionally, TPTD was linked to an increased risk of osteosarcoma in a phase III study [177], leading to considerable risk of cancer patients and contraindications for the following: pre-existing hypercalcaemia, severe renal impairment, metabolic bone diseases other than primary osteoporosis (including hyperparathyroidism and Paget's disease of bone), unexplained elevations of alkaline phosphatase, and previous radiation treatment to the skeleton [178]. Understandably, this significantly curtailed the use of TPTD in MRONJ patients.

Two more ongoing RCTs are currently investigating the effects of pentoxifylline and tocopherol on MRONJ patients. Both pentoxifylline and tocopherol have been employed in the treatment of osteoradionecrosis for many years. Pentoxifylline, a

methylxanthine derivative and phosphodiesterase inhibitor, enhances blood flow by increasing erythrocyte flexibility and vasodilation, while also modulating immunological activity. Tocopherol possesses antioxidant properties. It is believed that pentoxifylline and α -tocopherol may contribute to promoting wound healing and reducing scarring [179]. A recent study demonstrated that MRONJ patients with osteoporosis who received pentoxifylline and tocopherol experienced faster healing after tooth extraction and a lower incidence of recurrence compared to the control group [180]. Compared to TPTD, pentoxifylline and α -tocopherol do not carry the risk of increasing the incidence of osteosarcoma or disrupting bone metabolism, making them suitable for a wider range of patients.

Two out of thirteen RCTs [129, 130] indicated that applying APC to the tooth socket led to a lower proportion of MRONJ occurrences compared to the standard treatment (without APC). Additionally, three out of thirteen RCTs [131-133] combined APC with surgical interventions, resulting in a higher proportion of mucosal coverage compared to surgical intervention alone. However, the small sample size may have contributed to a lack of measurable effect. Moreover, methodological constraints of the trials were associated with a high risk of bias, contributing to uncertainty about any estimates of effect [161]. Therefore, although various strategies have been proposed to prevent or treat MRONJ, there was insufficient evidence to either claim or refute a benefit of any of the tested interventions for the prevention or treatment of MRONJ.

1.3 Tissue Engineering (TE) strategies for MRONJ prevention and treatment 1.3.1 Bone TE

The history of TE can be traced back four decades, revolutionising the approach to tissue and organ reconstruction [181]. Notably, TE strategies are based on scaffold materials combined with cells and/or growth factors to generate new tissues either *in vitro* or *in vivo*. These tissues, if the patients own cells (e.g. adult stem cells) are used, overcome the issue of immunogenicity, tissue rejection and consequent long-term use of immunotherapies [182].

For bone defect, bone TE (BTE) remains one of the most researched and clinically

challenging applications of TE. Large (typically >2 cm) bone defects caused by injuries, ageing, non-union fractures, and bone tumour resections, do not heal unaided [183, 184], in a considerable impact on morbidity. Currently, autologous bone grafting remains the 'gold standard' for repairing bone defects [185, 186]. However, autologous approaches have several drawbacks, including secondary trauma and morbidity at the donor site, often limited bone volume and is dependent on the quality of bone that can be harvested. In addition, the long duration of surgery and postoperative infection also limits the range of autologous bone grafting [187, 188].

The emergence of BTE has brought new hope to address this challenge. Integrating techniques involving biomaterials, growth factors, and cell engineering, BTE allows for custom designing of scaffolds that provide both mechanical support and bone regeneration. Currently, transcription factors involved in each phase of bone cell differentiation, maturation, and remodeling have been extensively studied (Fig 1.6). These findings provide insights into the development of BTE materials, that can be designed to specifically target these factors and promote bone regeneration.

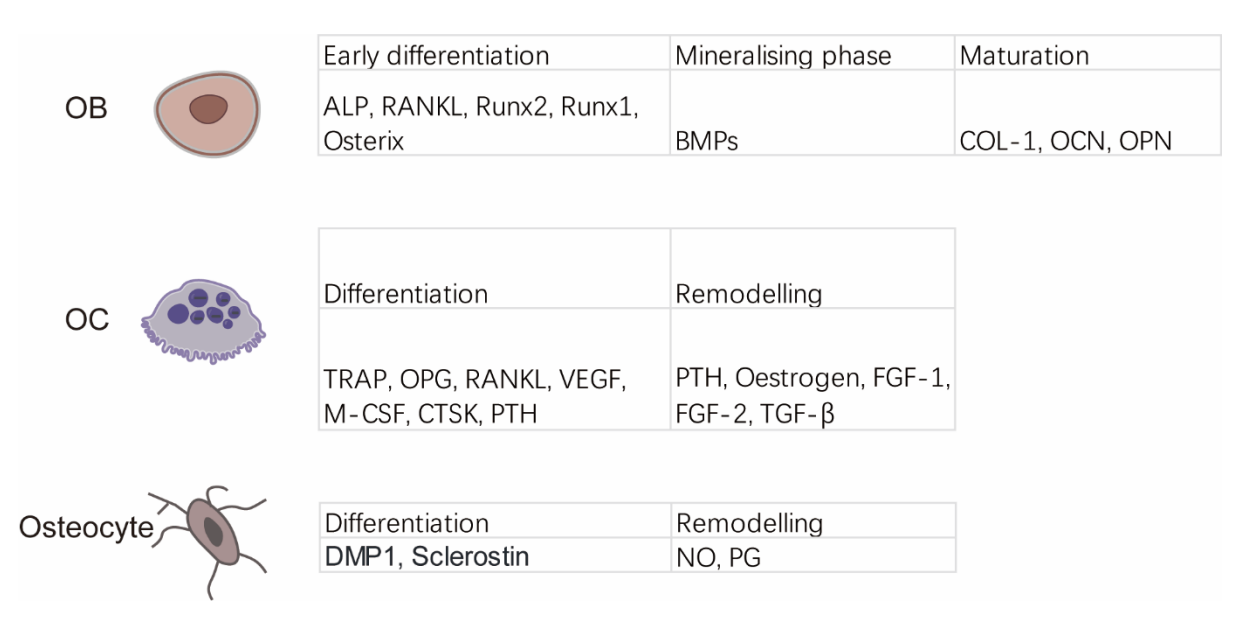


Fig 1.6 Transcriptional factors of bone cells in differentiation, maturation and remodelling phases [189-191]. RANKL, Receptor activator of nuclear factor kappa-B ligand. Runx2, Runt-related transcription factor 2. Osterix, Sp7 transcription factor. BMP, bone morphogenic protein. COL-1, Type I collagen. OCN, Osteocalcin. OPN, Osteopontin. TRAP, Tartrate-resistant acid phosphatase. OPG, Osteoprotegerin. VEGF, Vascular endothelial growth factor. M-CSF, Macrophage colony-stimulating factor. CTSK, Cathepsin K. PTH,

Parathyroid hormone. FGF, Fibroblast growth factor. TGF-β, Transforming growth factor beta. DMP1, Dentin matrix acidic phosphoprotein 1. NO, Nitric oxide. PG, Prostaglandin.

Therefore, BTE strategies can promote bone regeneration, prevent anoikis (in comparison to cell therapies) and offers mechanical support during tissue repair. These materials can be broadly classified, such as natural polymers, synthetic polymers, bioceramics, biodegradable metals, and carbon-based nanomaterials. Natural polymers such as collagen, chitosan, and alginate can closely mimic the natural bone matrix, making them suitable for TE and regenerative medicine applications. However, there are limitations such as relatively low mechanical strength, degradation, risk of infection, potential immunogenicity, and high cost [192-194]. Synthetic polymers such as polylactic acid and polyglycolic acid offer the advantages of tailored mechanical characteristics and controlled degradation rates. These materials are commonly used to fabricate biodegradable scaffolds for TE and drugdelivery systems [195-197].

Bioceramics have high compressive strength, can mimic the mineral in bone, can be white and can release ions with therapeutic properties, making them valuable in orthopaedic and dental applications [198, 199]. Bioceramics can be broadly classified into the following three types: crystalline ceramics, amorphous glasses, and partially crystalline BGs. BGs can be designed have controlled release to release of biologically active ions (e.g. Ca²+, Mg²+, Si⁴+, Cu²+, Sr²+, Li⁺, and Ag⁺ [200, 201]), to promote desirable cell and tissue responses (for example Co ions for HIF-1α stabilization for promoting angiogenesis [202]. These ions offer a more cost-effective alternative to biomolecules, such as growth factors (due to stable storage and ease of sterilisation) [203]. Further details on the biological effects of bioceramics and released ions are explained in Sections 1.3.2.

Biodegradable metals, specifically Mg and its alloys, have applications in the cardiovascular and orthopaedic fields [185, 204] and offer significant advantages in the context of orthopaedic implants. The ions released during degradation can exert additional osteometabolic regulatory effects, further facilitating the healing of bone

ailments. In addition, these materials gradually corrode inside the body, eliminating the need for implant removal surgery [205, 206]. Carbon-based nanomaterials such as carbon nanotubes and graphene (or graphene oxide) exhibit unique electrical, mechanical, and thermal properties. They have been explored for their potential in drug delivery, imaging, and biosensing applications because of their exceptional surface areas and reactivities [207, 208].

1.3.2 Tissue Engineering for oral and maxillofacial (OMF) region

The emergence of BTE has introduced new options for oral and maxillofacial (OMF) reconstruction. Notably, BTE materials have the potential to replace various components of the OMF complex, including teeth, jawbone, periodontium, temporomandibular joint, soft tissues, blood vessels, and nerves. Nevertheless, although the discipline has been established for several decades, clinical applications for reconstructing the OMF regions are currently limited, and challenges remain in translating the ideal model into clinical practice, in terms of complexity cost and efficacy [209].

The specific characteristics of the OMF region distinguish it from typical BTE applications, contributing to these challenges. First, OMF defects caused by tumours, trauma, or infections often exhibit complexity and involve both hard and soft tissue. All ectodermal, mesodermal, and endodermal tissue types are potential candidates for TE strategies and are present in the OMF regions. Furthermore, resolution of functional and aesthetic issues are both needed [210].

Another particular concern in OMF reconstruction is the potential exposure of the grafted tissue to the external environment. Constructs employed to restore defects involving the jaws, orbits, nose, and ears may come into direct contact with the mouth, sinuses (maxillary, ethmoidal, and frontal), nasal passages, and external environment. These areas have high moisture content and significant bacterial populations and are subjected to functional loads imposed by physiological activities, such as chewing [211].

Several alloplastic materials, such as polyether ether ketone, polymethyl methacrylate,

polyethylene, and titanium, have been introduced for treating large cranial defects, primarily focusing on brain protection and shape restoration rather than facilitating bone regeneration. Consequently, using these materials in such sizable defects often results in inadequate integration with the bone and soft tissues, potentially leading to problems such as implant exposure, infection, and the eventual need for implant removal [212, 213].

The OMF BTE field has been poised to develop innovative strategies to address these challenges, leading to the exploration of animal studies investigating various aspects of BTE applications in the OMF complex, particularly focusing on scaffold materials and growth factors. Hitherto, calcium phosphates, specifically tricalcium phosphate and hydroxyapatite (HA), have emerged as the predominant scaffold materials [209, 214]. In addition, various growth factors have been examined for their potential to regenerate the maxillofacial complexes. Notably, bone morphogenic protein (BMP) has gained widespread popularity among all subtypes because of its ability to significantly promote bone formation compared with that in control groups [215]. Currently, clinical trials are conducted on the OMF region mainly for limited defect sizes, such as maxillary sinus floor elevation [216, 217], alveolar cleft reconstruction [218, 219], periodontal defects [220] and tooth socket reservation [221, 222]. For critical-size defects in the OMF region, current research is still in the animal experimental stage and awaits further translation into clinical practice [209].

1.3.3 Tissue engineering for MRONJ

The current approaches to MRONJ discussed in Section 1.2, include prevention, conservative therapy, surgical interventions, and bisphosphonate drug holidays. However, none have been proven to be universally effective. Considering the intricate microenvironment and unique challenges associated with MRONJ, including compromised vasculature, susceptibility to infection, and poor tissue regeneration, TE strategies are being investigated for their potential to offer comprehensive and long-term solutions. These strategies involve using scaffolds, bioactive molecules, growth factors, and cell therapies, alone or in combination, to promote tissue regeneration

and restore the functional integrity of the affected region [223-226] (Fig 1.7). To understand the current knowledge on TE strategies for MRONJ, a literature review has been conducted follows the guidelines on the conducting of systematic scoping reviews from the Joanna Briggs Institute [227]. This method summarizes the evidence available on a topic to convey its broad and depth. The research question for this review was: "What are the characteristics, broad, and results of the existing research on the use of TE strategies in the management of MRONJ, from *in vitro*, *in vivo* to clinical?".

Only full-text papers reporting original data were included. Studies such as conference abstracts, review papers, letters to the editor, and opinion pieces were excluded. Additionally, studies focusing solely on MRONJ management without tissue engineering strategies were also excluded. Search of the Web of Science was conducted*1, up to date until September 30, 2023, and 205 papers were identified. After screening for relevance and quality, 54 papers were included in the final analysis, including 13 *in vitro*, 36 *in vivo*, and 5 RCTs studies (Fig 1.8A).

-

^{*1} Search terms (TOPIC words): ("tissue engineering" OR ("tissue" AND "engineering") OR "tissue engineering" OR "tissue scaffolds" OR ("tissue" AND "scaffold") OR "bone marrow cells" OR (bone AND marrow AND cells) OR "bone marrow cells" OR "MSC" OR "mesenchymal stem cells" OR (mesenchymal AND cell) OR "stem cell" OR (stem AND cell) OR (scaffold* OR glass* OR hydrogel OR ceramic* OR polymer OR fiber OR PLGA OR chitosan OR "growth factor*" OR biomaterial* OR BMP* OR "bone morphogenic protein")) AND (BRONJ OR MRONJ)

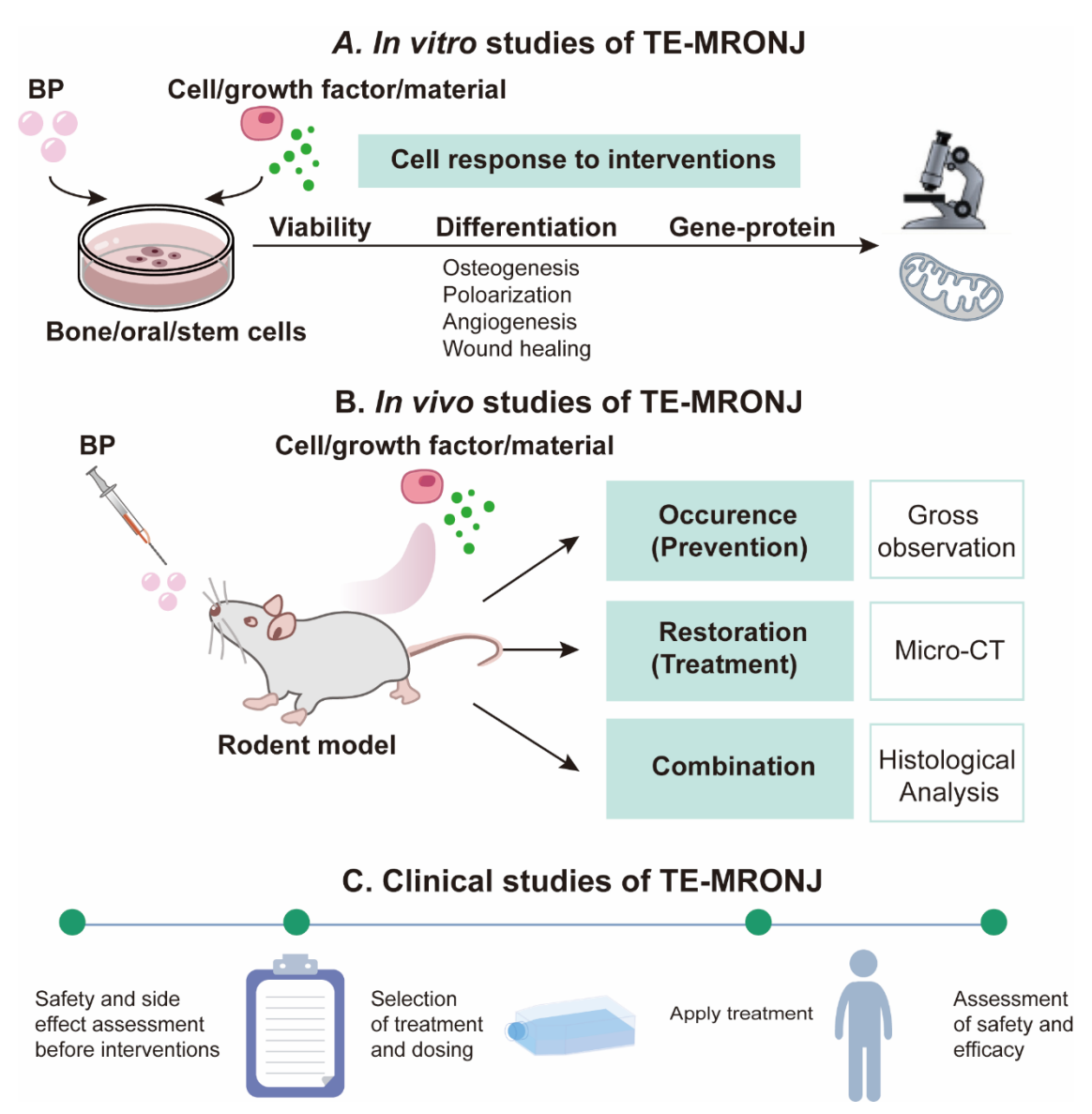


Fig 1.7 TE strategies for MRONJ: From *in vitro* **to clinical studies.** A. *In vitro* studies investigated the cellular response to TE interventions. B. *In vivo* studies majorly use rodent models to test both the prevention and treatment effect of TE interventions. C. Current clinical studies investigated the effect of growth factors on MRONJ or risking patients.

Both preventive and therapeutic approaches have been investigated in vivo (prevention: n=24, treatment: n=10, both: n=2) and clinical studies (prevention: n=2, treatment: n=3) (Fig 1.8B). For *in vitro* models, none of the 13 studies defined necrotic bone tissue, therefore cannot be classified as prevention or treatment.

Preventive models are defined as applying interventions prior to the formation of necrotic bone, and therapeutic models were established based on the confirmation of necrotic bone formation. Among the 13 *in vitro* studies, none created a cancer

microenvironment, whereas 2 out of the 36 *in vivo* studies established a cancer-based MRONJ model. Out of the five clinical studies, two exclusively involved osteoporosis patients, one included only cancer patients, and the remaining two encompassed both osteoporosis and cancer patients (Fig 1.8C).

All 13 studies utilized BP (ZA: n=10, AL: n=2) to generate MRONJ models. In the case of *in vivo* studies, 28 out of 36 employed ZA to create MRONJ models, with an additional 2 studies adding cyclophosphamide, and 1 study combined cyclophosphamide and VEGF inhibitor to develop anticancer-based models. Eight out of 36 *in vivo* studies combined ZA and dexamethasone (Dex), as excessive Dex dosage can induce osteoporosis (Fig 1.8D).

There were variations in the approach to TE interventions. Seven out of thirteen *in vitro* studies utilized cell therapy, while the other six studies employed material interventions. In the case of *in vivo* studies, 24 out of 36 utilized cell therapy, and 5 out of 36 applied materials. Furthermore, out of the 36 *in vivo*, 7 incorporated material-loaded cell therapy. All five clinical studies applied growth factors to MRONJ patients (Fig 1.8E).

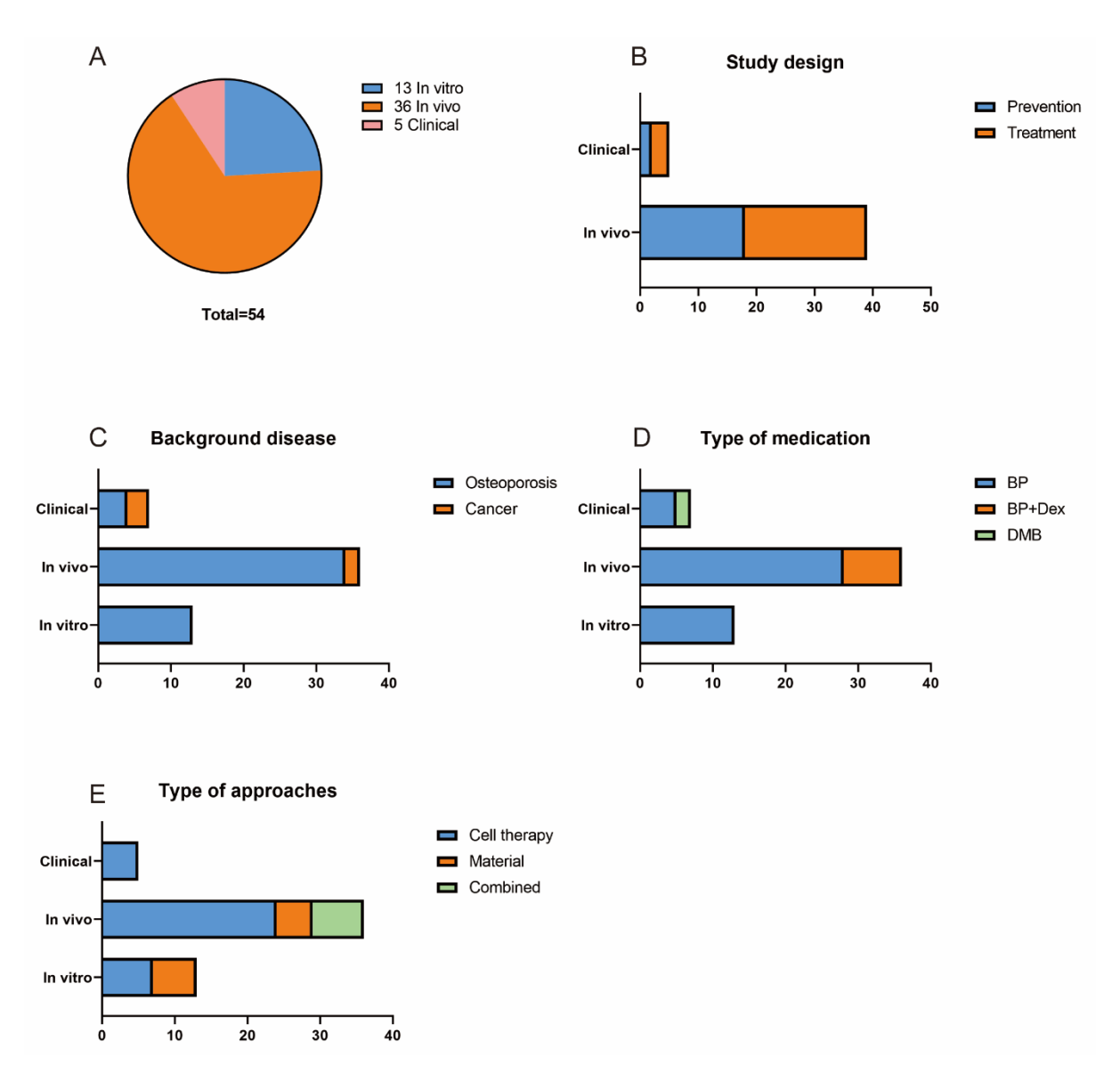


Fig 1.8 Characterization of TE studies for MRONJ. A. Number of *in vitro*, *in vivo* and clinical studies. B. Number of *in vivo* and clinical studies for prevention and treatment. C. Background disease (osteoporosis or cancer) of *in vitro*, *in vivo* and clinical studies. D. Types of medication (BP, BP+Dex and DMB) for *in vitro*, *in vivo* and clinical studies. E. Number of approaches (Cell therapy, material and combination) of *in vitro*, *in vivo* and clinical studies.

1.3.3.1 In vitro studies

Thirteen *in vitro* studies (Table 1.3) were conducted using 18 different cell types to investigate the use of TE therapy for the treatment of MRONJ. Among these studies, 9 of 13 utilised human cells, whereas the remaining 4 used rodent cells (Fig 1.9A). ZA was the major BP that triggered the MRONJ model, which represented 16 out of 18 studies, and 2 studies used AL. Various cell types were tested, with 5, 5, 3, 1, and 2 studies testing OBs, fibroblasts and keratinocytes, stem cells, endothelial cells, and

OCs and macrophages, respectively (Fig 1.9B). In terms of therapeutic strategies, 7 out of 13 studies employed growth factors or cell transplantation (Fig 1.9C), while the rest 6 studies utilized material-based approaches. Specifically, 4 out of 6 studies used hydrogels, and the other 2 used ceramic-glass materials (Fig 1.9D). Various potential pathways have been proposed to explain the effects of TE interventions, including promoting cell viability, proliferation or migration (n=8), osteogenesis (n=5), osteoclastogenesis (n=3), OB-OC cross talk (n=1) and angiogenesis (n=1). Inhibition of inflammation (n=3) and cell apoptosis (n=1) is also presented.

Table 1.3 List of in vitro TE studies

YEAR	CELL	TREATMENT	BP	POSSIBLE PATHWAYS
2023	HGF	Exosome from Adipose tissue- derived mesenchymal stromal cells (MSC(AT)s) loaded hydrogel	ZA	Cell viablity, migration, osteogenesis and inflammation [228]
2023	RAW 264.7 cells, human MSC	Antibiotic and geranylgeraniol (GGOH) loaded hydrogel		Osteoclastogenesis and osteogenesis [229]
2023	human MSC	Antibiotic and GGOH loaded hydrogel	ZA	Osteogenesis [230]
2023	RAW264.7 cells, MC3T3-E1	Zn ²⁺ releasing and AuNPs composite hydrogel	ZA	Macrophage polarisation and osteogenesis [231]
2021	Rat bone marrow- derived cells	Co-culture with Human Umbilical Cord Matrix-Derived MSC	ZA	Cell proliferation and viability, osteogenesis, OB-OC cross talk and inflammation [232]
2021	MRONJ patient BMSC	ADSC conditioned media	ZA	Cell migration and osteogenesis [232]
2020	HGF	Endothelial progenitors conditioned media	ZA	Cell viability and migration [233]
2019	HOK, HUVEC	Epidermal Growth Factor	ZA	Cell viability, migration and angiogenesis [234]
2019	HGF	Biphasic calcium phosphates (BCP)	ZA	Cell viability and migration [235]
2018	НОВ	Concentrated Growth Factors	ZA, AL	Cell viability and osteogenesis [236]
2016	RAW 264.7 cells	Water-soluble microfibrous borate glass	ZA	Osteoclastogenesis and ROS [237]
2016	HGF, huamn alveolar OB	PRGF	ZA	Cell proliferation, apoptosis and inflammation [238]
2014	Human fetal osteoblast cells (hFOB 1.19)	BMP-2	AL	Cell viability and OB induced osteoclastogenesis [239]

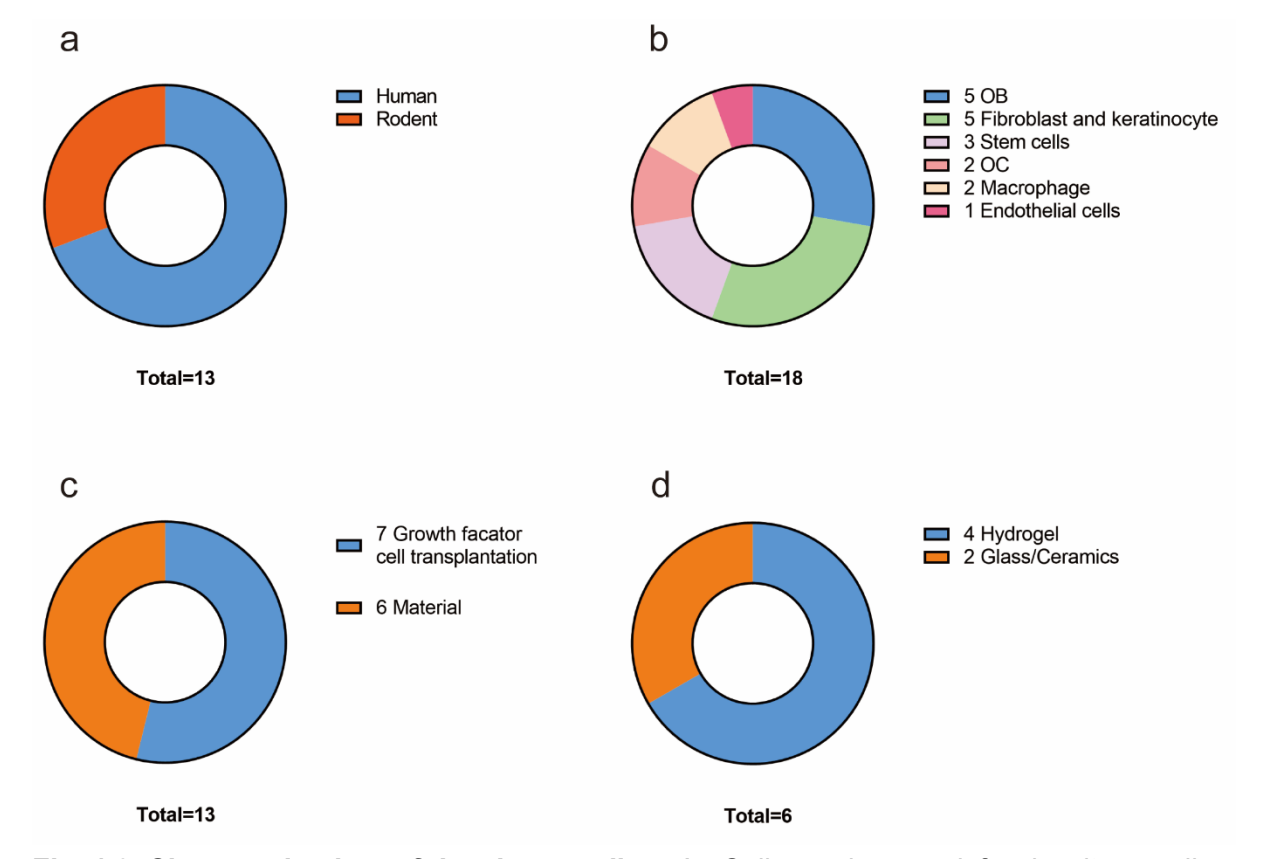


Fig 1.9 Characterisation of *in vitro* **studies.** A. Cell species used for *in vitro* studies, including human and animal cells. B. Cell types used in the included studies, including OBs, fibroblasts and keratinocytes, stem cells, OCs, macrophages and endothelial cells. C. TE types, including growth factor/ cell transplantation and material. D. Material type, including hydrogel and glass/ ceramics.

1.3.3.2 In vivo studies

Thirty-six *in vivo* studies, included in this analysis, are listed in Table 1.4. The models were established by administering BP to animals, followed by tooth extraction. Both preventive and therapeutic models were tested. In the preventive models, interventions were applied to the jawbone after BP application and tooth extraction. At this stage, the jawbone did not exhibit necrosis, and the effects of interventions were observed after 2-4 weeks.

Among these studies, 24 of 36 investigated the prevention of MRONJ. In addition, 10 of the 36 studies established an MRONJ model and confirmed it through imaging or histological examination. These studies have applied interventions at the necrotic site to test MRONJ treatment. Furthermore, 2 studies examined the effect both before and after necrotic bone was formed, therefore tested both preventive and therapeutic

effects. Rodents were the most commonly used animal models for in vivo studies, accounting for 32 of these 36 studies. Rabbits, minipigs, and dogs (n=2, 1, and 1, respectively) were used. Notably, ZA was consistently used as a BP intervention in all models, with 24 studies using it individually and 12 studies co-administering it with dexamethasone or cyclophosphamide (to mimic chemotherapy). The MRONJ model was established by extracting the molars 2-4 weeks after ZA administration. Regarding therapeutic applications, growth factor or cell transplantation approaches were preferred, accounting for 24 of these 36 studies. Hydrogels and ceramic glass materials were the preferred choices (n=4 for each), followed by collagen (n=3) and chitosan (n=1). Site application was the preferred method of administering therapies (n=28), whereas 3 out of 36 studies used intravenous injections to transplant cells. Animal studies have demonstrated that cell therapy may be beneficial for the prevention or treatment of MRONJ. Research has underscored the potential of stem cells as an effective treatment for MRONJ in animal models [224, 225, 240-242]. For instance, ADSCs have been have been shown to prevent the onset of MRONJ via the transforming growth factor β-1-mediated gingival wound healing in rabbits [243]. Sheets of MSCs derived from the periodontal ligament have been shown to enhance the healing of MRONJ lesions in both rat and beagle dog models [223]. A study led by Watanabe et al. investigated the effects of MSC-derived extracellular vesicles (MSC-EVs) in both in vitro and in vivo MRONJ models. Their findings revealed that MSC-EVs significantly reduced ageing in human bone marrow cells and fibroblasts. Furthermore, the study identified a reduction in the expression of cellular senescence genes such as p21 and pRB, and inflammatory markers such as interleukin (IL)-6, IL-8, matrix metalloproteinase (MMP)-1, and MMP-3 in vitro. Studies on rat models showed that the group treated with MSC-EVs exhibited enhanced wound healing at tooth extraction sites and a noticeable reduction in in senescent cells, compared to the untreated group [225].

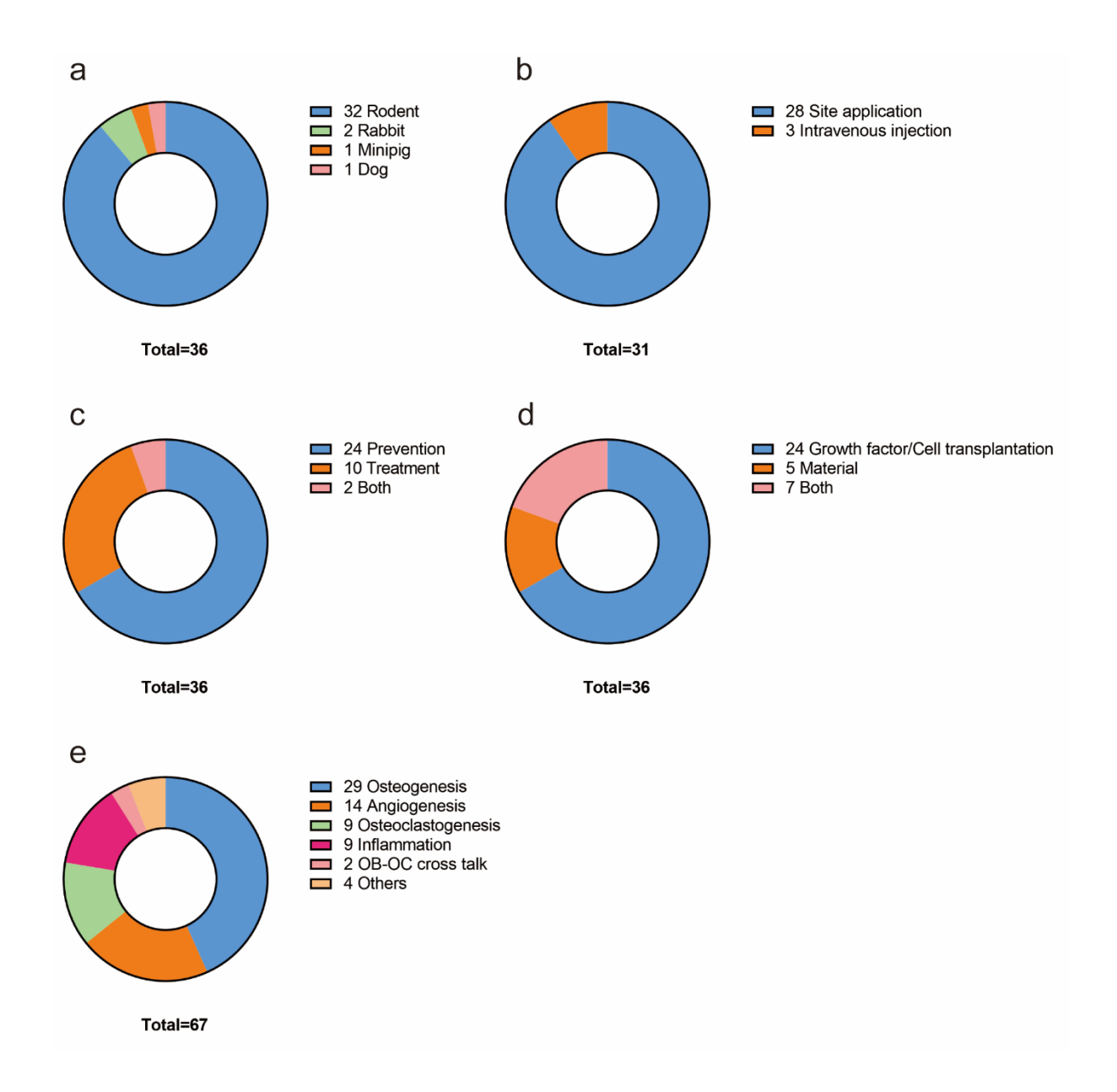


Fig 1.10. Characterization of *in vivo* **studies.** A. Species of animal models (Rodent, rabbit, minipig and dog). B. Model approach methods (Site application and intravenous injection). C. Study purpose (Prevention, treatment or both of them). D. TE types (Growth factor/cell transplantation, material or both of them). E. Pathway for interventions.

1.3.3.3 Clinical studies

Twenty-eight clinical studies were identified that focused on TE interventions for MRONJ treatment. After excluding case reports, pilot studies, case-control studies, and feasibility studies, five RCTs were included. These 5 RCTs were also a part of the RCT analysis (Table 1.2) described in Section 1.2.5, which involved the use of APC products for prevention (n=2) or treatment (n=3). Concurrently, out of 12 ongoing RCTs, five plan to administer growth factor products to MRONJ lesions. Of the three therapeutic studies, two applied APC following the removal of necrotic bone [244, 245]. Additionally, Park et al. combined BMP-2 with APC after surgery and observed that this regimen led to early resolution of MRONJ [244]. APC and BMP-2 were reported promoted bone regeneration, angiogenesis, and wound healing in all 5 RCTs. Their increasing use in MRONJ management underscores the importance of restoring functionality of both bone cells and vascular system. However, several challenges remain to be resolved. Sources of APC are limited, and the absence of mechanical support restricts their application in patients with MRONJ [209, 246]. Moreover, the defects resulting from advanced-stage MRONJ often require bone filling, grafting or substitution [63, 247, 248].

In addition to RCTs, other clinical case studies have validated that autologous cell transplantation can be a viable treatment for MRONJ [249-251]. A notable case by Cella et al. reported the complete recovery of a patient diagnosed with stage-0 MRONJ after injecting bone marrow stem cells into the lesion following a surgical procedure [250].

TE may offer new options for MRONJ management. There are, however, a significant constraint is that most existing data is derived from small animal models that do not wholly capture the complex pathophysiology of MRONJ, which necessitates a prudent approach when considering the translation of these findings to clinical settings. Moreover, current TE strategies and studies focus on growth factors and cell therapies. For large defects caused by MRONJ, scaffold materials are needed to provide mechanical support and attachment to cells. In addition, the release factors from scaffold are more suitable for long-term use compared to the temporary benefit from

plasma products. Therefore, there is a clinical need to explore the use of biomaterials, such as bioactive glass (BG), to determine their effectiveness in managing MRONJ.. Although human TE oral mucosa (TEOM) has not yet been approved for clinical applications, it has been proven that materials containing ions such as BGs and other substances like hydrogels can promote the healing and regeneration of oral soft and hard tissue [252, 253]. *In vitro* studies have shown that silver nanoparticles loaded in hydrogels can successfully deliver drugs with antimicrobial effects [254], and Srloaded hydrogels promote cellular activity and healing assays of gingival fibroblasts [255]. These characteristics suggest the potential of these ion-containing materials to serve as scaffolds for TEOM. Currently, the restoration of large-sized mucosa along with bone defects is achieved using autologous free flaps, where the mucosal part is replaced by skin tissue from the transferred flap. This can lead to a series of issues, including the loss of secretion function, undesirable hair growth in the oral cavity and scarring morbidity.

To review the validity and understanding mechanisms, we conducted (for the first time) an exhaustive literature review focusing on *in vitro* cell responses to BPs, as detailed in Section 1.5.

1.3.4 Bioactive glass (BG)

Bioactive glass (BG)

Since their inception by Prof. Larry Hench in 1969 [256], BGs have evolved significantly to yield a wide range of products for treating various medical conditions including clinically in bone repair [257] and chronic wound healing [258, 259]. These glassy materials are characterised by their non-equilibrium and non-crystalline nature, have been engineered to elicit specific biological responses. They possess the ability to adhere to both bone for implant coatings, release bioactive ions to induce bone or wound healing[260], or antimicrobial ions (e.g. Ag, Cu). Notably, BGs exhibit promising potential for multiple applications including treating bone defects, combating pathogens and malignancies through drug delivery, inorganic therapeutic ion release, and generating heat for magnetic-induced hyperthermia or laser-induced

phototherapy [261, 262]. In BTE, BGs can serve as a scaffold or as an implant coating [263].

Currently, global regulatory agencies have approved over 25 BG medical devices (Table 1.4), showcasing their diverse applications, including monolithic implants, bone void fillers, dentin hypersensitivity agents, wound dressings, and cancer therapeutics. The morphology and delivery systems of BGs have undergone significant transformations since the inception of the first devices based on 45S5 Bioglass®. The first BG composition, 45S5, has a composition of 45% SiO₂, 24.5% Na₂O, 24.5% CaO, and 6% P2O5 by weight [264] 45S5 represents the first development of a biomaterial with interfacial bonding strength. It can promote accelerated bone regeneration compared to bioactive HA ceramics [257, 265, 266]. When the BG comes into contact with bodily fluids such as blood or interstitial fluid, the surface of the BG reacts with ions in the bodily fluids. This reaction helps form a hydrated gel layer containing high calcium, phosphate, and silicon ion concentrations [262, 267, 268]. These ions can initiate the formation of HA crystals, which then grow on the surface of the BG, forming a layer of HA that is similar in composition and structure to the natural HA found in bones and dental tissues. This HA layer acts as a bioactive interface between the BG and bone, facilitating the exchange of ions and promoting the growth of new bone tissues [256, 268].

The composition of 45S5 included many initial commercial products were formulated with this composition and remain commercially available [269]. Additionally, alternative compositions such as S53P4 (53% SiO₂, 4% P₂O₅, 23% Na₂O, and 20% CaO by weight) [270] and 13-93B3 (5.5% Na₂O, 11.1% K₂O, 4.6% MgO, 18.5% CaO, 3.7% P₂O₅, and 56.6% B₂O₃ by weight) have been employed in various other devices [258, 259]. The formulations of the 25 approved BG products are listed in Table 1.5.

In 1985, the first commercialised product of the 45S5 Bioglass®—MEP® implant received approval from the Food and Drug Administration (FDA) for tissue reconstruction or bone substitution of the ear, nose and throat [60]. In 1988, another 45S5 product, EPI®, also gained FDA approval [271]. From then until 2000, additional 45S5 BGs, including ERMI® [272], PerioGlas® [273], Biogran [274], and NovaBone®

[275], were approved for periodontal restoration, while ArGlaes was approved for gingival repair [276, 277].

In 1999, TheraSphere [278] was granted FDA approval for the treatment of unresectable hepatocellular carcinoma. It comprises millions of microscopic glass spheres containing yttrium-90, which can emit radiation for the cancer therapy. Subsequently, BGs with compositions different from 45S5 entered the market, including CorGlaes (55 mol% P2O5) [279], UniGraft (Silicate) [280], S53P4 BGs BoneAlive® [281] and GlaceTM [270], StronBone® (Silicate) [282], DermaFuse/Mirragen (13-93B3) [258, 259], and BioMin® C (Silicate) [283]. However, the specific formulations for TheraSphere, Signify®, CorGlaes, UniGraft, Activa, SIGNAFUSE and BioMin® C have not been disclosed.

Table 1.4 Approved commercial BG products (*composition not publicly available)

Product Name	Approval Year	Composition	Applications field	Application tissue
MEP®	1985	45S5	ENT	Bone [264]
EPI®	1988	45S5	ENT	Bone [271]
ERMI®	1988	45S5	Dentistry	Bone [272]
PerioGlas®	1993	45S5	Dentistry	Bone [273]
Biogran	1995	45S5	Dentistry	Bone [274]
			Dentistry/General	
ArGlaes	1997	45S5	surgery	Soft tissue [276, 277]
TheraSphere	1999	Undisclosed	Radiology	Drug delivery [278]
NovaBone®	2000	45S5	Dentistry	Bone [275]
CorGlaes	2000	55 mol% P ₂ O ₅	General surgery	Bone [279]
UniGraft	2001	Silicate	Dentistry	Bone [280]
			0:-1/	
Medpor®-Plus™	2002	45S5	Cranial/ Maxillofacial	Bone [284, 285]
NovaMin®	2004	45S5	Dentistry	Tooth paste [286, 287]
BoneAlive®	2006	S53P4	Orthopedics	Bone [281]
Glassbone	2008	45S5	Orthopedics	Bone [288]
Cortoss®	2009	45S5	Orthopedics	Bone [289, 290]
				[,]
StronBone®	2010	Silicate	Dentistry	Bone/Tooth paste [282]
Vitoss BA	2011	45S5	Orthopedics	Bone [291, 292]
Signify®	2013	Undisclosed	Orthopedics	Bone [293]
			Cranial/	
Glace™	2014	S53P4	Maxillofacial	Bone [270]
NanoFuse	2015	45S5	Orthopedics	Bone [294]

DermaFuse/Mirr	•			
Agen	2016	13-93B3	General surgery	Soft tissue [258, 259]
Activa	2018	Undisclosed	Dentistry	Teeth [295]
OssiMend®	2019	45S5	Orthopedics	Bone [296]
BioMin® C	2020	Undisclosed	Dentistry	Tooth paste [283]
SIGNAFUSE	2020	Undisclosed	Orthopedic	Bone [297]

Table 1.5 Formulation (wt%) of 45S, S53P4, 13-93B3, A-W glass-ceramic and Stronbone™

Composition (wt%)	Na ₂ O	CaO	SiO ₂	P ₂ O ₅	CaF ₂	MgO	B ₂ O ₃	K ₂ O	SrO
45S5	24.5	24.5	45	6	0	0	0	0	0 [264]
S53P4	23	20	53	4	0	0	0	0	0 [270]
13-93B3	5.5	18.5	0	3.7	0	4.6	56.6	11.1	0 [258, 259]
Stronbone [™]	3.5	14.1	37.8	8.8	0	4.3	0	5.33	26.1[282]

Considering their restorative and osteoinductive properties, BGs offer a potential therapeutic strategy for MRONJ treatment. A study by Su et al. revealed that borate BG (BBG) prevented BP-induced MRONJ in a rat model by restoring osteogenesis and angiogenesis [298]. Although no such clinical trials have been performed, BGs have shown potential for MRONJ treatment.

1.3.5 Therapeutic ions released from BG

BG compositions are tailored to meet specific clinical needs, including those arising from cancer [278, 299, 300], hard and soft tissue defect [301, 302], infection [303, 304], and multiple objectives [305]. Increasing evidence suggests that the effect of BG *in vitro* [306-308] and *in vivo* [309] is primarily influenced by the dissolution products of BGs. The BG network can be modified to both determine the ion release rate, and the type of ion released, based on the clinical need. For example, a combination of Si, Sr and Cu therapy was proposed to treat myocardial infarction due to its regulatory effects on the angiogenesis of endothelial cell angiogenesis, M2 polarization of macrophages, and cardiomyocyte apoptosis [310]. the commercially available 45S5 and S53P4, are primarily used for bone and dental restoration, whilst borate-releasing13-93B3 is designed for soft tissue wound repair. The addition of specific ions into the BG network can alter the ion release rate, biological effect and clinical use. For example, example yttrium-90 was added into microscopic BG structure for enhanced radiation therapy for hepatic cancer (TheraSphere) [278].

Biological role of Si

Although Si-BGs have existed for over 50 years, our understanding of the cellular mechanisms influenced by Si remains incomplete. Turner et al. [311] provided a quantitative review of the literature on *in vitro* cell responses to Si concentrations and found that t there were increased occurrence of undesirable cellular outcomes above ~50ppm Si, and desirable cellular responses had a median of 30.2 ppm. This implies that Si concentration is crucial in determining cellular outcomes.

Si is known to be important in modulating the immune or inflammatory response [312-314] and in connective tissue formation particularly benefiting skin and bone [315, 316]. Research indicates a positive correlation between dietary Si and improved bone density [317, 318]. Additionally, adequate Si intake may reduce Alzheimer's disease risk [316, 319]. In healthy adults, serum Si levels typically vary between 100 to 310 μ g/L [320].

Although the exact mechanism of how Si promotes bone formation remains unknown, in vivo studies have shown that Si containing HA scaffold lead to significant higher mineral apposition rate and bone volume compared to Si-free group[321]. Si-BG promotes bone formation by releasing biologically relevant ions, particularly Ca, P, and Si [322, 323]. The release of Ca and P can lead to apatite formation in biological fluids, which may expedite bone repair independently of Si [202, 324], although Si-BGs exhibit enhanced bone-forming capabilities compared with non-Si bioceramics [325]. Research by Xynos et al. revealed that dissolution products from 45S5 Bioglass® activated genes vital for bone repair in vitro [309, 326]. Furthermore, other studies have shown that Si stimulates OB proliferation and collagen production [327]. In addition, Si-BG has been found to have an antimicrobial effect by altering the pH of the surrounding environment [328-330]. When Si-BG comes in contact with an aqueous environment, it releases Si ions and forms Si(OH)4, also known as tetrahydroxy silane, which increases the pH of the environment, creating an inhospitable environment for bacteria that are typically sensitive to changes in pH. In addition, Si-BG has also been found to enhance angiogenesis both in vitro and in vivo [331, 332].

Although Si is a component of BG, its presence in other types of materials has shown improvements in bone regeneration under pathological conditions such as insulin carriers [333], osteoporosis, and inflammation [334]. Lv et al. 2017) designed a nanofibrous composite scaffold material with a sustained release of Si ions and found that this scaffold promoted the adhesion, proliferation, and migration of human umbilical vein endothelial cells (HUVECs) and human keratinocytes *in vitro*. Moreover, it induces angiogenesis, collagen deposition, and re-epithelialisation at wound sites in a diabetic mouse model while inhibiting inflammatory reactions [335]. Dong et al. (2020) found that Si ions released from calcium silicate bioceramics partially restored the negative effects of high glucose on the osteogenic differentiation of bone marrow stromal cells [336]. Similarly, bone regeneration in an osteoporotic Sprague—Dawley rat model was enhanced by Si-released injectable bone cement [337]. Using Si-containing cement has also been reported can form a continuous calcific barriers in the exposed dental pulp tissue than in those without Si [338].

Boron ion

A borate-based 13-93B3 BG(56.6% B₂O₃) is used in product DermaFuse has been FDA approved for diabetic ulcers [339]. The cellular mechanism of this enhanced healing is unknown, but may involve the regulation of collagen and proteoglycans. Boron also enhances keratinocyte migration, potentially playing a crucial role in wound healing [340, 341] and play a significant role in restoring mineralization and VEGF expression in BMSC and HUVEC exposed to ZA [298].

Boron based BGs may also be used in bone regeneration, where B may enhance the integration of calcium into bones, joints, and cartilage [342]. Boron may also cause anti-inflammatory and antioxidant benefits [343, 344].

An *in vivo* rat model showed that borate bioactive glass prevents ZA-induced ONJ by restoring osteogenesis and angiogenesis, and µCT also demonstrated that BBG treatment significantly increased bone mineral density in the extraction sockets [298]. However, the rapid release of boron from materials can lead to undesirable effects if the dissolution rate is not properly controlled. MTT assays demonstrated a gradual

decrease in cell viability with increasing boron concentrations, ranging from 500 to 2000 ppm, whereas sodium ions exhibited no such toxicity [345].

Cobalt ion

In recent years, cobalt (Co)-doped BGs have shown promise for combining traditional bioactivity (bone-bonding and osteostimulatory characteristics) with pro-angiogenic effects linked to the release of Co. Co is known to stabilise hypoxia-inducible factor (HIF)-1α during bone formation by competing with Fe²⁺ ions, binding to the active site of prolyl hydroxylase domain protein 2, and blocking its function [346]. Co ions released from BGs have been shown to upregulate VEGF expression in different cell types, including HUVECs, MC3T3-E1 cells, and human fibroblasts [347-349]. Furthermore, Co pretreatment of BMSCs resulted in a higher degree of vascularisation and enhanced osteogenesis when these cells were implanted in skull bone defects in mice, compared to non-treated cells [350]. Additionally, Co restored primary rat OB mineralisation under hyperglycaemic conditions [351].

In addition to promoting and restoring bone regeneration, Co promotes wound healing, whether doped into BGs or used individually. Zhang et al. found that Co released from 13-93B3 BBG enhanced the proliferation, migration, and tube formation of HUVECs by upregulating HIF-1 α and VEGF. Additionally, Co-doped BBG accelerated full-thickness skin wound healing in a diabetic rat model by promoting angiogenesis and re-epithelialisation [352]. Solanki et al. found that Co-doped Si-BG fibres can increase the expression of HIF-1 α and VEGF in human keratinocyte cells compared to cells treated with only Co- or Si-BG, and HA formation did not occur [353].

Other ions

Other ions such as Zinc (Zn²⁺) [354, 355], Magnesium (Mg²⁺) [356, 357], Strontium (Sr⁺) [282, 358] and Potassium (K⁺) [359, 360] have also been proven to enhance bone or soft tissue regeneration when released from BGs. On substituting small amounts of Mg or Zn with Ca, the ion release remained sufficiently high to enable apatite precipitation. Additionally, Mg- and Zn-containing BGs are highly responsive to changes in particle size and relative surface area [361]. These ions are also hypothesized to play same roles (including antibacterial effect, osteogenesis,

angiogenesis and antioxidant) in managing MRONJ, both in terms of prevention and treatment.

Controlled release of multiple ions

BGs offer the capability for the controlled release of multiple therapeutic ions, by changing the glass network (e.g. introduction of ionic species such as Sr, Mg, Ag) and/or through different fabrication approaches (e.g. hybrid materials [362, 363], electrospun nanofibers [364, 365]. Combining BG particles in different bioresorbable polymers/hydrogels, also allows for the temporal control and release of different ions at different stages of the regeneration (e.g. pro-inflammatory initially to enhance healing and anti0microbial effects, followed by ions that promote ECM formation). This would allow the creation of a new generation of BGs with tailored BBG ion release for specific patients groups, with specific underlying diseases e.g. elderly, hyperglycaemic and patients undergoing BP therapy.

Besides BGs, the therapeutic ions can also be released from other biomaterials for bone regeneration. Mg²⁺ released from hydrogels showed good antibacterial and osteogenesis differentiation in a rat skull model [366]. In addition, Sr doped mesoporous silica nanoparticles [367] and Mg²⁺ coated collagen [368] can also promote bone regeneration.

1.4 Genetic factors associated with MRONJ

As mentioned in section 1.1.5, genetic predisposition is a potential pathophysiology of MRONJ [105, 106]. Currently, genetic screening methods, including whole exome sequencing (WES) [369], genome-wide association studies (GWAS) [370], gene expression profiling [371, 372], and oral microbe genome sequencing (MGS) [373, 374], have been used to investigate a wide range of genes that may demonstrate a genetic predisposition to developing MRONJ. After sequence screening, specific gene studies such as single-nucleotide polymorphism (SNPs) [375, 376], gene expression profiling [377], and polymerase chain reaction (PCR) [98, 378] are employed to investigate candidate genes or variants involved in MRONJ progression. Bacteria profiling is also performed to identify potential pathogenic bacteria involved in the

disease [98]. This approach focuses on selected pathogenic genes, variants, and microbes (Fig 1.11).

WES captures nearly all the protein-coding regions of the genome, known as the "exome" and is effective for identifying rare genetic variants, particularly in Mendelian diseases. However, WES does not provide information on the non-coding regions or other functional elements outside the exome [379]. In contrast, GWAS identifies genetic variations across the entire genome and is often used to identify genes associated with complex diseases such as diabetes and heart disease. One limitation of this method is that it requires a large sample size and identifies associations without proving causality [380-382].

Single nucleotide polymorphisms (SNPs) focus on individual changes in a single nucleotide and are useful for identifying specific variants related to diseases, pharmacogenetics, or traits. SNP studies have examined only specific predetermined sites in the genome [383]. Polymerase chain reaction (PCR) amplifies specific DNA segments and is used in a wide range of applications, including cloning, gene expression analysis, and diagnostics. Similar to other gene studies, PCR is limited to known sequences and does not provide a broad view of the genetic variation.

To characterise the knowledge gained by genetic studies, the web of science (core collection) database has been searched and 27 studies were defined* ². The importance of these studies lies in their potential to enhance our understanding of the multifactorial nature of MRONJ, contribute to the identification of high-risk patient groups, and aid in the development of more targeted and effective prevention and treatment protocols. This is particularly important in the context of personalized medicine, where understanding individual variations in disease susceptibility and response to treatment can lead to more effective and tailored healthcare interventions.

-

^{*2} Search term: genetic OR gene OR genom* (Topic) and BRONJ OR MRONJ (Topic)

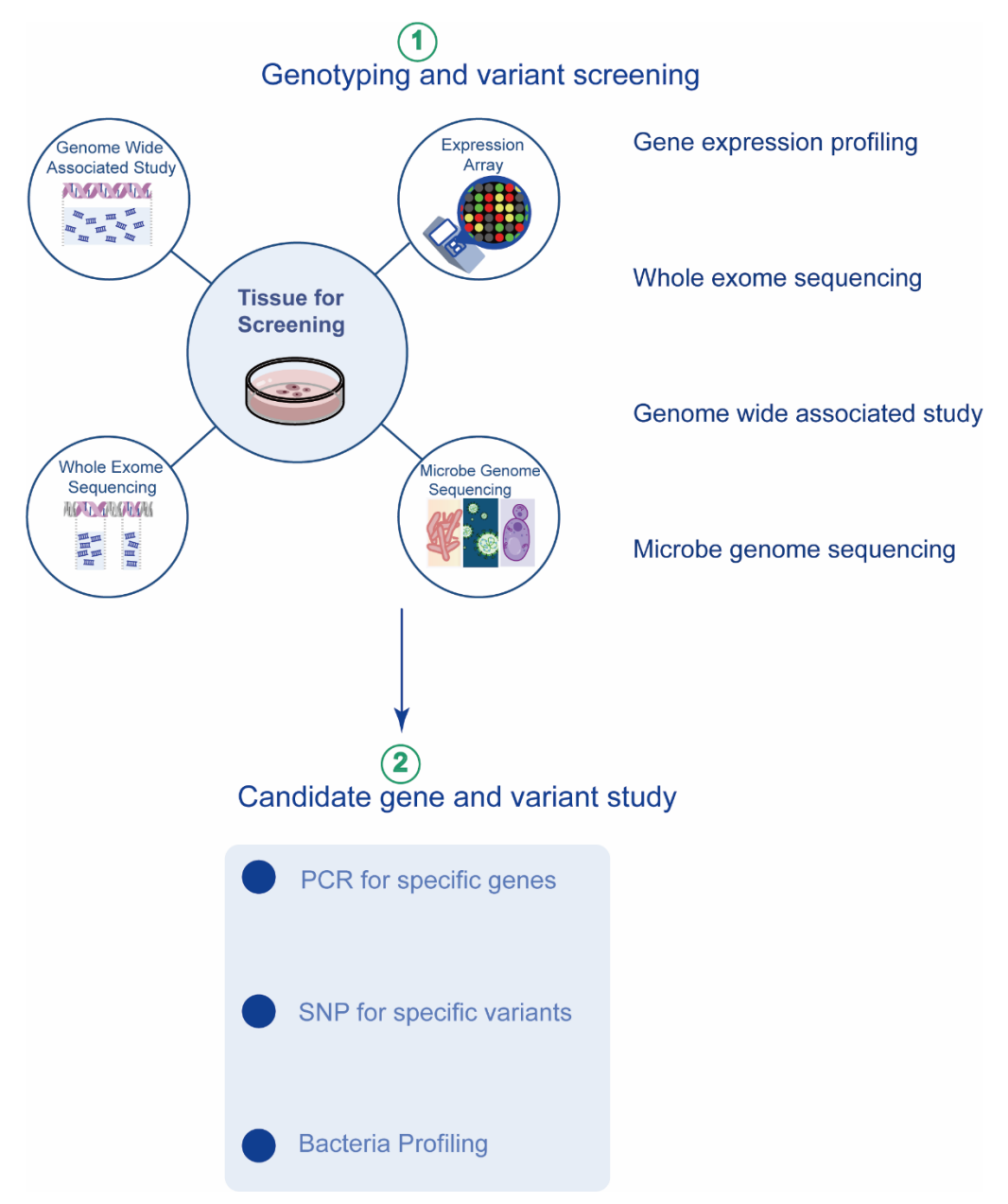


Fig 1.11. Overview of the clinical application of genome diagnostic approaches to MRONJ. Candidate genes are screened from gene expression profiling, WES, and GWAS studies (step 1) and verified by PCR and SNP (step 2). Similarly, the MGS results using patient saliva are followed by bacteria profiling.

1.4.1 Findings from GWAS, WES and single PCRs

1.4.1.1 Findings from GWAS and WES

Since 2008, four studies employing GWAS and four using WES have investigated the genetic factors in developing MRONJ in patients taking BPs (Fig 1.12 A). Although the results of these studies varied owing to the heterogeneity in samples and patient groups, they provided valuable information on the genetic factors associated with

MRONJ (Fig 1.12B).

After sequencing screening, some candidate SNPs have been identified and confirmed by single studies (Fig 1.12C). Sarasquete ME et al. found certain SNPs in cytochrome P450 family 2 subfamily C member 8 (CYP2C8) to be associated with an increased risk of BRONJ in patients with multiple myeloma [105], Martino et.al' s GWAS studied revealed that peroxisome proliferator-activated receptor gamma (PPAR-γ or PPARG) genes are related to a risk of developing BRONJ [106, 110]. Saliva samples from patients with breast cancer and osteoporosis showed that RNA Binding Motif Single Stranded Interacting Protein 3 (RBMS3) played role in determining the risk of BRONJ [384]. In another recent GWAS study published by Yang et al., the BLK proto-oncogene, Src family tyrosine kinase (BLK), Cathepsin B (CTSB), and Farnesyl diphosphate farnesyl transferase 1 (FDFT1) were all associated with MRONJ risk in both cancer and osteoporosis patients [370].

Similarly, various potential genes and SNPs were identified to be associated with diverse diseases by different studies. Kim et. al. found that CC homozygotes of rs2010963 and rs3025039 polymorphisms in VEGF were associated with an increased risk of BRONJ in a Korean population [385]. Yang et al. identified that the Silent information regulator sirtuin1(SIRT1) / HECT Domain And RCC1-Like Domain-Containing Protein 4 (HERC4) locus on chromosome 10 is associated with intravenous BP-induced ONJ in patients with cancer [386]. In 2019, Lee et al. identified different candidate genes in patients with cancer and osteoporosis, using WES, they identified AT-rich interaction domain (ARID), Heme binding protein 1 (HEBP1), Latent transforming growth factor beta binding protein 1 (LTBP1), and Plasmalemma vesicle associated protein (PLVAP) in patients who developed MRONJ after BP treatment for cancer, whereas Vascular endothelial growth factor A (VEGFA), DNA fragmentation factor subunit alpha (DFFA), and Family with sequence similarity 193 member A (FAM193A) to be differentially expressed in patients treated with BPs with osteoporosis [371]. In 2022, another Korean team found nine deleterious SNPs significantly associated with MRONJ in Keratin 18 (KRT18) and Poly (A) Binding Protein Cytoplasmic 3 (PABPC3) based on peripheral blood samples [369].

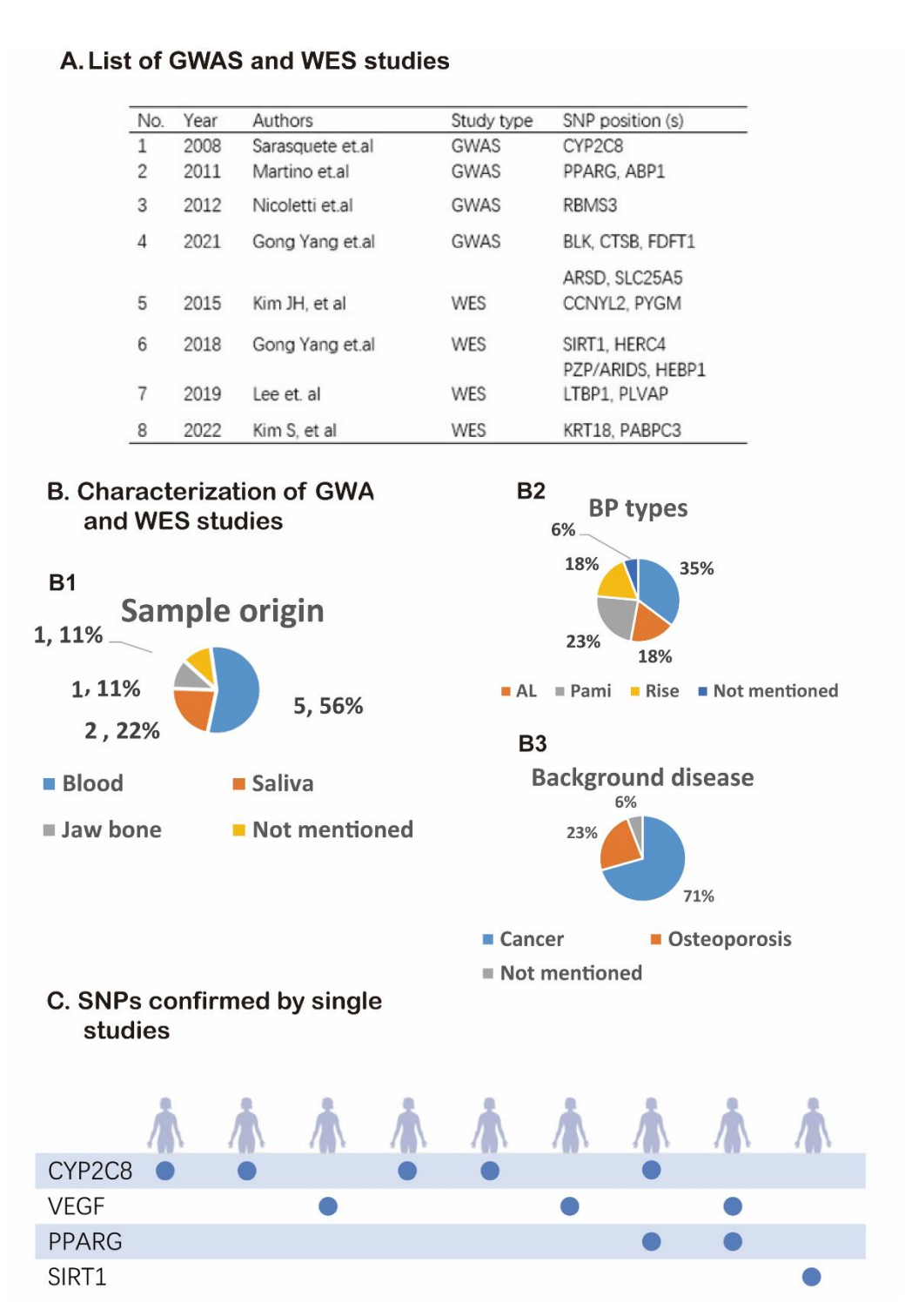


Fig 1.12 Summary of findings from genetic studies of BRONJ. A. Four GWAS and four WES studies have been performed according to a literature search*². B. The BP treatment, sample origin and background disease of the GWAS and WES studies.. C. An overview of the SNPs between patients treated with BPs who developed ONJ and those that did not, in different studies. .

1.4.1.2 Findings from candidate gene studies

To date, of the 9 studies investigating SNP in patients that developed MRONJ, compared to patients that didn't develop MRONJ, 5 reported SNP in the *CYP2C8* gene, whilst 3/9 studies reported SNP in the VEGF gene. This suggests that CYP2C8 (involved in the metabolism fatty acids) and VEGF may be associated with increased risk of developing MRONJ [372, 387-391]. However, contradictory results were reported in the other studies (Fig.1.12c).

Although the results of sequencing studies to date are limited and had contradictory conclusions, they suggested that genetic factors play a role in the development of BRONJ, providing insights that can be used to develop targeted interventions and personalised treatment plans for individuals with this condition.

1.4.2 Findings from microbiota

Microbiota sequencing studies conducted on BRONJ patients also had heterogenous outcomes. Yahara et al.[373] performed shotgun metagenome sequencing on patient saliva samples and identified 31 genes encoded by actinomyce that may be related to BRONJ. Candidate microbial studies by Li et al. [392] found higher expression of *Bacteroidetes, Spirochaetes, Synergistetes*, and *Tenericutes*, whereas *Proteobacteria* and *Actinobacteria* were lower in the inflamed bone tissue of BRONJ patients. Hallmer et al. [393] found anaerobic bacteria to be dominant in bone tissue samples from patients with BRONJ. On the other hand, an oral microbiome study showed that the composition was not directly linked to either BRONJ or N-BP exposure [98].

1.4.3 Differently Expressed Gene (DEG) identification from Gene expression omni bus (GEO)

GEO is a public repository of gene expression data maintained by the National Centre for Biotechnology Information (NCBI). It collects and curates a wide variety of gene expression datasets, including microarrays, RNA sequencing (RNA-seq) and other high-throughput genomic data. In 2008, one study characterising the microarray data from BRONJ patient samples showed a downregulation of the genes, *TSPAN13*, *SKAP2*, *MYBL1* and *HOXB2* [377].

1.4.4 Limitations of current findings

The variations in the results observed across different genetic studies could be attributed, at least in part, to different underlying diseases, medication regimens, sample origins, and sequencing techniques. Out of four studies that implemented GWAS, three used blood samples for sequencing, and one used saliva samples. Similarly, two of the four studies that implemented WES used blood samples, one used saliva, and the other used both blood and jaw-bone samples for sequencing. Additionally, the medications causing BRONJ differed among studies, and the background diseases included multiple myeloma, cervical cancer, prostate cancer, and osteoporosis. Therefore, the current knowledge of the genetic factors affecting BRONJ is still limited and needs further investigation, and studies with a larger sample size and higher homogeneity are necessary.

BRONJ patients have different microbiota compositions and oral health conditions as observed through microbiota studies, owing to variations in their medical histories, medication use, oral hygiene habits, and other factors, which can contribute to the observed differences in the results. Similar to GWAS and WES, the sample size and patient population in each study also varied, leading to differences in statistical power and the ability to detect significant differences or associations.

Despite the heterogeneity of the results, the gene experiments revealed possible cellular pathways involved in the development of MJONJ. GWAS and WES showed that SNPs in *CYP2C8*, *PPARG*, and *VEGF* were associated with the risk of BRONJ, these genes are responsible for direct and indirect angiogenesis and lipid metabolism pathways. *CYP2C8* converts arachidonic acid (AA) into epoxyeicosatrienoic acid [394], which plays a key role in the regulation of vascular tone and cardiovascular homeostasis [395]. *PPARG* directly regulates the expression of genes involved in lipid transport and metabolism, such as *FABP4*, *LXRA*, and *PGAR* [396]. *VEGF* and *VEGFA* are vital growth factors regulating vascular development and angiogenesis [397]. These results indicate that the risk of BRONJ is related to angiogenesis and lipid metabolism.

Chapter 2 Cellular response to BP: A literature review

Understanding how these cells respond to BPs at the cellular and molecular level is crucial to developing effective prevention and treatment strategies for BRONJ. Therefore, we examined the current literature on *in vitro* cell responses to BPs and their effect on the pathogenesis of BRONJ. A comprehensive search for *in vitro* studies investigating cell response to BPs in the context of BRONJ was conducted. By synthesising the data from these studies, we aimed to identify the patterns in cellular responses to BPs, the concentration of BPs and quantitatively demonstrate trends within the research field. The key aims of the work was to determine if there is commonality in the concentration dependent effects of BPs on cells, and if these differences were BP type dependent.

2.1 Search strategies and exclusion criteria

The Topic words 'osteonecrosis of the jaw' and 'in vitro' were used to search the Web of Science database, resulting in the collection of 257, an additional 8 papers were identified through other databases (Pubmed and Google scholar), in total 265 papers up until 31 July 2022. The exclusion criteria for this study included duplicate reports, reviews, conference abstracts, book chapters, and articles that did not quantitatively assess *in vitro* cellular responses to dissolution products or provide a description of the cell culture media used. After applying these exclusion criteria (as outlined in Fig 2.1), 123 studies were shortlisted and included in the analysis.

2.2 Data extraction and statistical analysis

The following data were extracted from each study: cell type, BP type, BP concentration and cell response to BP compared to control (untreated). In terms of cell response the concentration and type of BP that caused a significant decrease or negative outcome, no significant change, or a significant increase or positive outcome was recorded. Considering the sample size and heterogeneity of experimental

approach it was necessary to combine the cellular outcomes as nominally undesirable (e.g. decreased metabolic activity, proliferation, VEGF production or increased cell death) or desirable (e.g. increased metabolic activity, proliferation, VEGF production or decreased cell death). BP-induced cellular responses included; metabolic activity, cell proliferation, osteogenic differentiation, changes in levels of matrix metallopeptidase 9 (MMP-9), VEGF, and oxidative stress markers. Data points normality was tested using the Shapiro-Wilks test. If a normal distribution a one-way analysis of variance (ANOVA) was used to determine significant differences between the median [BP] that increased, decreased, or did not change cellular behaviour. When the groups presented data that were not normally distributed, a Kruskal-Wallis test was performed for multiple comparisons between the [BP] values for negative, no change, and positive cell responses.

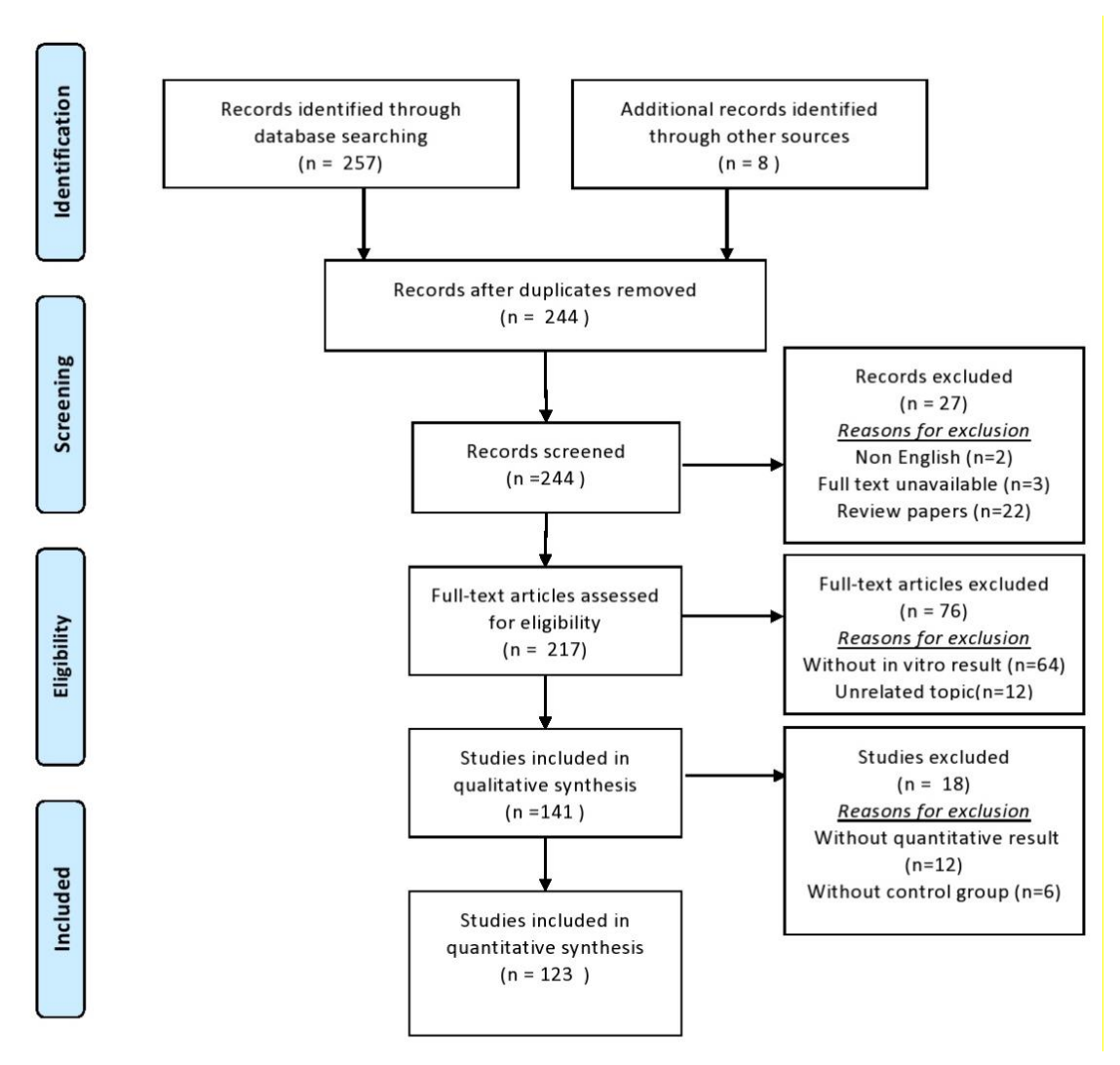


Fig 2.1. PRISMA flowchart of the article selection process. Initially, 264 (257 from Web of Science and 8 from other sources) studies were retrieved; after applying the exclusion criteria, 123 studies were used to extract data.

2.3 Results

2.3.1 Descriptive comparison of BPs analysed with the wider field

Among the 265 studies retrieved initially, papers were excluded mostly because they reported *in vivo* data (64/265, 24.1%) or review papers (22/265, 8.3%); or they did not quantitatively assess cellular responses to BPs (12/265, 4.5%; for example, reports containing cell growth images only), or lacked a suitable control group (6/265, 2.2%). A further 12 studies were found to be unrelated to the topic, were not in English (2/265, 0.7%) or where full text was unavailable (3/265) (Fig 2.2).

2.3.2 Quantification of the studies

The number of articles (N.a), number of data points (n), and percentage of total data points (n%) for cell types, cell species, cell behaviour characterization and BP types were presented (Fig1.14A). A variety of cell types from both rodents and humans were used to investigate BPs *in vitro* including OBs, fibroblasts, endothelial cells (HUVECs), macrophages, keratinocytes, OC, stem cells, and monocytes. Metabolic activity was the most frequently used cell assay, and ZA was the most frequently used as BP (Fig 2.2A).

2.3.3 Influence of BP concentration on cellular response

When combining all cellular response measures (metabolic activity, proliferation, apoptosis, protein production, etc.), it was observed that the concentration of BP that caused negative/undesirable cellular outcomes (of ~ 50 µM) was significantly different to the concentrations reported to cause no change or positive/desirable outcomes (p<0.0001). As BP concentration increased, the frequency of negative results also increased, and positive results decreased (Fig 2.2C). Additionally, metabolic activity assays contributed to most of the data, with osteoblast cells, human-origin cells, and ZA being the most frequently utilized *in vitro* model.

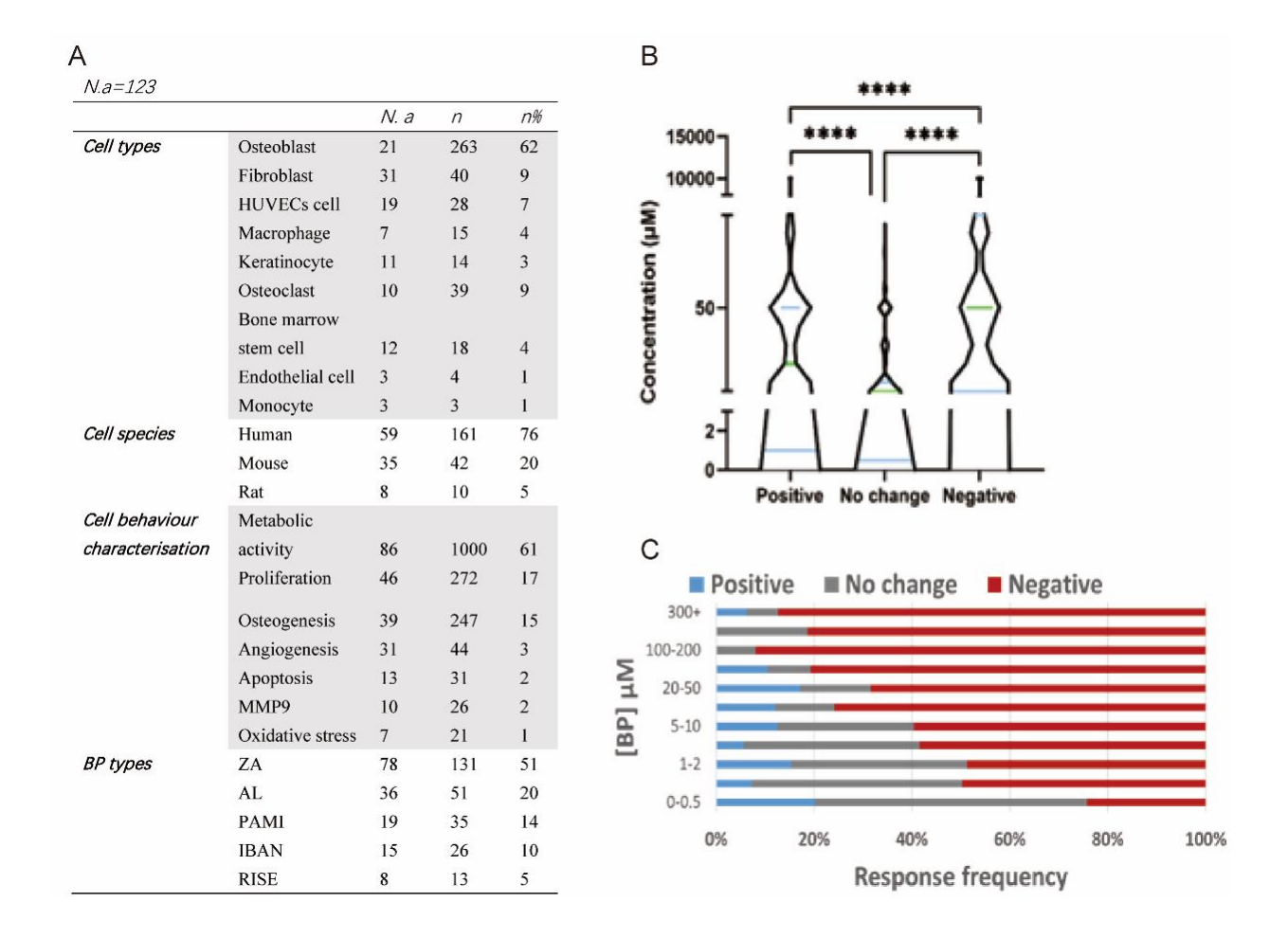


Fig 2.2 The effect of [BP] on cellular behaviour. (A) Quantification of the number of articles (N.a), number of data points (n), and percentage of total data points (n%) for cell types, cell species, cell behaviour characterization and BP types were presented. The (B) median [BP] and (C) frequency that is reported to cause a significant negative (decrease), no significant, or a positive (increase) difference in all observed cell responses *in vitro*, following exposure to BPs (*P<0.0001). [BP] above 50 μM was found to cause significantly negative outcomes, whilst positive and no responses occurred at lower concentrations (20 and 5μ M, respectively).

2.3.4 Methodology used to analyse in vitro response to BPs

Metabolic activity assays were used most frequently (70% of the studies), among which a high variance was observed in the type of assay used. MTT and CCK-8 assays were used the most (46 and 13%, respectively) compared to WST, Alamar blue, XTT, MTS, and calcein viability assays. All these tests require the formazan product as the reagent, but Alamar Blue avoids being invasive as the formazan is soluble. In contrast, other assays require dissolving the formazan crystals with Solvents, which adds an extra step and introduces potential variance, preventing continuation of the cell culture

[398]. Proliferation assays were used in only 16% of the studies, among which 80% used cell counting and 20% used DNA quantification (Table 2.1). The variance in assay type used may lead to variance when comparing different studies. To minimise the impact of these factors and obtain robust and reproducible results, it is important to carefully select and optimise the assay method, as well as control for potential confounding factors through appropriate experimental design and data analysis.

Table 2.1 Cell metabolic activity and proliferation assays used to determine cell response to BPs.

Cell behavior			
characterisation	Assay type	N	%
Metabolic activity (N.a=86)	MTT CCK WST Alamar/Cell Titer/Presto blue MTS XTT Calcein viability	458 129 78 65 32 24	46 13 8 7 3 2
Cell number (N.a=20)	Cell counting DNA quantificati on	218 54	80

2.3.5 Effect of BP concentration on cell metabolic activity and proliferation

Metabolic response to BPs (Fig 2.3A) was similar to the overall cell response, where the majority of studies (623 data points) showed that BPs caused undesirable effects (decreased metabolic activity) on bone cells, compared to 72 data points that showed desirable/increased metabolic activity and 305 data points where BPs did not significantly affect metabolic activity. Unsurprisingly, the concentration of BPs that caused undesirable outcomes (50 μ M) was significantly higher than the concentration of BP that caused a desirable/increased metabolic activity (10 μ M) (Fig 2.3A). For cell

proliferation, whilst the majority of studies (174 data points) were much higher than the number of data points that increased proliferation (45 data points). There was no significant difference between the BP concentration that caused increased or decreased proliferation (Fig 2.3B), although this may be due to the lower number of studies looking at proliferation compared to metabolic activity.

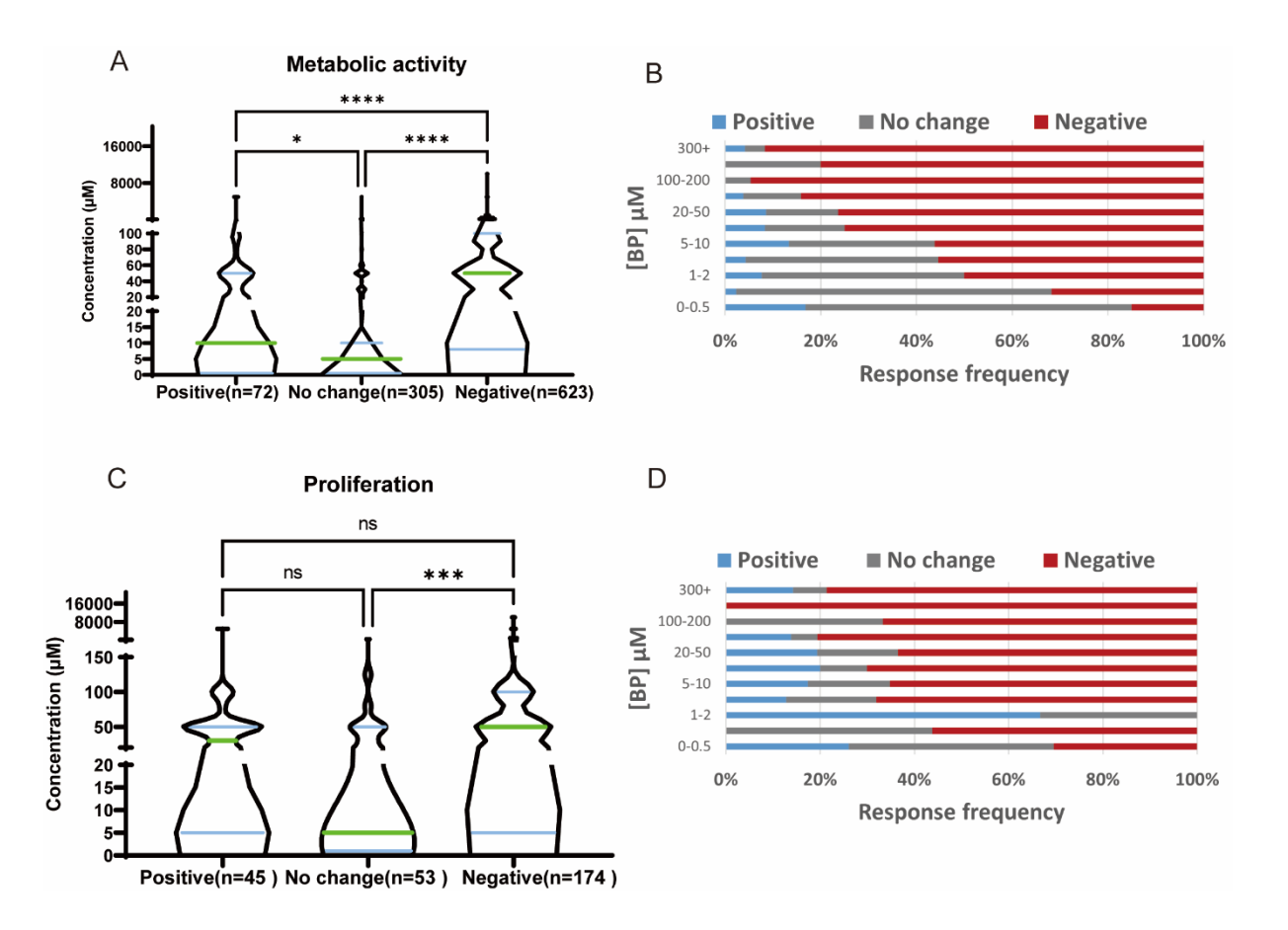


Fig 2.3 Effect of [BP] on cell metabolic activity and proliferation. The (A, C) median [BP] and (B, D) frequency that caused a significantly negative (decrease), insignificant, or significantly positive (increase) difference in metabolic activity and cell proliferation following exposure to BPs. For metabolic activity and proliferation, [BP] >50 μM was found to cause significantly negative outcomes, whilst positive and no responses occurred at lower concentrations (10 and 5 μM for metabolic activity, respectively; 30 and 5 μM for proliferation, respectively). *p<0.05, **p<0.01, ***p<0.005.

2.3.6 Does BP concentration influence cell response?

The effect of different BPs on cell behavior was investigated. The concentration of all BPs that caused undesirable outcomes was higher (P<0.0.5) than the concentration of BPs that caused no change, but only AL, CLO and IBAN showed a significant difference between the concentration of BP that caused negative outcomes compared to positive. (Fig 2.4 A-E, Table 2.2). The median BP concentration causing positive, no change, and negative effects on metabolic activity is listed in Table 1.8. It can be observed that among all BPs, ZA has the lowest concentration (20 μ M) decreasing metabolic activity and proliferation (12.5 μ M), while CLO has the highest concentration (75 μ M) increasing metabolic activity.

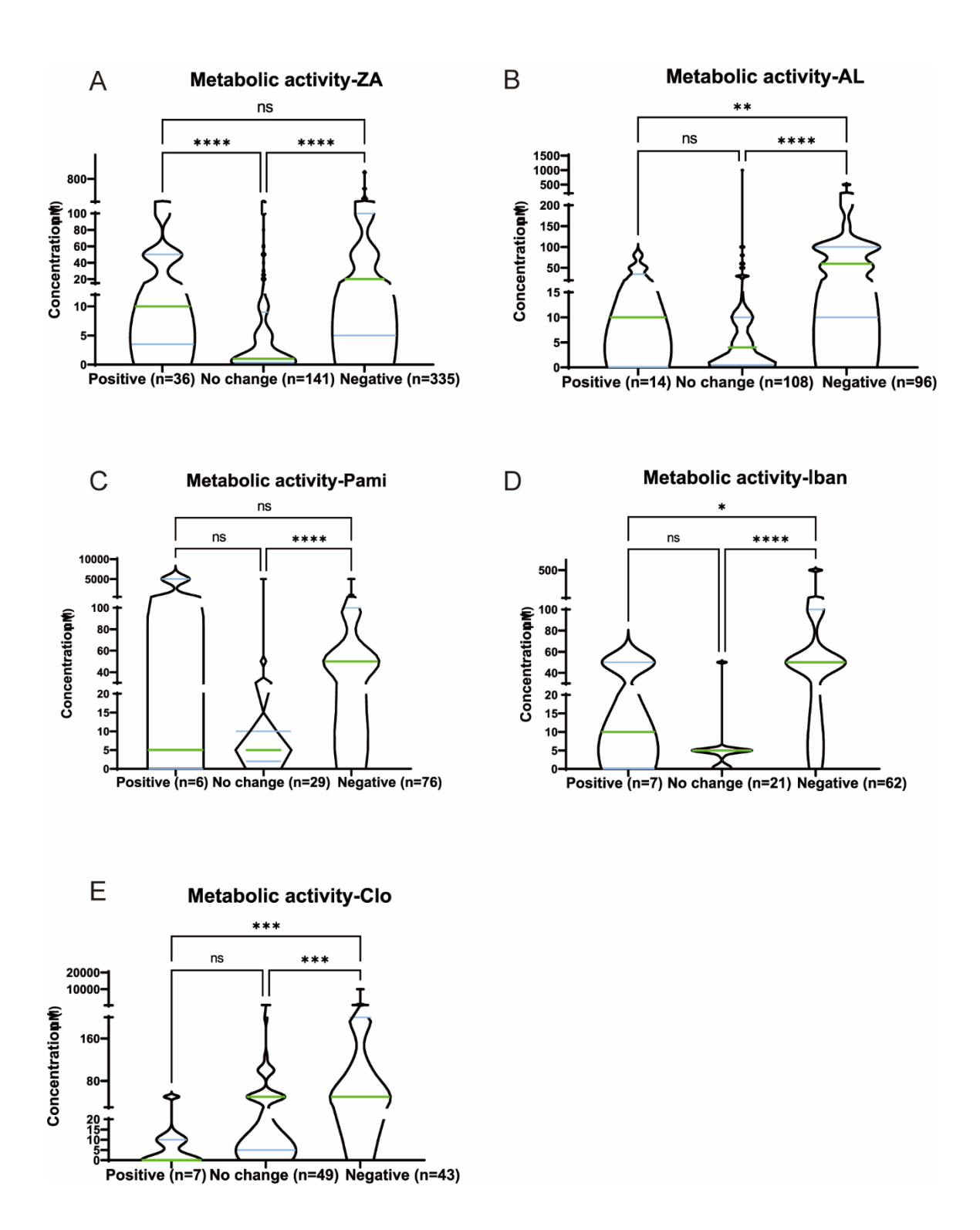


Fig 2.4. Effect of ZA, AL, IBAN, PAMI, and CLO on cell metabolic activity. The median concentrations that triggered positive, no change, and negative metabolic activity for (A) ZA were 10, 1, and 20 μM, (B) for AL were 10, 5, and 50 μM, (C) for PAMI were 5, 5, and 50 μM, (D) for Iban were 10, 5, and 100 μM, and (E) for CLO were 1, 50, and 150 μM, respectively. *p<0.05.

Table 2.2 Median of [BP] induced cell response (positive/increase, no change and

negative/decrease)

	Positive (μM)	No change (μM)	Negative (μM)
Metabolic activity	10	5	50
Proliferation	30	5	50
ZA metabolic activity	10	1	20
AL metabolic activity	10	5	50
Pami metabolic activity	5	5	50
IBAN metabolic activity	10	5	50
CLO metabolic activity	0.01	50	75
ZA proliferation	35	1	12.5
AL proliferation	18.5	5	50

2.3.7 Impact of varying concentrations of ZA and AL on cell proliferation rates

Similarly to metabolic activity there were differences in the response of cell proliferation to different types of BPs and different concentrations, but due to a lower number of data points (experiments performed) only ZA and AL were included for analysis. The BP concentration that was reported to cause a significant decrease in proliferation was higher than the concentration that caused no change (Fig 2.5) but not the concentration that caused an increase in proliferation. In total the number of data points that showed a decrease in proliferation in response to ZA and AL were much higher than the number of studies (data points) that showed an increase. In response to ZA 83 data points showed a decrease in proliferation, whilst 26 showed an increase in proliferation (Fig 2.5A). In response to AL, 21 data points had a decrease in proliferation, 19 exhibited no change; and 10 were reported to increase proliferation (Fig 2.5B).

A B

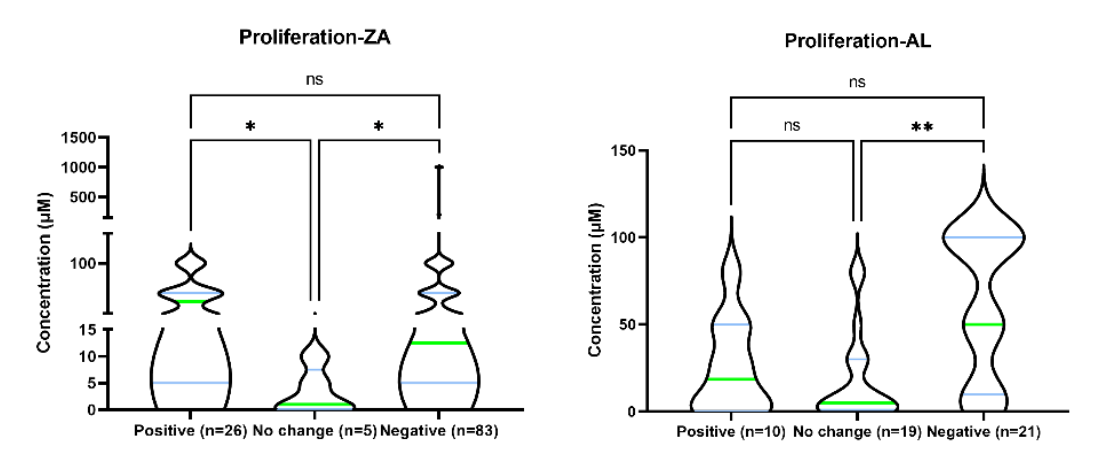
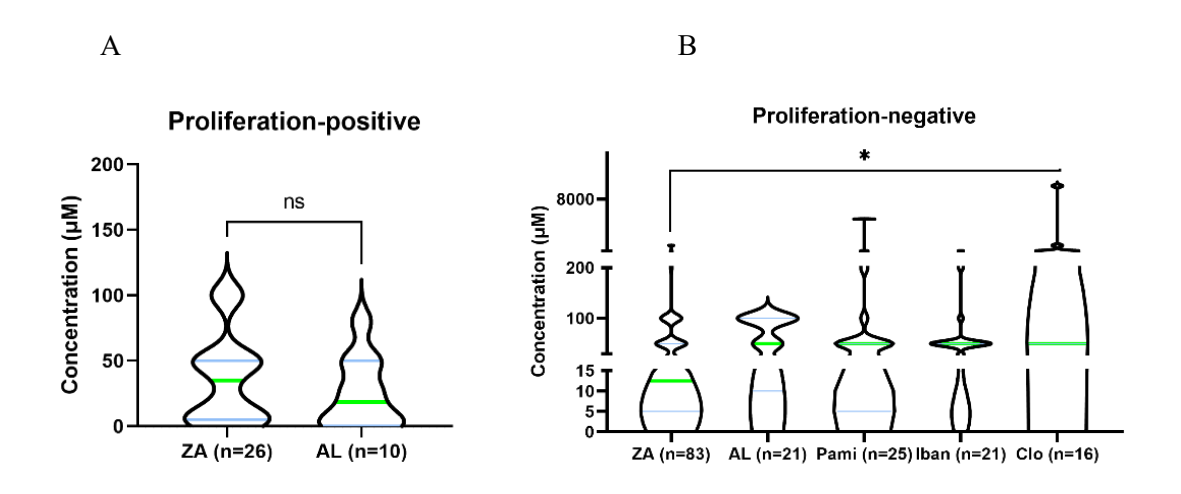


Fig 2.5. The effect of ZA and AL on cell proliferation. Median [ZA] and [AL] for negative, no change, and positive responses toward cell proliferation. The median concentrations that triggered positive, no change, and negative metabolic activity (A) for ZA were 35, 0.5 and 12 μ M, for AL were 12.5, 4.5 and 50 μ M (B). *p<0.05, **p<0.01.

2.3.8 How do other BPs affect cell proliferation?

No significant difference was observed between ZA and AL in their effect on promoting cell proliferation (Fig 2.6A). In contrast, the concentration of BPs reported to cause a decrease in proliferation was higher (P value) than ZA (Fig 2.6B-C). Despite the relatively few data points for non-nitrogen containing BPs (non n-BPs), a decrease in proliferation was observed at higher concentrations than nitrogen containing BPs (N-BPs), suggesting that N-BPs are more toxic compared to non-n-BPs.



C

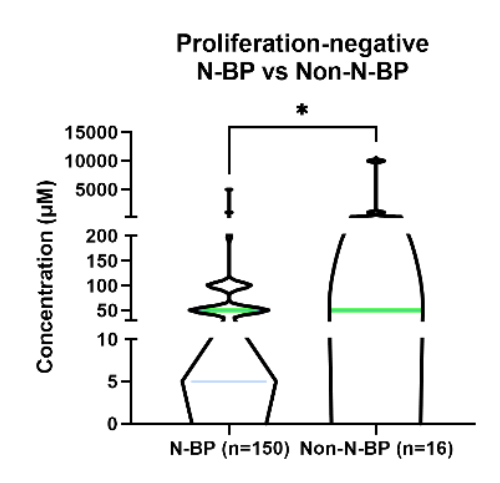


Fig 2.6. Comparison of the influence of different BPs on cell proliferation. The median [BP] of negative and positive responses toward cell proliferation is presented. A. For positive responses, no significant difference was observed between ZA and AL. B. For negative responses, significant differences were observed between ZA and CLO, as well as nitrogen-containing BP (N-BP) and non-nitrogen-containing BP (Non-N-BP) (C). *p<0.05.

2.3.9 The effect of BP Concentration on OB differentiation factors

ALP was the most commonly reported quantitative assay for determining OB differentiation. The reported concentration of BP that caused a decrease in ALP expression (10 μ M) was greater than the concentration of BP reported to cause an increase in ALP expression (0.1 μ M) (p<0.01) (Fig 2.7A). Col 1, OCN, RANKL and OPG did not exhibit any significant difference between the positive and negative responses, but there were only a few studies that reported these assays quantitatively (Fig 2.7B-E). For Runx2, a significant difference was observed for no change responses at concentrations (0.01 μ M), compared to negative responses (0.01 μ M) (p<0.001) (Fig 2.7F).

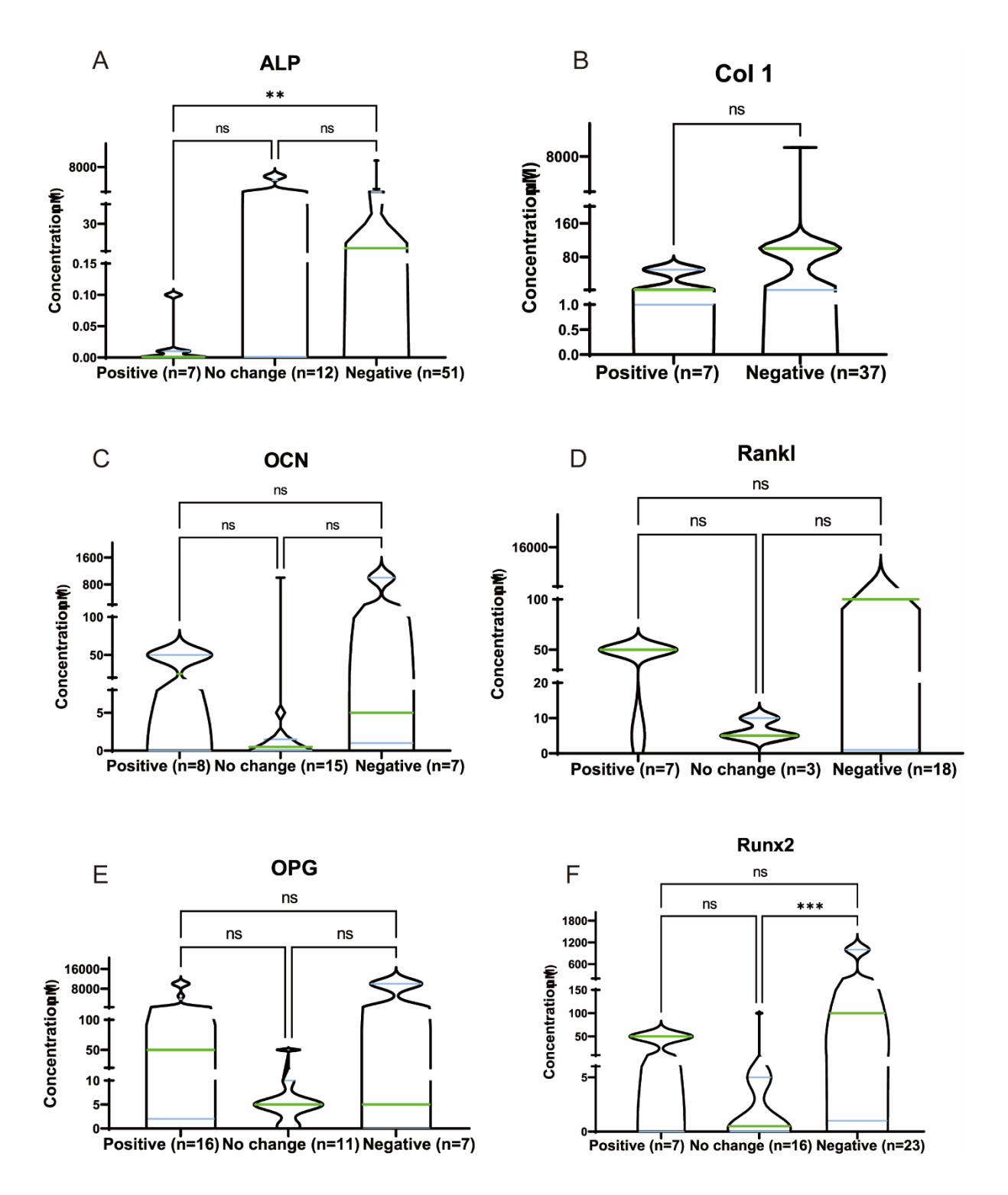


Fig 2.7. Influence of BP concentration on OB differentiation factors. The median [BP] of negative, no change, and positive responses toward cell proliferation are presented. A. For ALP activity, a significant difference was observed for positive responses at concentrations >0.01 μ M, compared to negative responses. B-E. For CoI1, OCN, RANKL and OPG, no significant difference was observed. F. For Runx2, a significant difference was observed in no change responses at concentrations >0.01 μ M, compared to negative responses. No significant difference in responses was observed for COL1, OCN, OPG, and RANKL. **p<0.01, ***p<0.005.

2.3.10 The effect of BP concentration on VEGF, oxidative stress markers and Mmp9

Interestingly the median [BP] that caused an increase in VEGF was higher (75 μ M) than the [BP] that caused a decrease in VEGF (1 μ M). There was no difference in the [BP] that caused increase or decrease in oxidative stress of MMP-9 production (Fig 2.8B-C). It is worth noting that the protein production or ROS production was not normalised to cell number, but considering that higher [BP] caused a decrease in cell number, if the results were normalised to cell number they may be enhanced.

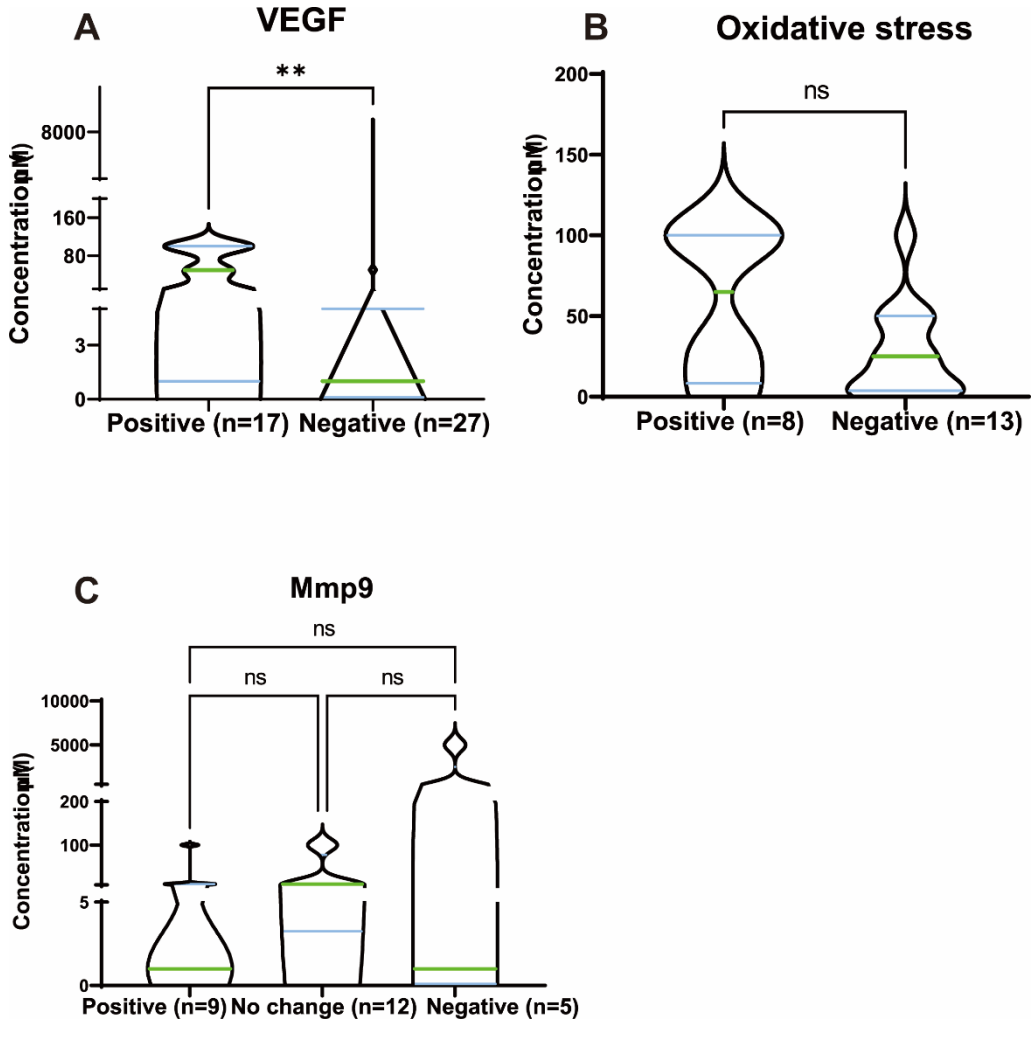


Fig 2.8. Influence of BP on VEGF, oxidative stress and Mmp9. A. A significant difference was observed on [BP] between positive and negative responses for VEGF (p<0.01). B-C. No significant difference in responses was observed for Mmp9 or oxidative stress markers. **p<0.01.

2.3.11 BP concentration affects metabolic activity and cell proliferation in

different cell types

There is considerable variation in the *in vitro* experimental approach and therefore variance in the outcomes. To investigate if there were different responses to BP among the various cell types used, the metabolic activity and proliferation data were compared between different cell experimental models to investigate BPs. . The median [BP] for positive responses was 10 µM (Fig 2.9A), and for negative responses was 50 µM (Fig 2.9B), for both human cells and non-human cells. A significant difference was observed in positive responses (Fig2.9C) between primary cells and immortalised cells (P<0.05), suggesting that immortalised cells are more likely to increase proliferation of metabolic activity in response to higher [BP]s. No significant difference was observed in negative responses (Fig 2.9D) between primary cells and immortalised cells, indicating similar toxicity sensitivity.

Compare to primary cells, immortalised cells normally allow increased self-renewal capacity and decreased variance between passages, as such they are easier to culture, cheaper and have more uniformed responses to external stimuli than primary cells [399, 400]. However, cell lines become immortal when they lose their cell cycle checkpoint pathways and circumvent the process of senescence [401]. It is clear that these cell models do not fully resemble the behavior of *in vivo* primary cells. In addition, cell lines may differ from the *in vivo* situation in important aspects [402]. Czekanska et. al compared proliferation and maturation potential of three osteoblast cell lines, SaOs2, MG-63, and MC3T3-E1 with primary human osteoblast (Hob) cells, and found similarities in cell proliferation and mineralization. However MG-63 cells behaved differently in ALP activity, mineralization potential and gene regulation [403]. Indicating, that to some extent, human cells and non-human cells exhibit similar responses to BP. This is somewhat surprising considering the know difference in cellular functions and cell diffrentiation. Scuteri et al. (2014) compared the *in vitro* differentiation ability of rat and human MSCs, and found that cells from different species exhibited differences in differentiation time and potential [404]. However, when it comes to the major pathway BP triggers in cells—the mevalonate pathway—human cells respond similarly to rat and mouse cells [405, 406]. This similarity might explain why human cells and rodent

cells respond similarly to BP in terms of metabolic activity.

No significant difference was observed in positive responses between stem cells and non-stem cells (Fig 2.9E). When comparing stem cell to non-stem cells, the [BP] reported to cause negative outcomes was lower (P<0.001) than the [BP] reported to cause a negative outcome in non-stem cells, suggesting that stem cells are more sensitive than non-stem cells, to BPs.

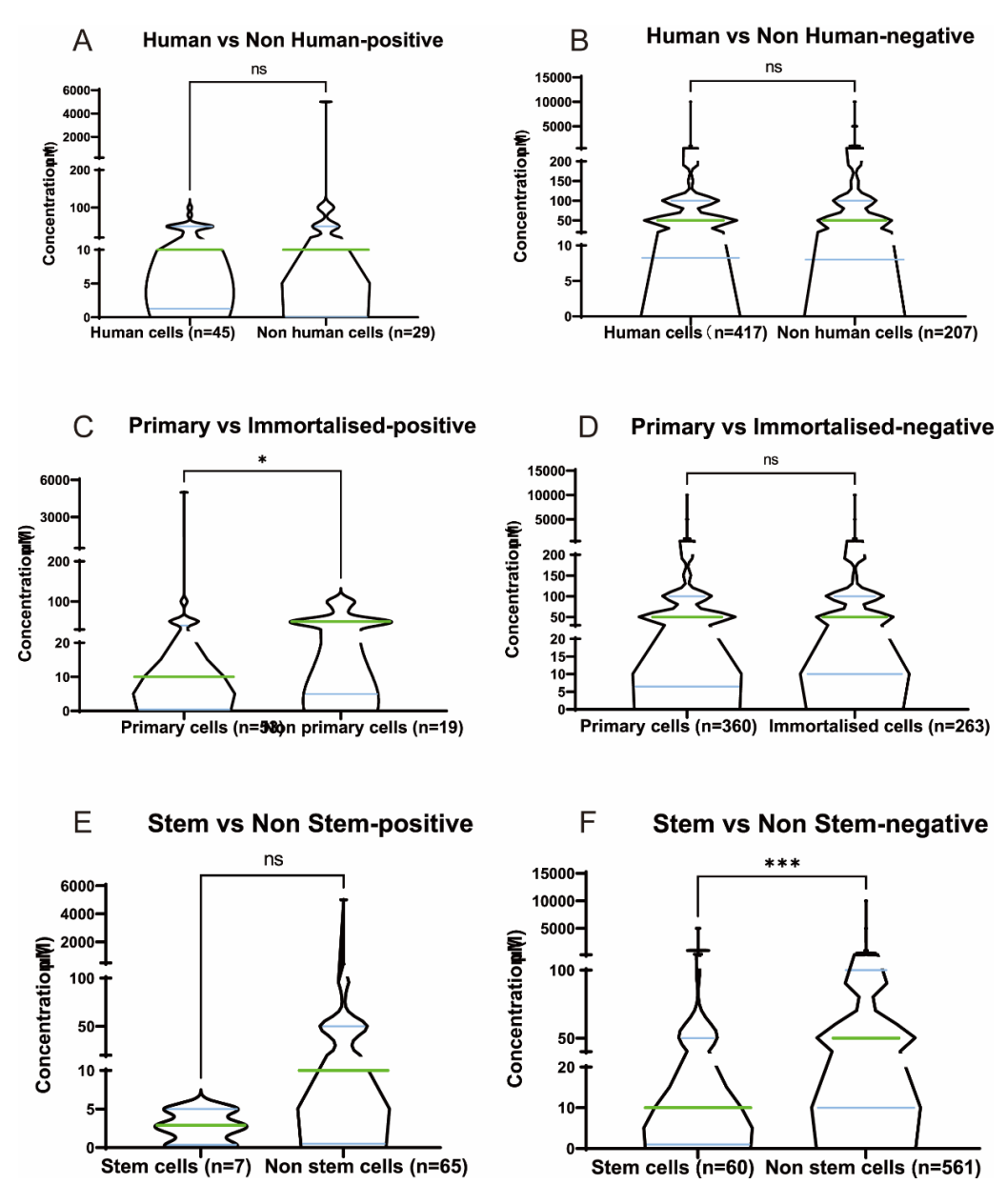


Fig 2.9 The influence of BP concentration on metabolic activity and cell proliferation in different cell types. The median [BP] of negative and positive responses to metabolic activity

or cell proliferation is presented. A-B. Positive and negative response of human cells and non-human cells. C-D. Positive and negative response of primary and immortalised cells. E-F. Positive and negative response of stem and non-stem cells. *p<0.05, ***p<0.001.

2.4 Discussion

Although our literature review conducted a comprehensive search based on existing knowledge, there are limitations in data collection, analysis, and interpretation. Firstly, the search terms could be further expanded to ensure inclusiveness, and studies published after August 1, 2022 should be included to gather the most up-to-date data. Secondly, currently, all the data, which include various cell and assay types, were analyzed together. This approach could lead to variations among individual groups, thereby resulting in vague interpretation of the results.

Another limitation of this review was that it only analysed *in vitro* studies, restricting it from fully capturing the complexity and variability of biological systems *in vivo*. The use of isolated cells or tissues may not accurately reflect the interactions between different cell types, organs, or physiological systems, which can affect the pharmacokinetics and safety of a drug. Additionally, *in vitro* studies may not fully represent the effects of factors such as metabolism, immune response, and organ-specific toxicity that can impact drug efficacy and safety. The complexity of the *in vivo* environment and non-human preclinical models, can however, increase variance/parameters and limit understanding of individual cell pathways more easily controllable and investigated *in vitro*. The works of this thesis were all *in vitro*, therefore need further *in vivo* study to provide more evidences.

Although BPs have been widely used to prevent metastatic cancer and treat bone diseases, the exact mechanism of how they work remains unclear, especially in non OC cells. Additionally, the mechanisms involved in the occurrence and progression of BRONJ are yet to be fully understood. While several *in vitro* and *in vivo* studies have proposed possible mechanisms involved, there is no clear agreement in the literature. Therefore, understanding what is known, within the literature about the role of BPs in the development of BRONJ would aide our understanding of both the aetiology and potential treatments of BRONJ. The section below aims to compile, in a systematic

manner, the known effects of BP on cellular responses In published in vitro studies.

2.4.1 BP affects cell behaviour in a concentration-dependent manner

As seen in section 2.3.3, the concentration of BP and type of BP influences cellular responses. ZA is more toxic than other BPs, and can trigger a negative response in cells at lower concentration, compared to other BPs. Likewise, CLO, a non-N-BP, is less effective than N-BP, and therefore, has a higher toxic concentration compared to N-BPs.

2.4.2 Overview of cell response to BP and possible pathways

BP on various cells

As summarised in the above sections, BPs have mainly negative effect on cell responses, including metabolic activity, proliferation, cell differentiation and specific functions. For non-absorbing cells (OB, fibroblast, keratinocyte and stem cells), BPs inhibit their growth, migrations, and induce apoptosis. For endothelial cells the ability of vessel formation was specifically inhibited, including reduced VEGF gene and protein expression, and reduced tube formation [79, 407-411]. BPs also inhibit antigen presentation in dendritic cells, leading to the inhibition of T cells and immune suppression [412, 413].

Besides direct reduction of OC function, BPs also played roles in the inhibition of OCs' differentiation. OCs are specialized cells derived from the monocyte/macrophage haematopoietic lineage, and activated via RANK/RANKL/OPG signalling pathway [414, 415]. BP can decrease OB expressed RANKL level, and thereby change the RANKL/OPG ratio, in favour of OC formation. Huang et. al found ZA inhibits osteoclastogenesis and resorption via suppressing RANKL-mediated NF-kappa B and JNK and their downstream signalling pathways [416].Additionally, BPs can interfere with the fusion process of macrophages, therefore reduce OC formation. K. Abe et. al found etidronate can directly inhibit RANKL-stimulated OC differentiation and fusion in RAW264.7 cells [417]. In addition, BPs can elevate M1 polarization, leading to chronic inflammation and tissue damage [418, 419] (Fig 2.10).

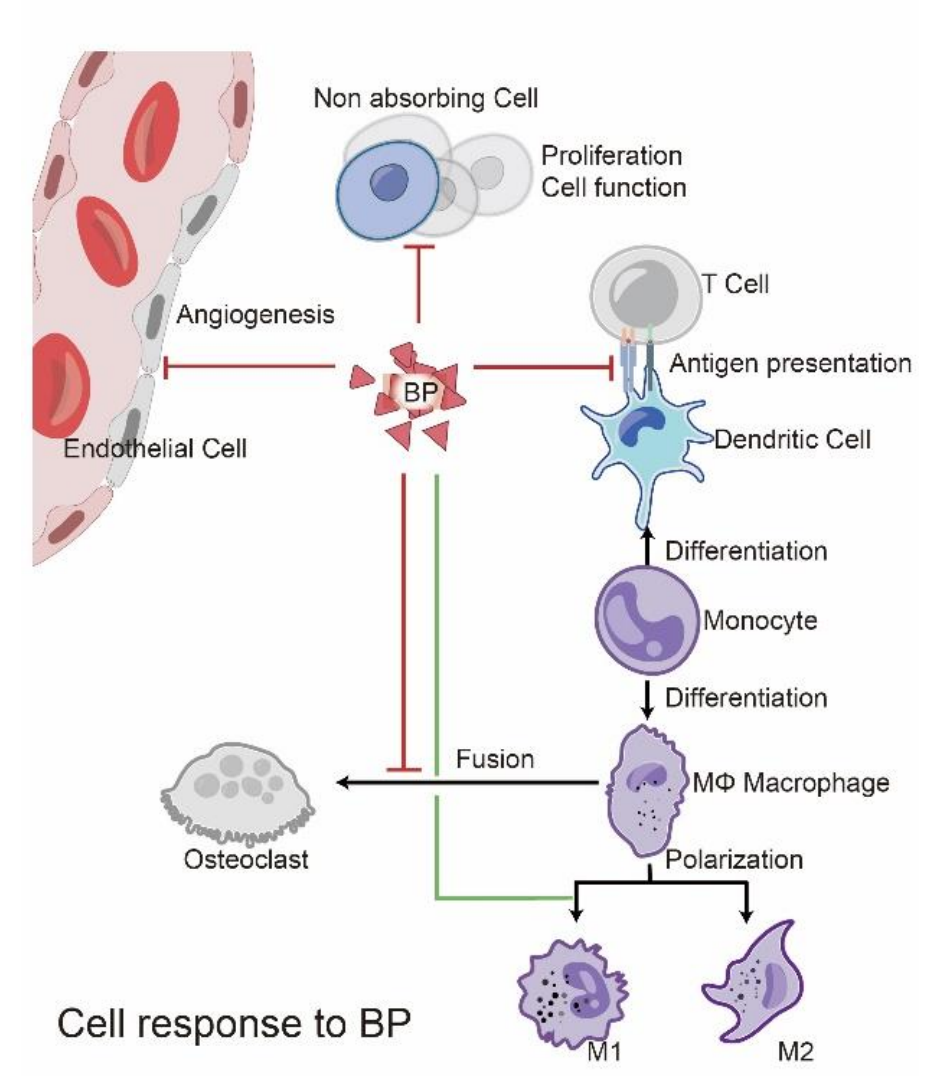


Fig 2.10. Overview of cell response to BPs. BPs can generally inhibit cell activity, growth, and specific functions, especially in the monocyte-macrophage-OC network. Red line represent inhibition while green line represent enhancement.

BP interactions with OBs

Our literature review showed BP affecting OB's cellular biophysiology via different possible pathways. These including increasing inflammation, apoptosis, and oxidative stress, and suppressing cellular functions such as osteogenic differentiation, osteoclastogenesis, and angiogenesis. Pathways were summarized in Fig 2.11. In a similar manner to BP's role in OC, the RANK/RANKL/OPG signalling pathway was also affect by BP in OB. OPG[420], RANKL [224, 416, 421], M-CSF and G-CSF [422] excreted by OB were inhibited by BPs, which induced inhibition of osteoclastogenesis. Meanwhile, the osteogenic gene expression, e.g., RUNX-2, OCN, OSC, BMP-2, BMP-2,

7 were also decreased in OB after exposure to BPs, leading to the impairment of osteogenic differentiation and bone forming [423-428]. Gao et. al found ZA regulated OB differentiation via MTORC1 pathway [429].

Other genes like COX-2 [430, 431], Tenascin C and Integrin Avb3 [432] have also been reported to be affected by BP. COX-2 gene expression can stimulate osteoclastogenesis by inhibiting OPG secretion, increasing RANKL expression in OB, and increasing RANK expression in OC [433]. Tenascin C and Integrin Avb3 genes are related to cell adhesion and migration, inhibition of them can affect these cell functions [431, 432].

Angiogenesis makers, including TGFβ1 [434], VEGFR [435], ANG-1 [436], which are involved in VEGF signaling pathway were also inhibited by BPs. The expression of CD54, CD80 and CD86 were also inhibited, which could effect OB interaction with immune cells and inflammation [412, 413]. IL-6, IL-8 and IL-1β were elevated and generate inflammation response [437-439].

Besides direct toxicity, BPs can also induce OB apoptosis via the classical caspase3/7 and NF-kB pathway[440]. Additionally, oxidative stress markers, including ROS, NO and iNOS were raised and lead to apoptosis [430], as well as cell cycle arrest [434, 441-444].

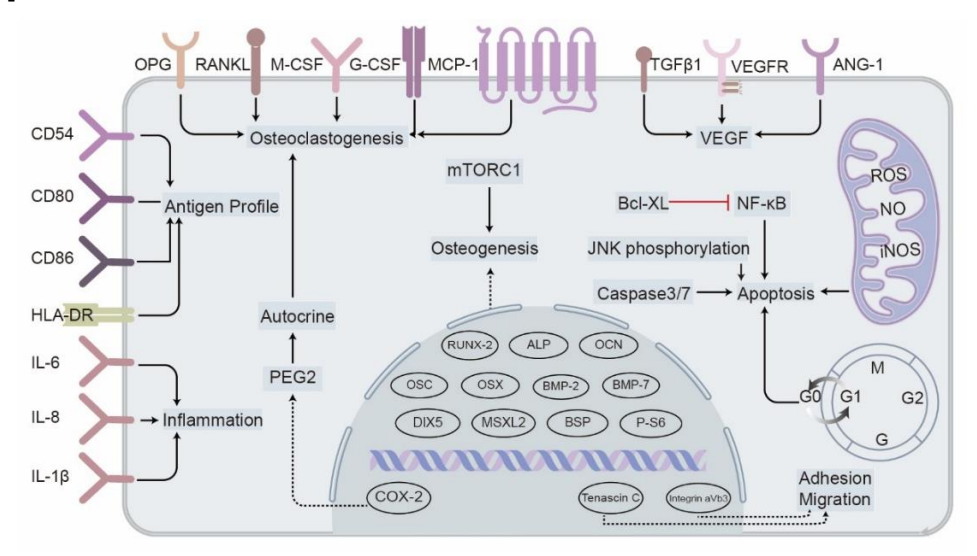


Fig 2.11. A summary of the possible pathways involved in OB response to BPs. Upon interaction with BP, responses from the cell membrane, cytosol, organelles, and nucleus are shown. Osteoclastogenesis, VEGF, antigen profile, inflammation, apoptosis pathways were involved in OB response to BP.

Chapter 3 General Methods and Materials

Using an *in vitro* bone nodule formation model, this thesis investigates the effects of BP on bone cells as well as therapeutic effect of ions released from bioactive glasses (ionic therapy) on BP treated bone cells. The osteoblast and osteoclast models were established to test the cellular responses of BPs, followed determination if ionic therapy can restore the inhibited cellular functions induced by BPs. The overview of the assays is summarised in Fig 3.1.

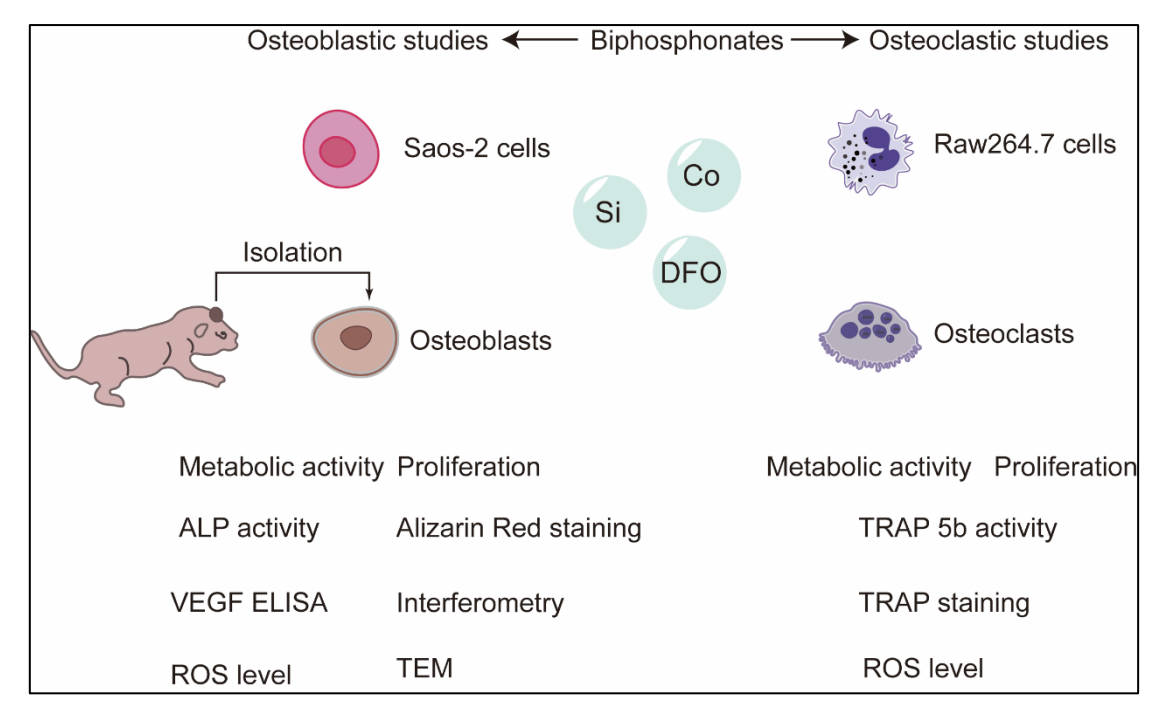


Fig 3.1 A schematic diagram of experimental set up. SaoS-2 cells and rat primary calvaria bone cells are used as osteoblastic models. Raw264.7 cells and selected sub-clone were used as osteoclastic models.

3.1 Cell culture models

3.1.1 Osteoblastic models

3.1.1.1 SaoS-2 cells culture

SaoS-2 cells (ECACC 89050205), an immortalised human osteosarcoma cell line was obtained from the European Collection of Animal Cell Cultures (ECACC, Salisbury, UK). In this study, the SaoS-2 cells were kept between passage numbers 11-14. The cells were cultured in McCoy's 5A (Modified) medium, GlutaMAX medium supplemented with 10% (v/v) Fatal bovine serum (FBS; Thermo Fisher Scientific) and

1% Penicillin streptomycin (P/S,Thermo Fisher Scientific), under 37°C and 5% CO2 (Binder GmbH, Tuttlingen, Germany).

For chapter 3 and chapter 5 experiments (osteoblast studies), the cells were seeded at a density of 60,000 cells/well (15,789 cells/cm²) in 12 well plates (Corning) and cultured for up to 7 days for the metabolic activity (Alamar Blue assay) and proliferation assays (DNA quantification assay). For ROS assays, the cells were seeded at 57,000 cells/well (30,000 cells/cm²) into 24 well plates (Corning) and cultured for up to 6 days.

3.1.1.2 Enzymatic primary rat osteoblasts isolation

Calvarial osteoblastic cells were isolated from 2 or 3-day-old Sprague-Dawley rats according to the sequential enzyme digestion protocol developed by Orriss et al. (2012) [445]. All animal experimentation protocols were approved by the University College London (UCL) Animal Care Services and were carried out in accordance with the UK Animals (Scientific Procedures) Act 1986 upholding the highest standards of ethical practice and care in all aspects of this research. In brief, the neonatal rats were euthanised, sterilised with 70% (v/v) ethanol and transferred to the flow cabinet. A scalpel incision was made along the skull to remove the skin before dividing the head in half. After removing the brain tissue, the jaw and excess cartilage tissues, the calvariae were washed with phosphate-buffered saline (PBS; Life Technologies) in a 5 mL Bijou tubes (Greiner Bio-One). PBS was then replaced with 1 mL (per calvaria bone) of 0.25% (v/v) trypsin solution containing 1 mM ethylenediaminetetraacetic acid (EDTA) (Sigma-Aldrich). Then the calvariae were incubated at 37°C in a 5% CO₂ (Binder GmbH, Tuttlingen, Germany). After 10 minutes incubation, trypsin was discarded and the calvariae were washed with a-modified essential medium (α-MEM; Life Technologies) containing nucleosides and supplemented with 10% fetal bovine serum (FBS; Thermo Fisher Scientific), 2 mM L-glutamine (Life Technologies) and 1% antibiotic/antimitotic (100 U/mL penicillin, 100 µg/mL streptomycin and 0.25 µg/mL amphotericin) (Sigma-Aldrich). The medium was then discarded and 800 µL of 0.2% w/v collagenase solution (per calvarial bone) (Sigma-Aldrich) were added and incubated for another 30 minutes at 37°C. The collagenase was then discarded and replaced with a fresh collagenase solution and incubated for further 60 minutes at

37°C. The final digestion was collected in 15 ml centrifuge tube (Corning), and the bones were washed with 5 mL α -MEM to collect the residual cells in the same centrifuge tube. The cells were centrifuged in an MSE MISTRAL 1000 bench top centrifuge (Sanyo Inst. Buckinghamshire, UK) for 5 minutes at 1500 rpm at room temperature. The supernatant was discarded and the cell pellet was then resuspended in 1 mL (per calvarial bone) of α -MEM, filtered with a 100 μM cell strainer (BD Biosciences) to remove any remaining bone tissue fragments. The cells were then plated into a 75 cm² tissue culture flask (T75; Corning), with 20 ml of α -MEM added. The flask was kept in incubator at 37°C for up to 3 days until a confluency was reached(Fig. 2.2).

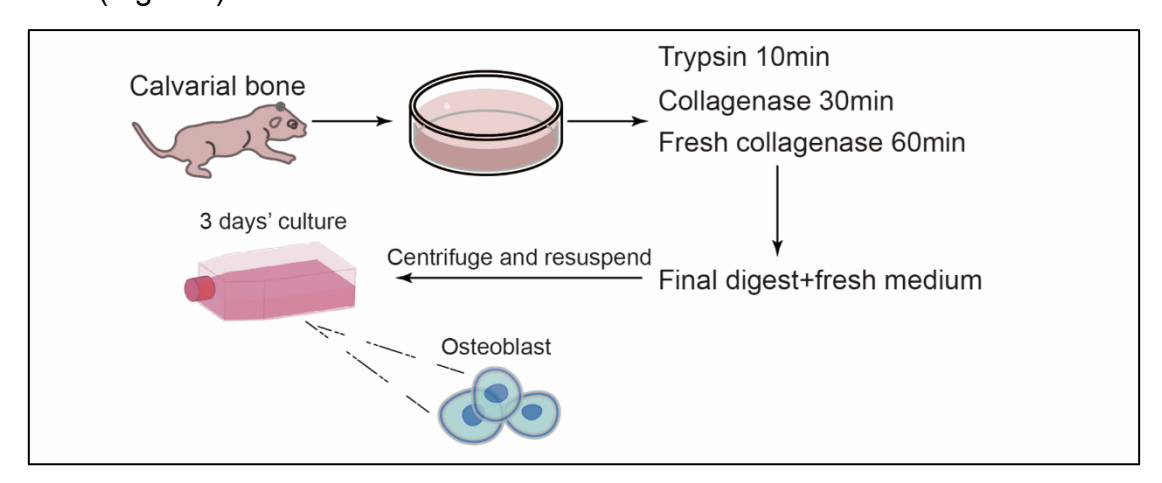


Fig 3.2 The process of enzymatic rat calvaria osteoblast isolation. Primary rat osteoblasts were isolated from 2 or 3-day-old Sprague-Dawley rats using the enzymatical digestion method. The calvariae bone were washed in PBS and incubated at 37° C in trypsin. After 10 minutes, the trypsin was discarded and the bones were incubated with 800 μL α-MEM(per calvaria bone) of collagenase for 30 minutes. Then the collagenase was replaced with fresh collagenase solution and incubated for another 60 minutes. The final digest was collected and transferred into centrifuge tube, and spun for 5 minutes at 1500 rpm. The cell pellet was resuspended in α-MEM and transferred into a 75 cm² flask, and incubate for 3 days till the cell reached confluency.

3.1.3 In vitro bone nodule formation

After reaching confluency, the primary rat osteoblasts were washed with 12 mL of PBS and incubated in 2ml of 0.25% (v/v) trypsin-EDTA for 5 minutes at 37°C trypsin was deactivated using 10 ml of α -MEM and the cell suspension was transferred to 15 ml tube for 5 minutes centrifuge at 1500 rpm at room temperature. The supernatant was discarded, and the cell pellet was resuspended in 1ml of α -MEM (per calvaria). A cell

count was performed using a haemocytometer (Optik Labor, depth 0.1 mm, cell size 0.0025 mm^2) and the cells were seeded at a density of 60,000 cells/well (15789 cells/cm²) in 12 well plate (Corning) in α -MEM, as mentioned in section 3.1.2.

To facilitate the removal of the nodules from the wells for interferometry and TEM measurements, 21 mm diameter Melinex disks (thickness: 175 μ M; Agar Scientific) were prepared with a laser cutter. The disks were then washed with water and soap, sterilised in 70% ethanol and rinsed in PBS and α -MEM (respectively) before transferring them into the plates. When the cells reached confluency in the wells (2-3 days after seeding), they were treated with BPs (ZA and AL 0.067, 0.2, 0.6 and 1.8 μ M) and BPs with sodium metasilicate (Na₂SiO₃) 0.5 μ M medium and maintained at 37°C for 21 days. All osteoblast conditioned mediums were prepared in α -MEM containing 2 mM β -glycerophosphate, 10 nM dexamethasone, and 50 μ g/ml ascorbate (all from Sigma-Aldrich) and were kept overnight in a ventilated T25 flask to stabilise the pH (described in section 2.5.1). Half of the medium was exchanged for fresh medium every 2-3 days.

3.2 Macrophages

RAW 264.7 cells are murine leukaemia virus transfected macrophage cell-line. In this study, the cells were obtained from the European Collection of Animal Cell Cultures (ECACC 91062702, Salisbury, UK) and then expanded with Dulbecco's Modified Eagle Medium (DMEM), GlutaMAX (Thermo Fisher Scientific) supplemented with 10% (v/v) (FBS) and 1% (v/v) penicillin streptomycin (P/S) (Sigma Aldrich) in a T75 tissue culture flask (Corning) and kept at 37 °C incubator with 5% CO2. After 2-3 days, when the cells reached confluency, they were passaged in 1:5 ratios using a cell scraper (Fisher). Low passage numbers (<20) were used to avoid genetic drift. The cells were seeded at a density of $3 \times 10^4 / \text{cm}^2$ in 6 well plates (Corning) for up to 6 days [446]. ZA or AL 0.067, 0.2, 0.6 and 1.8 μ M were added as BP treatment, and medium without BP was served as a control.

3.3 Osteoclasts

3.3.1 Osteoclastic sub-clone generation

Osteoclastic sub-clone of RAW 264.7 cells were generated using an adapted methodology firstly reported by Cuetara et.al [447]. Briefly, the heterogeneous RAW264.7 cell (p11) were seeded in a 6 well plate with a density of 8 cells per well. After 6 weeks, single cell colony was transferred one by one to a 48 well plate by using a 10 µl pipette tip. After another 4 weeks of culture in the 48 well plate, the well become confluent and were further transferred into two 6 well plates. Another 4 weeks additional culture was followed to let the cells become confluence. Cells from the 6-well plate were then transferred and seeded at a density of 30,000/cm2 in 48 well plates, and 3ng/ml RANKL was added at the beginning of this round. At day 6, the cell suspensions were passaged and culture in 6 well plates. In 6 well plates, TRAP staining was performed to screen the osteoclastic subclones. The colony exhibited TRAP most strongly was kept as an osteoclastic subclone and stored in frozen cryovials for the future studies (Fig 3.3).

In this study, an osteoclastic sub-clone 11 (C10), which respond strongest to TRAP staining and cultured by Dr Amy Yutong Li was used as the osteoclastic cell line [448].

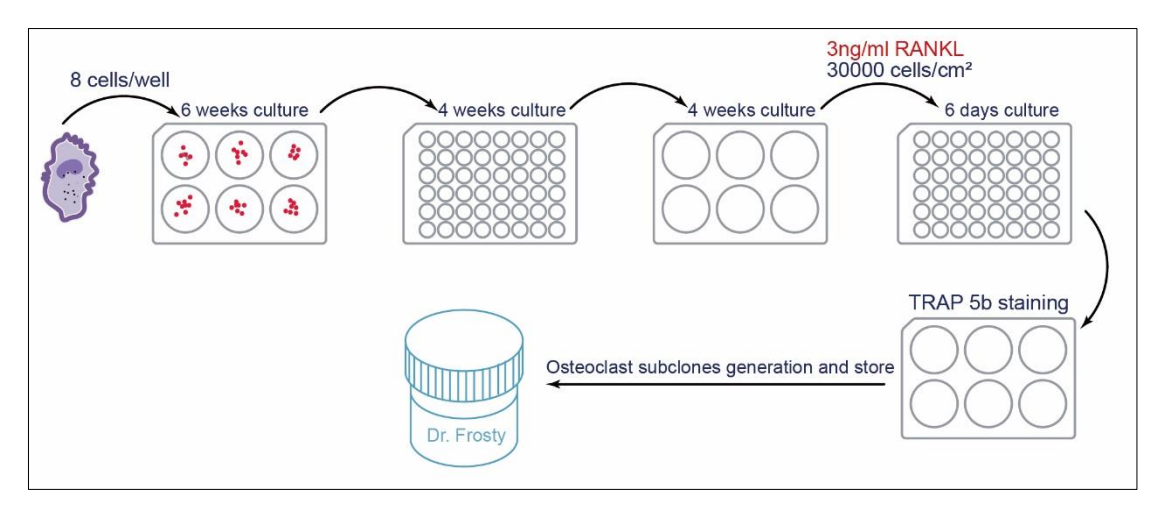


Fig 3.3 Osteoclastic sub-clone generation from Raw264.7 cells [5]. A schematic illustrating the selectin process of osteoclastic sub-clone. Initial seeding at a lower density (8 cells/well in 6 well plate) and subsequent transition to a higher seeding density (30,000 cells/cm² in 6 well plate). The sub-clone exhibiting the most significant response to TRAP staining was kept for future use.

3.3.2 Sub-clone culture and osteoclastic differentiation

Selected osteogenesis sub-clone,C10, was used for proliferation and differentiation assays. The C10 cells were expanded in high glucose DMEM GlutaMAX supplemented with 10% (v/v) FBS and 100 U/ml penicillin and 100 ug/ml streptomycin and seeded at 3,000 cells/cm² in 6 well plates. After 24 hours of seeding, 3 ng/ml RANKL was added to induce osteoclast differentiation and 20 ng/ml RANKL was used as a positive control. ZA and AL at concentrations of 0.067, 0.2, 0.6 and 1.8 μ M was added for BP conditions. Additionally, Si 0.5 mM, DFO 2 μ M or Cobalt 12.5 μ M was added to different BP conditions to assess the restoration of OC.

3.4 Preparation of conditioned mediums

Conditioned mediums were prepared based on different assays with the stock and working concentrations of Si, Co ions, DFO, ZA and AL listed in Table 3.1.

Table 3.1. List of reagents of conditioned mediums, stock and working concentrations

Treatment	Reagent	Stock concentration	Working concentrations
Si ²⁺	Na ₂ SiO ₃	5 mM	0.5 mM
Co ²⁺	CoCl ₂	200 mM	12.5 µM
DFO	DFO	100 μΜ	5 µM
ZA	ZA	1 mM	0.067, 0.2, 0.6, 1.8 μM
AL	AL	1 mM	0.067, 0.2, 0.6, 1.8 μM

3.4.1 Sodium metasilicate (Na₂SiO₃)

A stock solution of sodium metasilicate at a concentration of 5 mM was prepared in medium for each cell line. The mixture was filtered using a 0.2 µM PES syringe filter and the Si ion release profile was then measured using Inductively Coupled Plasma (ICP). The solution was then further diluted to 0.5, 1 and 2 mM in medium and kept in a T25 ventilated flask in incubator at 37 C and 5% CO² for 24 hours prior to applying to the cells.

3.4.2 Cobalt Chloride (CoCl₂)

Cobalt chloride solution was used to obtain cobalt ions (Co²⁺). A 200 mM stock solution was made by dissolving cobalt (II) chloride hexahydrate (CoCl₂.6H2O;) in distilled deionised water and the mixture was filtered using 0.2 µM PES membrane syringe filter (Corning). After measuring the exact Co ion release profile using ICP, the solution

was further diluted in α -MEM to achieve the concentrations of 12.5 μ M.

3.4.3 Deferoxamine mesylate salt (DFO)

DFO was prepared at a stock concentration of 100 µMin ddH₂O. Then diluted to 5 µM

and pre-incubated in a normoxia incubator for 24 hours before applying to the cell

cultures.

3.4.4 BP medium

Stock solution of zoledronic acid monohydrate (Sigma-Aldrich) and alendronate

sodium trihydrate (Sigma-Aldrich) at a concentration of 1 mM was prepared in DDH₂O

for different cells. The mixture was filtered using a 0.2 µM PES syringe filter. The stock

solutions were diluted to working concentrations (0.067, 0.2, 0.6 and 1.8 µM) and

preconditioned in a incubator at 37°C for 24 hours before applying to the cells.

3.5 Metabolic activity: AlamarBlue Assay

AlamarBlue is a colormetric, non-toxic reagent that detects metabolic activity

quantitatively in live cells. The reagent is called resazurin, which is cell permeable and

colored blue as an indicator.

At specific time points (day 1, 3 and 7 for SaoS-2 cells and day 1, 3 and 6 for Raw264.7

cells), the cell culture medium was removed from the well plates and stored in a -80°C

freezer for the ELISA assays. PBS 1mL was used to wash each well and then 1mL

10% (v/v) AlamarBlue dissolved in the medium was added. Three additional wells were

prepared with no cells for background. The whole process was conducted protected

from light. Then the plates were covered with aluminum pieces and kept in an

incubator at 37 °C. After 2 hours, the color of liquid turned from blue to pink due to

reducing resazurin to resorufin. At this time point, 100µL of the solution in each well

was transferred into a 96-well black plate (Thermo Fisher Scientific) and read in a

fluorescent microplate reader (Fluoroskan Ascent FL, Helsinki, Finland) at an

excitation wavelength of 530nm and an emission wavelength of 620nm.

3.6 Proliferation rate: Total DNA Assay

76

A total DNA quantification kit (Sigma-Aldrich) was used to detect the cell number and proliferation at specific time points (day 1, 3 and 7 for SaoS-2 cells and day 1, 3, 6 for Raw264.7 cells). This kit quantified the amount of double strand DNA by using the fluorescent dye benzimide (Hoechst33258). The assay was performed on the same well and plate with AlamarBlue assay. After the metabolic activity assay finished, the pink liquid was discarded and the wells were washed with PBS twice to make sure any remaining dye was removed. 500 µL of deionized distilled water (ddH₂O; Milli-Q, Millipore) was then added into the wells and the cells were lysed under eight freezethaw cycles at -80°C and room temperature. Once the last cycle finished, the cell lysate was checked under the microscope to ensure the cells were fully lysed. Then 100uL cell lysate was mixed with 100µL of Hoechst dye diluted to a working concentration of 20 μg/mL (Hoechst:10X assay buffer: ddH₂O, 1:1000:9000) in 96 well black plates. Fluorescence was quantified in a fluorescent microplate reader (excitation wavelength: 355nm, emission wavelength: 460nm). Serial dilution of calf thymus DNA standards (0-100µg/mL) was done according to the manufacturer's illustration and a standard curve was generated to calculate actual DNA concentration.

3.7 Alkaline Phosphatase Activity

Alkaline phosphatase enzyme activity is a common biomarker to measure the osteogenic differentiation of osteoblasts. On days 1, 7, 14 and 21, ALP activity (ALP; Abcam) was detected calorimetrically according to the manufacturer's protocol. 50 µLcell lysates and 50µL of 5mM pnitrophenyl phosphate (pNPP), a phosphate substrate, were mixed in a 96-well clear plate at room temperature and avoiding exposure to light. The ALP enzyme of the cells can convert the color of pNPP from clear to yellow (p-nitrophenol, pNP) by dephosphorylating it. After a one hour incubation at room temperature, once the color change was observed, 20µL stop solution (NaOH) was added to stop the reaction. Then the plate was read for absorbance at 405nm with a multimode microplate reader (TECAN Infinite M200 PRO, Switzerland). A standard curve of pNP was generated following the manufacturer's protocol to calculate the concentration of pNP. ALP activity was then normalized to

total protein content determined using a BCA protein assay kit (Merck).

3.8 VEGF ELISA

Angiogenesis of primary osteoblasts was measured using a VEGF ELISA kit (Quantikine kit; R & D Systems, Abington, UK) on day 1 and day 7. After termination of the day 1 or day 7 experiment, the supernatants were collected and centrifuged using a plate centrifuge (Hettich Universal 320R, Andreas Hettich GmbH & Co. KG, Tuttlingen, Germany) at 1500 rpm for 5 minutes at 4°C to remove cellular debris. When both the day 1 and day 7 samples were ready, the assay was performed according to the manufacturer's protocol.

In brief, 200µL supernatant was mixed with 50µL assay diluent in 96-well plates (provided in the kit). Then the plates were carefully sealed with plate sealer (provided with the kit) and kept on an orbital shaker incubated at room temperature for 2 hours. After 2 hours, the wells were washed with ddH₂O 5 times and gently tapped onto a paper towel to remove excess liquid. After adding 200µL of VEGF conjugate to each well, the plates were incubated for another hour on the orbital shaker at room temperature. Then the plates were washed using ddH₂O another five times and incubated with 200µL of substrate solution at room temperature. This process was protected from light. After 30 minutes, when the mixture's color changed, the plates were measured using a microplate reader at 450nm with a wavelength correction of 540nm (Fig 3.4). The absorbance reading was converted to a final concentration by calculation with a standard curve. The VEGF concentration was normalized to DNA content.

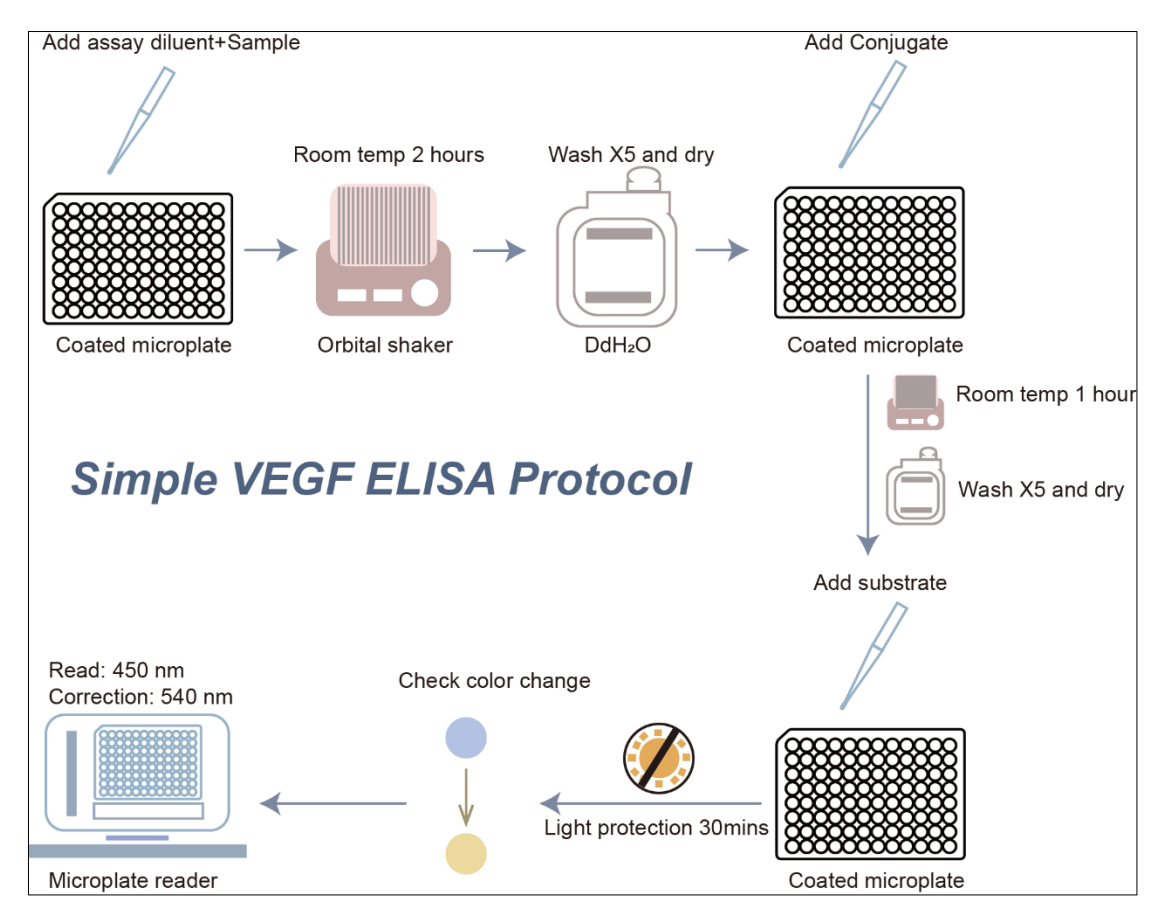


Fig 3.4 R&D VEGF ELISA protocol steps. When all samples were collected, 50μL of assay diluent and 200μL of supernatant were mixed in the VEGFA antibody coated 96-well plate Then the steps described above were followed.

3.9 Alizarin Red Calcium Staining Assay

Alizarin red staining (ARS; Sigma-Aldrich) is an anthraquinone-based dye used to mark calcium deposits in the cells. Once chelated to the cells, an ARS calcium complex is formed and shows the calcium abundant area as red.

For primary osteoblasts, after 21 days' culture, the medium was removed and the cells were washed three times with PBS. Then 1mL of 4% paraformaldehyde (PFA; Sigma-Aldrich) was added into each well to fix the cell and the plates were incubated at room temperature for 15 to 30 minutes. After removing the fixative, ddH₂O was used to wash each well 3 times. During fixing process, 40 mM of ARS was made and kept at a 4.1 to 4.5 pH level. To make sure the pH was reached, acetic acid (1M) was added drop by drop, while monitoring the pH using a calibrated Corning pH meter 240 (Corning Inc., NY, USA). After washing, 1mL of 40mM of ARS was added to each well and

incubated for 20 to 30 minutes. Once the dye was removed, the plates were again washed with ddH2O until all the remaining dye was cleared. A light microscope (EVOS XL Core, Thermo Fisher Scientific) was then used to take images at 4X and 10X magnification.

3.10 Measurement of reactive oxygen species (ROS)

Cellular ROS measurement

To quantify the cellular oxidative stress, 2',7'-Dichlorofluorescin di-acetate (H₂DCF) (Sigma-Aldrich) fluorescent dye is used. Once interact with ROS (such as hydrogen peroxide (H₂O₂), hydroxyl radicals (HO•) and peroxy radicals (ROO•), but not superoxide ions), the H₂DCF would be oxidised and can be observed under fluorescent microscope and quantitatively measured. Before using, the H₂DCF dye was aliquoted in absolute methanol (20mM) and perfused with nitrogen and stored in -80°C, 200μl for each vial to avoid being oxidized. Briefly, the seeding density for RAW264.7 or SaoS-2 cells were 3 x 10⁴. The cells were allowed to attach for 24-hour before treatments. At 30 minutes before terminating the experiment, 500 μM H₂O₂ was applied to act as a positive control. PBS was warm up to dissolve the dye. At treatment completion, the media was quickly removed by flipping on a paper towel and adding the warm dye solution (10 μM H₂DCF in warm PBS) followed by 30 minutes of incubation avoiding from light. The fluorescence was measured at the end using a fluorescence microplate reader (Fluoroskan Ascent FL, Thermo Labsystems, UK), the excitation wavelength was 485 nm and emission wavelength of 538 nm.

3.11 Quantification of osteoclast formation

3.11.1 TRAP staining

Once osteolcasts experiment was finished, the wells with cells were fixed in 2.5% glutaraldehyde for 30 minustes. After that, a staining using TRAP stain kit (leukocyte acid phosphatase kit, Sigma Kit 387-A) was performed. Briefly, the fixative was removed and washed with war PBS, then 1ml freshly prepared TRAP stain following the manufacturer's protocol was added to the sample. Osteoclasts were defined as

TRAP- positive cells with two or more nuclei and/or clear evidence of resorption pit formation. The total number of osteoclasts was counted under a light microscope.

3.11.2 TRAP 5b activity

To quantify the mature osteoclasts activity, TRAP 5b assay was conducted. In this study, TRAP 5b activity was measured in RAW264.7 cell cultures by calculating the conversion of naphthol ASBI phosphate to naphthol AS-BI in the presence of sodium tartrate with heparin as a specific TRAP 5a inhibitor under acidic (pH5) conditions. At the end of osteoclast culture, the wells were washed with warm PBS for 3 times. Then lysed by 6 freeze-thaw cycles in molecular grade DNA/RNase free water and checked under microscope to confirm they were fully break down. After that, 1 mg/ml naphthol AS-BI phosphoric acid/4pNPP was added in 0.1 M glycine buffer (with 0.1mM ZnCl₂, 0.1mM MgCl₂ and 20mM sodium tartrate (pH = 5.0)was added to the lysate. Then the cells were left in a 37°C, non-CO₂ regulated incubator for 1hour. The reaction was stopped with 1M NaOH, then the plate was read at 405nm on a colorimetric plate reader.

3.12 Bone nodule morphological study

3.12.1 Measuring Nodule Dimensions Using Interferometry

After 21 days' culture, the bone nodule grown on melinex were fixed in 4%PFA, and incubate at room temperature for 15 minutes. Then washed with ddH₂O and left on bench overnight to remove excess water.

For the characterization, the nodules at the centre of the Melinex disc (36 mm² square-shaped area) were assessed with Nexview-NX2 3D optical interferometer(Zygo, Middlefield, CT, USA) using 2.75X objective lenses, 0.5X zoom and a scan length of 145 µM. The height and area were analysed in Mx software and ImageJ, respectively.

3.13 Statistical analysis

The study's data was obtained from experiments conducted at least thrice, with the number of data points (n) indicated in Fig legends. The mean \pm standard deviation (SD) was used to express the data, and GraphPad Prism 9 software (GraphPad, CA, USA) was utilized for statistical analysis. Significance between conditions was determined via different statistical approaches: Student's-t-test with Welch's corrections was used for two data sets, while one-way ANOVA and Holm-Sidak's multiple comparisons test were used for more than two data sets. Significance levels were expressed as p < 0.05 (*), p < 0.01 (***), and p < 0.001 (****), with p-values less than 0.001 (****) considered extremely significant (Table 3.2).

Table 3.2 Star symbols for specific statistical meanings.

- ,		J	
Symbol	Statistical meaning	Statistical meaning	
ns	P>0.05		
*	P<0.05		
**	P<0.01		
***	P<0.001		
***	P<0.0001		

Chapter 4 Osteoblast response to BP

4.1 Introduction

BRONJ and OB studies

Since the first case series on BRONJ was reported in 2003 [449], research in BRONJ is increasing, mirroring the increased use of BPs (e.g. from 2.1% to 9.7% in postmenopausal women from 1993-1998 in US) [450] and incidences of BRONJ (ranging from 0.8% to 12%) [451]. As the clinical use of BPs is to inhibit OC function, it is unsurprising that the majority of both *in vivo* and *in vitro* studies have focused on their interaction with OC (Fig 4.1 A). There is, however, increasing realisation that other cells such as OB may also be important in the response to BPs and may be causing osteonecrosis. As can be seen in Fig 4.1 B, the rate of papers on BPs and OBs is increasing rapidly.

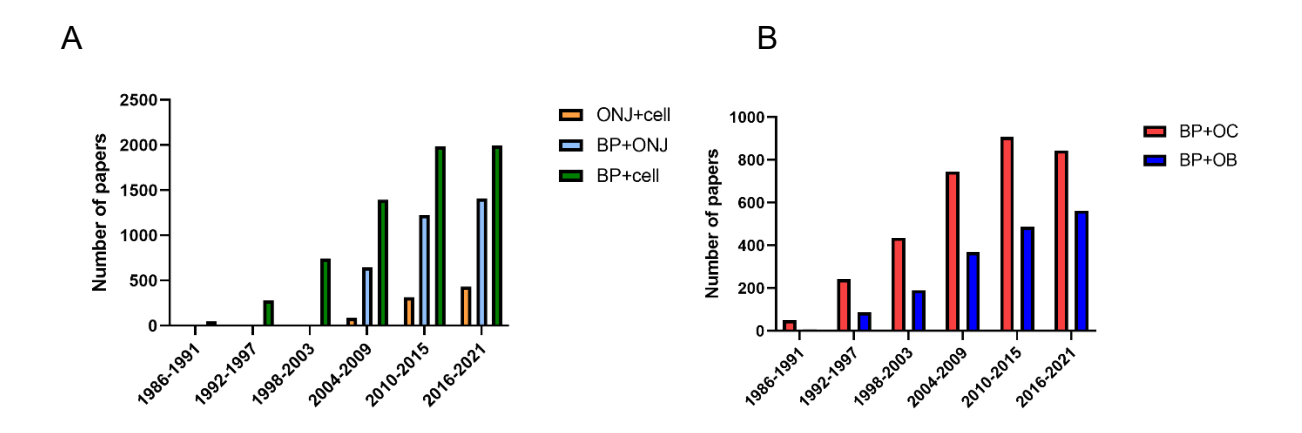


Fig 4.1. Quantity of research papers on the topic of BP, osteonecrosis of the jaw (ONJ) and cells*3. Since 1986, there has been a noticeable increase in research papers focusing on BP. However, it was not until 2004 that papers specifically studying ONJ started to gain attention (A). There are more studies focused on OC response to BPs compared to OB response to BPs, but the difference is reducing in recent years, which indicates the realisation of the importance of OBs in ONJ (B).

Research has shown that OB mineralisation can be inhibited by ZA after 14 days' culture *in vitro* [452], but little is known about the exact mechanism of BP on OB.

^{**}Web of science database has been searched to get an overview of this research field. From 1983 to 2015, the results of searching strategy "bisphosphonate" (Topic) AND cell (Topic) or "in vitro" (Topic)".

Inducing apoptosis (non-N-BP) and the inhibiting mevalonate pathway (N-BP), are the two pathways reported to cause toxicity in OCs response to BP (explained in chapter 4, Introduction part), and this may also be valid in OBs [453]. Another study has also suggested that non-N-BP can induce apoptosis in OBs but it is not clear whether it has followed the same mitochondrial pathway as OC or not [454]. N-BP is also associated with the mevalonate pathway inside OB metabolism. As a mevalonate pathway activator, geranylgeraniol (GGOH) has been proved to be able to restore ZA-induced inhibition of cell viability [453, 455]. Besides cellular metabolic activity, various other pathways have been suggested to play a role in the inhibition of bone formation in response to BPs. These include inhibited OB differentiation [21], reduced VEGF production [22, 23], elevated oxidative stress [456], as well as inflammation responses [437]. Therefore, it's essential to understand the exact pathways how OB response to BPs.

From in vivo to in vitro studies

Significant advances have been made in understanding BRONJ, but its pathophysiology remains incompletely understood. Whilst *in vivo* BRONJ models provide an understanding of connected systemic effects, the complex, multiparameter nature means that the understanding of BPs interactions with individual cells is more difficult. *In vitro* studies offer an isolated environment, removing the complexity of entire organism physiology, and simplifying the direct cause-and-effect relationships. Using a systematic approach to search the literature, we undertook a systematic review to explore the specific cellular response (as discussed in chapter 2, section 2.5) to BPs. and found 34 papers that studied OBs response to BPs. Out of the 34 papers reviewed, only 21 specifically investigated OBs metabolic activity interactions with BPs (total of 263 data points). A concentration-dependent effect on OBs metabolic activity response to BP was exhibited (Fig 4.2). There were only four papers (18 data points) reporting a significant increase in metabolic activity, rather than a decrease (19 papers and 166 data points). The literature search found that the median BP concentration that caused negative outcomes (e.g. decreased cell number or metabolic activity) at

55.2 μ M was higher than the BP concentration that had no effect or an increased effect (P<0.0001) (Fig 4.2 A). There was no difference in the BP concentration, that caused positive/increased metabolic activity or proliferation and no effects. A concentration-dependent effect was also observed among different types of BPs. The BP that OBs were most tolerant of (i.e. highest median concentration that caused a negative/decreased effect) was Clo (200 μ M). ZA had the lowest reported median concentration to generate a decrease/negative response in cells (12.61 μ M) metabolic activity and proliferation suggesting that ZA is the BP with the most toxic effect on OBs. However, only ZA and Iban showed a significant difference (P<0.05) (Fig 4.2 B).

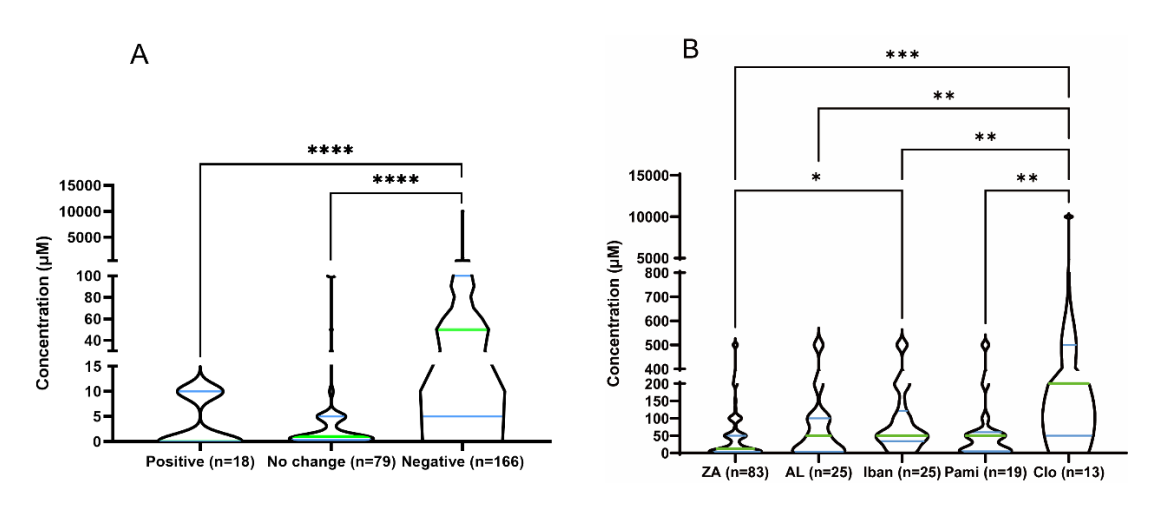


Fig 4.2 The effect of BPs on OBs metabolic activity and proliferation (A). The median BP concentration that caused decrease (55.2 μ M), p<0.0001, was significantly higher than the concentrations that caused an increase (0.1 μ M) and no change (1 μ M). (B). Non-N-BP (Clo) had higher median concentration to trigger negative response on OBs compared to N-BPs whilst ZA had the lowest. (P<0.01). (n=number of data points).

The expression of osteogenic differentiation factors, ALP, COL1, and RUNX2 have been reported to be inhibited by BPs in a concentration-dependent manner. In our literature review, 15 papers have studied RANKL and 9 papers have studied OPG (number of papers-updated) response to BPs. It was found that BPs can affect expression of these factors. Among the papers, 3/15 reported OC an increase in the osteoclast inhibiting factor RANKL by OBs, while 8/15 reported a decrease, and the remaining papers showed no change. A total of 5/9 papers showed an increase of OPG protein response to BPs and3/9 showed a decrease and the rest one showed no

significant difference. Also, in 5 papers that studied RANKL/OPG ratio, 4/5 showed an increase and 1/5 showed a decrease.

[BP] and OB differentiation factors

The median and quartile concentrations of OBs differentiation factors are presented in Table 4.1. For ALP, COL1, and RUNX2, the median concentrations of BPs that led to an increase were 0.001, 2, and 50 µM, respectively, which were lower than the concentrations causing a decrease, at 5, 100, and 100 µM, respectively. However, for OCN, 25 µM triggered an increase while 5 µM triggered a decrease. While numerous genes and proteins associated with various pathways have been examined, only a single study conducted a rescue experiment to validate the involvement of a specific pathway. In this study, Feng Gao et al [457] evaluated OB differentiation response to ZA. They discovered that differentiation was partially restored upon addition of Rapamycin , an inhibitor specific to mTORC1. This finding suggests a potential role of the mTORC1 pathway in this context.

Table 4.1 Median concentration (μM) of BPs reported to cause significant changes in OB differentiation factor expression.

	Increase (Quartile)	No change (Quartile)	Decrease (Quartile)
ALP	0.001 (1 × 10^-6, 0.01)	0.55 (0. 001,\ ' 456+51)	5 (1, 100)
COL1	2 (1, 50)	N/A	100 (1, 100)
RUNX2	50 (0.01, 50)	0.5 (0.01, 5)	100 (1, 1000)
OCN	25 (1 × 10^-6, 50)	0.5 (1 × 10^-6, 1.5)	5 (1, 1000)
RANKL	50 (5, 50)	5 (5, 10)	100 (1, 1 × 10^4)
OPG	50 (0.01, 3775)	5 (0.5, 10)	5 (0.01, 1 × 10 ⁴)

^{*}Unit: µM

4.2 Investigating OBs responses to BPs: Methodological approaches

A key novelty of the research presented in this chapter is the use of a primary bone cell model of bone formation over 21 days. Our literature review showed that only 2

out of 123 studies cultured OB longer than 14 days. In a study, Acil et al. evaluated the viability and inflammatory cytokine expression of ZA treated HOB, gingival fibroblasts, and SaOs-2 over a period of 28 days. However, they did not provide any data on mineralization [437]. Moreover, Borsani et al. conducted a cultured of HOB treated with ZA and AL for up to 21 days using lizarin red staining. Despite this no discernible mineralisation structure could be observed from the limited images provided [423].

We also found that only 3 out of 123 studies cultured cells between 7 to 14 days. In 18 out of 21 papers investigating OBs response to BPs, 9 papers used metabolic activity with the average duration of experiment of 4.6 days bone differentiation factors were studied. Besides, we selected ZA and AL as they are commonly used clinically [53] and are the most commonly studied (in our literature search ZA was used in 78/123 papers and AL in 36/123 papers).

The size and number of *in vitro* bone nodules revealed the extent of tissue engineered bone forming. To characterise these nodules, calcium (Alizarin red) and phosphate (Von Kossa) staining were often performed. In our literature review, 13 out of 21 papers used Alizarin red staining, and 3 out of 21 used Von Kossa staining to investigate the calcium deposited after BP intervention. However, staining alone cannot distinguish between mineral deposits and mineralised collagen fibre cells [458, 459]. Tissues other than bone can also generate calcification, but without ordered mineralisation of collagen fibres extracellularly [27-29]. Abnormal tissue calcification has less organised crystalline organisation compared to mature lamellar bone and does not interact with collagen fibres in an ordered manner [460, 461]. Zafar, S et al. did TEM on ZA treated fibroblasts, which revealed that cells in the presence of ZA showed irregularly shaped nuclei, dilated normal rough endoplasmic reticulum, and numerous vacuoles [462]. However, to our knowledge, no ultrastructure analysis has been performed on BP treated OB.

4.3 Chapter aims

1. To investigate the effects of ZA and AL on OB proliferation, metabolic activity and

in vitro bone nodule formation.

2. To investigate the effects of ZA and AL on the ROS production of OBs.

4.4 Testable null hypotheses

- 1. ZA and AL do not affect the proliferation and metabolic activity of SaOs-2 cells.
- 2. ZA and AL do not affect the ROS production of SaOs-2 cells.
- 3. ZA does not affect the rat OBs, ALP, VEGF and bone nodule formation.

4.5 Methods and materials

Based on Scheper et al.'s model, the appropriate ZA concentration in BRONJ bone tissue ranges from 0.4 to 4.6 μ M [463]. Alfredo et. al also provided an approach using ultra performance liquid chromatography coupled to tandem mass spectrometry, and found the ZA concentration in BRONJ patients' bone ranges from 10^-3 to 9.4^10-3 μ M [464]. In here, SaOs-2 cell-line and primary rat OBs were cultured as described in Chapter 2 (Section 2.1.1). Briefly, SaOs-2 cells were treated with either 0.067, 0.2, 0.6, or 1.8 μ M of ZA or AL and kept in an incubator at 20% O2. The metabolic activity and proliferation rate were measured on days 1, 3, and 7. ROS production was measured with 0.067, 0.2 or 1.8 μ M of ZA or AL treatment, at time point of days one, three, and seven.

Primary rat OBs were cultured as described in Chapter 2 (Section 2.1.2). Briefly, cells were treated with either 0.067, 0.2 or 1.8 μM of ZA and kept in an incubator at 20% O₂. Due to the limited number of cells obtained from calvarial bone, a reduction in the number of variables was required, which led to the omission of the 0.6 μM concentration. ALP activity and VEGF expression of the cells were measured on day 1 and 7. Bone nodules were further characterised using Alizarin red calcium staining and interferometry on day 21.

4.6 Results

4.6.1 The effect of ZA on SaOs-2 cells metabolic activity and proliferation

Higher dose of ZA exhibited inhibition of metabolic activity and proliferation of SaOs-2

cells while lower dose did not. Specifically, ZA at concentration of 1.8 μ M decreased the metabolic activity from day 3 (P<0.05) compared to the control (no treatment) and also showed a decrease from day 3 to day 7. Whereas, ZA at concentrations of 0.067, 0.2 and 0.6 μ M did not change the metabolic activity significantly (Fig 3.3). In a similar manner to the metabolic activity, ZA 0.067, 0.2 and 0.6 μ M did not change the DNA concentration or proliferation rate compared to the control. However, ZA 1.8 μ M decreased DNA concentration and proliferation compared to the control at all time points (P<0.001).

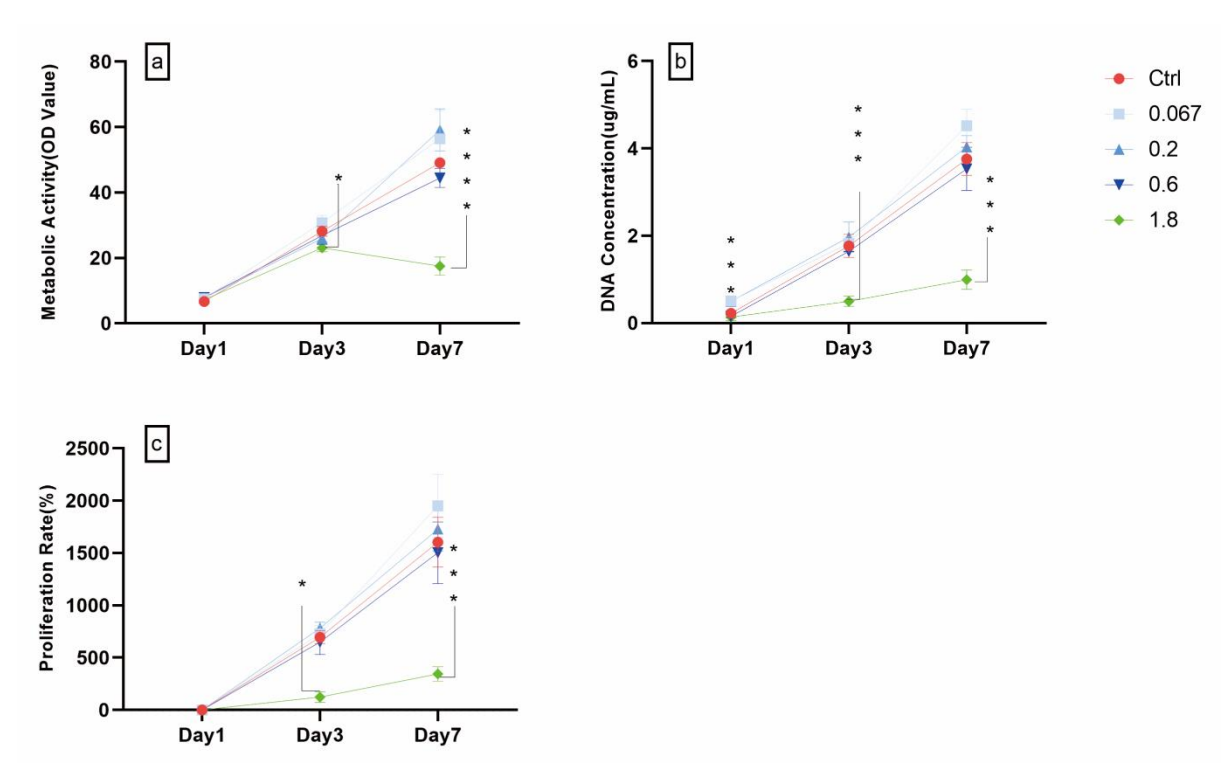


Fig 4.3 The effect of ZA on metabolic activity and proliferation of SaOs-2 cells. ZA concentrations below 1.8 μ M did not affect a) metabolic activity. b) proliferation and c) proliferation rate. Values are mean \pm SD; n= 5. * P<0.05, *** P<0.001, **** P<0.0001.

4.6.2 The effect of AL on SaOs-2 cells metabolic activity and proliferation

Similarly, AL 1.8 uM exhibited a significant decrease in metabolic activity on day 3 compared to the control group. Lower concentrations of AL did not have a noticeable impact on metabolic activity. AL 1.8 uM also led to a significant reduction in proliferation compared to the control. This effect closely resembled the results observed with ZA 1.8 uM, indicating similarities between the two BPs in terms of inhibiting proliferation

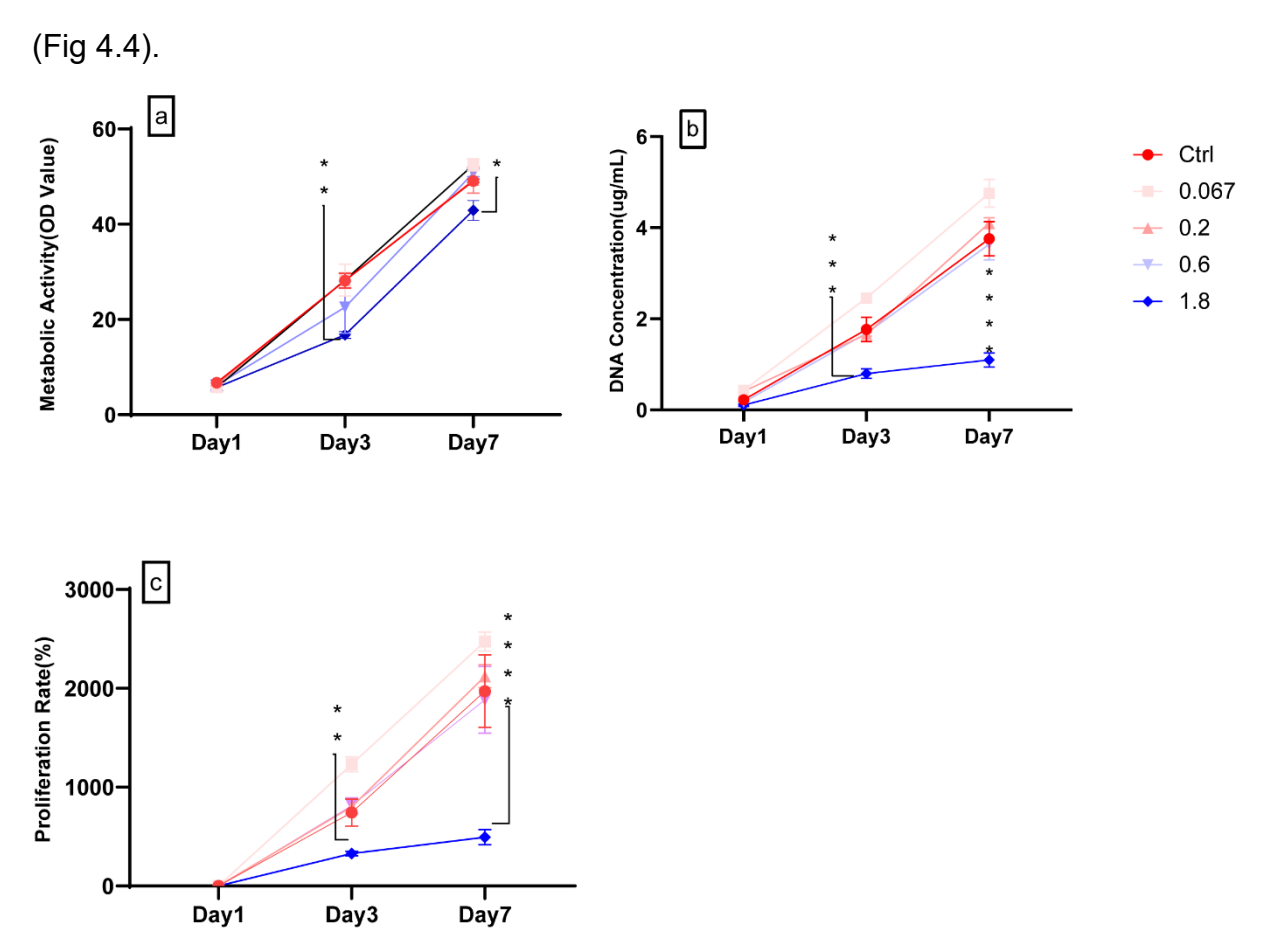


Fig 4.4 The effect of AL on metabolic activity and proliferation of SaOs-2 cells. Concentrations below 1.8 μ M AL did not affect a) metabolic activity, b) proliferation and c) proliferation rate. Whilst AL 1.8 μ M inhibited metabolic activity on both day 3 and day 7, cell number and proliferation rate (P<0.0001). Values are mean \pm SD; n= 5. **** P<0.0001, *** P<0.001.

4.6.3 The effect of ZA on SaOs-2 cells ROS production

To evaluate the oxidative stress induced by BPs, ROS production of ZA treated SaOs-2 cells was measured. The results were normalised to the fold of untreated cells (control). It can be observed that the ROS production was promoted by ZA. The total ROS production was increased by 0.067, 0.2, and 1.8 μ M ZA on day 1 (P<0.0001) and day 3 (P<0.01, P<0.0001, respectively). A concentration dependent manner was exhibited at day one and day three. At day seven, 0.067 and 0.2 μ M ZA increased the total ROS production (P<0.01) but not the 1.8 μ M ZA (Fig 4.5a).

After normalisation with the DNA concentration, a similar trend was observed. All concentrations ZA increased ROS production per unit DNA at day one (P<0.001), day

three (P<0.001) and day seven (P<0.01 (0.067 and 0.2 μ M), P<0.001 (1.8 μ M), respectively). A concentration dependent manner was observed at day three (Fig 3.5b).

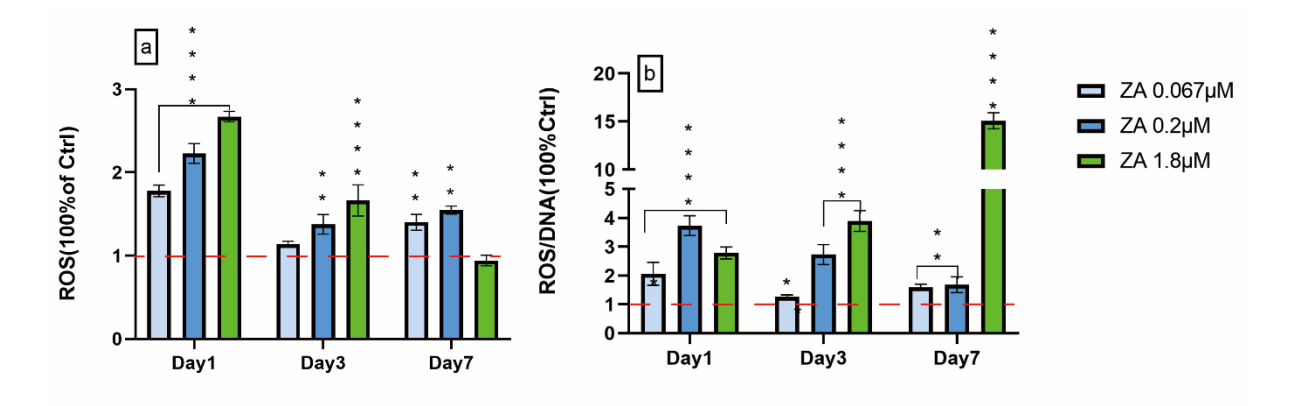


Fig 4.5 The effect of ZA on ROS production of SaOs-2cells. Concentrations below 1.8 μ M ZA increased total ROS (a) and ROS per unit DNA (b). Whilst a concentrations at 1.8 μ M did not affect total ROS at day seven. Values are mean \pm SD; n= 5. Red dotted line: control. **** P < 0.0001, *** P < 0.001, ***, P < 0.01.

4.6.4 The effect of AL on SaOs-2 ROS production

Similarly, ROS production was elevated by AL. At day one, the total ROS production was increased by 0.067, 0.2, and 1.8 μ M AL (P<0.0001) and a dose dependent manner was observed. At day three, only 1.8 μ M AL (P<0.01) increased the total ROS production and none of the three concentrations has induced an increase at day seven (Fig 4.6a). For ROS production per unit DNA, all concentrations AL had an increase at days one, three and seven. At day one, 0.067, 0.2 and 1.8 μ M AL increased the ROS per unit DNA to two-fold onwards (P<0.0001). At day three, 0.067 (P<0.01), 0.2 (P<0.0001) and 1.8 (P<0.0001) μ M AL increased ROS per unit DNA but no more than two-fold. At day seven, 0.067 and 0.2 μ M AL (P<0.0001) increased ROS per unit DNA to two-fold onward, while 1.8 μ M AL (P<0.001) also made an increase lower than two-fold (Fig 4.6b).

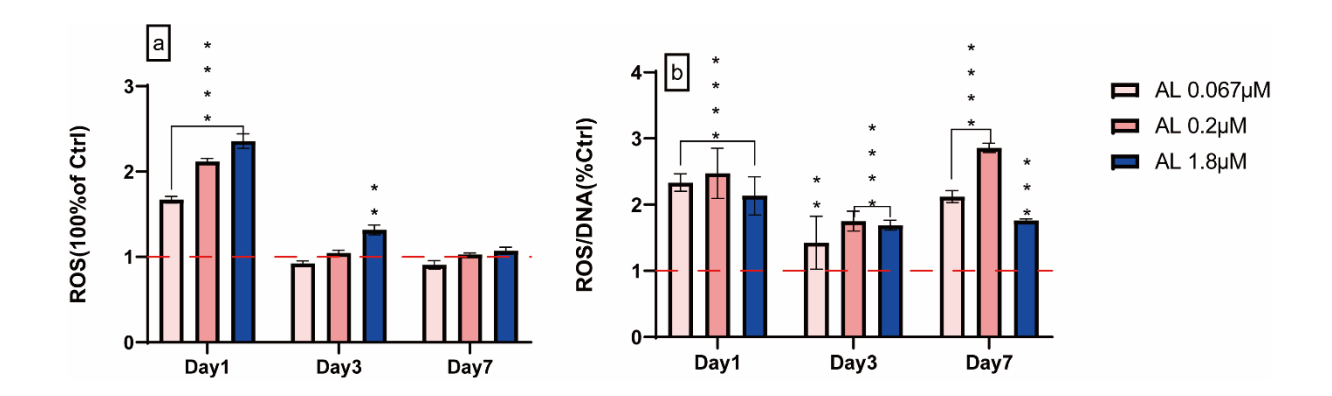
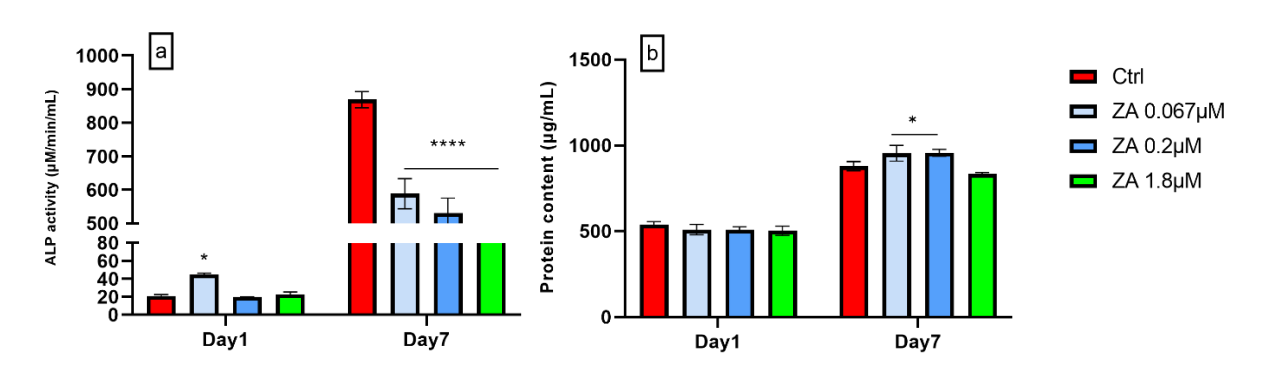


Fig 4.6 The effect of AL on ROS production of SaOs-2 cells. a) All concentrations AL increased total ROS production at day one (P<0.0001). AL 1.8 μ M increased ROS at day three (P<0.01). b) All concentrations AL increased ROS per unit DAN. Values are mean \pm SD; n= 5. Red dotted line: control. **** P < 0.0001, *** P< 0.001.

4.6.5 The effect of ZA on OB ALP production

ZA exhibited an inhibitory effect on ALP production, which is an early differentiation marker of OB. At day one, 0.067 μ M ZA increased (P<0.05) total ALP production while 0.2 and 1.8 μ M ZA did not make any change. At day seven, all concentrations of ZA decreased (P<0.0001) total ALP production and a concentration dependent manner was observed (Fig 4.7a). Protein content was also measured at day one and day seven. At day one, there was no difference of all concentrations ZA, and at day seven, 0.067 and 0.2 μ M ZA exhibited an increase (P<0.05) (Fig 4.7b). Normalised ALP production per unit protein showed 0.067 and 1.8 μ M ZA increased (P<0.0001, P<0.05, respectively) the normalized ALP activity at day one. At day seven, all concentrations ZA showed a decrease (P<0.0001) with a concentration dependent manner (Fig 4.7c).



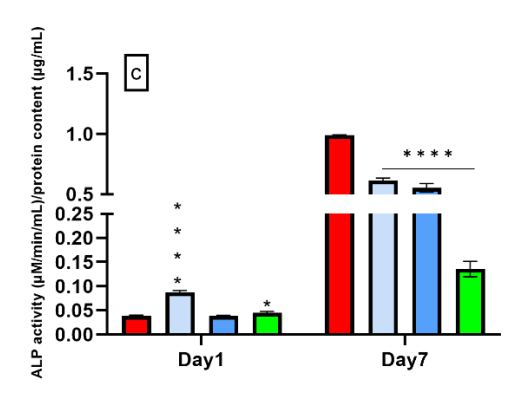
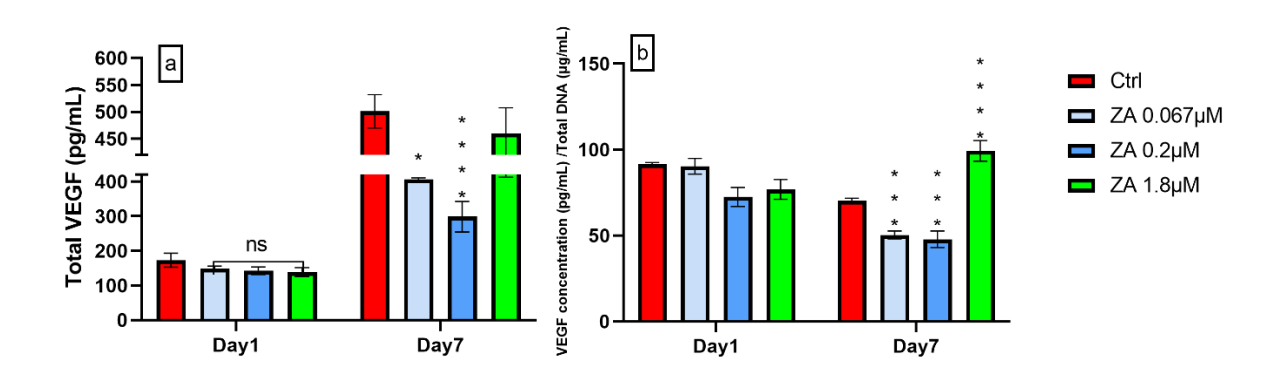


Fig 4.7 ALP production of ZA treated primary OB. a) ZA 0.067 μM increased total ALP production at day one. All concentrations ZA decreased total ALP at day seven (P<0.0001). b) ZA 0.2 and 1.8 μM increased protein content at day seven (P<0.05). c) ZA 0.067 and 1.8 μM increased ALP per unit protein content at day one. All concentrations ZA decreased ALP per unit protein content at day seven. Values are mean \pm SD; n= 5. **** P < 0.0001, *** P< 0.001.

4.6.6 The effect of ZA on OB VEGF production

Also, ZA affected VEGF production, indicating its involvement in angiogenesis activity. At day1, 0.067, 0.2 and 1.8 μ M ZA did not change the total VEGF production or VEGF per unit DNA. However, at day7, both total VEGF and VEGF per unit DNA were decreased by 0.067 (P<0.05, P<0.0.001, total VEGF and normalized VEGF respectively) and 0.2 μ M ZA (P<0.0001, P<0.01, total VEGF and normalized VEGF respectively). And at day7, VEGF per unit DNA was increased by 1.8 μ M ZA (P<0.0001), and DNA concentration was decreased by 0.2 and 1.8 μ M ZA(Fig 4.8a and 4.8b).



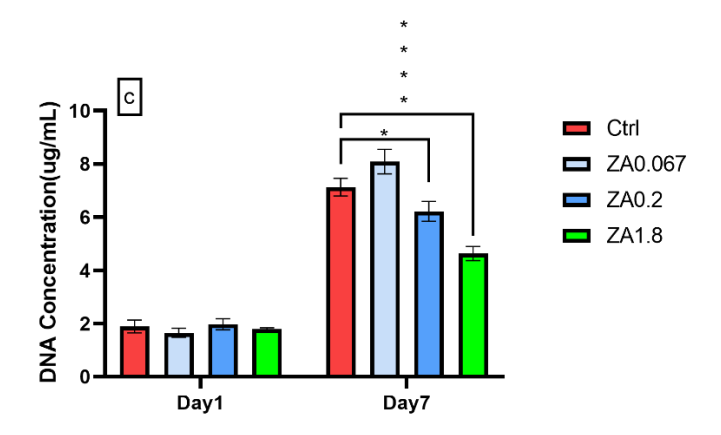


Fig 4.8 VEGF production of ZA treated primary OB. a) ZA 0.067 and 0.2 μ M decreased total VEGF at day 7. b) ZA 0.067 and 0.2 μ M decreased VEGF per unit DNA at day 7 while 1.8 μ M ZA increased VEGF per unit DNA. c). ZA 0.2 and 1.8 μ M decreased DNA concentration at day 7. Values are mean \pm SD; n= 5. **** P < 0.0001, *** P< 0.001.

4.6.7 ZA effect on bone nodule formation

ZA was shown to inhibit bone formation. Widespread mature mineralised nodules were formed in control conditions without ZA. Whilst, ZA 0.2 and 1.8 μM -treated OB showed an inhibition of bone nodule formation. ZA 0.067 μM formed fewer and smaller nodules compared to the control, while ZA 0.2 and 1.8 μM resulted in complete inhibition. Nodules in control were stained positive for Alizarin red and showed a discrete trabecular morphology. Although ZA 0.2 μM did not form mature bone structure, bright red regions confirmed the presence of calcium even in dystrophic mineralised areas. ZA 1.8 μM did not form any bone-like structures or mineralised areas. Interferometry images also confirmed presence of large dense nodules that are higher than the culture surface in control and dystrophic mineralisation in ZA 0.2 μM (Fig 4.9).

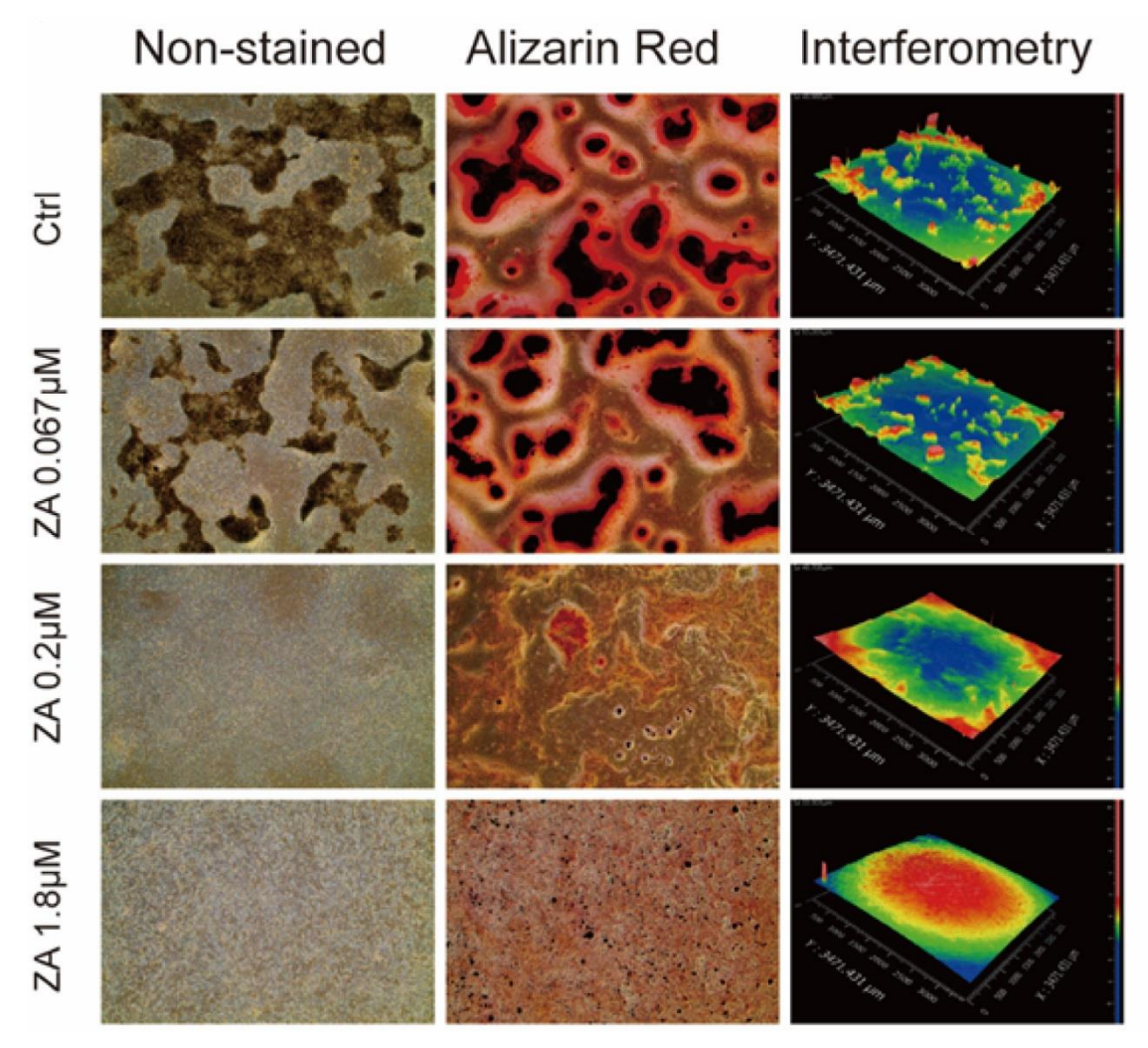


Fig 4.9 Images of bone nodules formed after 21 days' culture. The left column showed microscopic images of non- stained culture plates. There were more nodules formed at control conditions than ZA $0.067~\mu$ M. ZA 0.2 and $1.8~\mu$ M did not form any bone like structure. However, ZA $0.2~\mu$ M formed areas of dystrophic mineralisation while ZA $1.8~\mu$ M did not form any identifiable areas of mineralisation. Interferometry images showed that more and bigger nodules formed at control condition compared to ZA $0.067~\mu$ M. And ZA $0.2~and~1.8~\mu$ M presented flat surface morphologies.

4.6.8 ZA 1.8 uM inhibited Alizarin red staining areas and maximum height of bone nodules

To quantitatively measure the calcium deposition area and height, Image J software and interferometry were used. At day21, ZA 0.067μM significantly (P<0.01) increased the stained area compared to the control. ZA 0.2μM did not show significant difference compared to control while ZA 1.8μM decreased nodule formation significantly (P<0.001). A dose-dependent decrease was observed in ZA 0.067, 0.2 and 1.8μM with the increase of concentration (Fig 4.10 A). The maximum height of bone nodules was

measured by interferometry. It can be observed that ZA 0.067μM significantly increased the maximum height compared to the control. And ZA 0.2 and 1.8μM showed a significant decrease compared to the control (Fig 4.10 B).

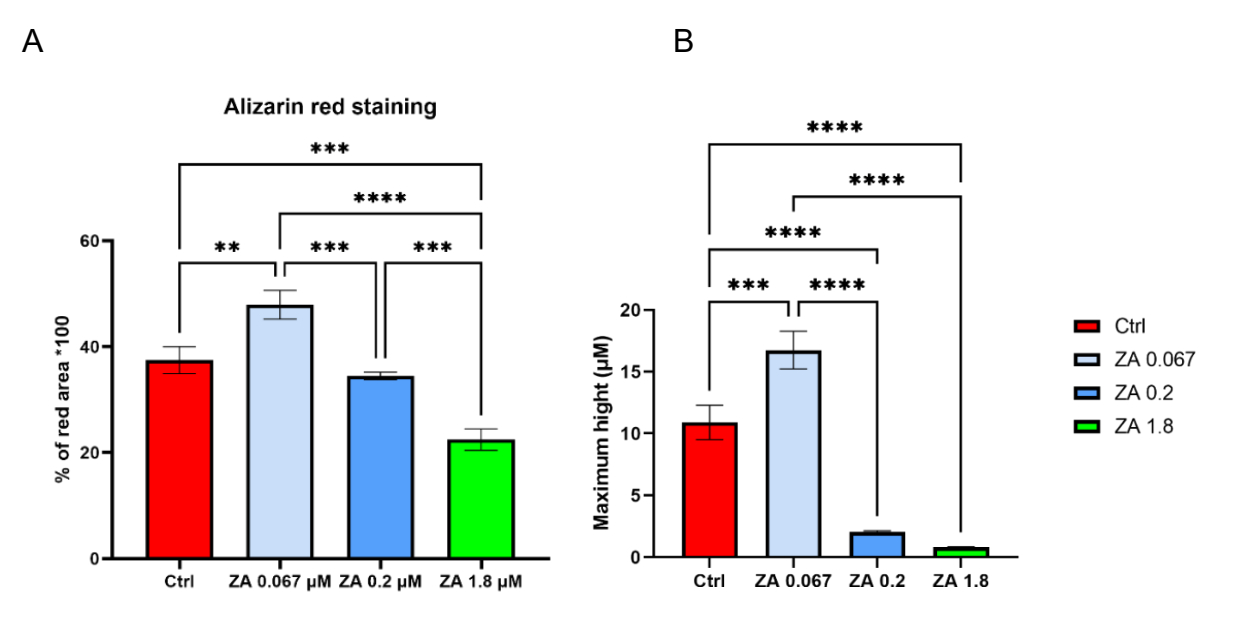


Fig 4.10 Quantitatively analysis of bone nodules. A). Alizarin red staining by Image J. The percentage of red stained area is presented. ZA 0.067 μM significantly increased the red area compared to the control, while ZA 1.8 μM showed a reduction. ZA 0.2 μM did not show significant difference compared to the control. B). Maximum height of bone nodules was measured by interferometry. Comparing to control, ZA 0.067μM generated a significant increase while ZA 0.2 and 1.8μM generated a reduction. Values are mean \pm SD; n= 5. **** P < 0.0001, *** P< 0.001.

4.7 Discussion

4.7.1 How does ZA affect OB metabolic activity and proliferation

Our results showed that ZA inhibits OB metabolic activity and DNA concentration in a dose-dependent manner. In previous research, various different approaches were used to measure metabolic activity and proliferation. However, some *in vitro* studies claimed that proliferation was measured using metabolic activity assays such as CCK8, without providing results related to DNA content or cell numbers.

Compare to the results seen in the literature (20 μ M significantly reduced the metabolic activity, Fig 2.16 A), the toxic concentrations of ZA we saw in our experiments were lower (1.8 μ M). This might have been caused by the heterogeneity of cells and different

culture times in the literature. The OB types from literature include not only immortalised SaOs-2 cells but also primary OBs from both rodent and human sources. According to our literature review, the metabolic activity and proliferation of immortalised cells were more tolerant than primary cells. And there was no significant difference between human cells and non-human cells. In addition, the culture time varied from 1-28 days.

For primary OBs, non-toxic concentrations are needed to investigate the effect of ZA on bone nodule formation and differentiation. Although the exact mechanism of how ZA affect OB metabolic activity or proliferation has not been further studied yet, the above results provided evidence to determine the threshold concentration for the following studies.

4.7.2 How AL affects OB metabolic activity and proliferation

Similar to ZA, 1.8 μ M AL also inhibited the metabolic activity, DNA concentration and proliferation rate of SaOs-2 cells from day3. Although the median concentration according to our literature review is much higher than that at 50 μ M, our experiment showed 1.8 μ M AL is already toxic to SaOs-2 cells. This may have been caused by the different cell types and culture times used in the literature, like ZA studies showed. Most previous studies used MTT assay for metabolic activity and cell number counting for proliferation. This may induce differences to our results as we use alamarBlue assay for metabolic activity and DNA concentration for proliferation. Pourgonabadi, S. et al. found 3 μ M AL significantly reduced metabolic activity of SaOs-2 cells after three days' culture but 1.5 μ M AL did not. In addition, the assay they used was MTT [465]. No study was found to use alamarBlue or DNA quantification for AL treated OBs.

4.7.3 How ZA affects OB ROS production

ZA and AL were used as the BP intervention for SaOs-2 ROS and primary OB due to its prevalence in both experimental and clinical settings. Compared to other oral BPs (AL, RISE, IBAN), intravenously administered ZA and PAMI have a higher reported incidence of MRONJ [62, 466]. Additionally, ZA was the most frequently used BP in

relevant studies reviewed, making it the most readily comparable choice for our experiment (n=83 compared to n=25 for AL).

Our results showed that ZA (0.067 to 0.6 μ M) increased both the total ROS production and ROS per unit DNA in SaOs-2 cells. An increase in ROS production was observed in dose dependent manner on day 3. There was limited data point of ROS results from our literature review, and no direct results for ROS production on BP treated OB. However, the [BP] (60 μ M) cause an overall increasing ROS was higher than our experimental results. And it can be observed that the level of ROS production is quite varied depending on the cell type. For example, De Colli et al. found 100 μ M ZA increased ROS in human gingival fibroblasts [467]. Yuan, H also found 0.1 μ M ZA could increase ROS in Raw264.7 cells [237].

4.7.4 How AL affects OB ROS production

Similar as ZA, AL increased total ROS production in a dose dependent manner. And our literature review showed that the cellular response to BP can be varied depending on the cell types, for example, the difference between oral cell and non-oral cell ROS. Taniguchi et al. exposed human periodontal ligament fibroblasts (HPdLFs) in 30 µM AL for 48 hours and the ROS level was elevated at least two-fold compared to the control group. No significant ROS generation was observed in normal human dermal fibroblasts (NHDFs) [456]. The exact way oral cells and non-oral cells perform differently is currently unknown. Vermeer, J. A. F et al. compared the response of risedronate between jaw-bone OCs and long bone OCs and the results showed that jaw-bone OCs could uptake more risedronate and presented more resistance to apoptosis compared to long bone cells [468]. Besides, to our knowledge no literature has reported the ROS level of AL treated OB. Therefore, our results can be a reference for the following studies and researchers.

4.7.5 How does ZA affects OB ALP production

ZA and AL exhibited a similar effect on metabolic activity, DNA concentration and ROS production, and SaOs-2 cells performed more sensitive to ZA. ZA was selected as the

BP intervention for SaOs-2 ROS and primary OB due to its prevalence in both experimental and clinical settings. Compared to other oral BPs (AL, RISE, IBAN), intravenously administered ZA and PAMI have a higher reported incidence of MRONJ [62, 466]. Additionally, ZA was the most frequently used BP in relevant studies reviewed, making it the most readily comparable choice for our experiment (n=83 compared to n=25 for AL).

Alkaline Phosphatase (ALP) is a key enzyme in the early stage of bone development, the ALP activity is frequently used as a marker for bone formation. We measured ALP activity on day 1 and day 7. On day1, ALP activity was elevated by ZA 0.067 µM, whilst inhibited by higher concentrations. On day 7, ALP activity was significantly reduced by ZA, both total and normalized ones. For the higher concentration, it might be caused by the direct toxic effect (inducing OB apoptosis). For the lower concentrations, it might be related to the inhibition of OB differentiation. That is to say, ZA can affect OB differentiation directly.

Literature showed the median concentration of BPs to inhibit ALP activity was 5 μ M, which is higher than our result. However, this median includes all types of BP and various types of cells. The heterogeneity of BPs and cells may induce different results. For a late response in OB differentiation, examination of bone nodule formation is the tactic. The calcification is measured using Alizarin red staining and then characterisation of the nodule can follow.

4.7.6 How ZA affects OB angiogenic response?

Generally, BP has an inhibition effect on angiogenesis. ZA decreased VEGF production, both in terms of the total amount and per cell. This may be due to ROS induced pathways. Our research demonstrated in SaOs-2 cells that ZA increased ROS production, and others have also reported that ZA increases ROS in primary cells [469] and immortalized cells [470]. Other researchers have also reported that BPs can affect VEGF production. According our literature research, the median [BP] increase VEGF was 70 μM and decrease was 1 μM (Fig 1.20 A). Interestingly, previous research has shown that ROS induces VEGF expression in macrophage [469], endothelial cells

4.7.7 How ZA affects OB bone nodule formation

To our knowledge this is the 1st report of the quantitative effects of ZA on bone nodule formation *in vitro*. ZA was demonstrated to inhibit bone formation in a concentration manner above 0.2 μM, but interestingly low levels of ZA (0.067 μM) increase the volume and height of the bone nodules. This is consistence with the clinical effect of ZA, which can increase bone mineral density [473, 474]. Research showed that ZA cannot only inhibit OC activity, but also enhance OB differentiation to stimulate bone forming *in vivo* [475, 476].

The increase in bone nodule formation may be linked to the increased proliferation and ALP at day 1 in our experiments with 0.067 µM ZA. Whilst it is believed that the in vivo increase BMD is primarily due to OC inhibition, our results also suggest that increased calcium deposition may also occur via OBs exposed to low levels of ZA. According to our literature review, BP can increase osteogenic factors at some time points. For example, Rise 0.05 µM, ZA 0.01 µM, AL 0.01 µM and Iban 50 µM can increase RUNX2 and BMP2 gene expression [477, 478]. And 0.001 µM ZA increased OCN gene expression and protein [429]. Also, 1 µM AL [479], 50 µM Iban and Clo [480] increased COL1 gene expression. These findings showed that a relatively low concentration can increase osteogenic differentiation to some extent, which may have contributed to the increased bone formation. ZA concentration above 0.2 µM decreased in vitro bone nodule formation. According to our results, the mechanism can be considered as the inhibition of ALP and VEGF production as well as the increase of ROS production. This is consistent with our literature, which reminds us that BP can inhibit OB functions including osteogenic differentiation and the increase of oxidative stress. The actual concentration of BP in the human body is difficult to measure, as BP chelates to HA individually, and invasive intervention cannot be applied. Theoretically, the in vivo concentration of BP can be measured on an animal model, via resection of the model bone. However, no such study has been performed so far.

4.7.8 How do ZA and AL potentially affect other types of cells?

As mentioned in the above sections, ZA and AL have been shown to significantly inhibit the metabolic activity, proliferation, and differentiation of OB, while increasing ROS production. ZA exhibits greater toxicity on OB compared to AL, possibly due to its more efficient binding with OB or its longer duration of effective action. Similarly, both ZA and AL have been found to inhibit cell differentiation in various other types of cells, including endothelial cells, fibroblasts, and stem cells (Chapter 1, section 1.5). Regarding OC, the specific mechanisms of how N-BP and Non-N-BP work at the cellular level have been studied for years. However, the exact *in vitro* concentrations required to trigger negative effects remain to be investigated. To determine the concentration range of BPs for subsequent studies, the response of OC to ZA and AL will be investigated in Chapter 5.

Chapter 5 Osteoclast response to BP

5.1 Introduction

Numerous types of cells *in vitro*, both bone cells and non-bone cells, are affected by BP. Our literature review (chapter 2) revealed that 13% of studied cells investigated OC and macrophages. As a bone destructive cell, OC plays a vital role in bone remodelling. BP can either kill OC via direct toxicity (Non-N-BP) or inhibit them by blocking the mevalonate pathway (N-BP) [52, 53]. Whether killed or inhibited, the damaged OC induces the delay of the turnover of bone and is considered to be a major cause of BRONJ. Owing to the dysfunctional degradation of OC, normal bone remodelling is disrupted, and studies have found OC inhibition played central role of the necrosis [63].

OC differentiation

OC differentiates from the monocyte/macrophage lineage. The pluripotent haematopoietic stem cell located inside bone marrow gives rise to the colony forming unit-monocyte (CFU-M) inside the marrow. CFU-M is a progenitor of the monocyte precursor. Once monocytes are released into the blood stream, they move to bony tissue and transform into mononuclear OC. Finally, the mononuclear OC fuses to multi-nucleated OC, which resorbing bone (Fig 5.1.a) [481, 482].

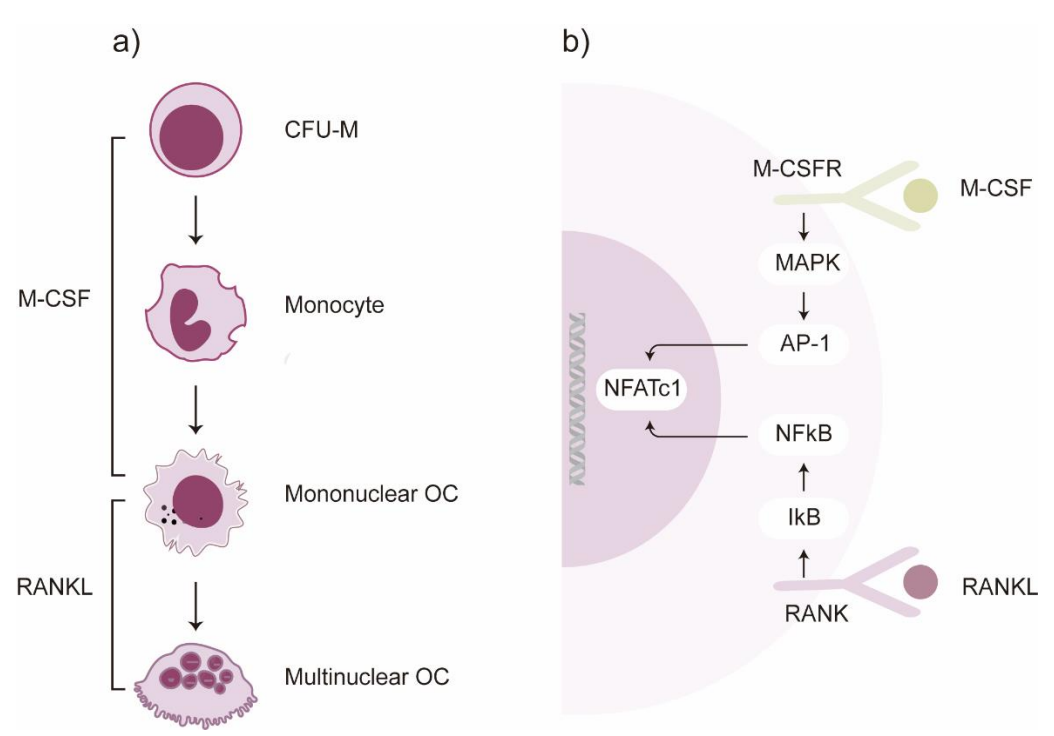


Fig 5.1. The process of OC formation. a. OC differentiation factors. OC originates from CFU-M, which is formed due to the release of monocyte-colony stimulating factor (M-CSF). CFU-M first differentiates to a monocyte, which further differentiates to mononuclear OC. b. The combination of M-CSF and M-CSFR activates the MAPK pathway and AP-1, therefore inducing NFATc1 activation and stimulating the formation and proliferation of pre-OCs. RANKL activates NFκB via its receptor and leads to the expression of NFATc1. OC, osteoclast; CFU-M, colony forming unit-monocyte; M-CSF, monocyte-colony stimulating factor; M-CSFR, monocyte colony stimulating factor receptor.

Osteoclastogenesis is supported by two major regulators, namely monocyte-colony stimulating factor (M-CSF) for the initial process and the receptor activating NFkB (RANKL) for the subsequent differentiation (Fig 4.1.b). M-CSF binds to its receptor (M-CSFR) and activates the activator protein-1 (AP-1) by triggering the mitogen activated protein kinase (MAPK) phosphorylation cascade, which induces cell proliferation. Thereafter, RANKL binds to its receptor RANK and activates the nuclear factors of activated T-cells cytoplasmic 1 (NFATc1), which is the main regulator of OC transcription factors, and triggers the formation of mature OC [483, 484]. These factors include dendritic cell-specific transmembrane protein (DC-STAMP), H+ATPase, TRAP, cathepsin K (CSTK), and matrix-metallo-protease 9 (MMP9). DC-STAMP regulates cell fusion and the formation of multi-nucleated OCs, H+ATPase, and TRAP facilitate the degradation of the inorganic component of bones, and CSTK and MMP9 are

responsible for the degradation of the organic component of bones [485, 486].

OC interacts with OB via a complex network, and the RANK/RANKL/OPG system forms one of the most vital pathways of this network. OB produces both RANKL and OPG, which can competitively trigger the formation or inhibition of OC. Binding of RANK to RANKL activates OC differentiation, whereas blocking of RANKL by OPG inhibits osteoclastogenesis [487].

OC and BP

As OC is the primary cell types that uptake BP continuously, it is important to have focused studies investigating the OC response to BP. In particular, the long-term effect and the crosstalk between OC and other cells involved in the bone remodelling process should be investigated.

In general, BP has a high affinity for binding with divalent metal ions, particularly calcium ions, owing to the presence of negatively charged phosphonate groups and the hydroxyl group in its side chain [52, 53, 488]. Hence, BP closely binds with the surface of HA in bony tissues; this high affinity of BP also results in its quick removal from circulation but ensures a long-term presence in the skeletal system [8]. Clinical trials have shown that the effect alendronate (AL) can be detected even five years after a one dose injection alone [9]. In humans, when the resorptive OCs are active in the bone's surface, BP is released from HA and then taken up by OC via endocytosis across the ruffled borders of OC [10].

Currently, the pathways through which OC interacts with BP have been explained, depending on the types of BP. Non-N-BPs do not have nitrogen in their side chains, resulting in a distinct pathway for OC inhibition . Non-N-BPs induce cytotoxicity in OC via a mitochondrial pathway, ultimately triggering cell apoptosis [11]. In contrast, N-BPs disturb the mevalonate pathway in OC, which prevents protein prenylation, finally resulting in cell apoptosis [52, 53] (Fig 5.2).

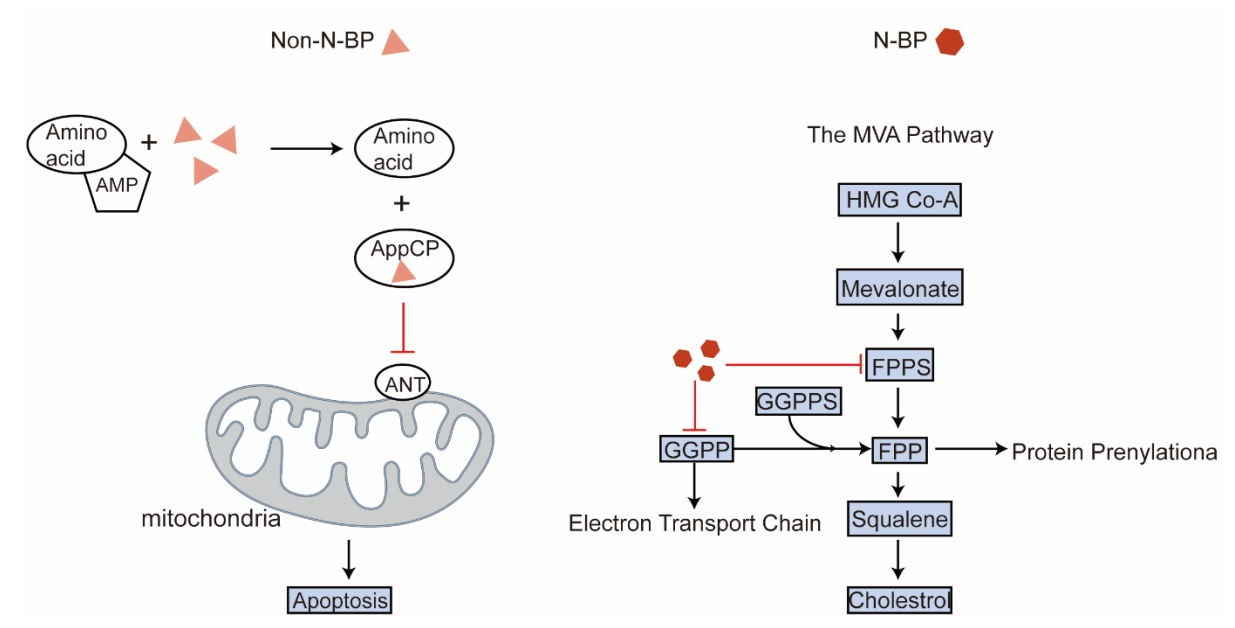


Fig 5.2. OCs response to Non-N-BP and N-BPs via two different pathways. Non-N-BP is metabolised and combines with denosine-5'-[(β , γ)-methyleno] triphosphate (AppCP), and the resulting product is toxic to the adenine nucleotide translocator (ANT) (a component of the mitochondrial permeability transition pore), thereby triggering mitochondrial permeabilisation and caspase-3 mediate apoptosis. Administration of N-BP impairs the synthesis of farnesyl diphosphate synthase (FPPS) and geranylgeranyl pyrophosphoate (GGPP) in the mevalonate pathway, which inhibits protein prenylation and cholesterol production and results in cell apoptosis.

From our literature review (Chapter 2), we collected 33 proliferation data points of OC response to all BPs (both Non-N-BP and N-BP) from 15 papers, and 127 metabolic activity data points from 18 papers. There were three data points of a positive response of OC metabolic activity or proliferation to BP, and hence, only no change and negative effects were recorded in the present study. No significant difference was observed between the BP concentration and OC proliferation. Further, the concentration of BP which caused a negative effect (10 µM) was significantly higher than no change 5 µM)P<0.01) (Fig 5.3 b). There were fewer data points about OC than OB on the BP toxicity (proliferation and metabolic activity). This may suggest that BP functions as an OC inhibitor, potentially contributing to the limited data availability. Consequently, the studies on the proliferation and metabolic activity of BP on OC provide minimal information.

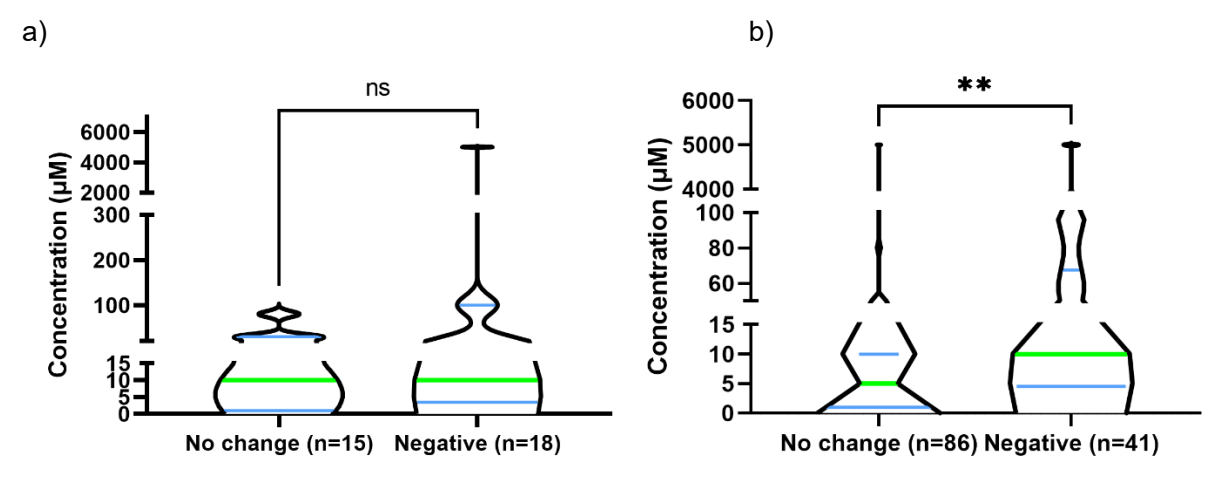


Fig 5.3. Concentration dependent response of OCs reported from the literature* BP. There was no difference in the concentration of BPs that caused a decrease in proliferation compared to the concentration reported (in the literature) to cause no change, with the medium concentration causing both a no change and increase in proliferation $\sim 10 \underline{\mu} M$ (a). A concentration dependent effect of BPs on metabolic activity was, however, observed where the mean BP concentration reported to cause a decrease in metabolic activity was higher than the BO concentration that was reported to cause no change (b) (**: P<0.01). The median concentration of no change was $5\mu M$ and for negative effect was $10\mu M$.

This chapter employed *in vitro* models to investigates the mechanism of BP interaction with OCs and their precursors. Raw264.7 cells, derived from a mouse leukaemia cell line, were used as models for both macrophage inflammatory response and OC studies [489, 490]. However, these cells exhibited considerable heterogeneity [491], posing challenges in result reproducibility across laboratories, cell batches, and experiments. For example, the OC-like precursors in Raw264.7 cells have been shown to possess varying capacities to form functional OCs [492, 493]. To address this, we screened OC subclones for macrophages and the OC studies and followed the protocol described in Chapter 2 (Section 2.3). Research within our group has also proved the homogeneity of this OC subclone and its enhanced OC-forming capacity. Both undifferentiated and differentiated Raw264.7 cells were examined.

This study represents the first investigation using the OC subclone of Raw 264.7 cells for BP study, with both differentiated and undifferentiated cells. This chapter includes assessments of proliferation, metabolic activity, ROS, TRAP5b activity, and TRAP staining to measure the BP effect on OCs.

5.2 Chapter aims

This chapter investigates the mechanisms by which ZA and AL modulate the proliferation, metabolic activity, ROS production and OC differentiation in Raw264.7 C10 cells (a OC subclone).

5.3 Testable hypotheses

- 1. ZA and AL affect the proliferation and metabolic activity of either undifferentiated or differentiated C10 cells.
- 2. ZA and AL affect the ROS production of either undifferentiated or differentiated C10 cells.
- 3. ZA and AL affect the OC differentiation (TRAP5b activity and TRAP staining) of differentiated C10 cells.

5.4 Methods and materials

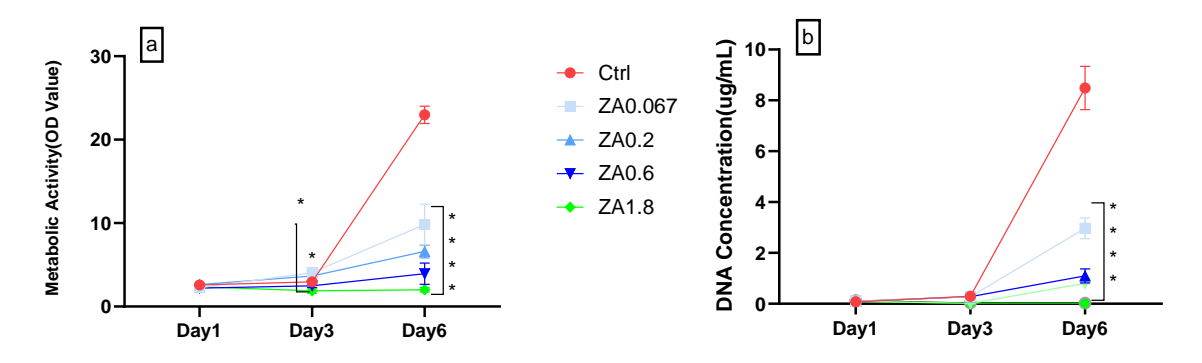
Raw264.7 macrophages and OC sub-clone C10 were cultured as described in Chapter 2 (Section 2.3). For macrophage studies, Raw264.7 cells were seeded at 3x10⁴ cells/cm² in 6 well plates. For OC studies, C10 subclone cells were seeded at 3x10⁴ cells/cm² in 6 well plate 24 hours after seeding, 3ng/ml RANKL was added to generate OC differentiation and 20ng/ml RANKL was used as a positive control.

Briefly, cells were treated with either ZA at concentrations of 0.067, 0.2, 0.6 or 1.8 μ M or AL at concentrations of 0.067, 0.2, 0.6, 1.8 or 5.4 μ M and kept in an incubator at 20% O₂. Untreated cells (without BPs) served as controls. The metabolic activity and proliferation rate were measured on days 1, 3 and 6 for both RAW cells and C10 subclone. ROS production was also measured on day 3. Additionally, TRAP 5b activity measurement and TRAP staining were performed on C10 sub-clone on day 5 (Section 2.11).

5.5 Results

5.5.1 The effect of ZA on the metabolic activity and proliferation of undifferentiated Raw264.7 cells

ZA exhibited an inhibition on cellular metabolic activity and proliferation on Raw264.7 cells. On day 3, ZA 1.8 μ M reduced metabolic activity (P < 0.05), while ZA 0.067 μ M increased metabolic activity (P < 0.05); concentrations in between did not cause any change. On day 6, all concentrations of ZA (0.067, 0.2, 0.6 and 1.8 μ M) decreased metabolic activity (P < 0.0001) compared to control. DNA concentration did not show any significant changes on days 1 and 3, irrespective of the ZA concentration. However, on day 6, the DNA concentration was significantly decreased by all concentrations of ZA (0.067, 0.2, 0.6, and 1.8 μ M) (P < 0.0001) (Fig 5.4).



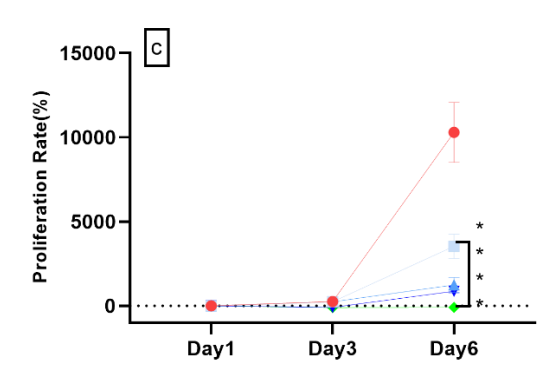


Fig 5.4 The effect of ZA on the metabolic activity and proliferation of undifferentiated Raw264.7 cells. All concentrations of ZA decreased metabolic activity (a), cell number (b) and proliferation rate (c). Metabolic activity was also decreased by 1.8 μ M ZA on Day 3.(Number of wells = 4). ctrl, control.*, P<0.05. **, P<0.01. ****, P<0.001. *****, P<0.0001.

5.5.2 The effect of AL on the metabolic activity and proliferation of undifferentiated Raw264.7 cells

Similar as ZA, AL treatment also showed a concentration dependent effect on the metabolic activity and proliferation by undifferentiated (monocyte-like) Raw264.7 cells. With concentrations of AL below 1.8µM AL not causing a decrease in metabolic activity

or proliferation (Fig 5.5). A concentration of 0.6 AL did not cause a decrease in metabolic activity or proliferation, where as a concentration of 0.6 ZA did, suggesting that ZA is more toxic to monocytic cells.

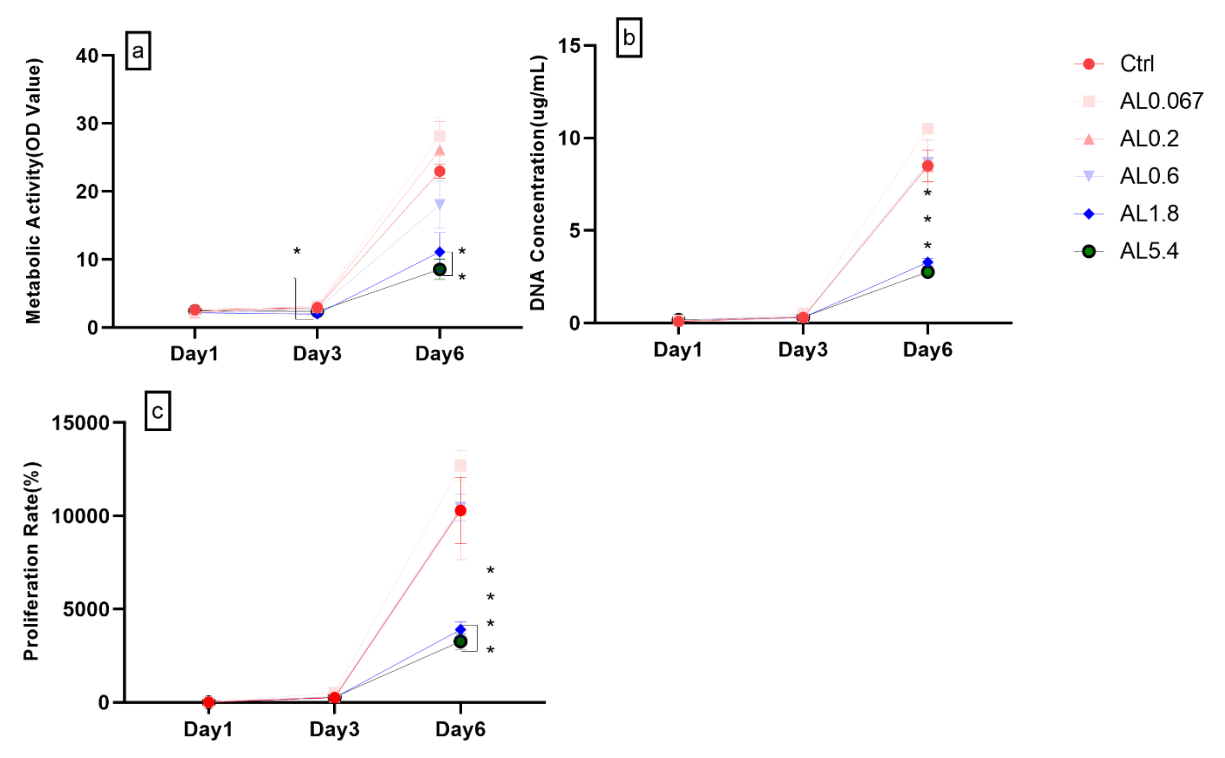
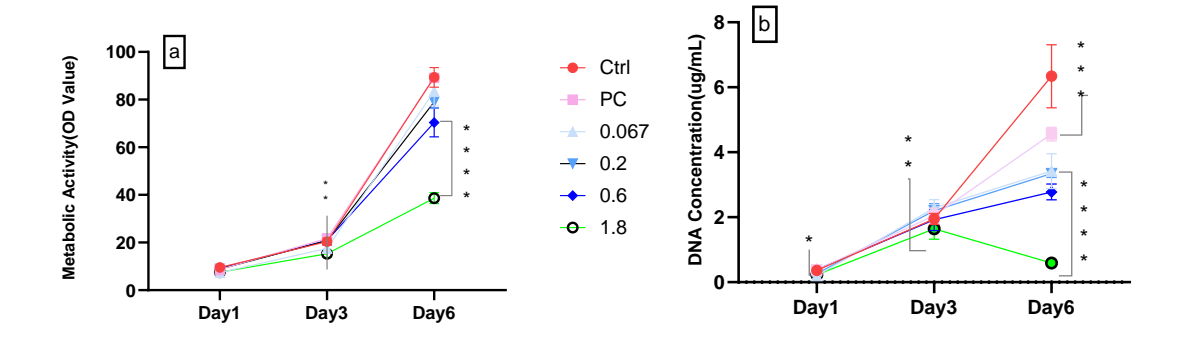


Fig 5.5 The effect of AL on the metabolic activity and proliferation of undifferentiated Raw264.7 cells. a) metabolic activity was decreased by 5.4 μ M AL on day 3 (P < 0.05) as well as by 1.8 and 5.4 μ M AL on day 6. b) DNA concentration was decreased by 1.8 and 5.4 μ M AL on day 6. c) Proliferation rate was decreased by 1.8 and 5.4 μ M AL on day 6. (Number of wells = 4). Ctrl, control. *, P<0.05. ***, P<0.01. ****, P<0.001. *****, P<0.0001.

5.5.3 The effect of ZA on the metabolic activity and proliferation of differentiated Raw264.7 cells

On day 3, a significant reduction in metabolic activity was observed only at ZA 1.8 μ M compared to the control. By day 6, this decrease extended to ZA concentrations of 1.8 μ M and 0.6 μ M. No other lower concentrations showed significant changes. On day 1, proliferation decreased at ZA concentration of 1.8 μ M compared to control. By day 3, reductions were observed at ZA concentrations of 1.8 and 0.6 μ M. By day 6, proliferation decreased across all ZA concentrations (Fig 5.6). Although all concentrations of ZA decreased proliferation on day 6, the differentiated Raw264.7 cells (OCs) showed a difference in the decreasing of metabolic activity at concentrations of 0.6 and 1.8 μ M on day 6, compared to undifferentiated Raw264.7

cells (monocyte-like cells) (0.067 μ M increased and 1.8 μ M decreased on day 3, all concentrations on day 6, Fig 5.4a). Additionally, OCs exhibited an earlier negative response in DNA concentration compared to monocytes, with 1.8 μ M on day 1, and 0.6 and 1.8 μ M on day 3, as well as all concentrations on day 6 (for monocytes, Fig 5.4b).



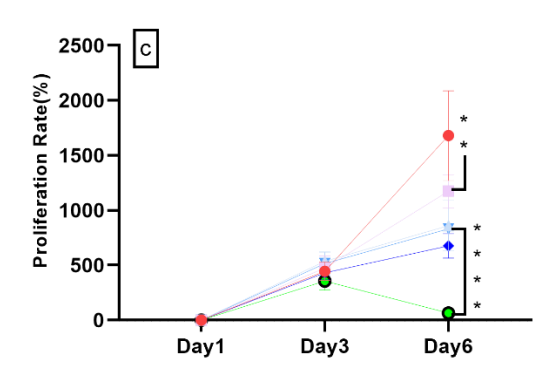


Fig 5.6 ZA inhibited the metabolic activity and proliferation of differentiated Raw264.7 cells. a) Metabolic activity was decreased by 1.8 μ M ZA on day 3, whereas it was decreased by 0.6 and 1.8 μ M ZA on day 6. b) DNA concentration was decreased by 1.8 μ M ZA on days 1, 3, and 6. All concentrations of ZA decreased DNA concentrations on day 6. c) Proliferation rate was decreased by 0.6 and 1.8 μ M ZA on day 6. (Number of wells = 4, number of experiments = 1). **, P<0.01. ***, P<0.001. ****, P<0.0001.

5.5.4 The effect of AL on the metabolic activity and proliferation of differentiated Raw264.7 cells

AL had lower concentration on the metabolic activity and proliferation of differentiated OCs (1.8 and 5.4 μ M on day 3, Fig 5.7a) compared to undifferentiated Raw264.7 monocyte-like cells (5.5 μ M on day 6, Fig 5.5a). In addition, OCs decreased the DNA concentration earlier (From day 1 upon, Fig 5.4b) compared to monocyte like cells

(Day 6, Fig 5.5b), while had a higher concentration to decrease DNA concentration or proliferation (5.4 μ M, Fig 5.7b-c) compared to monocyte-like cells (1.8 μ M, Fig 4.5b-c). Interestingly the positive control (20 μ M RANKL) also decreased proliferation and this may be due to differentiation (P < 0.001) (Fig 5.7b & c).

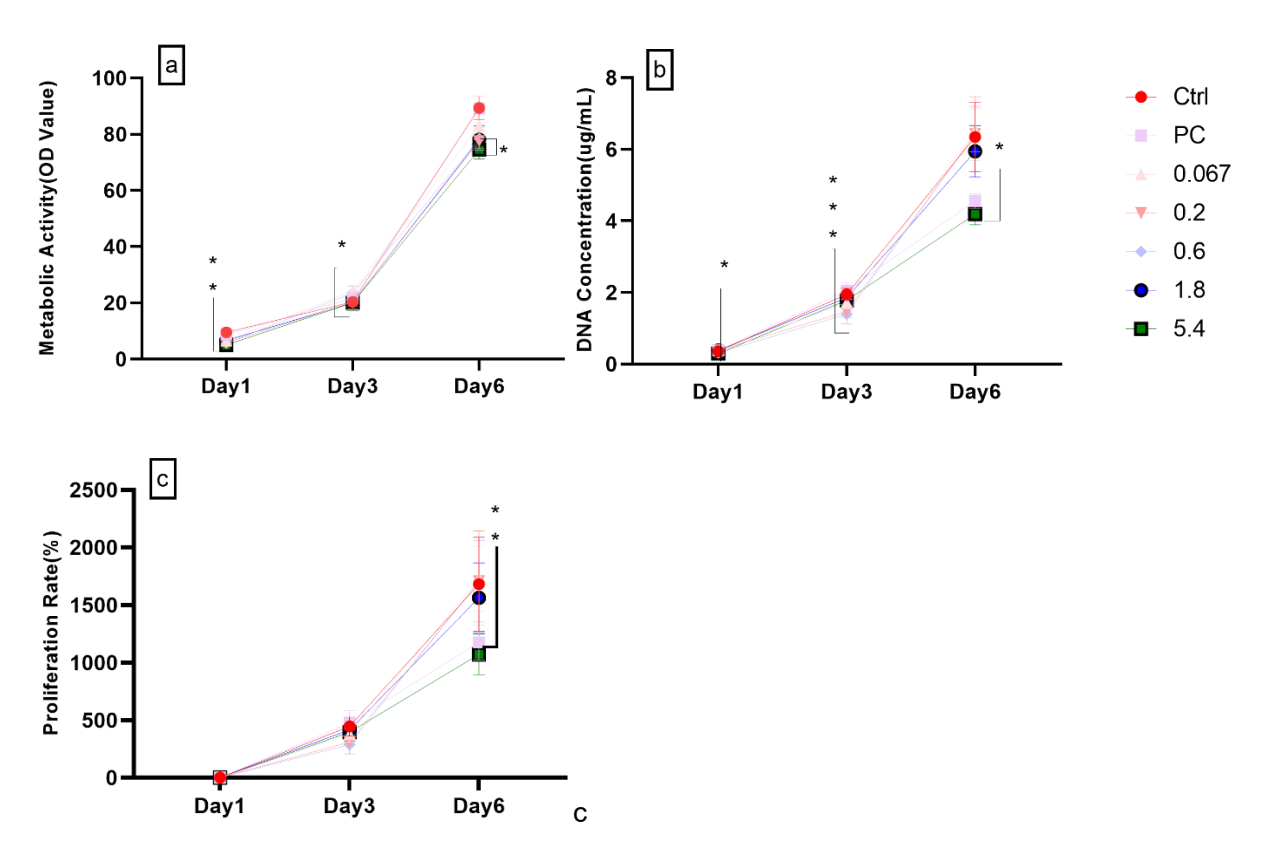


Fig 5.7 The effect of AL on the metabolic activity and proliferation of differentiated Raw264.7 cells. AL caused a decrease in OC metabolic activity by 1.8 and 5.4 μ M on days 1, 3, and 6 (a). DNA concentration was also decreased by 5.4 μ M AL decreased on days 1, 3, and 6. The positive control (20 ng/mL RANKL) also decreased DNA concentration on day 6. c) Proliferation rate was decreased by both 5.4 μ M AL and the positive control on day 6. (Number of wells = 4). ctrl, control; PC, positive control. *, P<0.05. ***, P<0.01. ****, P<0.001.

5.5.5 The effect of ZA on ROS production on undifferentiated C10 Raw264.7 cells

All concentrations of ZA (0.067, 0.2, 0.6 and 1.8 μ M) caused a significant increase in total ROS activity and per unit DNA compared to control with respective p values (P < 0.001, P < 0.0001, P < 0.05, and P < 0.001, respectively). A ZA concentration-dependent increase in ROS per unit DNA was observed (Fig 5.8).

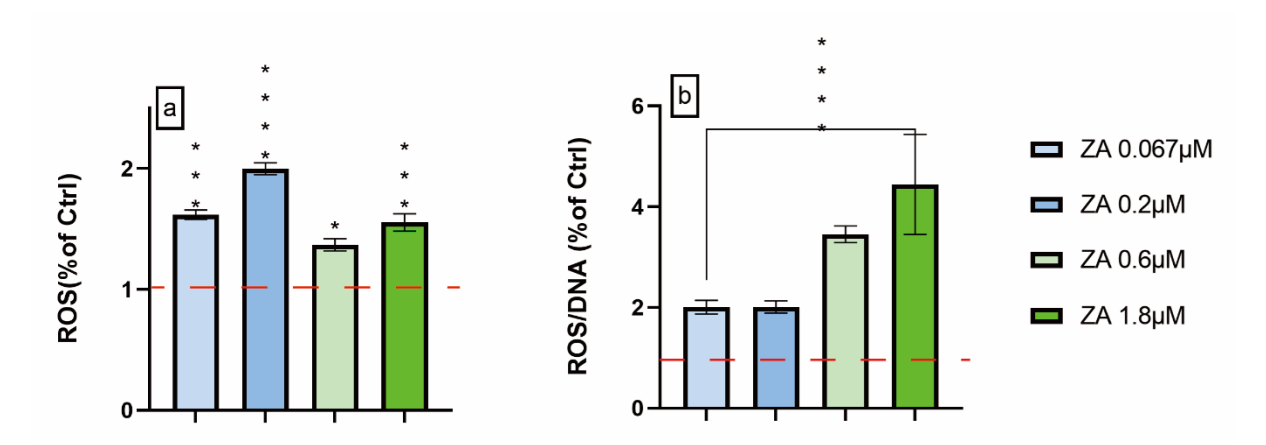


Fig 5.8 The effect of ZA on ROS production on undifferentiated RawC10 cells. All concentrations of ZA increased total ROS availability (a) and ROS availability/DNA (b). AL caused a concentration dependent increase in ROS/<u>DNA.</u> (total number of wells = 4). Red dotted line: control (untreated). *, P<0.05. ***, P<0.01. ****, P<0.001. *****, P<0.0001.

5.5.6 The effect of AL on ROS production in undifferentiated C10 Raw264.7 cells

Similarly, differences were observed between AL treated cells and control. AL at concentrations of 0.067, 0.2, 0.6 and 1.8 μ M increased both total ROS production and ROS production per unit of DNA (P < 0.0001, P < 0.0001, P < 0.0001, and P < 0.001, respectively). Compared to ZA (more than 4 fold of the control), AL (less than 2 fold of the control) triggered less ROS/DNA on the highest concentration (1.8 μ M), while similar at the lower concentrations (0.067, 0.2 and 0.6 μ M).

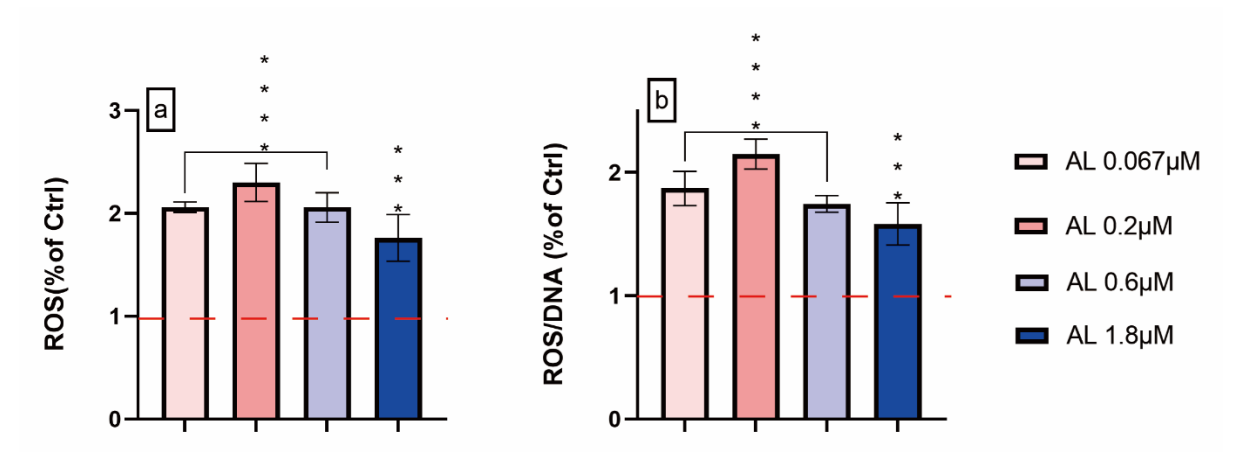


Fig 5.9 The effect of AL on ROS production in undifferentiated RawC10 cells. a) All concentrations of AL increased total ROS production). b) All concentrations of AL increased ROS per unit of DNA. (Number of wells = 4, number of experiments = 2). Red dotted line: control. ***, P<0.001. ****, P<0.0001.

5.5.7 The effect of ZA on ROS production in differentiated C10 Raw264.7 cells

To assess the oxidative stress induced by ZA, the total ROS production was measured in differentiated C10 RAW264.7 cells treated with difference concentrations of ZA (0.067, 0.2, 0.6, and 1.8 μ M). In the positive control, 20ng/ml RANKL was added. The results were normalised based on the values obtained for the control (without ZA treatment), and we compared the ROS production induced by ZA compared to that of the control. Positive control and cells treated with ZA concentrations of 0.067, 0.2 and 0.6 μ M increased the total ROS production (P < 0.01, P < 0.01, and P < 0.001, respectively), and the positive control and cells treated with 0.067, 0.2, 0.6 and 1.8 μ M of ZA also showed an increase in ROS production per unit DNA (P < 0.001).

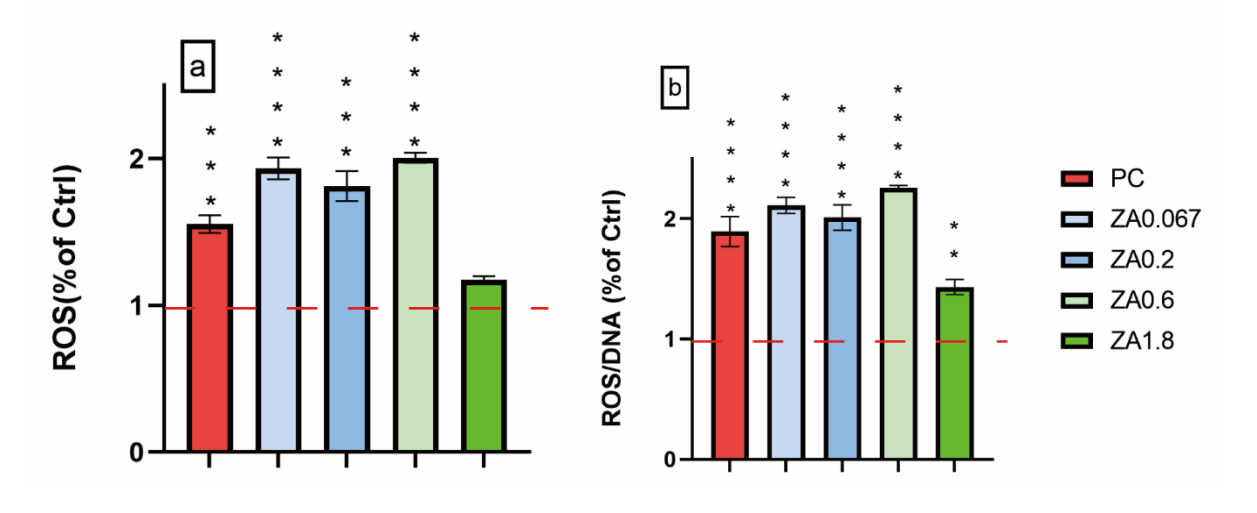


Fig 5.10 ROS production of the ZA treated differentiated Raw C10 cells. a) Total ROS was increased under 0.067, 0.2 and 0.6 μ M ZA. b) All concentrations of ZA increased ROS per unit of DNA. (Number of wells = 4, number of experiments = 2). PC, positive control. Red dotted line: control. ***, P<0.01. ****, P<0.001. ****, P<0.0001.

5.5.8 The effect of AL on ROS production in differentiated C10 Raw264.7 cells

To assess the oxidative stress induced by AL, the total ROS production was measured in differentiated C10 Raw264.7 cells treated with different concentrations of AL (0.067, 0.2, 0.6 and 1.8 μ M AL). In the positive control, 20ng/ml RANKL was added. The results were normalised based on the values obtained for the control (without AL treatment), and the rate of oxidative stress induced by AL was compared to that of the control. All concentrations AL increased both total and per unit DNA ROS production. (P < 0.05). Compared to ZA, AL on 1.8 μ M still had a significant increasing (P<0.05)

on the total ROS production.

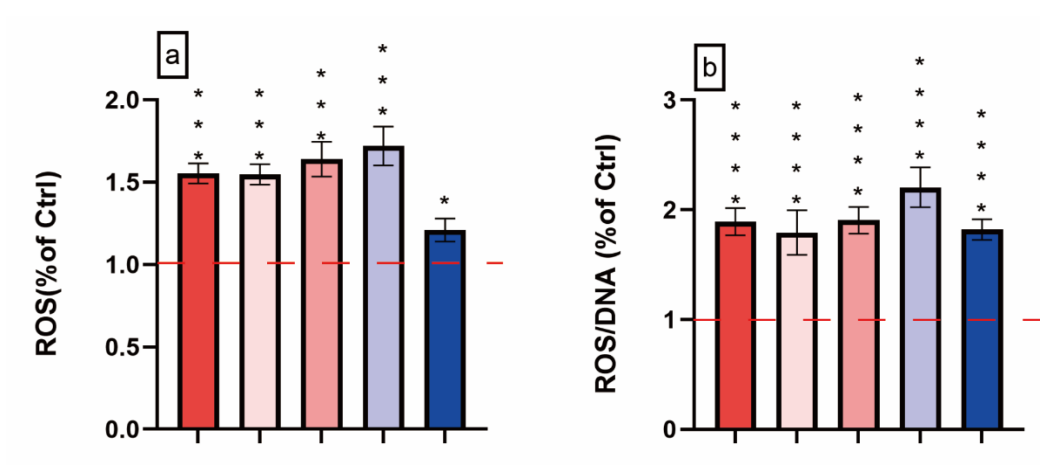


Fig 5.11 ROS production of AL treated differentiated RawC10 cells. a-b) All concentration of AL increased the total ROS and ROS per unit DNA. (Number of wells = 4, number of experiments = 2). PC, positive control. Red dotted line: control. *, P<0.05. **, P<0.01. ****, P<0.001. *****, P<0.0001.

5.5.9 The effect of ZA on differentiated C10 Raw264.7 cells

Cells under all concentrations of ZA successfully formed OCs. However, the morphology of OC differed depending on the experimental conditions. The control, positive control, and cells treated with 0.067 μ M ZA, exhibited round and full multinuclear cells, whereas those treated with 0.2 and 0.6 μ M of ZA appeared flatter. Cells treated with 1.8 μ M ZA showed collapsed multinuclear cells. The positive control (20 ng/ml RANKL) led to the formation of the most OCs significantly more than those formed under other conditions (P < 0.01). Compared to the control, treating the cells with 0.067 and 0.2 μ M of ZA did not make a significant difference to the number of OCs (P > 0.05). However, ZA at concentrations of 0.6 and 1.8 μ M decreased the number of OCs (P < 0.01) (Fig 5.12 a-b).

The TRAP 5b activity assay was performed to measure the impact of ZA on OC differentiation. ZA at concentrations of 0.067, 0.2, and 0.6 μ M significantly decreased TRAP 5b activity (P < 0.001, P < 0.01, and P < 0.01, respectively). However, no significant difference was observed between ZA-treated cells and control group at ZA concentration of 1.8 μ M (P > 0.05) (Fig 5.12 c).

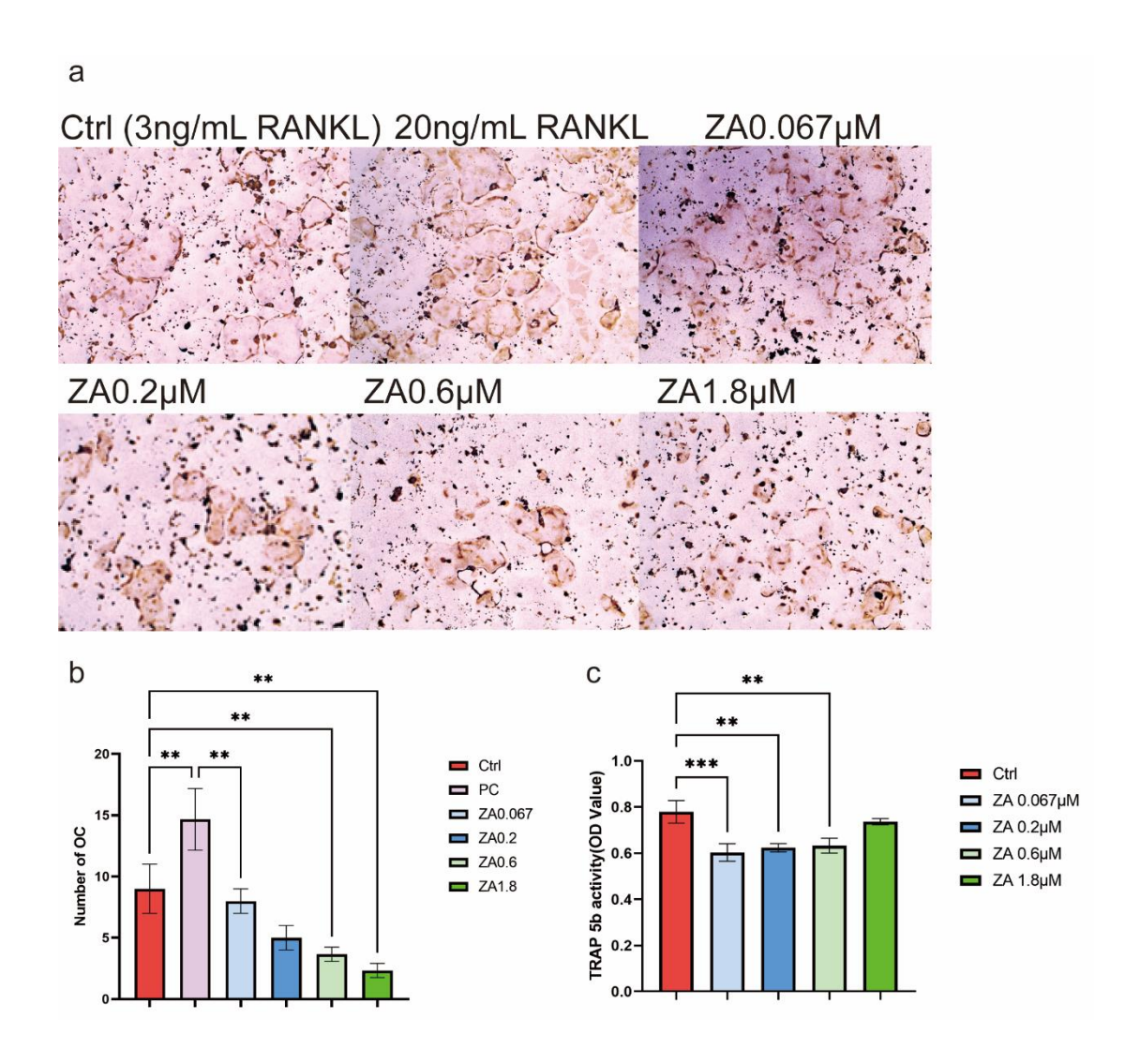


Fig 5.12 The effect of ZA on OC differentiation results of differentiated C10 Raw264.7 cells. a. Microscopic images of TRAP staining of ctrl, positive ctrl and ZA treated C10 cells. b. Quantification of number of OCs formed in different conditions. c. TRAP 5b activity of ZA treated OC. Ctrl, control. PC, positive control, TRAP 5b quantification was <1 and oversaturated and is therefore not shown. **, P<0.01. ***, P<0.001.

5.5.10 The effect of AL on differentiated C10 Raw264.7 cells

All conditions were able to form OCs successfully and the cellular morphology remained similar. Compared to the control, cells treated with AL (at concentrations of 0.067, 0.2, 0.6, and 1.8 μ M) did not exhibit a significant decrease in the number of OCs. Although the number of OCs reduced in AL-treated cells in a dose dependent manner, this difference was not statistically significant (P > 0.05).

The TRAP 5b activity assay was performed to measure to assess the impact of AL on OC differentiation. AL at a concentration of $0.067~\mu M$ did not change the TRAP 5b

activity compared to the control, whereas AL at concentrations of 0.2, 0.6, and 1.8 μ M significantly decreased TRAP 5b activity (P < 0.05, P < 0.001, and P < 0.01, respectively) (Fig 5.13).

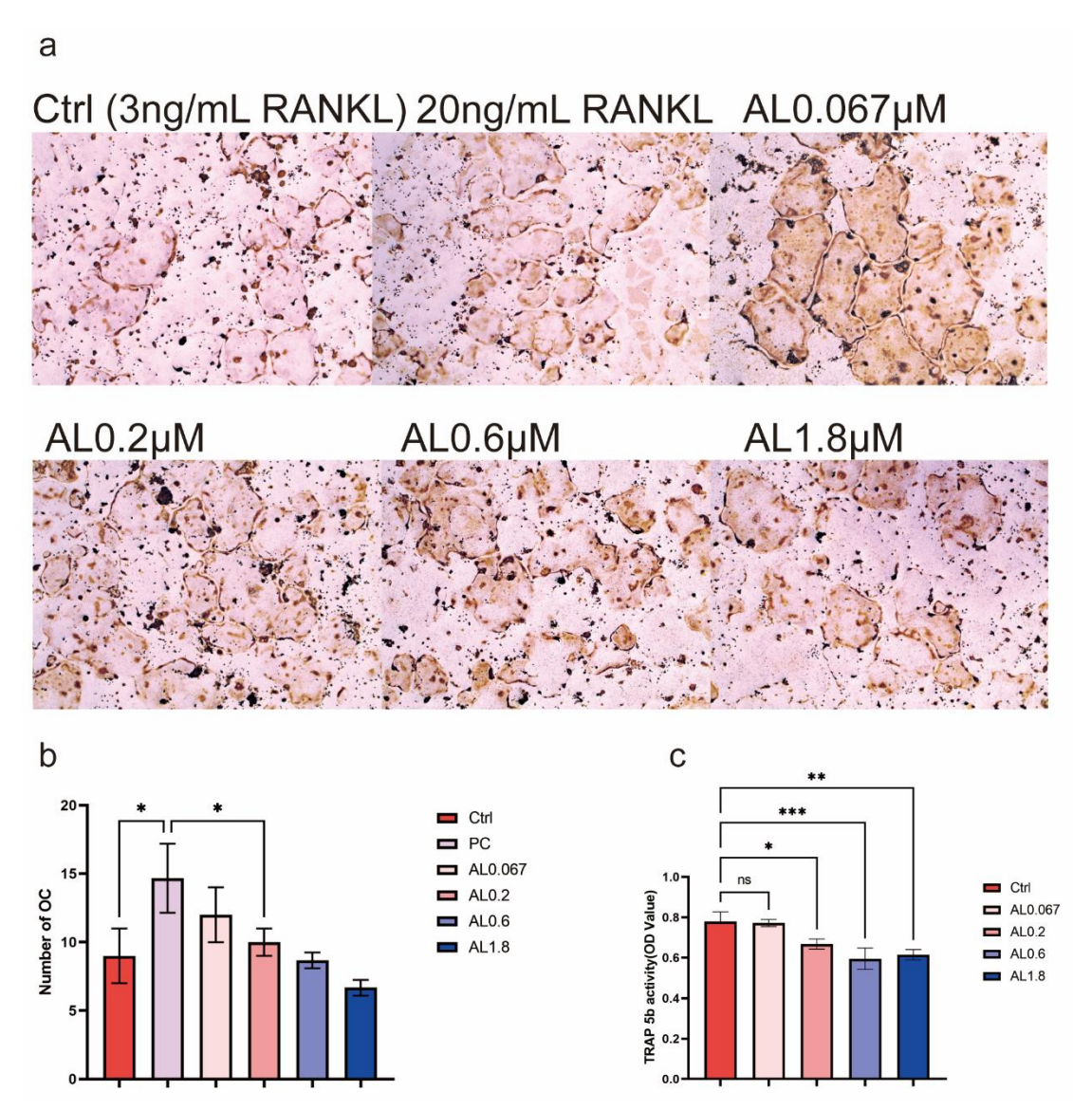


Fig 5.13 The effect of AL on TRAP differentiation results of differentiated C10 Raw264.7 cells. a. Microscopic images of TRAP staining of control, positive control, and AL-treated C10 cells. b. Quantification of number of OCs observed under control, positive control, and the different concentrations of AL. c. TRAP 5b activity of AL treated OC. Ctrl, control; PC, positive control, TRAP 5b quantification was <1 and oversaturated and is therefore not shown.*, P<0.05. ***, P<0.01. ****, P<0.001.

5.6 Discussion

5.6.1 How does ZA and AL affect the metabolic activity and proliferation of the Raw264.7 macrophage?

Our results showed that ZA concentrations above 0.2 µM inhibited the metabolic activity, DNA concentration and proliferation of Raw264.7 cells. This observation is similar to those reported in published studies, which suggested that concentrations of ZA at 0.1 and 0.5 ZA can significantly reduce the viability of Raw264.7 cells [418, 494, 495]. However, in another study (MTT, 72 hours) addition of 1 µM ZA showed no effect on metabolic activity [496]. These differences may be attributed to the differences in the metabolic assays, cell seeding concentration, media and the inherent heterogeneity of Raw264.7 cells. The heterogeneity of Raw264.7 cells suggests that the cell lines contain sub-clones with different abilities to form OCs [3], which can, in turn, induce heterogeneity of cell characteristics in different studies and experiments. These may also contribute to the different results of ZA on the viability and proliferation of Raw264.7 cells.

A concentration dependent effect of AL of metabolic activity and cell number was also observed.. As presented in chapter 1, AL exhibited relatively lower toxicity compared to ZA, and where a higher concentration of AL (50 μ M) to decrease the metabolic activity compared to ZA (20 μ M) (Chapter 2,). Whilst no published studies, to our knowledge, have tested the effect of AL on undifferentiated or differentiated Raw264.7 cells, there have been investigations on the effect of AL on macrophages/OCs and in a similar manner to our study showed a concentration 60-100 μ M reduced metabolic activity or proliferation [497, 498].

5.6.2 How does ZA and AL affect the metabolic activity and proliferation of differentiated Raw264.7 C10 subclones?

Our results showed that ZA concentrations above 0.2 μ M can inhibit the metabolic activity, DNA concentration and proliferation of differentiated Raw264.7 C10 subclones. This finding is consistent with those reported in previous studies [416, 418, 494, 499]. Huang et al. reported that 1 μ M ZA inhibited OC formation from Raw264.7 cells (the number of OC and resorptive pits decreased), but the metabolic activity and proliferation were not measured [416]. Gu et al. determined the metabolic activity of Raw264.7, in response to ZA, using the CCK-8 assay and found that 5 μ M ZA can

significantly inhibit the cells' metabolic activity [499]. Other studies have also shown that RANKL can promote monocyte differentiation and inhibit proliferation [500]. However the study above (by Suchita et. al., 2023) also used a much higher concentrations of RANKL (10 ng/ml) than the present study (3 ng/mL), and this may affect both metabolic activity and proliferation. Vuoti et. al (2023) demonstrated that RANKL caused a concentration dependent effect on monocyte proliferation and differentiation, but the effect is saturated with relatively low RANKL concentrations [501]. Huang et al. (2019) cultured both Raw264.7 cells and RANKL-induced Raw264.7 cells with ZA, and observed similar inhibition of proliferation as reported within here. They attributed OC formation suppression to inhibition of the NF-kB and JNK signalling pathways [502]. Similarly, Dong et al. (2018) reported that ZA inhibited differentiation and resorption capacity in OCs derived from Raw264.7 cells, potentially through the adenosine-activated protein kinase (AMPK) pathway [503].

In terms of understanding why cells are more tolerant of higher AL concentrations compared to ZA, when the mode of action of the N-BPs is believed to be similar (inhibiting intracellular FPPS [53]), this may be due to affinity of the respective chemicals to Ca or P in HA crystals. Ca is important in a number of cellular processes e.g. mitochondrial function and apoptosis. Other studies have also demonstrated that AL is less toxic than ZA on oral keratinocytes and fibroblasts [504] and *in vivo* [505].

5.6.3 How does ZA and AL affect the ROS production of Raw264.7 macrophages and OCs?

All concentrations of ZA and AL increased both total ROS and ROS per unit DNA in both undifferentiated (macrophage) and differentiated Raw264.7 (OC) cells. This is consistent with the literature that have reported that N-BPs can induce SaOs-2 cells and Salivary Adenoid Cystic Carcinoma Cell Line (SACC-83 cell) apoptosis via increasing cellular and mitochondrial [506, 507], and ZA 30 μ M increases ROS levels in oral fibroblast [456], and ZA 100 μ M induce OC apoptosis via increasing ROS production [508]. This suggests that although AL is less toxic than ZA (requiring a higher concentration, 0.6 μ M, to achieve the same effect as ZA's 0.067 μ M), it can

nonetheless elevate ROS levels similar to ZA, suggesting that the increased inhibition of ZA on cell proliferation and metabolic activity may not be just due to increased ROS levels but interactions with further cellular pathways, such as apoptosis or cell cycle regulation pathway.

A limitation of measuring ROS production in the OC differentiated C10 subclone, is that both undifferentiated macrophages and OCs are present in the culture (despite washing), and it is uncertain what the contribution both cell types are making to the total ROS production. A further complication is how to normalise ROS production in OC differentiated cells, when each OC is multinucleated and contains different amount of DNA.

5.6.4 How does ZA and AL affect TRAP 5b activity and OC formation of differentiated Raw264.7 C10 subclones?

TRAP 5b activity was decreased by 0.067, 0.2, and 0.6 μ M ZA, but not 1.8 μ M This contradicts the results obtained for OC formation as TRAP staining showed that 1.8 μ M ZA reduced OC formation. Others have also reported that N-BPs inhibit both OC formation [507]. Similarly, TRAP 5b activity was decreased by AL concentrations above 0.067 μ M, but no difference was observed between the number of OCs treated with AL and control, as determined by TRAP staining. The difference observed between the quantitative TRAP5b assay and the TRAP staining, may be due to the low amounts of DNA present in 1.8 μ M ZA cultures, and the differences in the sensitivity of DNA quantification and TRAP5b assay.

5.6.5 The protocol of Raw264.7 cells differentiation to OC and sub clone screening

The ability of cells to form functional bone resorbing OCs is disputed [491, 509], and this may be is limited due to the heterogeneity of this macrophage cell line [510]. To induce OC formation from macrophages, high doses of RANKL are often used, ranging from 30 to 100 ng/ml in different studies, and both DMEM and α -MEM were used for

Raw264.7 cell culture [237, 416, 498, 499]. However, our study demonstrated that a lower dose of 3 ng/ml was sufficient to generate functional OCs capable of dentin resorption (or though in lower amounts than primary cells[1]. Nevertheless, debates exist regarding whether OCs differentiated from Raw264.7 cells truly represent primary OCs and exhibit resorptive capabilities [511, 512]. Similarly to our protocol, Mira-Pascual et al. screened Raw264.7 cells by stimulating them with RANKL and found that the generated subclone of OCs was able to demineralise hydroxyapatite [491]. Here we demonstrate that the Raw264.7 clone is a suitable cell line for measuring differences to BPs, but there is still a need to compare the results to primary human OCs.

5.6.6 What are the possible pathways of BP-induced effect on Raw264.7 cells?

Other studies have also reported that ZA impairs the differentiation of OCs, as evidenced by decreased TRAP activity and impaired resorption assay [237, 416, 498]. PCR and Western blot analysis have demonstrated that ZA inhibits the expression of OC-related genes (CTR, RANK, TRAP, DC-STAMP, CTSK, and MMP-9) [237, 416, 499], providing insights into the potential pathways through which ZA affects OC function. Additionally, ZA treatment has been shown to increase the number of ROS-positive cells [237], which is consistent with the findings in our present study in which ZA and AL were found to increase ROS production. Furthermore, Zhao et al. found that ZA treatment on Raw264.7 cells led to an increase in M1 polarisation. Also, qPCR analysis revealed elevated expression of iNOS, TNF α , and IL-6 genes, along with increased protein levels of TNF α , IL-1 β , and IL-6, as well as enhanced ROS production [418]. These findings suggest that the shift towards M1 phenotype caused by ZA may operate through inflammation and oxidative stress pathways. Similarly, our results also revealed that oxidative stress played roles in the process of BP inhibited osteoclastogenesis.

5.6.7 How do BPs affect OB-OC cross-talk?

Bone remodeling is under dynamic balancing, and BP may play roles not only in single

cells but also in cellular interactions, thereby affecting the bone healing process. Our results showed that ZA and AL can affect both OB and OC differentiation. However, the cross-talk between OB and OC under BP intervention has not yet been investigated in this thesis. Also, our literature review indicated that there was no significant difference in the expression of receptor activator of RANKL and OPG between positive and negative responses based on limited data points. This suggests that the cross-talk between OB and OC should be emphasized in future research.

Chapter 6 Can Si restore BP induced inhibition of OB?

6.1 Introduction

As discussed in Chapter 1, BRONJ is a newly recognised complication associated with BP prescriptions. BP can affect OB by decreasing cell metabolic activity, proliferation, migration, angiogenesis, osteogenesis, and other cell functions, as well as by promoting negative effects such as inflammatory responses via the ROS pathway [470]. Various experimental therapies, including material-based approaches, have been proposed [161]. Both *in vitro* [229, 235, 237] and *in vivo* [513, 514] studies have revealed that ion-releasing materials can restore the BP-induced inhibition of osteogenesis or angiogenesis. For example, Bo can compete with BP on the apatite surface, potentially mitigating the adverse effects of BP [515, 516], and Zn can reverse BP-induced M1 macrophage polarisation [229]. Although the exact mechanism of action is still not fully elucidated and there is a long way to go before clinical application, these findings suggest that the ions released from BG or other materials could be considered as an option for treating BRONJ.

Si-BG promotes bone formation by releasing biologically relevant ions, such as Ca, P, and Si [322, 323, 517, 518]. Compared to non-Si-containing BGs, Si-BG has demonstrated an improved capability for bone formation [325]. It is believed to play a crucial role in enhancing bone formation and regeneration. It can form a hydroxyapatite (HAP) surface layer that binds to bone and also acts as a pro-osteoinductive component [519, 520].

Despite the invention of Si-BG more than 50 years ago, there is still relatively limited knowledge regarding the cellular mechanisms of Si. Even though the exact mechanisms underlying the therapeutic effects of Si are not fully understood, its ability to promote bone formation has led to its application as a therapeutic component in bone biomaterials such as BG, ceramics, and polymers. These materials have been utilised in the treatment of bone defects resulting from conditions such as tumours, infections, trauma, and other pathological conditions [203, 519, 521]. Currently, 16 Si-BGs out of 24 commercial BGs have been approved for clinical use.

In Chapter 4, ZA and AL were shown to inhibit OB cell metabolic activity, proliferation, ALP activity, and VEGF production, as well as to increase ROS production. Moreover, the *in vitro* bone nodule formation experiment showed that ZA above 0.2 μM significantly inhibits bone formation. Considering the effect of Si on promoting angiogenesis and osteogenesis, as well as ROS scavenging, it is possible to use it as a therapeutic approach for BRONJ (Fig 6.1). Previous studies have shown that functional OB restoration can be achieved by targeting the specific molecules involved in these pathways. Yazici, T et al. found that Se treatment reduces ZA-induced Saos-2 cell apoptosis and oxidative stress [470]. Xiao, L applied a melatonin-releasing hydrogel to H₂O₂-induced cell apoptosis in MC3T3-E1 cells and showed that cell viability and the deterioration of osteogenesis were reversed [522].

Consistent with Chapter 4, soluble Si ions were introduced into BP-treated OBs to observe their restorative effects. Two cell types were used as *in vitro* models of OB: Saos-2 cells and rat primary calvarial cells. ROS production, VEGF production, and bone formation in Si- and BP-treated OBs were analysed to determine whether Si can reverse BP's inhibition of OB.

6.2 Chapter aims

This chapter investigates the effects of Si on the proliferation, metabolic activity, ROS production. We also investigate if Si can restore BP inhibited osteoblast function.

6.3 Testable null hypotheses

- 1. Si 2 mM does not affect the proliferation, ROS production, VEGF production or metabolic activity of BP treated SaOs-2 cells.
- 2. Si 0.5 mM does not affect the ZA treated primary OB's bone formation.

6.4 Methods and Materials

SaOs-2 cell-line and primary rat OBs were cultured as described in Chapter 3 (Section 3.1.1). Briefly, SaOs-2 cells were treated with either Si 0.5, 1 and 2 mM, and kept in an incubator at 20% O₂. Metabolic activity, proliferation rate and ROS production were

measured at days 1, 3 and 7, and VEGF (days 1 and 7) and ALP (days 1, 7, 14 and 21) were measured. SaOs-2 cell treated with either 0.067, 0.2, or 1.8 μM of ZA or AL combined with/without 2 mM Si, then ROS production was measured at days 1, 3, and 7. Cells without any treatment were used as a control. Si concentration 2 mM (SaOs-2 cell) and 0.5 mM (primary OB) was determined according to previous results of our research group [1, 351].

Primary rat OBs were cultured as described in Chapter 3 (Section 3.1.2). Briefly, cells were treated with either 0.067, 0.2 or 1.8 μM of ZA and with/without Si 0.5 mM and kept in an incubator at normoxia (20% O₂). Due to the limited number of cells obtained from calvarial primary bone a reduced number of variables was required, which meant omitting 0.6 μM. Cells without any treatment were used as a control. ALP activity and VEGF expression of the cells were measured at days 1 and 7. VEGF production was measured at day 7. Bone nodules were further characterised using Alizarin red calcium staining and interferometry at day 21.

6.5 Results

6.5.1 Effect of Si on the metabolic activity, DNA concentration, and proliferation of SaOs-2 cells

To assess the effect of Si and DFO on the metabolic activity and proliferation, alamarBlue and DNA were quantified in the Saos-2 cells. DFO 5 μ M was used as a positive control. On day 7, DFO decreased the metabolic activity (P<0.0001) compared to the control. Si concentrations of 0.5, 1, and 2 mM did not change the metabolic activity on days 1, 3, or 7. On day 3, the total DNA decreased following the use of DFO 5 μ M (P<0.05). Si concentrations of 0.5, 1, and 2 mM did not change the total DNA content on days 1, 3, or 7. On day 7, treatment with 2 mM Si increased the cell proliferation rate (P<0.05). On day 7, DFO 5 μ M decreased the proliferation rate (P<0.001) while Si 2 mM increased it (P<0.001).

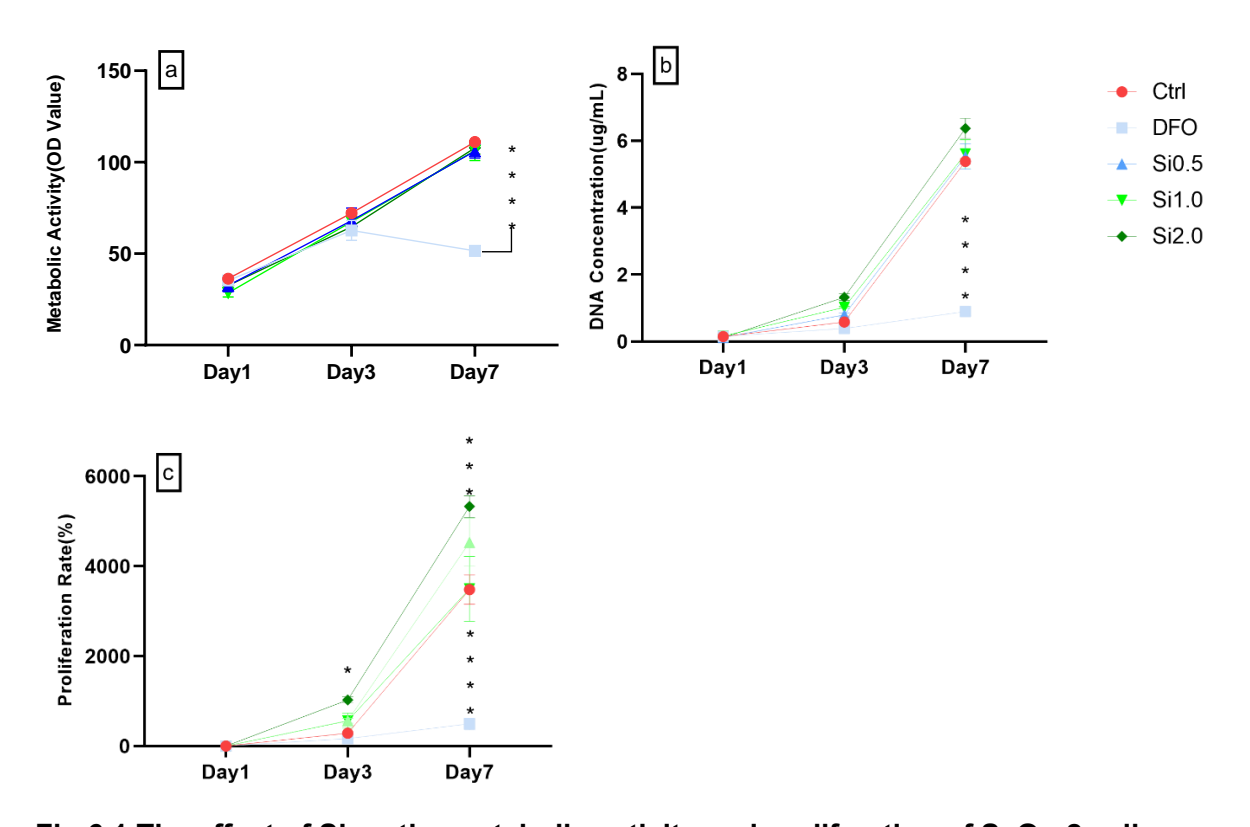


Fig 6.1 The effect of Si on the metabolic activity and proliferation of SaOs-2 cells. a) DFO decreased the metabolic activity on day 7. b) Si 2 mM increased the DNA concentration on day 3 (P<0.05) while DFO decreased the DNA concentration on day 7. c) Si 2 mM increased the proliferation rate on day 3 (P<0.05) and day 7. DFO decreased the proliferation on day 7. (Number of wells = 4). *, P<0.05. ***, P<0.001. ****, P<0.0001.

6.5.2 The effect of Si on ROS availability in SaOs-2 cells

To evaluate the ROS production induced by 0.5, 1, and 2 mM of Si, 2,7-dichlorofluorescin was used. H_2O_2 and DFO 5 μ M were used as positive and negative controls respectively. DFO 5 μ M decreased the total ROS on day 3 and day 7 (P<0.05, P<0.0001 respectively). On day 7, Si concentrations of 0.5, 1, and 2 mM did not affect the total ROS or ROS per unit of DNA (Fig 6.2).

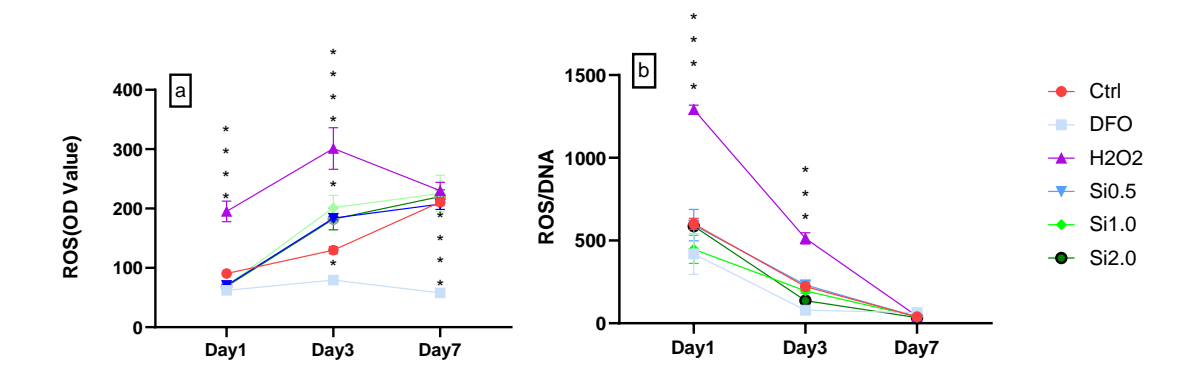


Fig 6.2 The effect of Si on ROS production by Saos-2 cells. H_2O_2 served as a positive control. a) 0.5, 1, and 2 mM of Si increased the total ROS and DFO decreased the ROS on day 3. b) All the Si concentrations and DFO did not significantly affect the ROS per unit of DNA. (Number of wells = 4). *, P<0.05. ****, P<0.001. *****, P<0.0001.

6.5.3 Effect of Si on the ROS in BP-treated Saos-2 cells

BP increases ROS production in SaOs-2 cells (Chapter 4). To evaluate the effect of Si on BP-treated SaOs-2 cells, 2 mM of Si was added to BP-treated Saos-2 cells and ROS production was measured on days 1, 3, and 7.

Adding 2 mM of Si to the Saos-2 cells partially reversed the increase in ROS production induced by ZA; both the total ROS production and ROS per unit DNA were decreased (Fig 6.3 a). A similar trend was observed in AL-treated SaOs-2 cells in terms of total ROS production and ROS per unit DNA (Fig 6.3 b).

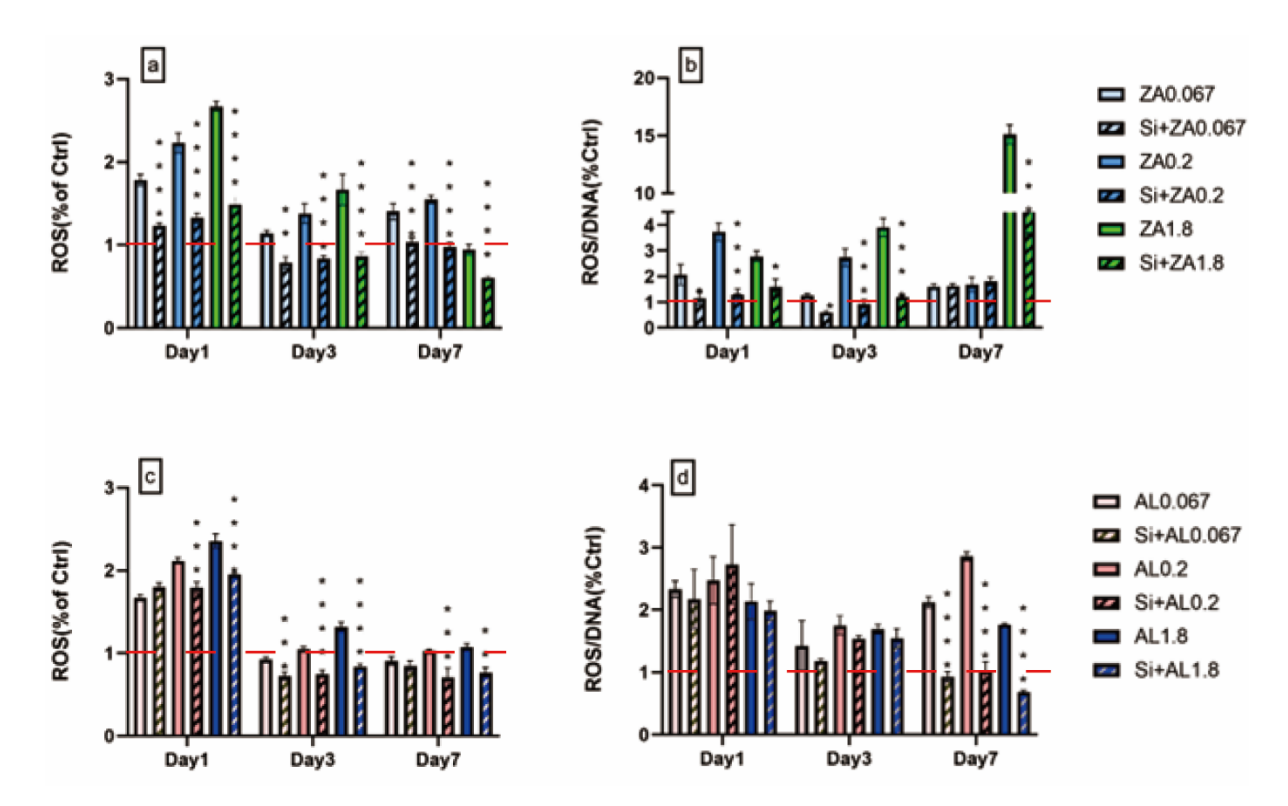


Fig 6.3. Si effect on the ROS in BP-treated SaOs-2 cells. a) On days 1, 3, and 7, adding 2mM of Si significantly decreased the total ROS production of ZA 0.067, 0.2, and 1.8 μM treated SaOs-2 cells. b) On day 1, Si 2 mM significantly decreased the ROS production per unit DNA of ZA 0.2 and 1.8 μM treated SaOs-2 cells. On day 3, Si 2 mM significantly decreased the ROS production per unit DNA of ZA 0.067, 0.2, and 1.8 μM treated SaOs-2 cells. On day 7, Si 2 mM significantly decreased the ROS production per unit DNA of ZA 1.8 μM treated SaOs-2 cells. c) On day 1 and day 7, Si 2 mM significantly decreased the total ROS production of AL 0.2 and 1.8 μM treated SaOs-2 cells. On day 3, Si 2 mM significantly decreased the total ROS production of AL 0.067, 0.2, and 1.8 μM treated SaOs-2 cells. d) On day 7, Si 2 mM significantly decreased the ROS production per unit DNA of AL 0.067, 0.2, and 1.8 μM treated SaOs-2 cells. (Number of wells = 4). ***, P<0.01. *****, P<0.001. *******, P<0.0001.

6.5.4 Si effect on ZA treated OB DNA concentration and proliferation

On day 1 and day 7, the DNA concentration of primary OB treated with Si and Si+ZA was measured. There was no significant difference observed among all the conditions on day 1. However, on day 7, ZA at concentrations of 0.2 and 1.8 µM significantly decreased the DNA concentration compared to the control (P<0.05, P<0.0001, respectively). Furthermore, the addition of Si at a concentration of 0.5 mM did not reverse the inhibition (P>0.05) (Fig 6.4).

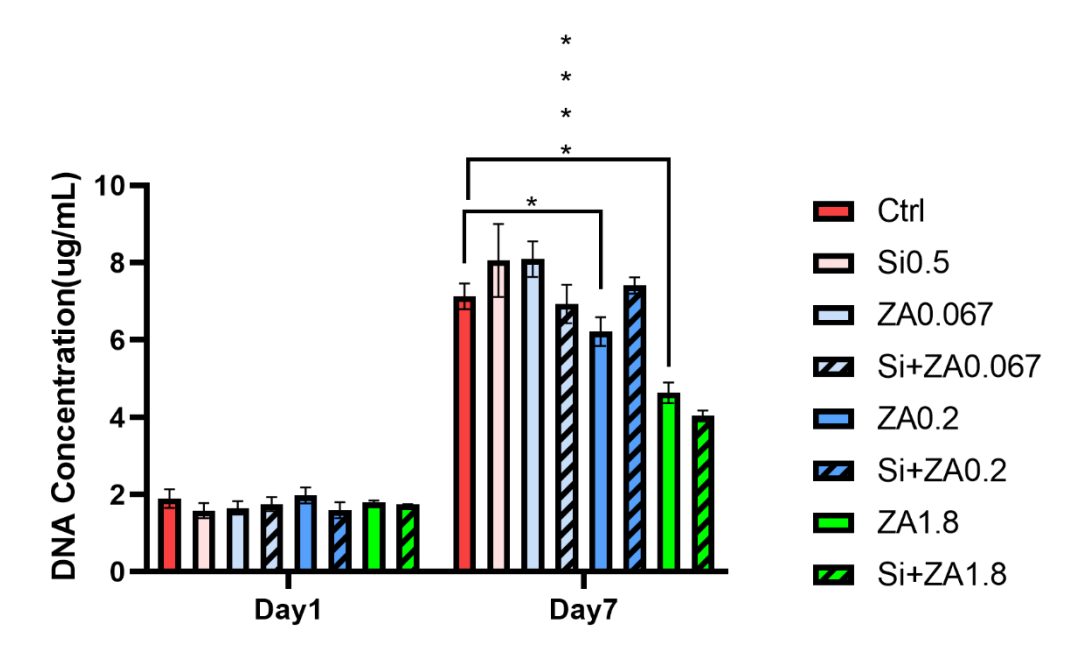


Fig 6.4. Si effect on the DNA concentration in ZA-treated primary OB. No significant difference was observed among all conditions on day 1. On day 7, ZA at concentrations of 0.2 μ M and 1.8 μ M significantly decreased DNA concentration. Adding Si did not reverse the inhibition. (Number of wells = 4, number of experiments = 1). *, P<0.05. ****, P<0.0001.

6.5.5 Si treated OB VEGF

To measure the effect of Si on OB angiogenesis, a VEGF assay was performed on Si 0.5, 1, and 2 mM treated primary OBs on days 1 and 7. On day 1, Si 1 mM increased the total VEGF production per unit DNA (P<0.001). On day 7, Si 0.5 mM significantly increased both the total VEGF and VEGF per unit of DNA (P<0.0001 and P<0.001, respectively), and Si 2 mM decreased both the total VEGF and VEGF per unit of DNA (P<0.0001 and P<0.001, respectively) (Fig 6.5).

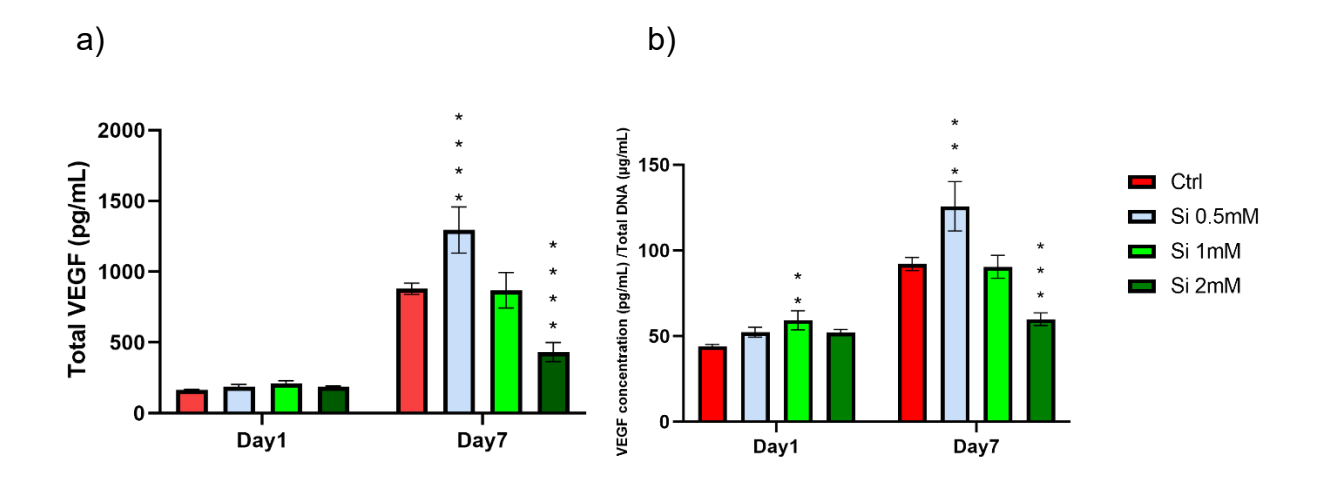


Fig 6.5 VEGF production of Si treated primary OB. a) Si 0.5 mM increased the total VEGF on day 7 (P<0.0001). Si 2 mM decreased the total VEGF on day 7 (P<0.0001). b) Si 1 mM increased the VEGF per unit DNA on day 1 (P<0.01). Si 0.5 mM increased the VEGF per unit DNA and Si 2 mM decreased the normalised VEGF on day 7 (P<0.001). (Number of wells= 3, number of experiments = 1). **, P<0.01. ****, P<0.001. *****, P<0.0001.

6.5.6 Si+ZA treated OB VEGF

To investigate whether Si can restore ZA-induced angiogenesis inhibition, a VEGF assay was performed on Si 0.5 mM as well as ZA 0.067, 0.2 and 1.8 μ M (with and without Si 0.5 mM) treated OBs on days 1 and 7. On day 1, adding Si 0.5 mM decreased the VEGF per unit DNA in the ZA 0.067 μ M treated OBs, and increased the VEGF per unit DNA in the ZA 0.2 and 1.8 μ M treated Obs. On day 7, both the total VEGF and VEGF per unit DNA of ZA 1.8 μ M treated OBs were increased by adding Si 0.5 mM (Fig 6.6).

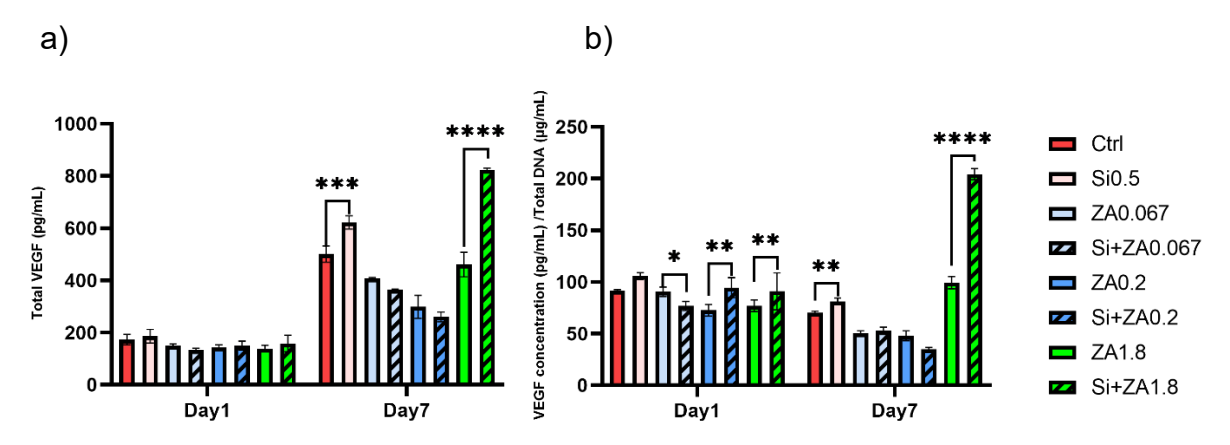


Fig 6.6 VEGF production of ZA and ZA + Si treated primary OB. a) On day 7, adding Si 0.5 mM increased the total VEGF of ZA 1.8 μM treated OBs. b) On day 1, adding Si 0.5 mM

decreased the VEGF per unit DNA of ZA 0.67 μ M treated OBs, and increased the VEGF per unit DNA of ZA 0.2 and 1.8 μ M treated OBs. On day 7, adding Si 0.5 mM increased the total VEGF of ZA 1.8 μ M treated OBs. (Number of wells = 3, number of experiments = 1). **, P<0.01. ***, P<0.001. ****, P<0.0001.

6.5.7 Si-treated OB bone nodule formation

On day 21, the primary OB-formed bone nodules were imaged under a microscope. Alizarin red staining was performed to characterise calcium storage. Interferometry was applied to the Melinex disc to calculate the number and size of the nodules (Fig 6.7). Quantitative analysis by Image J and interferometry showed that Si 0.5 mM formed more ARS areas and produced the maximum height of the nodules (Fig 6.8).

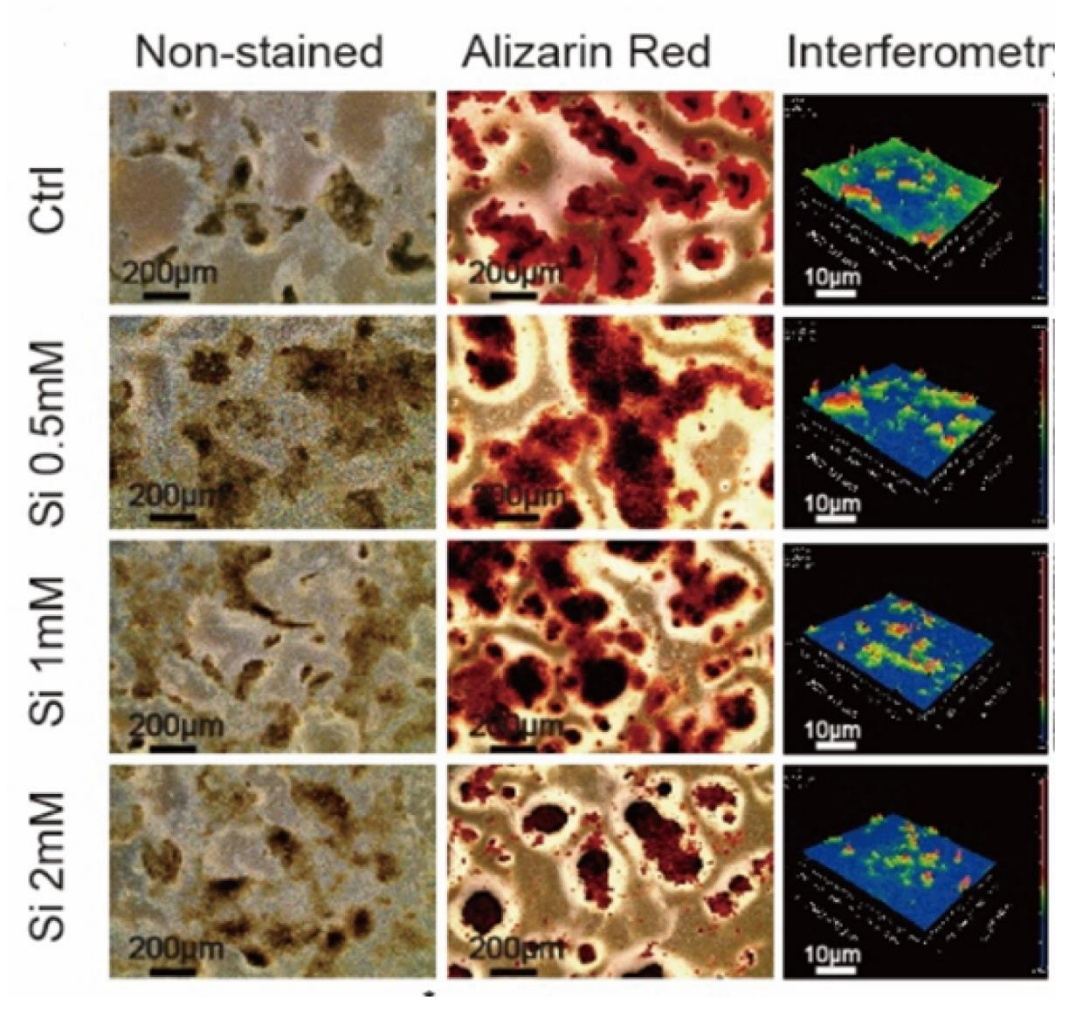


Fig 6.7 Day21 image, ARS and interferometry of primary OB bone nodule formation. Non-stained, microscopic images of the control and Si 0.5, 1.0, and 2.0 mM treated nodule formation. Alizarin red was used to determine calcium storage in the conditions. Interferometry was used to characterise the size and number of the nodules.

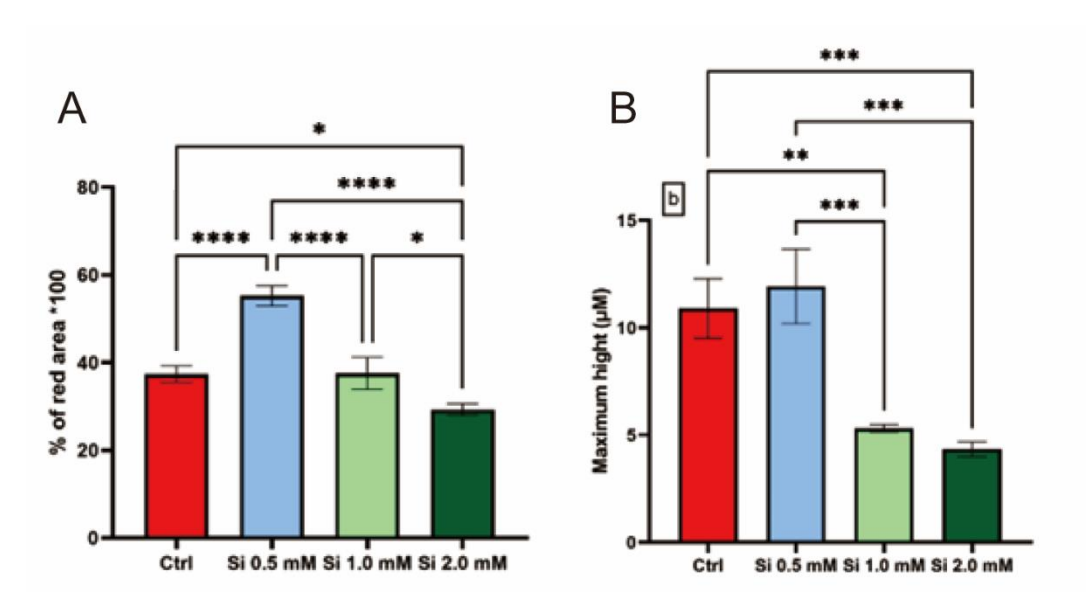


Fig 6.8. Quantitative analysis of the bone nodule formation. A. a) Percentage of the red area of the ARS image. Si 0.5 mM significantly increased the red area compared to the control, Si 1.0 mM, and Si 2.0 mM. Si 2.0 mM significantly decreased the red area compared to the control. No significant difference was observed between Si 1.0 mM and the control. B. Interferometry analysis was performed to measure the maximum height of the nodules. Si 1.0 mM and 2.0 mM significantly reduced the maximum height compared to the control, while Si 0.5 mM did not show a significant difference compared to the control. (Number of wells = 3, number of experiments = 1). *, P<0.05. **, P<0.01. ****, P<0.001. *****, P<0.0001.

6.5.8 Si+ZA treated OB bone nodule formation

To investigate the effect of Si on ZA treated OB, a bone nodule formation assay was conducted for 21 days. Si 0.5 mM was added to OB treated with ZA at concentrations of 0.067, 0.2, and 1.8 µM to determine if it could reverse the inhibitory effect induced by ZA. On day 21, the primary OB formed bone nodules, which were then imaged under a microscope. Alizarin red staining was performed to assess calcium storage (Fig 6.9 A). Interferometry was used on the Melinex disc to calculate the number and size of the nodules. Quantitative analysis using Image J and interferometry revealed that Si 0.5 mM in combination with ZA 0.067 µM resulted in a larger area of Alizarin red staining and maximum height of the nodules compared to the control. In contrast, ZA at concentrations of 0.2 and 1.8 µM significantly inhibited the area of Alizarin red staining and the maximum height compared to the control (Fig 6.10). Although the addition of Si 0.5 mM did not alter the inhibition, microscopic images taken on day 7 showed that Si 0.5 mM was able to reverse the inhibition of collagen formation caused

by ZA 0.067 μM and 0.2 μM (Fig 6.9 B).

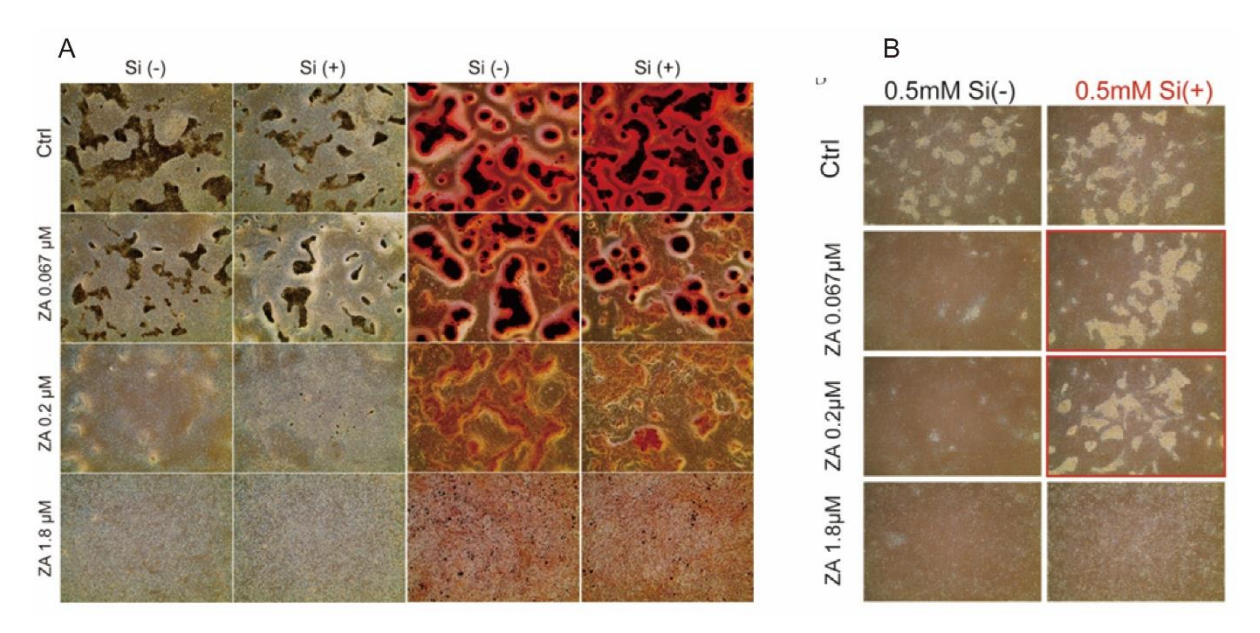


Fig 6. 9 Day 21 and day 7 microscopic image of ZA and ZA+Si treated OB. A. Adding Si 0.5 mM did not reverse the inhibitory effect on bone formation induced by ZA. However, it should be noted that ZA at a concentration of 1.8 μM could not be reversed by adding Si 0.5 mM. B. Adding Si 0.5 mM was able to reverse the inhibition of collagen formation caused by ZA at concentrations of 0.067 μM and 0.2 μM. However, it should be noted that ZA at a concentration of 1.8 μM could not be reversed by adding Si 0.5 mM.

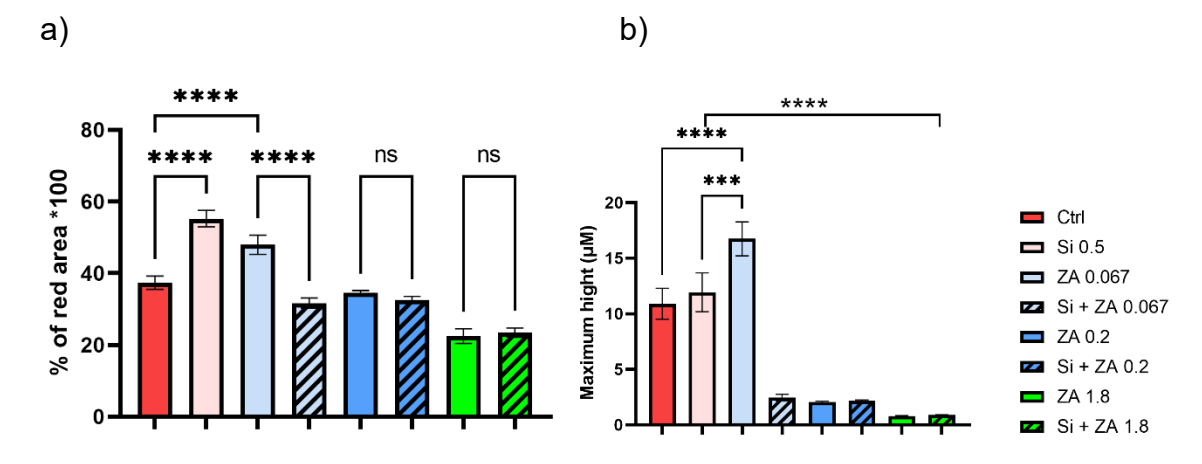


Fig 6. 10 Quantitative analysis of the bone nodule formation. a). The percentage of the red area in the Alizarin red staining (ARS) image was analysed. ZA at a concentration of 0.067 μM or Si 0.5 mM significantly increased the red area compared to the control. However, adding Si 0.5 mM did not reverse the inhibitory effect induced by ZA at concentrations of 0.2 μM and 1.8 μM compared to the control. b). Interferometry analysis revealed that ZA at a concentration of 0.067 μM significantly increased the maximum height compared to the control. Adding Si 0.5 mM did not show a significant difference compared to the control. (Number of wells = 3, number of experiments = 1). ****, P<0.001. ******, P<0.0001.

6.6 Discussion

6.6.1 How does Si affect SaOs-2 cell metabolic activity and proliferation?

The exact mechanism by which Si interacts with cells remains unclear. In this section, the metabolic activity and proliferation of SaOs-2 cells following exposure to different concentrations (from 0.5 to 2 mM) of Si were measured to determine non-toxic concentrations for OB. None of the concentrations of Si changed the metabolic activity or DNA concentration compared to the control, and higher concentrations (2 mM) of Si increased the SaOs-2 cell proliferation rate. The effect of Si on cell viability and proliferation varies depending on the Si type, concentration, and cell type. A systematic review [523] analysed the published literature and found that Si concentrations above 40 ppm were significantly more likely to cause a decreased (undesirable) cellular response, such as decreased cell viability or proliferation. For example, a study showed that high concentrations of Si ions at 5 mM suppressed BMSC cell proliferation [520], while Si 25 μ g/ml increased hDFC proliferation and Si 100 μ g/ml decreased [524].

6.6.2 How does Si affect primary OB bone nodule formation?

Si 0.5 mM exhibited an increase in bone formation compared to the control, whereas Si 1 and 2 mM did not inhibit bone formation. However, Si 1 mM and 2 mM treated primary OBs formed less bone compared to Si 0.5 mM. This increase may be associated with the enhanced collagen formation induced by Si. Si is a natural trace element found in the mammalian diet, and increasing evidence suggests that it may be vital for bone and connective tissue health [314, 525]. Research has shown that Si can increase type I collagen production in the form of a BG60S dissolution component [526], and that orthosilicic acid at physiological concentrations stimulates type I collagen synthesis [527]. Si can also be internalised into cells without cell destruction [528]. This harmless Si uptake may be involved in increased proliferation and collagen production.

6.6.3 How does Si affect SaOs-2 cell ROS production

Studies demonstrate that Si-BG possesses intrinsic antioxidant activity [529]. Notably,

Si acts as a ROS scavenger, reducing both acellular and cellular ROS production [1]. Our results showed Si increased Saos-2 cell total ROS production on day 3, but did not change the ROS per unit DNA. As mentioned in section 6.4.1, this may have been caused by the increase in the cell number of Si-treated SaOs-2 cells.

6.6.4 How does Si reverse BP inhibited early bone nodule formation

Si has been revealed to have the effect of promoting bone remodelling. Our results showed on day 7, Si partially reversed ZA 0.067 and 0.2 μ M collagen formation. ZA 0.067, 0.2, and 1.8 μ M treated OBs did not form collagen. Adding Si 0.5 mM to ZA 0.067 and 0.2 μ M treated OBs can partly reverse the collagen formation. However, Si 0.5 mM did not reverse collagen formation in the ZA 1.8 μ M treated OBs. This may indicate that Si is mainly involved in the collagen-forming stage of bone regeneration.

6.6.5 How does Si affect primary OB angiogenesis

Si, Si-BG, and Si-containing nanoparticles have been extensively reported to promote angiogenesis both *in vivo* and *in vitro* [524, 530, 531]. Similarly to ALP activity, VEGF production in the Si-treated OBs increased on day 7 of the Si 0.5 mM intervention. Si 1 mM did not alter VEGF expression on day 7, whereas Si 2 mM induced a decrease. This concentration-dependent effect revealed that lower doses of Si can increase VEGF production, whereas higher doses can induce a decrease.

Chapter 7 Can HIF mimetics restore BP induced inhibition of OC?

7.1 Introduction

7.1.1 The role of HIF in bone regeneration and remodelling

Dropping oxygen levels leads to a condition known as hypoxia, which plays an important role in bone repair [532]. Microvascular damage following bone fracture causes hypoxic pressure, leading to the activation of a series of downstream pathways, mainly those involving hypoxia-inducible factor (HIF) and HIF stabilisation. HIF is a transcription factor essential in healthy bone regeneration and bone remodelling [533, 534]. The HIF pathway regulates genes essential for cellular adaptation to hypoxia and coordinates tissue regeneration including the ones responsible for angiogenesis, erythropoiesis, glucose metabolism, and cell survival [535-538].

The HIF pathway comprises HIF- α subunits, including HIF- 1α and HIF- 1β , which contain basic helix-loop-helix protein domains that enable heterodimerisation, DNA binding, and formation of downstream genes [539, 540]. Under conditions of normal oxygen levels (normoxia), HIF- 1α is continuously degraded due to the activity of prolyl hydroxylase domain proteins (PHDs). During this process, cellular iron (Fe²⁺) inhibits PHD function and allows HIF- 1α translocation to the nucleus along with hypoxia response element (HRE) activation [541]. While under hypoxic conditions, PHD activity is inhibited via various pathways, leading to HIF- α stabilisation [534] (Fig 7.1 upper).

Hypoxia plays a crucial role in bone fracture repair by creating a hypoxic environment due to microvascular damage following the fracture, resulting in HIF-1 α stabilisation [542, 543]. This leads to the production of inflammatory and angiogenic factors mediated by HIF-1 α , initiating the inflammatory phase necessary for normal bone regeneration [544, 545]. Hypoxia and HIF-1 α stabilisation are also important for various processes involved in bone marrow-derived mesenchymal stem cells (BMSCs), including recruitment, proliferation, and regulation of differentiation into chondrocytes and OBs [546, 547]. Moreover, HIF-1 α has been shown to upregulate

numerous pro-angiogenic genes, such as VEGF and bFGF, in cells associated with fracture repair [548, 549]. Additionally, when ordered bone formation occurs during the remodelling phase, HIF stabilisation is critical for osteoclastogenesis [550, 551], OC function [552, 553], and OB-OC cross talk [554].

Therefore, artificial stabilization of HIF-1 α has gained attention as a potential therapeutic approach to enhance bone regeneration and has implications in the field of bone tissue engineering. The stabilisation of HIF can be achieved by some chemicals, which are called HIF mimetics. They can inhibit the degradation of HIF-1 α at a normal oxygen level, such as cobalt chloride (CoCl₂), dimethyloxalylglycine (DMOG) and desferrioxamine (DFO). They target the HIF pathway via distinct mechanisms. Co has been reported to stabilise HIF-1 α by competing with iron ions (Fe²⁺), binding to the PHD-2 active site[555]. DFO downregulates PHD-2 and factor inhibiting HIF (FIH) activity via Fe chelation, due to their dependence on this ion [556], whereas DMOG competes with 2-oxoglutarate and binds to both PHD-2 [557] (Fig 7.1).

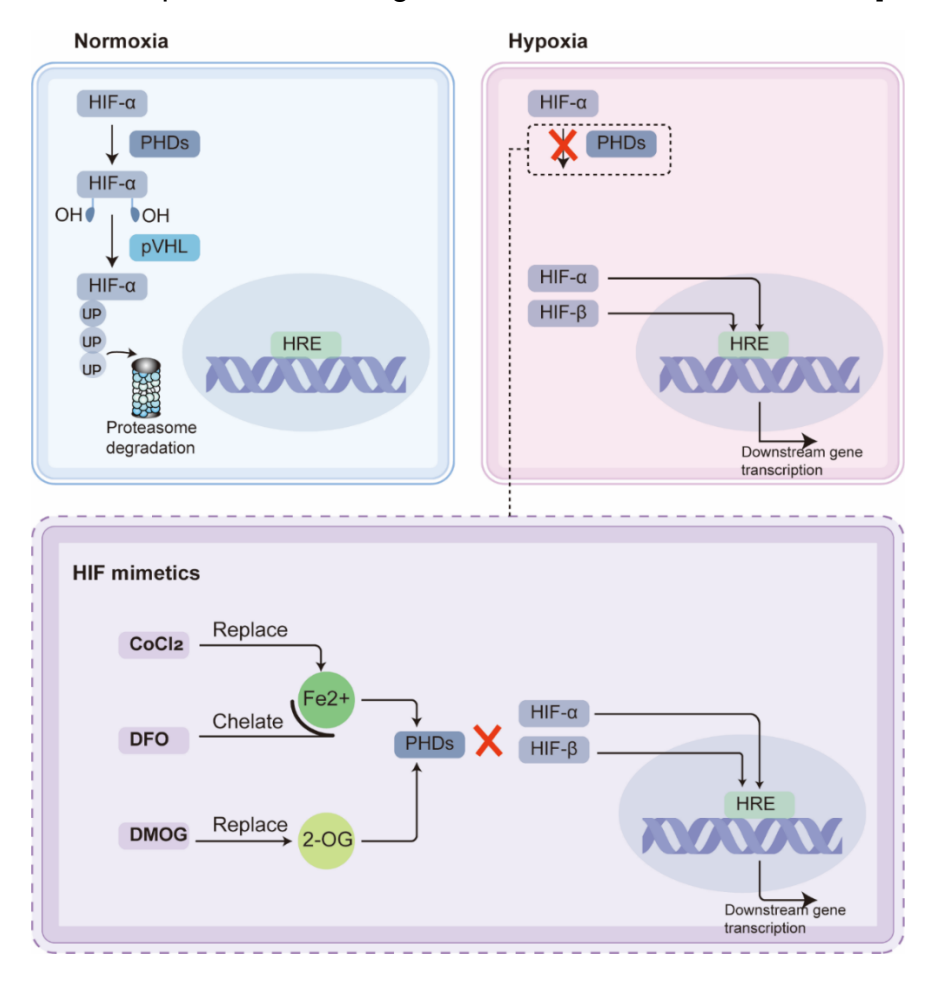


Fig 7.1. Hypoxia inducible factor (HIF) pathway and HIF mimetics. Under normoxia (left), HIF-1α is hydroxylated by oxygen sensing prolyl hydroxylase domain proteins (PHDs) family, including PHD1, PHD2, and PHD3. This hydroxylation occurs in the presence of oxygen, 2-oxoglutarate (2-OG) as substrates, and Fe2+ as a cofactor [558, 559]. Subsequently, hydroxylated HIF- α interacted with von Hippel-Lindau protein (pVHL) promoting HIF- α ubiquitin protein (UP) proteasome degradation. In hypoxia (right), the activity of PHDs is inhibited, leading to the stabilisation of HIF- α . Stabilised HIF- α then translocates into the nucleus forming a dimer with HIF- β , binding to hypoxia response elements (HREs).

Whilst the HIF pathway is undoubtably important in angiogenic signalling and restoring the vasculature in bone repair, the direct effect of HIF-1α on OC behaviour and resorption process is uncertain. Furthermore, the lack of oxygen (real hypoxia) and HIF-1α stabilisation may have different effects on bone regeneration. In OC, hypoxia (1% O₂) can induce a 3-fold increase in the number of OCs compared to that observed with 20% O₂, thereby contributing to bone resorption [560]. Studies have shown that hypoxia increases the production of reactive oxygen species (ROS), which is necessary for differentiation and activation of OCs [560-562].

Stabilised HIF-1α by L-mimosine, a prolyl hydroxylase (PHDs) domain inhibitor can increase the gene expression of genes involved in OCs differentiation and activation, such as RANKL and NFATc1 [563]. In addition, HIF stimulate the production of proinflammatory cytokines such as TNF-α (tumour necrosis factor alpha) and IL-1β (interleukin-1 beta) [564]. These cytokines can further promote OCs' differentiation and activation, which is independent of RANKL, which leads to increased bone resorption [565, 566]. In addition, OB-OC cross talk can be mediated by HIF via the RANKL pathway. HIF further stimulates OC activity by increasing RANKL production in OBs [567].

Additionally, HIF promotes angiogenesis by regulating multiple steps in the process. HIF can increase the expression of proangiogenic factors and their receptors, such as VEGF, PIGF, PDGFB, ANGPT1, and ANGPT2, which promote endothelial cell proliferation, migration, and survival [568, 569]. Furthermore, HIF enhances the recruitment of bone marrow-derived endothelial progenitors to angiogenic sites, further promoting vessel formation [39]; it also upregulates the expression of matrix

metalloproteinases (MMPs), which degrade extracellular matrix proteins and allow endothelial cells to migrate and form new vessels, especially in cancer [570].

7.1.2 HIF-1α and BRONJ

Evidence suggests that the HIF-1 α pathway is involved in the development of BRONJ. HIF-1 α expression has been shown to be increased in the jaws of patients with BRONJ, which may contribute to the development of osteonecrosis by promoting inflammation and impairing bone healing [571, 572]. BPs exert anti-angiogenic effects by inhibiting the growth of new blood vessels, which may be beneficial in treating certain types of cancer [573, 574]. Evidence also suggests that BPs affect the HIF pathway, which plays an important role in the regulation of angiogenesis. Tang et al. found that BPs suppress insulin-like growth factor 1-induced angiogenesis via the HIF-1 α /VEGF signalling pathways in human breast cancer cells [575]. However, conflicting results have also been reported, with some suggesting that BPs may actually inhibit HIF-1 α activity [576].

The HIF pathway may play a role in the development of BRONJ; however, it also shows the potential for treating this condition. Although no therapeutic strategy has been developed so far, HIF mimetics can be considered possible therapeutic targets to treat BRONJ. By stabilising HIF-1 α , bone healing can be promoted, and the risk of BRONJ can be reduced.

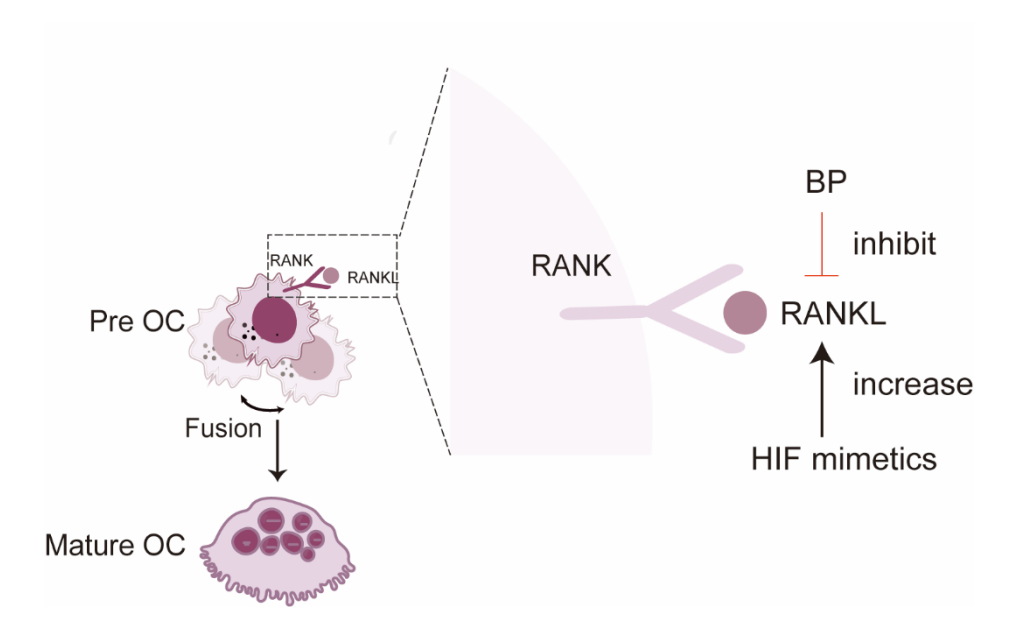


Fig 7.2. Hypothesis of HIF mimetics restoring BP-induced OC inhibition. HIF mimetics converse BP-induced RANKL inhibition, and therefore restore OC formation.

Co BG was found to both stabilise HIF-1α and increase VEGF expression [202]. VEGF can directly promote osteoclastogenesis via PI3K/AKT/mTOR pathway [577], or stimulate RANKL production in fibroblast [578], therefore promote bone resorption, Our group's work has also proved that hypoxia mimetics (CoCl₂ and DMOG) can partly restore hyperglycaemia inhibited bone nodule formation, possibly via increasing ALP [351]. Additionally, Co could mediate bone remodelling via increasing inflammation and angiogenesis, therefore promoting osteoclastogenesis [1]. Furthermore, our work also showed DFO can increase OC differentiation on both cell number and TRAP 5b activity [1]. DFO is an iron chelator [579], which can inhibit PHD via chelating with Fe²⁺, and therefore also works as an HIF stabiliser.

The current findings by our group and knowledge from the literature, indicate that BG ion release can regulate both OB and OC formation, Si can enhance bone formation, Si can inhibit OC formation, and Co can promote OC formation. Controlled release of Co or Si ions by BGs (or different BGs) could therefore offer a means of regulating bone formation and remodelling, depending upon the underlying disease conditions. In order to examine how each ion/molecule reversed the effect of BP OB and OC, cell toxicity and differentiation assays were performed.

7.2 Chapter aims

Considering the restorative effects of HIF mimetics on bone and wound healing in patients with inhibited regeneration, this chapter investigates whether Co and DFO restore functionality in BP-treated OC cells in terms of proliferation, metabolic activity, ROS, OB differentiation and OC differentiation.

7.3 Testable hypotheses

- 1. Co (25 μ M) does not affect ROS production (of monocytes or differentiated OCs) OCs, or OC differentiation, in ZA and AL treated culture.
- 2. DFO (2 µM) does not affect of monocytes or differentiated OCs) OCs, or OC

differentiation, in ZA and AL treated culture.

7.4 Methods and Materials

OC sub-clone C10 were cultured as described in Chapter 2 (Section 2.3). C10 subclone cells were seeded at $3x10^3$ cells/cm² in 6 well plate 24 hours after seeding, 3ng/ml RANKL was added to generate OC differentiation and 20ng/ml RANKL was used as a positive control. After that, OC cells were treated with either ZA 0.067, 0.2, 0.6 or 1.8 μ M or AL 0.067, 0.2, 0.6, 1.8 or 5.4 μ M, with/without Co 25 μ M or DFO 2 μ M treatment and were kept in an incubator at 20% O₂. Cells without any treatment were used as a control. The ROS production (day 3), TRAP 5b activity (day 5) measurement and TRAP staining (day 5) were performed (Section 3.11).

7.5 Results

7.5.1 DFO and Cobalt on ZA and AL treated OC ROS production

To evaluate the effects of ZA, AL, DFO, and Co on the oxidative stress level of OCs, ROS assays were performed on day 3. ZA (0.067, 0.2, and 0.6 μ M) significantly increased total ROS and ROS per unit DNA. Co (25 μ M) significantly increased total ROS and ROS per unit DNA. In contrast, the addition of DFO (2 μ M) or Co (25 μ M) can significantly reduce the increase in ROS caused by ZA (0.067, 0.2, and 0.6 μ M) (Figs 6.3 A, B). Similarly to ZA, AL (0.067, 0.2, and 0.6 μ M) significantly increased total ROS and ROS per unit DNA. Moreover, the addition of DFO (2 μ M) or Co (25 μ M) can significantly reduce the increase in ROS caused by AL (0.2, 0.6, 1.8 μ M) (Figs 7.3 C,D).

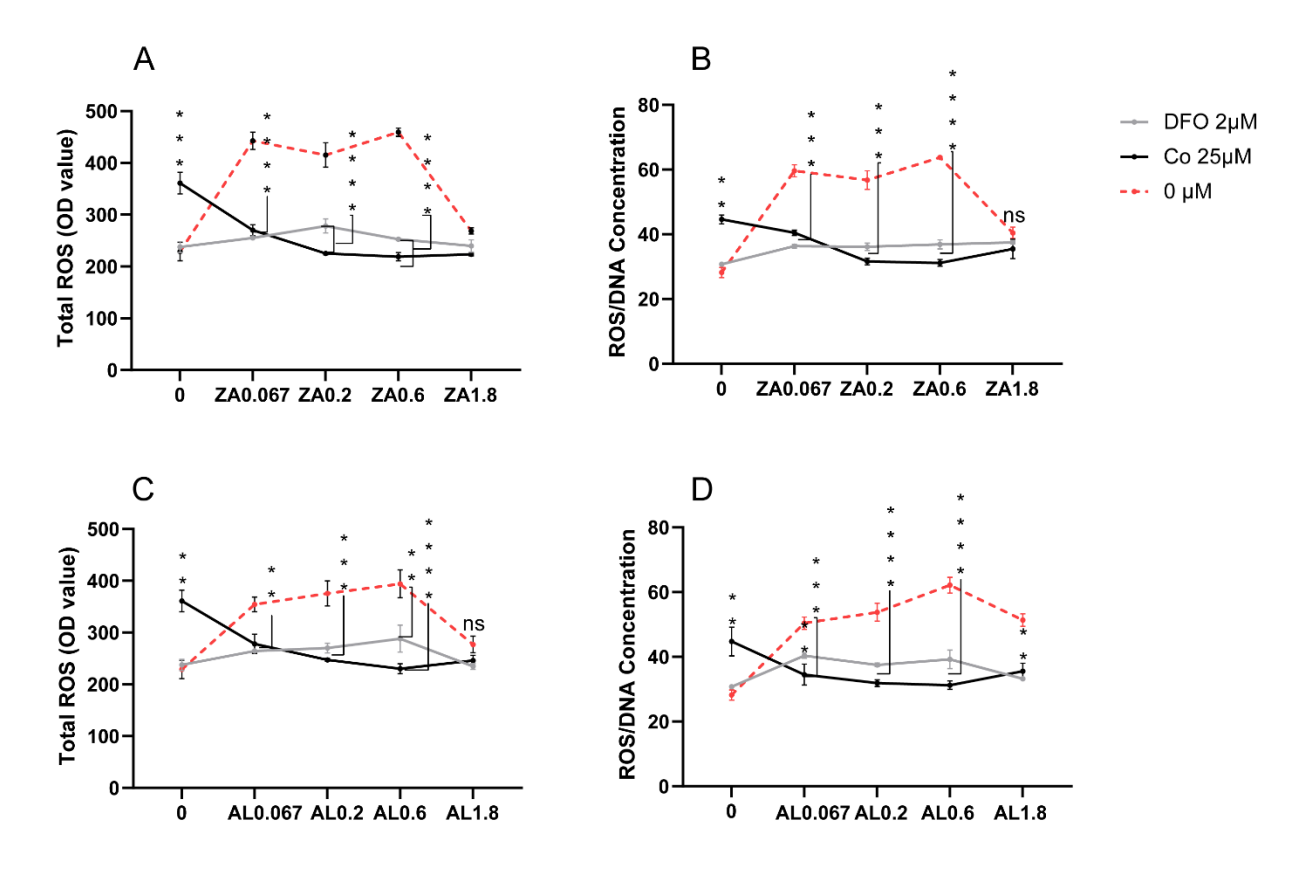


Fig 7.3. The effect of DFO and Co on ZA and AL induced ROS production. BPs (ZA [a-b] and AL [c-d]) increased ROS availability in a concentration dependent manner. Co and DFO both inhibited total ROS production and ROS production unit DNA (Number of wells = 3). **, P<0.01. ***, P<0.001. ****, P<0.0001.

7.5.2 Effect of DFO and Co on TRAP 5b activity in ZA- and AL-treated OCs

To evaluate the effect of ZA, AL, DFO, and Co on OC differentiation, TRAP 5b assays were performed on day 5. ZA (0.067, 0.2, and 0.6 μ M) decreased TRAP 5b activity significantly (P<0.0001). The addition of DFO (2 μ M) or Co (25 μ M) significantly reversed the decrease in TRAP 5b activity induced by ZA (0.067, 0.2, and 0.6 μ M) (Fig 7.4 A). Similarly to ZA, AL (0.067, 0.2, 0.6, and 1.8 μ M) decreased TRAP 5b activity significantly (P<0.01, P<0.0001, P<0.0001, and P<0.0001, respectively). The addition of DFO (2 μ M) or Co (25 μ M) significantly reversed the decrease in TRAP 5b activity induced by all concentrations of AL (P<0.001) (Fig 7.4 B).

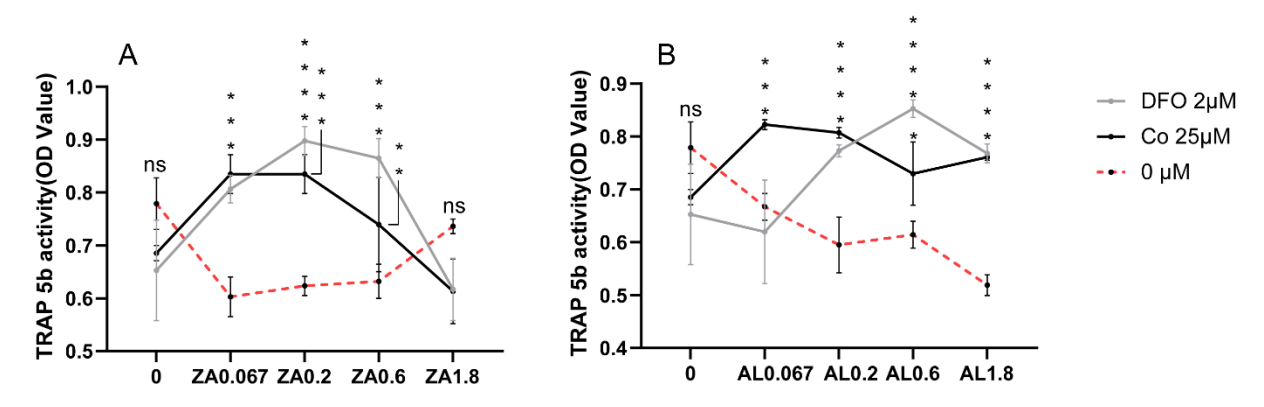


Fig 7.4 Effect of DFO and Co on TRAP5b activity in ZA- and AL-treated OCs. BPs (ZA [a] and AL [b]) decreased TRAP5b activity availability in a concentration dependent manner. (Number of wells = 3). **, P<0.01. ***, P<0.001. ****, P<0.001.

7.5.3 Effect of Co on ZA-treated OC TRAP staining

TRAP staining revealed that ZA inhibited OC formation. On day 5, ZA (0.6 and 1.8 μ M) significantly decreased the number of OCs (P<0.01 and P<0.001, respectively). The addition of Co (25 μ M) partially reversed the ZA-induced (0.6 and 1.8 μ M) inhibition of OC formation (P<0.05) (Fig 7.5).

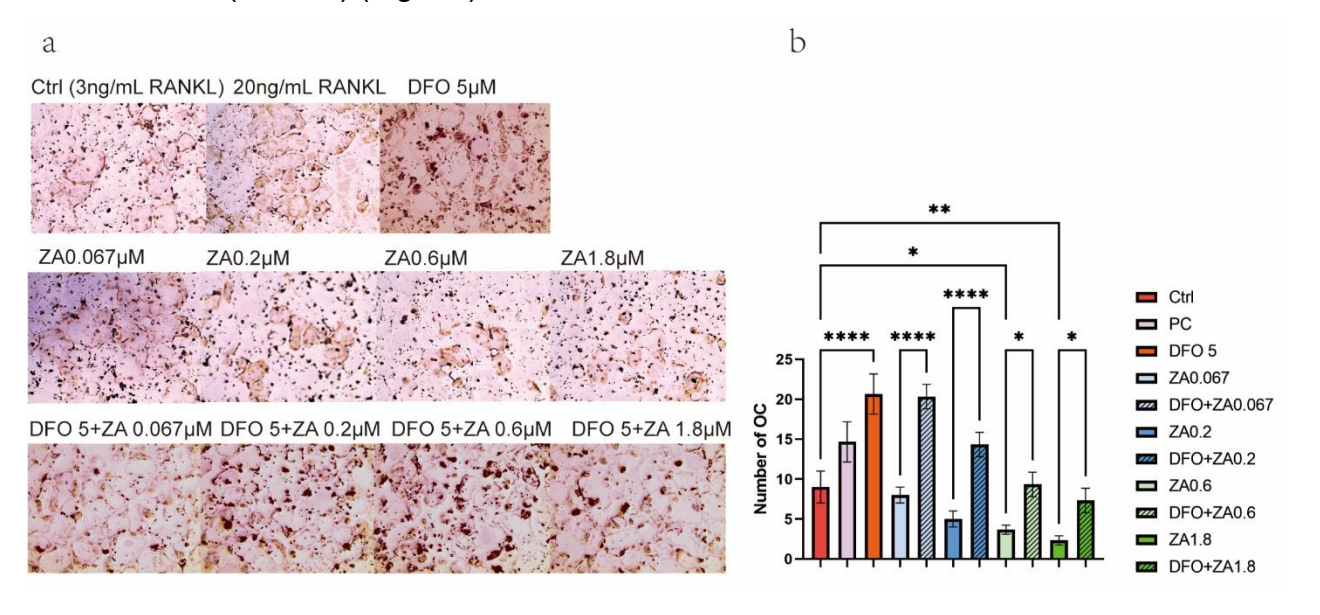


Fig 7.5. TRAP staining of OCs treated with ZA and Co+ZA. ZA (0.6 and 1.8) μ M decreased the number of OCs, compared to the control. The addition of Co (25 μ M) partially reversed the ZA-induced (0.6 and 1.8 μ M) inhibition of OC formation. ZA at concentrations of 0.067 and 0.2 μ M did not change the number of OCs. Positive Control (PC) = 20ng RANKL. (Number of wells = 3). *, P<0.05. ***, P<0.01. ****, P<0.001.

7.5.4 Effect of Co on AL-treated OC TRAP staining

TRAP staining revealed that AL inhibited OC formation. On day 5, no significant difference was observed among the OCs treated with AL and AL combined with Co (25 µM), or among the treated OCs and the control (Fig 7.6).

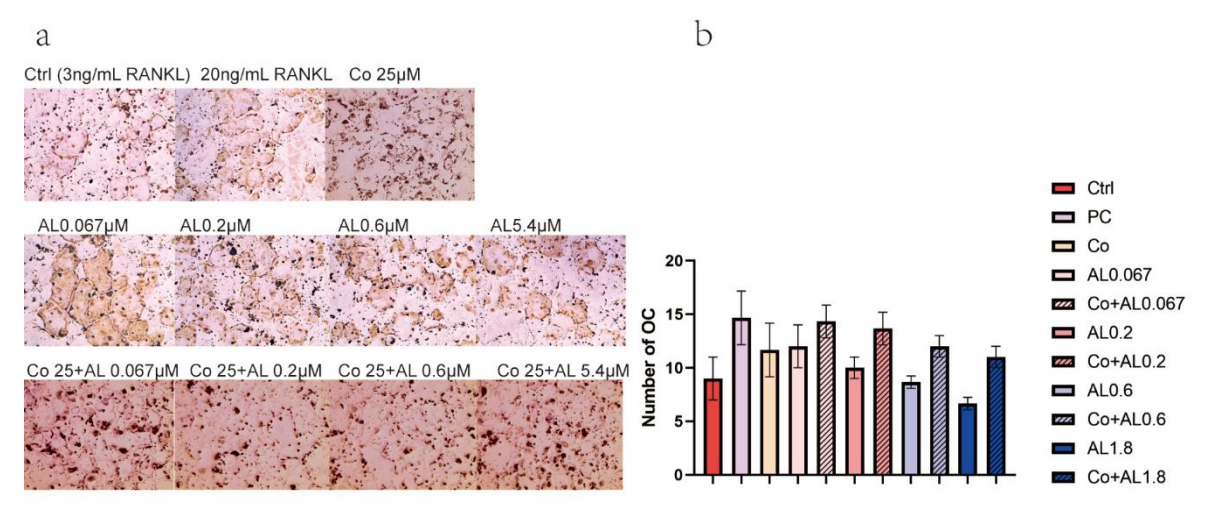


Fig 7.6. TRAP staining of AL- and Co-treated OCs. No significant difference was observed among the OCs treated with AL and AL combined with Co (25 μ M), or among the treated OCs and the control. (Number of wells=3).

7.5.5 Effect of DFO on ZA-treated OC TRAP staining

TRAP staining revealed that ZA inhibited OC formation. On day 5, ZA (0.6 and 1.8 μ M) significantly decreased the number of OCs (P<0.01 and P<0.001, respectively). DFO (5 μ M) significantly increased the number of OCs, compared to the control (P<0.0001). The addition of DFO (5 μ M) significantly reversed the decrease in the number of OCs after ZA (0.067, 0.2, 0.6, and 1.8 μ M) treatment (P<0.0001, P<0.0001, P<0.05, and P<0.05, respectively) (Fig 7.7).

a b

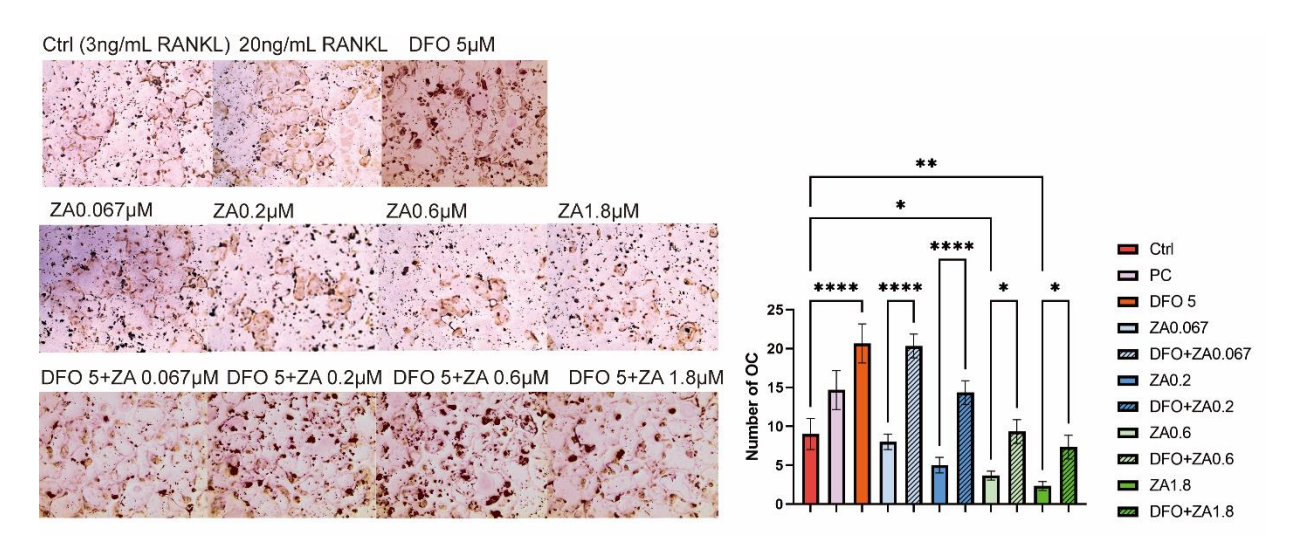


Fig 7.7. TRAP staining of OCs treated with ZA and ZA+DFO. ZA (0.6 and 1.8 μ M) significantly decreased the number of OCs. DFO (5 μ M) significantly increased the number of OCs, compared to the control. The addition of DFO (5 μ M) significantly increased the number of OCs after ZA (0.067, 0.2, 0.6, and 1.8 μ M) treatment. (Number of wells = 3). *, P<0.05. **, P<0.01. ***, P<0.001. ****, P<0.001. ****, P<0.0001.

7.5.6 Effect of DFO on AL-treated OC TRAP staining

TRAP staining showed that none of the AL concentrations changed the number of OCs. In contrast, compared to the control, DFO (5 μ M) significantly increased the number of OCs (P<0.0001). The addition of DFO (5 μ M) significantly increased the number of OCs that were treated with different concentrations of AL (P<0.001) (Fig 7.8).

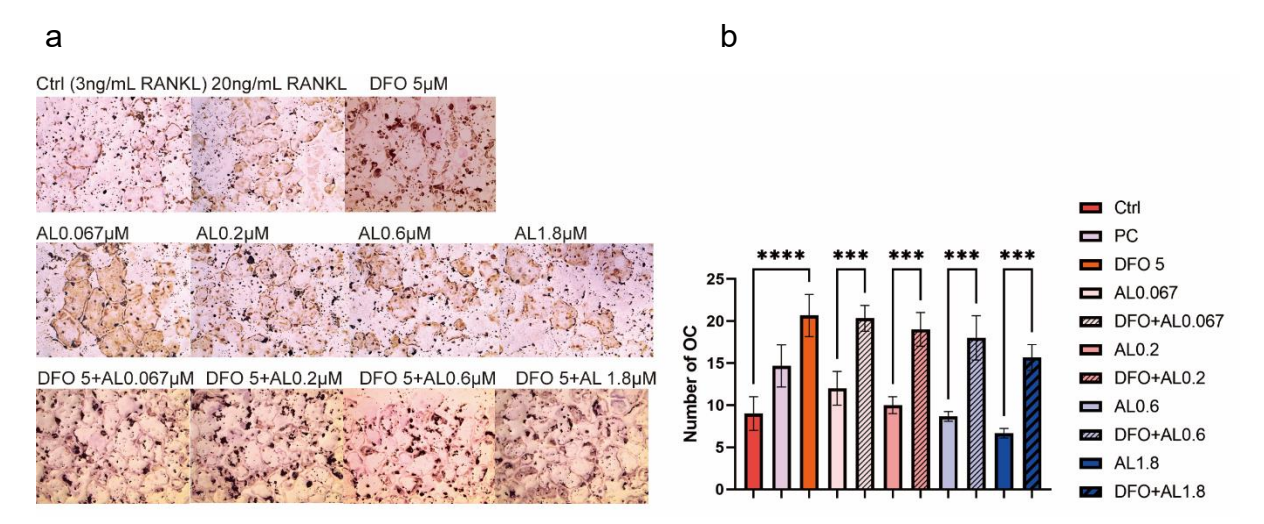


Fig 7.8. TRAP staining of OCs treated with AL and AL+DFO. None of the AL concentrations changed the number of OCs. DFO (5 μ M) alone and in addition to AL significantly increased the number of OCs. (Number of wells = 3). ***, P<0.001.

7.6 Discussion

7.6.1 Mechanism through which Co affects OC ROS

ROS availability is important for OC differentiation and inhibition of ROS has been demonstrated to inhibit OC differentiation (examples). Indeed, recent work with our group has shown that inhibition of ROS with oxygen scavengers or Si ions (via inhibition of the Fenton reaction) reduces OC generation [1]. Here we show the opposite that an inhibition of ROS with Co and DFO increased OC formation. It has been reported that Co ions increase ROS of Raw264.7 macrophages [580], Jurkat cell lines [581] and PC12 cells [582]. Moreover, Co is categorised as a d-block metal ion, like other transition metals, and it holds significant application value in chemical and catalytic reactions. Co ions can initiate the release of iron, thereby stimulating the Fenton reaction [583], which increases ROS production. *C. elegans* studies have revealed that this process might be mediated by mitochondrial-associated mechanisms [584]. In addition, Co works as a PHD inhibitor, mimicking hypoxia and leading to ROS generation via the HIF pathway [585-587].

7.6.2 Mechanism through which Co affects OC TRAP 5b activity and OC formation

Our results showed Co did not significantly change OC TRAP 5b activity or OC cell formation on day 5. Hypoxia and HIF mimics have been reported to increase OC differentiation both *in vitro* and *in vivo*. TRAP staining of bone marrow macrophages (BMM) from C57BL/6 mice has shown that TRAP activity and resorption measurement can be elevated by Co ions released from BG [588]. Co ions can also enhance osteolysis and aseptic implant loosening by affecting OC function via the HIF pathway [589]. The difference between our results and those of previous studies may be a result of the differences in cell types and assays used. TRAP activity includes TRAP 5a and TRAP 5b activity, and TRAP 5b has been reported as a sensitive parameter for monitoring OC activity [590, 591].

7.6.3 Mechanism through which Co reverses BP-induced ROS increase in OCs The addition of Co (25 µM) to ZA- and AL-treated OC can significantly reverse the

increased ROS production. N-BPs are reported to induce oxidative stress via the ROS pathway [506, 507]. Co has been reported to have a dual effect on ROS production. As an OB-OC cross talk agent, ROS is required in the process of OC formation, However, excessive ROS can also lead to disturbance of cellular functions. The accumulation of mitochondrial ROS cause damage to proteins, nucleic acids, lipids, membranes and organelles, which can lead to activation of cell death processes such as apoptosis [592]. Co protoporphyrin can reduce cellular ROS levels by mediating antioxidative genes [593]. However, Co has also been reported to induce cell apoptosis by increasing mitochondrial ROS [594]. For the first time, our results have shown that Co can reverse BP-induced increase in ROS production. While the exact pathway remains unknown, this offers a new potential therapeutic approach.

7.6.4 Mechanism through which Co reverses the inhibition of TRAP 5b activity and OC formation by BP

The addition of Co (25 µM) to ZA- and AL-treated OC significantly reversed the inhibition induced by ZA and AL. Therefore, Co can partially mitigate the ZA- and AL-induced damage to OC differentiation. Currently, BP is considered to inhibit OC by interfering with the mevalonate pathway. As an HIF mimetic, the mechanism through which Co affects this pathway remains unclear. Reports have shown that Co increases enzymes involved in the mevalonate pathway in *Fusarium graminearum* and the halophilic archaeon *Halolamina pelagica* CDK2 [595, 596]. However, no direct evidence of the mechanism through which Co influences the cellular mevalonate pathway has been reported.

7.6.5 Mechanism through which DFO affects OC ROS

DFO is an iron chelator and can reduce cellular ROS levels by inhibiting the Fenton reaction. The effect of DFO on ROS can be bilateral. Research has shown that DFO can also increase cellular and mitochondrial ROS in MCF-7 cells [597]. However, our results revealed that DFO (5 μ M) did not change total ROS or ROS per unit DNA in OCs, compared to the control. This could be a result of the differences in seeding

density, the time point of the assay, and the cell types used.

7.6.6 Mechanism through which DFO affects OC TRAP 5b activity and OC formation

The addition of DFO (5 μ M) to ZA- or AL-treated OCs can partly reverse the inhibition of TRAP 5b activity and OC formation by BPs. This indicates that ZA and AL may decrease OC differentiation as HIF inhibitors, which could in turn be reversed by HIF mimetics such as DFO. The number of OCs increased significantly by adding DFO (5 μ M). This is the first report of BPs and DFO exerting adverse effects towards each other. This can help develop potential therapeutic targets.

7.6.7 Mechanism through which DFO reverses BP-induced ROS increase in OCs

The addition of DFO (5 μ M) can reverse the elevated ROS production induced by ZA or AL. Considering no difference has been observed between the OCs treated with DFO (5 μ M) and the control, DFO may exert its ROS scavenger role above a particular threshold, such that when ROS accumulation reaches a specific level, it can be scavenged by DFO. However, there are no previous reports on the same.

7.6.8 Correlation between TRAP 5b activity and OC cell number

Our results demonstrate differences between TRAP 5b activity and the number of OC cells. Regarding the effect of Co treatment on TRAP 5b, we observed an elevation in the 0.067 µM ZA group, but TRAP staining did not reveal any differences. Conversely, in the 1.8 µM ZA group, although TRAP staining indicated an increase in OC formation under Co treatment, there was no significant difference in TRAP 5b activity. This suggests that the TRAP 5b assay may have a narrower detection range compared to TRAP staining and is more sensitive to subtle changes.

Furthermore, the TRAP 5b assay demonstrated that Co can restore the inhibitory effects of all AL concentrations, but TRAP staining did not reveal any significant differences. This indicates that the TRAP 5b assay detects restorative effects within a narrower concentration range. However, at high toxic concentrations (1.8 µM ZA), the

TRAP 5b assay did not show any response, whereas TRAP staining revealed differences.

Additionally, our findings for DFO also exhibited differences between the results of the TRAP 5b assay and TRAP staining. The TRAP 5b assay did not show any difference between the 5 μ M DFO and 5 μ M DFO + 1.8 μ M ZA groups, whereas TRAP staining revealed differences, similar to the results for Co. This suggests that TRAP 5b may not respond when cell toxicity reaches a threshold, whereas TRAP staining can still provide relevant information.

Chapter 8. Overall discussion

This study investigated the effects of BPs on bone cells and demonstrated that BPs have a concentration-dependent effect on metabolic activity, proliferation, ROS production, inhibited *in vitro* bone formation and OC differentiation. This thesis also explores the potential of ionic therapies (Si and Co ions) to restore the function of BP-treated OBs and OCs. Our findings revealed that Si treatment restored early bone formation (day 7), possibly by decreasing the ROS levels. Additionally, Co (and the iron chelator DFO) restored ZA-inhibited OC differentiation. This chapter discusses the possibility of using a combination of therapeutic ions to treat BRONJ, the limitations of the current study, the validity and need for improvement in *in vitro* models of ONJ, and future research directions.

8.1 Limitations of the methodological approaches

This study had several limitations. First, only *in vitro* studies were conducted during the experimental period. As discussed previously, *in vitro* studies do not accurately reflect the complex environment of living organisms, and the results obtained may not be representative of the actual interactions and processes that occur *in vivo*. Additionally, the use of isolated OB and OC may not fully capture the complexity of the multiple cell types present in the bone tissue. The simpler, *in vitro* models, do however, allow greater understanding of the impact of different factors on cell function.

8.1.1 Validity of the in vitro bone models

This thesis demonstrates the potential for therapeutic ions (Si and Co) to help restoring BP-treated bone cell function using *in vitro* models. The relevance of the model to *in vivo* ONJ could be improved. This study used immortalised cells (SaOs-2 cells and Raw264.7 cells) and primary rodent cells (neonatal rat calvarial OB model, as described by Orriss et al. [598]). Human primary OBs and OCs would be ideal for studying bone formation and resorption due to their species-specific characteristics.

Human primary OBs and OCs have the advantage for studying BRONJ and studying bone formation/resorption owing to their species-specific characteristics. Human OBs, however, exhibit higher variability within a single isolation population and between individuals from which they were isolated [599]. They also have reduced bone formation capacity than the established rat model used in our study [600, 601]. It is important to have repeatability in the testing in vitro effects and also to be able to reliably form bone, if studying bone formation. Similarly, human OCs differ from rodent OCs in morphology [602], differentiation markers [414], bone resorption capacity [603], and expansion potential [604]. However, the use of human cells presents specific challenges, in terms of variability between patients [605], expansion potential [606] and availability [607]. The Raw264.7 cell line is the most commonly used OC cell line in the literature and overcomes some of the limitations of the primary monocytes in terms of variability and expansion potential; however, there is considerable debate as to whether the cell line is capable of producing bone resorbing OCs (Hume 2002, Cuetara 2006). It has been reported that the Raw264.7 cell line remains heterogeneous, meaning the percentage of RANKL-sensitive cells varies with the cell culture and passage number/conditions [511, 608]. Therefore, a more stable OC cell line with improved bone resorption capacity is needed. The tissue source of the bone cells may be also be important for the relevance of the in vitro models. In our study we used cranial derived bone cells. Jaw bone is reported to be a combination of intermembranous and endochondral ossification [609] and OB derived from the jaw have been shown to have specific differences to other bone cells [610, 611], these include higher osteogenic potential, augmented capacity and lower rate of collagen maturation. In our study, comparing OB from the mandible and long bones could be the next experimental step to investigate the role of regional specific factors in BRONJ development. The multicellular environment, particularly the presence of proinflammatory cells in affected tissues, plays a crucial role in BRONJ development [612]. Studies have reported increased levels of both systemic and local inflammation in patients with BRONJ [613], suggesting that incorporating specific inflammatory cells or related cytokines could improve the relevance and complexity of the BRONJ model.

8.1.2 Two dimensional (2D) or Three dimensional (3D) in vitro models?

In vitro bone formation has been shown to be influenced by environmental conditions (pH, oxygen levels, temperature, etc.) [351, 614, 615] and the physicochemical environment (e.g. mechanics and whether on a 2D or 3D environment). Payr et al (2021) compared 2D- and 3D-cultured OBs (on polystyrene) derived from elderly females and found that the 3D-cultured OBs exhibited significantly higher levels of osteogenic markers (OPG, Col1, and OP) compared to their 2D counterparts (OPG, Col1, and OP) [616]. In a study by Buttery et al., the osteogenic differentiation of embryonic stem cells was enhanced in 3D environments compared to 2D environments [617]. OC activity has also been investigated in 2D and 3D environments. Kleinhans et al., conducted a study using human monocyte-derived OCs cultured in both 2D and 3D systems and found that larger OCs were formed in 3D culture, but no significant difference was observed in terms of the sealing zone and resorption activity [618].

OB and OC co-culture systems have also been used and may provide a more comprehensive understanding of bone remodelling mechanisms and bone-related diseases [619]. In 2D co-culture models, OBs and OCs can be direct-contact cultures, or separated spatially through the use of semi-permeable membranes (e.g. Transwell® plates) [620]. Direct 2D models, however, allow for direct cell interaction, usually achieved by seeding both bone-building and bone-resorbing cells in the same culture container [621]. Co-culture systems also require similar cell culture media, which poses practical problems *in vitro* where the functionality of both OB and OCs, require different supplements.

8.1.3 Bone characterisation approaches

In vitro bone nodules can be characterised using various methods, such as calcium staining, measurement of physical size, and analysis of inner structures. Alizarin red staining (ARS) is a commonly used *in vitro* approach to investigate bone formation and stain calcium. According to our literature review, 12/123 studies used ARS to measure calcium storage, and 4/123 used Von Kossa staining, (which detects calcium

and phosphate deposition). No studies were, however, found that provided a robust analysis of the biochemical or physicochemical properties of the bone, or the volume of bone formed in response to BPs. Both ARS and Von Kossa staining can be semiquantitatively measured using software, such as ImageJ, or by dissolving the dyes for quantitative analysis. Analysis of the stained area can provide data for comparing the mineralisation levels between conditions. However, a major limitation of the use of calcium and phosphate stains is that they cannot distinguish between other mineral salts that may spontaneously form in cell cultures with high calcium and phosphate levels (e.g. calcium carbonate). Research within our group has shown alizarin staining of dystrophic minerals/apatite surrounding cells as opposed to extracellular mineralised collagen fibres, as found in bone. Furthermore, these methods cannot distinguish between different types of mineralisation, such as hydroxyapatite and other calcium phosphates. Or if the mineral is embedded within the collagen fibres, like bone. It would have been beneficial to examine the ultra-structure of the bone through TEM and/or biochemically characterise the formed bone using either FTIR or Raman spectroscopy [622, 623]. TEM facilitates the determination of HA crystals within the ECM, whereas biochemical analysis facilitates the comparison of both proteins and minerals present compared with native bone [624].

8.1.4 Lack of in vivo data

Due to limited resources during the pandemic, this thesis did not include *in vivo* data. Currently, animal research has played a pivotal role in understanding the mechanism of BRONJ, particularly in the development of complex models and investigation of human-observed risk factors. These models involve creating osteoporosis or cancer models, followed by the induction of ONJ, often in combination with or without oral infection or dental extraction as triggers. Through animal models, it is possible to determine the *in vivo* dose range of BP that induces BRONJ, study comprehensive pathogenic mechanisms and risk factors, and test corresponding preventive and therapeutic measures.

To find out the existing knowledge of model building, a search in the Web of Science

using terms related to *in vivo* studies and MRONJ yielded 272 papers⁴. Holtmann et al. conducted a review of studies on both *in vitro* and *in vivo* BRONJ models up to June 2018. Out of 139 studies, 87 were conducted *in vivo*, 46 were *in vitro*, and six involved both *in vivo* and *in vitro* experiments [625]. They compared 93 studies that utilised animals, including rats (n=46), mice (n=30), dogs (n=6), minipigs (n=3), sheep (n=2), and rabbits (n=1). Their findings were in line with what has already been observed in patients [117, 626, 627] undergoing BP therapy: tooth extractions appear to significantly increase the susceptibility to ONJ in rodents, particularly in rats. Furthermore, all three minipig models confirmed that the administration of BPs, in combination with tooth extractions, induces BRONJ [628-630]. Aguirre et al., after reviewing 240 studies (including BP and other medications inducing ONJ) up to June 2021, similarly as Holtmann's review, concluded that larger species provided accurate clinical and histopathological outcomes, and rodent models also proved reliable, as they were all able to generate necrotic jaw-bones under BP and inflammation intervention, with or without tooth extraction [631].

Base on the findings from the above animal studies, appropriate plan to acquire *in vivo* data for future study can be designed. These including animal and intervention selections, dosage of timing of medications, with or without tooth extraction. In addition, as mentioned in chapter1, there was less cancer models compared to osteoporosis models, despite cancer patients have much higher incidence of MRONJ.

8.1.5 Lack of mechanistic studies

While this thesis identifies potential pathways through which therapeutic ions exert their effects, it lacks a detailed mechanistic test for the *in vitro* bone model. Although our previous study showed that the bone nodule formed by rat OB has similar components, inner structure, and surface morphology to real bone, as confirmed by TEM, Raman, and SEM analysis [351], mechanistic tests are necessary to quantify

-

^{**}Web of science database has been searched to get an overview of this research field. From 2009 to 2023, the results of searching strategy "BRONJ OR MRONJ* (Topic) AND "in vivo OR animal OR rat OR mice OR dog OR minipigs OR sheep OR rabbit (Topic)".

the impact of BP on bone mechanical properties. Currently, techniques such as bending, compression, torsion, tensile and shear test are frequently used to measure the mechanical properties of bone replacement materials [632-635]. In future studies, these mechanistic analyses will be performed on *in vitro* models treated with BP and ions to further investigate their impact.

8.2 Therapeutic ions

8.2.1 Regulation of OB and OC

Inhibited bone remodelling may play an essential role in the pathophysiology of BRONJ (Chapter1, section 1.1.4). Therefore, targeting the balance between bone formation and resorption (and OB-OC cross talk) through the release of ions may prove to be a promising approach for restoring bone formation. BPs, as reported in this thesis and previously [456, 562] increase ROS production. While ROS is an essential component of cell metabolism and OC differentiation [636] and as a signalling factor [636] high levels of ROS can be toxic. Su et. al. (2020) investigated the potential of BBGs as a management strategy for BRONJ. Their study, conducted in an animal model, demonstrated that BBG administration significantly reduced the incidence of BRONJ-like lesions by decreasing ROS levels [81]. Si may also act as a ROS scavenger. Kakabadse et al. (1960) previously discussed the antioxidant capabilities of Si, highlighting its role in the reaction between Na₂SiO₃ and H₂O₂ [637]. By reducing the available ferrous ions, Si can diminish free radical production by inhibiting the Fenton reaction. This effect has been observed in environmental studies, particularly in water treatment, where dissolved SiO₂ enhanced the stability of H₂O₂ in groundwater containing ferrous iron [638].

Si has also been shown to increase the activity of antioxidant enzymes, such as superoxide dismutase, catalase, and glutathione peroxidase, which help to further scavenge ROS and protect against oxidative damage [639]. The combination of metal ion binding and increased antioxidant enzyme activity makes silicate an effective ROS scavenger.

Similarly, Co acts as HIF mimetics by directly stabilising the HIF protein, thereby

enhancing its activity and promoting downstream effects typically observed in response to low oxygen levels. Co stabilises HIF by replacing iron in the HIF molecule and preventing its destruction by the Von Hippel-Lindau (VHL) protein, a key component of the oxygen-sensing pathway [640]. In contrast, DFO chelates iron, reducing cellular iron levels, and stabilising HIF [641]. Once stabilised, HIF-1α can indirectly promote OC differentiation and function via various pathways. It can upregulate the expression of genes associated with OC activity, such as RANKL, VEGF, and pro-inflammatory cytokines, leading to increased bone resorption [563]. As discussed in Chapter 6, BP can mediate HIF-1α through multiple pathways. Ge et al., found that ZA decreased HIF-1α protein levels in HUVEC cells through the PI3K/AKT/mTOR and MAPK pathways, but had no effect on HIF-1α mRNA levels or promoter activity [642]. Li et al., cultured SH-SY5Y cells with cobalt and etidronate and found that etidronate alleviated the cobalt-induced increase in HIF-1α [643]. BP mediates OC by decreasing RANKL expression [644]. Although it is difficult to determine whether BP-induced MRONJ occurs through the HIF pathway, HIF mimetics can be used to restore BP-induced OC inhibition. Further studies are necessary to elucidate the interactions among HIF, RANKL, and BRONJ.

In conclusion, Si and Co ions are playing different roles in restoring BP inhibited bone regeneration: Si is for OB and Co is for OC. Although studies has proved Co is also promoting OB activity and bone forming [351], Si can reduce OC differentiation via inhibiting Fenton reaction. In addition, the releasing rate of Si and Co are different. It has been reported the dissolution of Si was around 9–16 mg/l for the slower flow rate, 0.04 ml/min, at 24 h [645]. The different characteristics of Si and Co require further studies on the cooperation approaches to optimizing the regenerative effect of BGs.

8.2.2 Concerns and toxicity of using ions in clinical settings

Although the therapeutic ions have been tailored into BGs for medical use for years, there are concerns that they may be toxic to the human body. Therefore, the dosage and releasing rate of BGs are essential in clinical settings. Regarding Si, the review work within our group showed that *in vitro* [Si] above 52 ppm is more likely to generate

undesirable outcomes, while [Si] below 30.2 ppm would cause desirable cellular responses [311]. And for Co, the 13-93B3 BBG has been used soft tissue regeneration, and no signs of cytotoxicity were observed for 100 μ g/ml particle concentrations on MG-63 cells [646], 125 μ g/ml for HUVECs cells [647].

It has been confirmed that both the Si-containing 45S5 and Co-containing 13-93B3 BGs are safe for patients, but the long-term effect of ions has also raised concerns. BGs release ions at a steady rate, which can range from a few hours to several months [648]. However, load-bearing devices that can be used in orthopedics over the long term and have the ability to regenerate living bone are not yet available clinically [262]. Therefore, for future studies, further investigation into the long-term effects of BGs and ions is necessary.

8.3 Potential confounding factors of this thesis

The potential confounding factors in this thesis include variations in cell types and the limited sample size. Firstly, the SaOs-2 cells used in the study were at passage numbers ranging from 11 to 14. Due to the repetition of experiments and the long duration of the pandemic, not all cells were from the same passage number, resulting in variations among passages. Additionally, the Raw 264.7 cells used are known for their high heterogeneity, and variations among cell clusters may introduce bias. To mitigate this, we utilized the screened OC subclone of Raw 264.7 cells for the OC study, which significantly reduces the chance of bias. Secondly, the limited sample size (4 biological repeats and 3 technical repeats) may also lead to bias. A larger sample size with statistical approach is necessary for future studies in order to obtain more reliable and robust results.

8.4 Future work

8.4.1 Experiments to confirm findings

The future research plan includes further understanding of the mechanism of BRONJ and how ions work, as well as exploring the repurposed use of BGs for both prevention and treatment of BRONJ (Fig 7.1). A gene array would allow analysis of how BPs affect

bone cells and how therapeutic ions prevent or restore bone formation. According to our literature review, the expression of genes involved in bone remodelling, angiogenesis, and oxidative stress is affected by BP interventions. Further studies are required to investigate the effects of Si on early bone formation. These include the measurement of BMP2, BMP4, ALP, and COL1 expression. It is also important to note that if Si and Co are released from BG materials, the effects of other ions present in the BG dissolution products (e.g. Ca, P, and Na) on BP-treated cells should be considered. Previous studies have shown that Ca and P, released from bioceramics, can affect bone formation [649, 650]. Moreover, the combination of different ions may cause different bone responses [651].

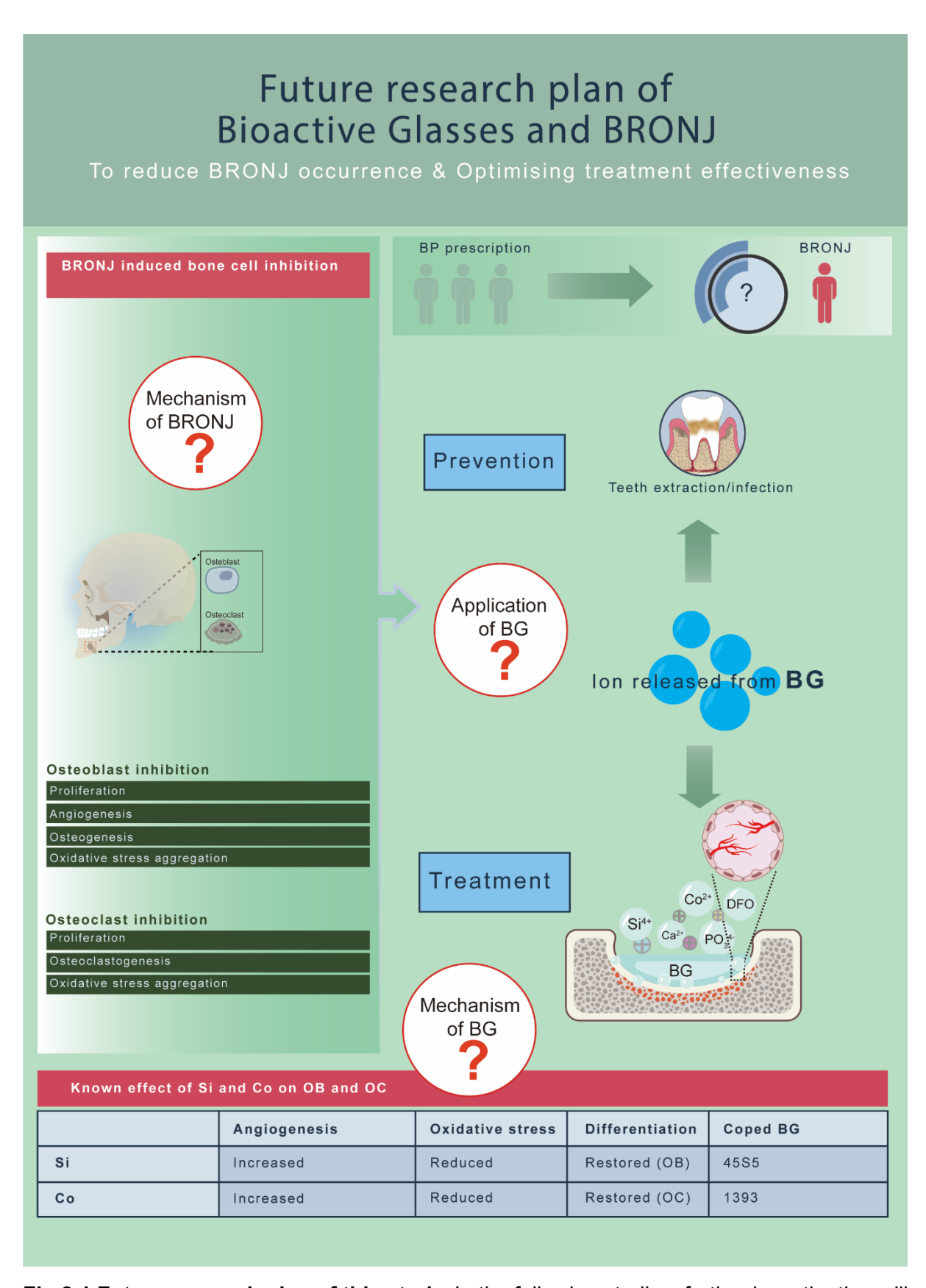


Fig 8.1 Future research plan of this study. In the following studies, further investigation will be carried out to understand the mechanism of BRONJ and how ions work. Additionally, the potential repurposing of currently used BGs for the prevention and treatment of BRONJ will

be explored.

Finally, a BRONJ animal model was established to test the *in vivo* effects of ions and BGs. Based on the literature, a normal rodent model with BP injection can be used as an osteoporosis BRONJ model, and tumour-bearing rodents combined with BP injection can be used as a cancer BRONJ model.

8.4.2 Application of ionic therapy to prevention and treatment

This thesis investigated the ions (Si and Co) individually, as opposed to multiple ions released from BGs. This innovative approach allows for the tailoring of BGs with specific ion release profiles for different patient cohorts and the development of new BGs capable of releasing different therapeutic components, such as Si and Co, at various stages of BRONJ. For instance, the release of Si may be targeted towards the early stages of BRONJ, as it can reverse the inhibition of collagen formation induced by BPs, and Co intervention may be released prior to the release of other ions that promote osteogenesis, which could be achieved by manufacturing bi-layered BG particles or bioactive additive manufacturing processes utilising different materials. Invasive dental procedures (e.g. tooth extraction and implantation) increase the risk of BRONJ [652]. As a preventive measure, BG with therapeutic ions can be applied to the surgical area to promote bone remodelling and decrease oxidative stress. In addition, BG can be combined with surgical intervention to treat existing necrotic bones.

Beyond the aspects of BRONJ discussed in this thesis, newer OC-targeting drugs associated with MRONJ require further investigation. While BPs are known to cause MRONJ, other cancer drugs have been reported to induce ONJ, including monoclonal antibodies, such as denosumab, rapamycin inhibitors, such as everolimus, TNF- α inhibitors, such as adalimumab, and tyrosine kinase inhibitors, such as sunitinib [63]. Therapeutic ions may need to be tailored to MRONJ induced by different drugs; for instance, DMB, the second most common drug that induces MRONJ, inhibits OC by targeting RANKL; therefore, therapeutic agents that stimulate RANKL, such as HIF

mimetics, may be effective. Everolimus targets the mTOR pathway; therefore, Sr-substituted 45S5 may be a potential treatment option because Si-45S5 can enhance bone regeneration via the Akt/mTOR pathway [358].

While ions and BG may be considered as management strategies for both the prevention and treatment of MRONJ, it is important to balance the effects of drugs and ions. For example, ions released from BG may reduce the anticancer effects of drugs or neutralise the OC inhibition effects necessary for osteoporosis treatment. Additionally, the timing of ion and BG application should be carefully considered depending on whether they are intended for treatment or prevention. Therefore, it is crucial to conduct an assessment to determine an appropriate approach.

8.5 Conclusion

In conclusion, BRONJ is a rare but challenging condition without an effective treatment. The roles of BP-induced OB and OC inhibition in the onset and progression of BRONJ have been established. The development of materials that can restore both OB and OC functions through ion release in a BG model has the potential to provide promising approaches for the prevention and treatment of BRONJ. This research highlights the need for an *in vitro* model that mimics BRONJ and the importance of the locally controlled release of therapeutic ions from BG. The development of this model will allow for a deeper understanding of the pathophysiology of BRONJ and the development of effective therapies.

Appendix A.

Table A-1 *In vivo* studies of TE strategies for MRONJ

		Prevention	Cell/growth factor				
	Animal	or Treatment	or material application	Interventions	Medication	Possible pathways	Ref
2023	Rodent	Prevention	Cell/growth factor	exosome from Adipose tissue-derived mesenchymal stromal cells (MSC(AT)s)	ZA	Cell viablity, migration, osteogenesis and inflammation	[228]
2023	Rodent	Prevention	Material	multifunctional composite hydrogel	ZA	Macrophage polarisation, osteogenesis, bacteriostasis and inflammation	[231]
2022	Rodent	Prevention	Material	Biodegradable Mg implant	ZA, ZA+ VEGFR inhibitor	VEGF, calcitonin gene-related peptide (CGRP)	[513]
2022	Rodent	Prevention	Material	HA and/or collagen sponge	ZA	Osteogenesis, inflammation	[653]
2022	Rodent	Treatment	Cell/growth factor	Angiogenesis factor (A- Heal) or ABMDO (Autologous Bone Marrow Derived Osteoblasts)	ZA	Osteogenesis, angiogenesis	[654]
2022	Rodent	Treatment	Cell/growth factor	Surgical resection followed by applying A- PRF or L-PRF reinforced by PBM	ZA	autologous platelet concentrations (APC) products	[655]
2022	Rodent	Prevention	Material	Beta tricalcium phosphate	ZA	Osteogenesis	[656]
2021	Rodent	Treatment	Cell/growth factor	hUC-MSCs intravenously to rat	ZA	Osteogenesis, osteoclastogenesis and PTH pathway	[224]
2021	Rodent	Prevention + Treatment	Cell/growth factor	BMP-2	ZA/cyclophosph amide	Osteogenesis, angiogenesis	[657]
2021	Rodent	Prevention	Cell/growth factor+material	PRP	ZA	APC products	[658]

2021	Rodent	Prevention	Cell/growth factor	dental pulp stem cell- conditioned medium	ZA	Osteogenesis and angiogenesis	[659]
2021	Rodent	Prevention	Cell/growth factor	Small extracellular vesicles derived from adipose tissue (sEV-AT)	ZA+Dex	Angiogenesis	[660]
2021	Rodent	Treatment	Cell/growth factor	Surgical remove+platelet-derived growth factor-BB (PDGF-BB)	ZA	Osteogenesis and angiogenesis	[661]
2021	Rabbit	Treatment	Cell/growth factor	huamn ADSC transplantation	ZA	Osteogenesis and osteoclastogenesis	[232]
2021	Rodent	Prevention	Cell/growth factor	VEGF	ZA	Osteogenesis, angiogenesis and inflammation	[662]
2020	Rodent	Prevention	Cell/growth factor	Extracellular Vesicles of Stem Cells	ZA	Osteogenesis, angiogenesis and inflammation	[225]
2020	Rodent	Prevention	Cell/growth factor+ material	Allogeneic Bone Marrow Mesenchymal Stem Cell	ZA	Osteogenesis and angiogenesis	[663]
2020	Rodent	Prevention	Material	Calcium Phosphate Ceramic	ZA	Osteogenesis	[514]
2020	Rodent	Prevention	Cell/growth factor	β-ТСР	ZA	Osteogenesis	[664]
2020	Rodent	Prevention	Cell/growth factor	EPC conditioned media or endothelial growth media (EGM-2)	ZA+Dex	Angiogenesis	[233]
2019	Rodent	Treatment	Cell/growth factor + hydrogel	Adipose-Derived Stem Cells and BMP-2	ZA	Osteogenesis, osteoclastogenesis, OB- OC cross talk and angiogenesis	[665]
2019	Rabbit	Prevention	Cell/growth factor	Adipose-derived stem cells	ZA+Dex	Osteogenesis, gingival wound healing	[666]
2019	Rodent	Prevention	Cell/growth factor	autologous PRP	ZA	Osteogenesis and angiogenesis	[667]
2019	Rodent	Prevention	Cell/growth factor+ chitosan	human parathyroid hormone (hPTH)	ZA	hPTH pathway	[668]
2019	Dog	Prevention	Cell/growth factor	Allogeneic multipotent mesenchymal stromal cell sheet	ZA+Dex	Osteogenesis and inflammation	[240]

2019	Rodent	Prevention	Cell/growth factor+ hydrogel Cell/growth	bFGF	ZA	Osteogenesis	[669]
2019	Rodent	Prevention	factor+ hydrogel	rhBMP-2	ZA	Osteogenesis and osteoclastogenesis	[226]
2019	Rodent	Prevention	Cell/growth factor	supernatant of Human Dental Pulp Stem Cells	ZA	Osteogenesis, osteoclastogenesis and OB-OC cross talk	
2018	Rodent	Treatment	Cell/growth factor	Cytokine Mixtures Mimicking Secretomes from MSC	ZA+Dex	Osteogenesis, osteoclastogenesis and angiogenesis	[670]
2018	Rodent	Prevention	Cell/growth factor	noncultured stromal vascular fraction (SVF) cells transplantation	ZA+ cyclophosphami de	Osteogenesis, osteoclastogenesis and angiogenesis	[671]
2017	Rodent	Prevention	Cell/growth factor+ collagen sponge	rhBMP-2	ZA	Osteogenesis and inflammation	[672]
2016	Rodent	Treatment	Cell/growth factor	Multipotent mesenchymal stromal cell sheet	ZA+Dex	Osteogenesis and angiogenesis	[241]
2015	Rodent	Treatment	Cell/growth factor	conditioned media from mesenchymal stem cells	ZA+Dex	Osteogenesis, osteoclastogenesis and inflammation	[242]
2015	Rodent	Prevention	Cell/growth factor	adipose-derived stem cells (ASCs) with or without previous stimulation with bone morphogenetic protein 2 (BMP-2) and platelet- rich plasma (PRP)	ZA	Osteogenesis	[673]
2013	Minipig	Treatment	Cell/growth factor	Allogeneic BMMSC transplantation via intravenous infusion	ZA	Osteogenesis, osteoclastogenesis and inflammation	[674]
2010	Rodent	Prevention + Treatment	Cell/growth factor	Systemic infusion with mesenchymal stem cells (MSCs)	ZA+Dex	Immunomodulatory	[675]

References

- 1. Li, A.Y., *Understanding the role of orthopaedic implant dissolution ions in bone remodelling*, in *Division of Surgery*. 2019, University College London: London, UK.
- 2. Ruggiero, S.L., et al., American Association of Oral and Maxillofacial Surgeons position paper on bisphosphonate-related osteonecrosis of the jaws--2009 update. J Oral Maxillofac Surg, 2009. **67**(5 Suppl): p. 2-12.
- 3. Lo, J.C., et al., *Prevalence of Osteonecrosis of the Jaw in Patients With Oral Bisphosphonate Exposure.*Journal of Oral and Maxillofacial Surgery, 2010. **68**(2): p. 243-253.
- 4. Rogers, S.N., et al., A survey of consultant members of the British Association of Oral and Maxillofacial Surgeons regarding bisphosphonate-induced osteonecrosis of the jaws. British Journal of Oral and Maxillofacial Surgery, 2009. **47**(8): p. 598-601.
- 5. Gordon, B., WOMEN WORKERS AND OCCUPATIONAL-HEALTH THE VICTORY OF THE FRENCH MATCH WORKERS OVER PHOSSY-JAW. Mouvement Social, 1993(164): p. 77-93.
- 6. Steele, M.C. and F.A. Ive, *RECURRENT FACIAL ECZEMA IN FEMALES DUE TO STRIKE ANYWHERE MATCHES*. British Journal of Dermatology, 1982. **106**(4): p. 477-479.
- 7. Lopez, S. and D. Felsenberg, What is "phossy jaw"? Osteologie, 2012. 21(2): p. 70-71.
- 8. Marx, R.E., Uncovering the Cause of "Phossy Jaw" Circa 1858 to 1906: Oral and Maxillofacial Surgery Closed Case Files-Case Closed. Journal of Oral and Maxillofacial Surgery, 2008. **66**(11): p. 2356-2363.
- 9. Isaac, S. "Phossy jaw" and the matchgirls: a nineteenth-century industrial disease. 2018; Available from: https://www.rcseng.ac.uk/library-and-publications/library/blog/phossy-jaw-and-the-matchgirls/.
- 10. Carlton, G. *Inside 'Phossy Jaw,' The Deadly Condition That Plagued 19th-Century Matchstick Girls*. 2021; Available from: https://allthatsinteresting.com/phossy-jaw.
- 11. Lehmann, E., *Phosphorus and evil match industry.* University of Saskatchewan Undergraduate Research, 2017. **3**(2).
- 12. de Meijere, A., *Adolf von Baeyer: Winner of the Nobel Prize for Chemistry 1905*. Angewandte Chemie-International Edition, 2005. **44**(48): p. 7836-7840.
- 13. Francis, M.D. and D.J. Valent, *Historical perspectives on the clinical development of bisphosphonates in the treatment of bone diseases.* Journal of Musculoskeletal & Neuronal Interactions, 2007. **7**(1): p. 2-8.
- 14. Von Baeyer H, H.K., *Acetodiphosphoriga sauer*. Ber, 1897. **30:1973**.
- 15. Blaser B, W.K., Germscheid HG, Wollmann K, *Ueber 1-Hydroxyalkan-1,1-diphosphonsäuren.* Z Anorg Allg Chem, 1971. **381**: p. 247-259.
- 16. Francis, M.D., J.A. Gray, and W.J. Griebstein, *The Formation and Influence of Surface Phases on Calcium Phosphate Solids*, in *Advances in Oral Biology*, P.H. Staple, Editor. 1968, Elsevier. p. 83-120.
- 17. Francis, M.D. and W.W. Briner, *EFFECT OF PHOSPHONATES ON DENTAL ENAMEL IN-VITRO AND CALCULUS FORMATION IN-VIVO*. Calcified Tissue Research, 1973. **11**(1): p. 1-9.
- 18. Fleisch, H., R.G.G. Russell, and M.D. Francis, *DIPHOSPHONATES INHIBIT HYDROXYAPATITE DISSOLUTION IN VITRO AND BONE RESORPTION IN TISSUE CULTURE AND IN VIVO*. Science, 1969. **165**(3899): p. 1262-8.
- 19. Bassett, C.A.L., et al., *DIPHOSPHONATES IN TREATMENT OF MYOSITIS OSSIFICANS*. Lancet, 1969. **2**(7625): p. 845-&.
- 20. Fogelman, I., et al., *The use of whole-body retention of Tc-99m diphosphonate in the diagnosis of metabolic bone disease.* J Nucl Med, 1978. **19**(3): p. 270-5.

- 21. Francis, M.D. and I. Fogelman, *99mTc Diphosphonate Uptake Mechanism on Bone*, in *Bone Scanning in Clinical Practice*, I. Fogelman, Editor. 1987, Springer London: London. p. 7-17.
- 22. Watts, N.B., et al., INTERMITTENT CYCLICAL ETIDRONATE TREATMENT OF POSTMENOPAUSAL OSTEOPOROSIS. New England Journal of Medicine, 1990. **323**(2): p. 73-79.
- 23. Storm, T., et al., EFFECT OF INTERMITTENT CYCLICAL ETIDRONATE THERAPY ON BONE MASS AND FRACTURE RATE IN WOMEN WITH POSTMENOPAUSAL OSTEOPOROSIS. New England Journal of Medicine, 1990. **322**(18): p. 1265-1271.
- 24. Bone, H.G., et al., *Ten years' experience with alendronate for osteoporosis in postmenopausal women.*New England Journal of Medicine, 2004. **350**(12): p. 1189-1199.
- 25. Saag, K.G., et al., *Alendronate for the prevention and treatment of glucocorticoid-induced osteoporosis.*New England Journal of Medicine, 1998. **339**(5): p. 292-299.
- 26. Cummings, S.R., et al., Effect of alendronate on risk of fracture in women with low bone density but without vertebral fractures Results from the fracture intervention trial. Jama-Journal of the American Medical Association, 1998. **280**(24): p. 2077-2082.
- 27. Liberman, U.A., et al., EFFECT OF ORAL ALENDRONATE ON BONE-MINERAL DENSITY AND THE INCIDENCE OF FRACTURES IN POSTMENOPAUSAL OSTEOPOROSIS. New England Journal of Medicine, 1995. **333**(22): p. 1437-1443.
- 28. Reginster, J.Y., et al., Randomized trial of the effects of risedronate on vertebral fractures in women with established postmenopausal osteoporosis. Osteoporosis International, 2000. **11**(1): p. 83-91.
- 29. Harris, S.T., et al., Effects of risedronate treatment on vertebral and nonvertebral fractures in women with postmenopausal osteoporosis A randomized controlled trial. Jama-Journal of the American Medical Association, 1999. **282**(14): p. 1344-1352.
- 30. Chesnut, C.H., et al., *Effects of oral ibandronate administered daily or intermittently on fracture risk in postmenopausal osteoporosis*. Journal of Bone and Mineral Research, 2004. **19**(8): p. 1241-1249.
- 31. Reid, I.R., et al., *Fracture Prevention with Zoledronate in Older Women with Osteopenia*. New England Journal of Medicine, 2018. **379**(25): p. 2407-2416.
- 32. Filleul, O., E. Crompot, and S. Saussez, *Bisphosphonate-induced osteonecrosis of the jaw: a review of 2,400 patient cases.* Journal of Cancer Research and Clinical Oncology, 2010. **136**(8): p. 1117-1124.
- 33. Ibrahim, T., L. Mercatali, and D. Amadori, *Bone and cancer: the osteoncology.* Clin Cases Miner Bone Metab, 2013. **10**(2): p. 121-3.
- 34. Sousa, S. and P. Clézardin, *Bone-Targeted Therapies in Cancer-Induced Bone Disease*. Calcified Tissue International, 2018. **102**(2): p. 227-250.
- 35. Hong, S., et al., Bone metastasis and skeletal-related events in patients with solid cancer: A Korean nationwide health insurance database study. PLoS One, 2020. **15**(7): p. e0234927.
- 36. Gastanaga, V.M., et al., *Prevalence of hypercalcemia among cancer patients in the United States.* Cancer Med, 2016. **5**(8): p. 2091-100.
- 37. Boussios, S., et al., *Metastatic Spinal Cord Compression: Unraveling the Diagnostic and Therapeutic Challenges.* Anticancer Res, 2018. **38**(9): p. 4987-4997.
- 38. Hameed, A., et al., *Bone disease in multiple myeloma: pathophysiology and management.* Cancer Growth Metastasis, 2014. **7**: p. 33-42.
- 39. Bernstein, Z.S., E.B. Kim, and N. Raje, *Bone Disease in Multiple Myeloma: Biologic and Clinical Implications*. Cells, 2022. **11**(15).
- 40. Diel, I.J., et al., *Improved quality of life after long-term treatment with the bisphosphonate ibandronate in patients with metastatic bone disease due to breast cancer.* European Journal of Cancer, 2004. **40**(11):

- p. 1704-1712.
- 41. Yuen, K.K., et al., *Bisphosphonates for advanced prostate cancer.* Cochrane Database of Systematic Reviews, 2006(4).
- 42. Costa, L. and P.P. Major, Effect of bisphosphonates on pain and quality of life in patients with bone metastases. Nature Reviews Clinical Oncology, 2009. **6**(3): p. 163-174.
- 43. Hunter, D., *Hunter's Diseases of Occupations, 2nd ed.* 1957, London: English University Press.
- 44. Miles, A.E.W., *PHOSPHORUS NECROSIS OF JAW PHOSSY-JAW*. British Dental Journal, 1972. **133**(5): p. 203-+.
- 45. Marx, R.E., *Pamidronate (Aredia) and zoledronate (Zometa) induced avascular necrosis of the jaws: A growing epidemic.* Journal of Oral and Maxillofacial Surgery, 2003. **61**(9): p. 1115-1117.
- 46. Broome, M., B. Jaques, and C. Madrid, *The return of phossy jaw?* Revue De Stomatologie Et De Chirurgie Maxillo-Faciale, 2008. **109**(3): p. 203-205.
- 47. Ashcroft, J., *Bisphosphonates and phossy-jaw: breathing new life into an old problem.* Lancet Oncology, 2006. **7**(6): p. 447-449.
- 48. Hellstein, J.W. and C.L. Marek, *Bisphosphonate osteochemonecrosis (bis-phossy jaw): Is this phossy jaw of the 21st century?* Journal of Oral and Maxillofacial Surgery, 2005. **63**(5): p. 682-689.
- 49. Berthold, H.K., I.J. Diel, and I. Gouni-Berthold, *Phossy jaw revisited Do bisphosphonates cause bisphossy jaws?* Drug Safety, 2004. **27**(12): p. 920-920.
- 50. Cremers, S., et al., A pharmacokinetic and pharmacodynamic model for intravenous bisphosphonate (pamidronate) in osteoporosis. Eur J Clin Pharmacol, 2002. **57**(12): p. 883-90.
- 51. Ensrud, K.E., et al., Randomized trial of effect of alendronate continuation versus discontinuation in women with low BMD: results from the Fracture Intervention Trial long-term extension. J Bone Miner Res, 2004. 19(8): p. 1259-69.
- 52. Reszka, A.A. and G.A. Rodan, *Nitrogen-containing bisphosphonate mechanism of action*. Mini Rev Med Chem, 2004. **4**(7): p. 711-9.
- 53. Drake, M.T., B.L. Clarke, and S. Khosla, *Bisphosphonates: mechanism of action and role in clinical practice.*Mayo Clin Proc, 2008. **83**(9): p. 1032-45.
- 54. Fleisch, H., R.G. Russell, and M.D. Francis, *Diphosphonates inhibit hydroxyapatite dissolution in vitro and bone resorption in tissue culture and in vivo*. Science, 1969. **165**(3899): p. 1262-4.
- 55. Mostefa Side Larbi, M.A., et al., *Thermodynamic study of the interaction between calcium and zoledronic acid by calorimetry*. The Journal of Chemical Thermodynamics, 2016. **97**: p. 290-296.
- Walter, C., et al., *Influence of bisphosphonates on endothelial cells, fibroblasts, and osteogenic cells.* Clin Oral Investig, 2010. **14**(1): p. 35-41.
- 57. Ruggiero, S.L., et al., *Osteonecrosis of the jaws associated with the use of bisphosphonates: A review of 63 cases.* Journal of Oral and Maxillofacial Surgery, 2004. **62**(5): p. 527-534.
- 58. Germain, M.L., et al., *Osteonecrosis of the jaw in a patient with bisphosphonates therapy.* Drug Safety, 2005. **28**(10): p. 956-956.
- 59. Hoff, A.O., et al., *Osteonecrosis of the jaw in patients receiving intravenous bisphosphonate therapy.*Journal of Bone and Mineral Research, 2005. **20**: p. P61-P61.
- 60. Van Poznak, C.H., et al., *Osteonecrosis of the jaw in patients with metastatic breast cancer.* Journal of Bone and Mineral Research, 2005. **20**: p. P21-P21.
- 61. Rosella, D., et al., *Medication-related osteonecrosis of the jaw: Clinical and practical guidelines.* J Int Soc Prev Community Dent, 2016. **6**(2): p. 97-104.
- 62. Ruggiero, S.L., et al., American Association of Oral and Maxillofacial Surgeons position paper on

- medication-related osteonecrosis of the jaw--2014 update. J Oral Maxillofac Surg, 2014. **72**(10): p. 1938-56.
- 63. Ruggiero, S.L., et al., American Association of Oral and Maxillofacial Surgeons' Position Paper on Medication-Related Osteonecrosis of the Jaws-2022 Update. Journal of Oral and Maxillofacial Surgery, 2022. **80**(5): p. 920-943.
- 64. Ruggiero, S.L., et al., American Association of Oral and Maxillofacial Surgeons Position Paper on Medication-Related Osteonecrosis of the Jaw-2014 Update. Journal of Oral and Maxillofacial Surgery, 2014. **72**(10): p. 1938-1956.
- 65. Blair, H.C., et al., *Calcium signalling and calcium transport in bone disease.* Subcell Biochem, 2007. **45**: p. 539-62.
- 66. Aquino-Martínez, R., et al., Extracellular calcium promotes bone formation from bone marrow mesenchymal stem cells by amplifying the effects of BMP-2 on SMAD signalling. PLoS One, 2017. **12**(5): p. e0178158.
- 67. Bloodgood, R.A., *Calcium-regulated phosphorylation of proteins in the membrane-matrix compartment of the Chlamydomonas flagellum.* Exp Cell Res, 1992. **198**(2): p. 228-36.
- 68. Matthews, E.K., *CALCIUM AND MEMBRANE PERMEABILITY*. British Medical Bulletin, 1986. **42**(4): p. 391-397.
- 69. Bagur, R. and G. Hajnóczky, *Intracellular Ca(2+) Sensing: Its Role in Calcium Homeostasis and Signaling.*Mol Cell, 2017. **66**(6): p. 780-788.
- 70. Gao, S.Y., et al., *Zoledronate suppressed angiogenesis and osteogenesis by inhibiting osteoclasts formation and secretion of PDGF-BB*. Plos One, 2017. **12**(6).
- 71. Endo, Y., et al., *Underlying Mechanisms and Therapeutic Strategies for Bisphosphonate-Related Osteonecrosis of the Jaw (BRONJ)*. Biological & Pharmaceutical Bulletin, 2017. **40**(6): p. 739-750.
- Yoneda, T., et al., Bisphosphonate-related osteonecrosis of the jaw: position paper from the Allied Task Force Committee of Japanese Society for Bone and Mineral Research, Japan Osteoporosis Society, Japanese Society of Periodontology, Japanese Society for Oral and Maxillofacial Radiology, and Japanese Society of Oral and Maxillofacial Surgeons. Journal of Bone and Mineral Metabolism, 2010. 28(4): p. 365-383.
- 73. Kobayashi, Y., et al., *Zoledronic acid delays wound healing of the tooth extraction socket, inhibits oral epithelial cell migration, and promotes proliferation and adhesion to hydroxyapatite of oral bacteria, without causing osteonecrosis of the jaw, in mice.* Journal of Bone and Mineral Metabolism, 2010. **28**(2): p. 165-175.
- 74. Wehrhan, F., et al., Osteoclastic expression of higher-level regulators NFATc1 and BCL6 in medication-related osteonecrosis of the jaw secondary to bisphosphonate therapy: a comparison with osteoradionecrosis and osteomyelitis. J Transl Med, 2019. **17**(1): p. 69.
- 75. Aghaloo, T.L., A.L. Felsenfeld, and S. Tetradis, *Osteonecrosis of the jaw in a patient on Denosumab.* J Oral Maxillofac Surg, 2010. **68**(5): p. 959-63.
- 76. Marenzana, M. and T.R. Arnett, *The Key Role of the Blood Supply to Bone*. Bone Res, 2013. **1**(3): p. 203-15.
- 77. Filipowska, J., et al., *The role of vasculature in bone development, regeneration and proper systemic functioning.* Angiogenesis, 2017. **20**(3): p. 291-302.
- 78. Lespasio, M.J., N. Sodhi, and M.A. Mont, Osteonecrosis of the Hip: A Primer. Perm J, 2019. 23.
- 79. Ziebart, T., et al., *Bisphosphonates: restrictions for vasculogenesis and angiogenesis: inhibition of cell function of endothelial progenitor cells and mature endothelial cells in vitro.* Clinical Oral Investigations,

- 2011. **15**(1): p. 105-111.
- 80. Ohlrich, E.J., et al., *The bisphosphonate zoledronic acid regulates key angiogenesis-related genes in primary human gingival fibroblasts.* Archives of Oral Biology, 2016. **63**: p. 7-14.
- 81. Su, Z.F., et al., Borate bioactive glass prevents zoledronate-induced osteonecrosis of the jaw by restoring osteogenesis and angiogenesis. Oral Diseases, 2020. **26**(8): p. 1706-1717.
- 82. Aguirre, J.I., et al., Alendronate impairs angiogenesis and bone formation during the early stages of bone healing in an animal model for osteonecrosis of the jaw. Journal of Bone and Mineral Research, 2007. **22**: p. S74-S74.
- 83. Moccia, F., et al., Endothelial Ca(2+) Signaling, Angiogenesis and Vasculogenesis: just What It Takes to Make a Blood Vessel. Int J Mol Sci, 2019. **20**(16).
- 84. Martini, A., et al., *Angiotensin II regulates endothelial cell migration through calcium influx via T-type calcium channel in human umbilical vein endothelial cells.* Acta Physiologica, 2010. **198**(4): p. 449-455.
- 85. Faehling, M., et al., Essential role of calcium in vascular endothelial growth factor A-induced signaling: mechanism of the antiangiogenic effect of carboxyamidotriazole. Faseb j, 2002. **16**(13): p. 1805-7.
- 86. White, C.D. and D.B. Sacks, *Regulation of MAP kinase signaling by calcium*. Methods Mol Biol, 2010. **661**: p. 151-65.
- 87. Lyng, F.M., et al., *The involvement of calcium and MAP kinase signaling pathways in the production of radiation-induced bystander effects.* Radiat Res, 2006. **165**(4): p. 400-9.
- 88. Yadegari, A., et al., *The effect of melatonin on prevention of bisphosphonate-related osteonecrosis of the jaw: an animal study in rats.* Journal of the Korean Association of Oral and Maxillofacial Surgeons, 2020. **46**(4): p. 266-274.
- 89. de Sousa, F.R.N., et al., The effect of high concentration of zoledronic acid on tooth induced movement and its repercussion on root, periodontal ligament and alveolar bone tissues in rats. Scientific Reports, 2021. **11**(1).
- 90. Dimopoulos, M.A., et al., Osteonecrosis of the jaw in patients with multiple myeloma treated with bisphosphonates: evidence of increased risk after treatment with zoledronic acid. Haematologica-the Hematology Journal, 2006. **91**(7): p. 968-971.
- 91. Badros, A., et al., *Osteonecrosis of the jaw in multiple myeloma patients: Clinical features and risk factors.*Journal of Clinical Oncology, 2006. **24**(6): p. 945-952.
- 92. Bastos, P., et al., *In-vivo imaging of the microvasculature of the soft tissue margins of osteonecrotic jaw lesions*. British Dental Journal, 2017. **223**(9): p. 699-705.
- 93. Mine, Y., et al., Occlusal Trauma and Bisphosphonate-Related Osteonecrosis of the Jaw in Mice. Calcif Tissue Int, 2022. **110**(3): p. 380-392.
- 94. George, E.L., Y.-L. Lin, and M.M. Saunders, *Bisphosphonate-related osteonecrosis of the jaw: a mechanobiology perspective.* Bone Reports, 2018. **8**: p. 104-109.
- 95. Pabst, A.M., et al., *The influence of bisphosphonates on viability, migration, and apoptosis of human oral keratinocytes-in vitro study.* Clinical Oral Investigations, 2012. **16**(1): p. 87-93.
- 96. Landesberg, R., et al., *Inhibition of oral mucosal cell wound healing by bisphosphonates*. Journal of Oral and Maxillofacial Surgery, 2008. **66**(5): p. 839-847.
- 97. Marx, R.E., et al., *Bisphosphonate-induced exposed bone (osteonecrosis/osteopetrosis) of the jaws: risk factors, recognition, prevention, and treatment.* J Oral Maxillofac Surg, 2005. **63**(11): p. 1567-75.
- 98. Kalyan, S., et al., *Systemic immunity shapes the oral microbiome and susceptibility to bisphosphonate-associated osteonecrosis of the jaw.* J Transl Med, 2015. **13**: p. 212.
- 99. Roato, I., et al., Immune Dysfunction in Medication-Related Osteonecrosis of the Jaw. Int J Mol Sci, 2023.

24(9).

- 100. Ciobanu, G.A., et al., *Correlations between Immune Response and Etiopathogenic Factors of Medication-Related Osteonecrosis of the Jaw in Cancer Patients Treated with Zoledronic Acid.* International Journal of Molecular Sciences, 2023. **24**(18): p. 14345.
- 101. Yamachika, E., et al., *The influence of zoledronate and teriparatide on gamma delta T cells in mice.* J Dent Sci, 2017. **12**(4): p. 333-339.
- 102. Kalyan, S., et al., Can peripheral blood $\gamma\delta$ T cells predict osteonecrosis of the jaw? An immunological perspective on the adverse drug effects of aminobisphosphonate therapy. J Bone Miner Res, 2013. **28**(4): p. 728-35.
- 103. Ristow, O., et al., *Is bone turnover of jawbone and its possible over suppression by bisphosphonates of etiologic importance in pathogenesis of bisphosphonate-related osteonecrosis?* J Oral Maxillofac Surg, 2014. **72**(5): p. 903-10.
- 104. Gong, X., et al., Skeletal Site-specific Effects of Zoledronate on in vivo Bone Remodeling and in vitro BMSCs Osteogenic Activity. Scientific Reports, 2017. **7**(1): p. 36129.
- 105. Sarasquete, M.E., et al., *Bisphosphonate-related osteonecrosis: genetic and acquired risk factors.* Oral Dis, 2009. **15**(6): p. 382-7.
- 106. Kim, J.H., et al., *Genetic investigation of bisphosphonate-related osteonecrosis of jaw (BRONJ) via whole exome sequencing and bioinformatics*. PLoS One, 2015. **10**(2): p. e0118084.
- 107. Zhong, D.N., J.Z. Wu, and G.J. Li, Association between CYP2C8 (rs1934951) polymorphism and bisphosphonate-related osteonecrosis of the jaws in patients on bisphosphonate therapy: a meta-analysis. Acta Haematol, 2013. 129(2): p. 90-5.
- 108. Arduino, P.G., et al., *Vascular endothelial growth factor genetic polymorphisms and haplotypes in female patients with bisphosphonate-related osteonecrosis of the jaws*. J Oral Pathol Med, 2011. **40**(6): p. 510-5.
- 109. Basi, D.L., et al., *Matrix metalloproteinase-9 expression in alveolar extraction sockets of Zoledronic acid-treated rats.* J Oral Maxillofac Surg, 2011. **69**(11): p. 2698-707.
- 110. Kastritis, E., et al., Genetic factors related with early onset of osteonecrosis of the jaw in patients with multiple myeloma under zoledronic acid therapy. Leuk Lymphoma, 2017. **58**(10): p. 2304-2309.
- 111. Zebic, L. and V. Patel, Preventing medication-related osteonecrosis of the jaw. Bmj, 2019. 365: p. 11733.
- 112. Kos, M., Incidence and risk predictors for osteonecrosis of the jaw in cancer patients treated with intravenous bisphosphonates. Arch Med Sci, 2015. **11**(2): p. 319-24.
- 113. Moinzadeh, A.T., et al., *Bisphosphonates and their clinical implications in endodontic therapy.* International Endodontic Journal, 2013. **46**(5): p. 391-398.
- 114. 2023; Available from: https://www.nice.org.uk/.
- 115. Kos, M., et al., *Bisphosphonate-related osteonecrosis of the jaws: A review of 34 cases and evaluation of risk.* Journal of Cranio-Maxillofacial Surgery, 2010. **38**(4): p. 255-259.
- 116. Kwon, Y.D., et al., *Bisphosphonate related osteonecrosis of the jaws (BRONJ) in osteoporotic males.* Springerplus, 2016. **5**(1): p. 1468.
- Saad, F., et al., Incidence, risk factors, and outcomes of osteonecrosis of the jaw: integrated analysis from three blinded active-controlled phase III trials in cancer patients with bone metastases. Ann Oncol, 2012.
 23(5): p. 1341-1347.
- 118. Hallmer, F., et al., *Prevalence, initiating factor, and treatment outcome of medication-related osteonecrosis of the jaw-a 4-year prospective study.* Oral Surg Oral Med Oral Pathol Oral Radiol, 2018. **126**(6): p. 477-485.

- 119. Soriano, R.M. and M.D. J, *Anatomy, Head and Neck, Maxilla*, in *StatPearls*. 2023, StatPearls Publishing Copyright © 2023, StatPearls Publishing LLC.: Treasure Island (FL).
- 120. Breeland, G., A. Aktar, and B.C. Patel, *Anatomy, Head and Neck, Mandible*, in *StatPearls*. 2023, StatPearls Publishing

Copyright © 2023, StatPearls Publishing LLC.: Treasure Island (FL).

- 121. Brenneise, C.V. and C.A. Squier, *Blood flow in maxilla and mandible of normal and atherosclerotic rhesus monkeys.* J Oral Pathol, 1985. **14**(10): p. 800-8.
- 122. Diel, I.J., et al., *Pathophysiology, risk factors and management of bisphosphonate-associated osteonecrosis of the jaw: Is there a diverse relationship of amino- and non-aminobisphosphonates?* Crit Rev Oncol Hematol, 2007. **64**(3): p. 198-207.
- 123. Sigua-Rodriguez, E.A., et al., *Bisphosphonate-related osteonecrosis of the jaw: a review of the literature.* Int J Dent, 2014. **2014**: p. 192320.
- 124. Jadu, F., et al., A retrospective study assessing the incidence, risk factors and comorbidities of pamidronate-related necrosis of the jaws in multiple myeloma patients. Ann Oncol, 2007. **18**(12): p. 2015-9.
- 125. Teoh, L., et al., Medication-related osteonecrosis of the jaw: Analysing the range of implicated drugs from the Australian database of adverse event notifications. Br J Clin Pharmacol, 2021. **87**(7): p. 2767-2776.
- 126. Urade, M., [Diabetes mellitus and bisphosphonate-related osteonecrosis of the jaws]. Clin Calcium, 2009. **19**(9): p. 1332-8.
- 127. Di Fede, O., et al., *BRONJ in patients with rheumatoid arthritis: a multicenter case series.* Oral Dis, 2016. **22**(6): p. 543-8.
- 128. Zhang, W., et al., *The Role of the Immune Response in the Development of Medication-Related Osteonecrosis of the Jaw.* Front Immunol, 2021. **12**: p. 606043.
- 129. Poxleitner, P., et al., Tooth extractions in patients under antiresorptive therapy for osteoporosis: Primary closure of the extraction socket with a mucoperiosteal flap versus application of platelet-rich fibrin for the prevention of antiresorptive agent-related osteonecrosis of the jaw. J Craniomaxillofac Surg, 2020. **48**(4): p. 444-451.
- 130. Mozzati, M., et al., A dental extraction protocol with plasma rich in growth factors (PRGF) in patients on intravenous bisphosphonate therapy: a case-control study. Joint Bone Spine, 2011. **78**(6): p. 648-9.
- 131. Park, J.H., J.W. Kim, and S.J. Kim, *Does the Addition of Bone Morphogenetic Protein 2 to Platelet-Rich Fibrin Improve Healing After Treatment for Medication-Related Osteonecrosis of the Jaw?* J Oral Maxillofac Surg, 2017. **75**(6): p. 1176-1184.
- 132. Giudice, A., et al., *Can platelet-rich fibrin improve healing after surgical treatment of medication-related osteonecrosis of the jaw? A pilot study.* Oral Surg Oral Med Oral Pathol Oral Radiol, 2018. **126**(5): p. 390-403.
- 133. Yüce, M.O., E. Adalı, and G. Işık, *The effect of concentrated growth factor (CGF) in the surgical treatment of medication-related osteonecrosis of the jaw (MRONJ) in osteoporosis patients: a randomized controlled study.* Clin Oral Investig, 2021. **25**(7): p. 4529-4541.
- 134. Ripamonti, C.I., et al., Decreased occurrence of osteonecrosis of the jaw after implementation of dental preventive measures in solid tumour patients with bone metastases treated with bisphosphonates. The experience of the National Cancer Institute of Milan. Ann Oncol, 2009. **20**(1): p. 137-45.
- 135. Bantis, A., et al., Bisphosphonate-induced osteonecrosis of the jaw in patients with bone metastatic, hormone-sensitive prostate cancer. Risk factors and prevention strategies. Tumori, 2011. **97**(4): p. 479-

83.

- 136. Montefusco, V., et al., Antibiotic prophylaxis before dental procedures may reduce the incidence of osteonecrosis of the jaw in patients with multiple myeloma treated with bisphosphonates. Leuk Lymphoma, 2008. **49**(11): p. 2156-62.
- 137. Ji, X., et al., *Antibiotic effects on bacterial profile in osteonecrosis of the jaw.* Oral Dis, 2012. **18**(1): p. 85-95.
- 138. Kishimoto, H., K. Noguchi, and K. Takaoka, *Novel insight into the management of bisphosphonate*related osteonecrosis of the jaw (BRONJ). Jpn Dent Sci Rev, 2019. **55**(1): p. 95-102.
- 139. Spanou, A., et al., *Primary wound closure and perioperative antibiotic therapy for prevention of bisphosphonate-related osteonecrosis of the jaw after tooth extraction.* Quintessence Int, 2020. **51**(3): p. 220-228.
- 140. Vandone, A.M., et al., *Impact of dental care in the prevention of bisphosphonate-associated osteonecrosis of the jaw: a single-center clinical experience.* Ann Oncol, 2012. **23**(1): p. 193-200.
- 241. Zheng, Y., et al., Low-level laser therapy prevents medication-related osteonecrosis of the jaw-like lesions via IL-1RA-mediated primary gingival wound healing. BMC Oral Health, 2023. **23**(1): p. 14.
- 142. Shim, Y.H., et al., *Analysis of Factors Associated with the Postoperative Healing of Medication-Related Osteonecrosis of the Jaw in Patients with Osteoporosis*. J Clin Med, 2021. **10**(16).
- 143. Yuan, A., et al., Gingival fibroblasts and medication-related osteonecrosis of the jaw: Results by realtime and wound healing in vitro assays. Journal of Cranio-Maxillofacial Surgery, 2019. **47**(9): p. 1464-1474.
- 144. Walton, K., et al., *Medication related osteonecrosis of the jaw in osteoporotic vs oncologic patients-quantifying radiographic appearance and relationship to clinical findings*. Dentomaxillofac Radiol, 2019. **48**(1): p. 20180128.
- 145. Ripamonti, C.I., et al., Efficacy and tolerability of medical ozone gas insufflations in patients with osteonecrosis of the jaw treated with bisphosphonates-Preliminary data: Medical ozone gas insufflation in treating ONJ lesions. J Bone Oncol, 2012. 1(3): p. 81-7.
- 146. Freiberger, J.J., et al., What is the role of hyperbaric oxygen in the management of bisphosphonate-related osteonecrosis of the jaw: a randomized controlled trial of hyperbaric oxygen as an adjunct to surgery and antibiotics. J Oral Maxillofac Surg, 2012. **70**(7): p. 1573-83.
- 147. Morishita, K., et al., *Treatment outcomes of adjunctive teriparatide therapy for medication-related osteonecrosis of the jaw (MRONJ): A multicenter retrospective analysis in Japan.* J Orthop Sci, 2020. **25**(6): p. 1079-1083.
- 148. Sim, I.W., et al., *Teriparatide Promotes Bone Healing in Medication-Related Osteonecrosis of the Jaw: A Placebo-Controlled, Randomized Trial.* Journal of Clinical Oncology, 2020. **38**(26): p. 2971-+.
- 149. Varoni, E.M., et al., Conservative Management of Medication-Related Osteonecrosis of the Jaws (MRONJ): A Retrospective Cohort Study. Antibiotics (Basel), 2021. **10**(2).
- 150. Jasper, V., et al., Medication-related osteonecrosis of the jaw (MRONJ) stage III: Conservative and conservative surgical approaches versus an aggressive surgical intervention: A systematic review. Journal of Cranio-Maxillofacial Surgery, 2020. **48**(4): p. 435-443.
- 151. Sacco, R., et al., Microsurgical Reconstruction of the Jaws Using Vascularised Free Flap Technique in Patients with Medication-Related Osteonecrosis: A Systematic Review. Biomed Research International, 2018. **2018**.
- 152. Marcianò, A., et al., *Oral Surgical Management of Bone and Soft Tissues in MRONJ Treatment: A Decisional Tree.* Life (Basel), 2020. **10**(7).

- 153. Choi, N.R., et al., Surgical Treatment of Medication-Related Osteonecrosis of the Jaw: A Retrospective Study. Int J Environ Res Public Health, 2020. 17(23).
- 154. Giudice, A., et al., Can Surgical Management Improve Resolution of Medication-Related Osteonecrosis of the Jaw at Early Stages? A Prospective Cohort Study. Journal of Oral and Maxillofacial Surgery, 2020. 78(11): p. 1986-1999.
- 155. Mustakim, K.R., et al., Significance of medication discontinuation on bisphosphonate-related jaw osteonecrosis in a rat model. Scientific Reports, 2022. **12**(1): p. 21449.
- 156. Yoneda, T., et al., *Antiresorptive agent-related osteonecrosis of the jaw: Position Paper 2017 of the Japanese Allied Committee on Osteonecrosis of the Jaw.* J Bone Miner Metab, 2017. **35**(1): p. 6-19.
- 157. Anastasilakis, A.D., et al., Osteonecrosis of the Jaw and Antiresorptive Agents in Benign and Malignant Diseases: A Critical Review Organized by the ECTS. The Journal of Clinical Endocrinology & Metabolism, 2021. 107(5): p. 1441-1460.
- 158. Campisi, G., et al., *Medication-Related Osteonecrosis of Jaws (MRONJ) Prevention and Diagnosis: Italian Consensus Update 2020.* Int J Environ Res Public Health, 2020. **17**(16).
- 159. Khan, A.A., et al., *Diagnosis and management of osteonecrosis of the jaw: a systematic review and international consensus.* J Bone Miner Res, 2015. **30**(1): p. 3-23.
- 160. Ray, S., and others (eds), *Oxford Handbook of Clinical and Healthcare Research*, ed. S. Ray, et al. 2016: Oxford University Press.
- 161. Beth-Tasdogan, N.H., et al., *Interventions for managing medication-related osteonecrosis of the jaw.* Cochrane Database of Systematic Reviews, 2022(7).
- 162. Mozzati, M., et al., *Tooth extraction and oral bisphosphonates: comparison of different surgical protocols.* Joint Bone Spine, 2011. **78**(6): p. 647-8.
- 163. Mücke, T., et al., *Prevention of bisphosphonate-related osteonecrosis of the jaws in patients with prostate cancer treated with zoledronic acid A prospective study over 6 years.* J Craniomaxillofac Surg, 2016. **44**(10): p. 1689-1693.
- 164. Ristow, O., et al., Wound closure and alveoplasty after preventive tooth extractions in patients with antiresorptive intake-A randomized pilot trial. Oral Dis, 2021. **27**(3): p. 532-546.
- 165. Ristow, O., et al., Comparison of auto-fluorescence and tetracycline fluorescence for guided bone surgery of medication-related osteonecrosis of the jaw: a randomized controlled feasibility study. Int J Oral Maxillofac Surg, 2017. **46**(2): p. 157-166.
- 166. Giudice, A., et al., *Can Autofluorescence Guide Surgeons in the Treatment of Medication-Related Osteonecrosis of the Jaw? A Prospective Feasibility Study.* J Oral Maxillofac Surg, 2018. **76**(5): p. 982-995.
- 167. Sim, I.W., et al., *Teriparatide Promotes Bone Healing in Medication-Related Osteonecrosis of the Jaw: A Placebo-Controlled, Randomized Trial.* J Clin Oncol, 2020. **38**(26): p. 2971-2980.
- 168. Ohbayashi, Y., et al., A comparative effectiveness pilot study of teriparatide for medication-related osteonecrosis of the jaw: daily versus weekly administration. Osteoporos Int, 2020. **31**(3): p. 577-585.
- 169. Mijiritsky, E., et al., *Use of PRP, PRF and CGF in Periodontal Regeneration and Facial Rejuvenation-A Narrative Review.* Biology (Basel), 2021. **10**(4).
- 170. Shetye, A.G., et al., *Effect of advanced platelet-rich fibrin and concentrated growth factor on tissues around implants in maxillary anterior region.* J Indian Prosthodont Soc, 2022. **22**(2): p. 169-178.
- 171. Santini, D., et al., *Pamidronate induces modifications of circulating angiogenetic factors in cancer patients*. Clin Cancer Res, 2002. **8**(5): p. 1080-4.
- 172. Santini, D., et al., *Zoledronic acid induces significant and long-lasting modifications of circulating angiogenic factors in cancer patients*. Clin Cancer Res, 2003. **9**(8): p. 2893-7.

- 173. Anitua, E., et al., *The effects of PRGF on bone regeneration and on titanium implant osseointegration in goats: a histologic and histomorphometric study.* J Biomed Mater Res A, 2009. **91**(1): p. 158-65.
- 174. Anitua, E., M. Troya, and G. Orive, *Plasma Rich in Growth Factors Promote Gingival Tissue Regeneration by Stimulating Fibroblast Proliferation and Migration and by Blocking Transforming Growth Factor-81-Induced Myodifferentiation.* Journal of Periodontology, 2012. **83**(8): p. 1028-1037.
- 175. Govender, S., et al., Recombinant human bone morphogenetic protein-2 for treatment of open tibial fractures: a prospective, controlled, randomized study of four hundred and fifty patients. J Bone Joint Surg Am, 2002. **84**(12): p. 2123-34.
- 176. Pautke, C., et al., *Fluorescence-guided bone resection in bisphosphonate-associated osteonecrosis of the jaws.* J Oral Maxillofac Surg, 2009. **67**(3): p. 471-6.
- 177. Krege, J.H., et al., *Teriparatide and Osteosarcoma Risk: History, Science, Elimination of Boxed Warning, and Other Label Updates.* JBMR Plus, 2022. **6**(9): p. e10665.
- 178. Raloxifene and teriparatide for the secondary prevention of osteoporotic fragility fractures in postmenopausal women. NICE technology appraisal guidance [TA161], 2018.
- 179. Epstein, M.S., et al., Management of bisphosphonate-associated osteonecrosis: pentoxifylline and tocopherol in addition to antimicrobial therapy. An initial case series. Oral Surg Oral Med Oral Pathol Oral Radiol Endod, 2010. **110**(5): p. 593-6.
- 180. Colapinto, G., et al., Outcomes of a Pharmacological Protocol with Pentoxifylline and Tocopherol for the Management of Medication-Related Osteonecrosis of the Jaws (MRONJ): A Randomized Study on 202 Osteoporosis Patients. Journal of Clinical Medicine, 2023. **12**(14).
- 181. Ikada, Y., Challenges in tissue engineering. J R Soc Interface, 2006. 3(10): p. 589-601.
- 182. Qu, H.W., et al., *Biomaterials for bone tissue engineering scaffolds: a review.* Rsc Advances, 2019. **9**(45): p. 26252-26262.
- 183. Annamalai, R.T., et al., *Injectable osteogenic microtissues containing mesenchymal stromal cells conformally fill and repair critical-size defects.* Biomaterials, 2019. **208**: p. 32-44.
- 184. Zhang, X., et al., *Cell-free 3D scaffold with two-stage delivery of miRNA-26a to regenerate critical-sized bone defects.* Nature Communications, 2016. **7**(1): p. 10376.
- 185. Lee, J.W., et al., Long-term clinical study and multiscale analysis of in vivo biodegradation mechanism of Mg alloy. Proceedings of the National Academy of Sciences of the United States of America, 2016. **113**(3): p. 716-721.
- 186. Bhumiratana, S., et al., *Tissue-engineered autologous grafts for facial bone reconstruction.* Sci Transl Med, 2016. **8**(343): p. 343ra83.
- 187. Chagou, A., et al., *The association of stromal mesenchymal cells with the bone substitute for the treatment of non-union of long bones, an alternative to autologous spongy grafts: a case report.* Pan African Medical Journal, 2020. **37**.
- 188. Mehta, S., et al., Cost-Effectiveness Analysis of Demineralized Bone Matrix and rhBMP-2 versus Autologous Iliac Crest Bone Grafting in Alveolar Cleft Patients. Plastic and Reconstructive Surgery, 2018. 142(3): p. 737-743.
- 189. Zhu, S., et al., *Cell signaling and transcriptional regulation of osteoblast lineage commitment, differentiation, bone formation, and homeostasis.* Cell Discovery, 2024. **10**(1): p. 71.
- 190. Jiang, T., et al., *Role and Regulation of Transcription Factors in Osteoclastogenesis*. Int J Mol Sci, 2023. **24**(22).
- 191. Chan, W.C.W., et al., *Regulation and Role of Transcription Factors in Osteogenesis*. Int J Mol Sci, 2021. **22**(11).

- 192. Luo, Z.Y., et al., *Time-responsive osteogenic niche of stem cells: A sequentially triggered, dual-peptide loaded, alginate hybrid system for promoting cell activity and osteo-differentiation.* Biomaterials, 2018. **163**: p. 25-42.
- 193. Partlow, B.P., et al., *Highly Tunable Elastomeric Silk Biomaterials*. Advanced Functional Materials, 2014. **24**(29): p. 4615-4624.
- 194. Diba, M., et al., Composite Colloidal Gels Made of Bisphosphonate-Functionalized Gelatin and Bioactive Glass Particles for Regeneration of Osteoporotic Bone Defects. Advanced Functional Materials, 2017. **27**(45): p. 1703438.
- 195. Wilson, J.A., et al., *Magnesium Catalyzed Polymerization of End Functionalized Poly(propylene maleate)* and *Poly(propylene fumarate) for 3D Printing of Bioactive Scaffolds*. Journal of the American Chemical Society, 2018. **140**(1): p. 277-284.
- 196. Wang, S.F., et al., Molecularly Engineered Biodegradable Polymer Networks with a Wide Range of Stiffness for Bone and Peripheral Nerve Regeneration. Advanced Functional Materials, 2015. **25**(18): p. 2715-2724.
- 197. Cui, H.T., et al., *Biologically Inspired Smart Release System Based on 3D Bioprinted Perfused Scaffold for Vascularized Tissue Regeneration.* Advanced Science, 2016. **3**(8).
- 198. Bohner, M., et al., *Characterization and distribution of mechanically competent mineralized tissue in micropores of beta-tricalcium phosphate bone substitutes.* Materials Today, 2017. **20**(3): p. 106-115.
- 199. Jakus, A.E., et al., *Hyperelastic "bone": A highly versatile, growth factor-free, osteoregenerative, scalable, and surgically friendly biomaterial.* Science Translational Medicine, 2016. **8**(358).
- 200. Hoppe, A., N.S. Güldal, and A.R. Boccaccini, *A review of the biological response to ionic dissolution products from bioactive glasses and glass-ceramics*. Biomaterials, 2011. **32**(11): p. 2757-2774.
- 201. Zhou, Y., C. Wu, and J. Chang, *Bioceramics to regulate stem cells and their microenvironment for tissue regeneration.* Materials Today, 2019. **24**: p. 41-56.
- 202. Azevedo, M.M., et al., *Synthesis and characterization of hypoxia-mimicking bioactive glasses for skeletal regeneration.* Journal of Materials Chemistry, 2010. **20**(40): p. 8854-8864.
- 203. Chen, L., et al., *3D printing of a lithium-calcium-silicate crystal bioscaffold with dual bioactivities for osteochondral interface reconstruction.* Biomaterials, 2019. **196**: p. 138-150.
- 204. Cheng, P.F., et al., *High-purity magnesium interference screws promote fibrocartilaginous entheses* regeneration in the anterior cruciate ligament reconstruction rabbit model via accumulation of BMP-2 and VEGF. Biomaterials, 2016. **81**: p. 14-26.
- 205. Xing, F., et al., *Recent progress in Mg-based alloys as a novel bioabsorbable biomaterials for orthopedic applications.* Journal of Magnesium and Alloys, 2022. **10**(6): p. 1428-1456.
- 206. Wang, J.L., et al., *Biodegradable Magnesium-Based Implants in Orthopedics-A General Review and Perspectives*. Advanced Science, 2020. **7**(8).
- 207. Ruan, J., et al., Enhanced Physiochemical and Mechanical Performance of Chitosan-Grafted Graphene Oxide for Superior Osteoinductivity. Advanced Functional Materials, 2016. **26**(7): p. 1085-1097.
- 208. Shimizu, M., et al., *Carbon Nanotubes Induce Bone Calcification by Bidirectional Interaction with Osteoblasts*. Advanced Materials, 2012. **24**(16): p. 2176-2185.
- 209. Seppänen-Kaijansinkko, R., *Tissue Engineering in Oral and Maxillofacial Surgery Preface*. Tissue Engineering in Oral and Maxillofacial Surgery, ed. R. SeppanenKaijansinkko. 2019. V-V.
- Young, S., et al., *Chapter 65 Tissue engineering in oral and maxillofacial surgery*, in *Principles of Tissue Engineering (Fifth Edition)*, R. Lanza, et al., Editors. 2020, Academic Press. p. 1201-1220.
- 211. Jamalpour, M.R., et al., Clinical Functions of Regenerative Dentistry and Tissue Engineering in Treatment

- of Oral and Maxillofacial Soft Tissues. Applications of Biomedical Engineering in Dentistry, ed. L. Tayebi. 2020. 223-238.
- 212. Coulter, I.C., et al., Routine but risky: a multi-centre analysis of the outcomes of cranioplasty in the Northeast of England. Acta Neurochir (Wien), 2014. **156**(7): p. 1361-8.
- 213. Neovius, E. and T. Engstrand, *Craniofacial reconstruction with bone and biomaterials: review over the last 11 years*. J Plast Reconstr Aesthet Surg, 2010. **63**(10): p. 1615-23.
- 214. Stein, F., et al., *Vascularization in Oral and Maxillofacial Tissue Engineering*. Tissue Engineering in Oral and Maxillofacial Surgery, ed. R. SeppanenKaijansinkko. 2019. 97-122.
- 215. Basyuni, S., et al., *Systematic scoping review of mandibular bone tissue engineering*. British Journal of Oral and Maxillofacial Surgery, 2020. **58**(6): p. 632-642.
- 216. Bertolai, R., et al., *Bone graft and mesenchimal stem cells: clinical observations and histological analysis.*Clinical cases in mineral and Bone Metabolism, 2015. **12**(2): p. 183.
- 217. Pasquali, P.J., et al., *Maxillary sinus augmentation combining Bio-Oss with the bone marrow aspirate concentrate: a histomorphometric study in humans.* International Journal of Biomaterials, 2015. **2015**.
- 218. Al-Ahmady, H.H., et al., *Combining autologous bone marrow mononuclear cells seeded on collagen sponge with Nano Hydroxyapatite, and platelet-rich fibrin: Reporting a novel strategy for alveolar cleft bone regeneration.* Journal of Cranio-Maxillofacial Surgery, 2018. **46**(9): p. 1593-1600.
- 219. Behnia, H., et al., *Repair of alveolar cleft defect with mesenchymal stem cells and platelet derived growth factors: a preliminary report.* Journal of Cranio-Maxillofacial Surgery, 2012. **40**(1): p. 2-7.
- 220. Baba, S., et al., *Phase I/II trial of autologous bone marrow stem cell transplantation with a three-dimensional woven-fabric scaffold for periodontitis*. Stem cells international, 2016. **2016**.
- d'Aquino, R., et al., *Periosteum-derived micro-grafts for tissue regeneration of human maxillary bone.*Journal of Translational Science, 2016. **2**(2): p. 125-129.
- 222. Monti, M., et al., *In vitro and in vivo differentiation of progenitor stem cells obtained after mechanical digestion of human dental pulp.* Journal of Cellular Physiology, 2017. **232**(3): p. 548-555.
- 223. Kaibuchi, N., et al., *Novel Cell Therapy Using Mesenchymal Stromal Cell Sheets for Medication-Related Osteonecrosis of the Jaw.* Front Bioeng Biotechnol, 2022. **10**: p. 902349.
- 224. Yang, G., et al., Effect of Human Umbilical Cord Matrix-Derived Mesenchymal Stem Cells on Bisphosphonate-Related Osteonecrosis of the Jaw. Tissue Engineering and Regenerative Medicine, 2021. **18**(6): p. 975-988.
- 225. Watanabe, J., et al., *Extracellular Vesicles of Stem Cells to Prevent BRONJ.* Journal of Dental Research, 2020. **99**(5): p. 552-560.
- 226. Brierly, G.I., et al., *Investigation of Sustained BMP Delivery in the Prevention of Medication-Related Osteonecrosis of the Jaw (MRONJ) in a Rat Model.* Macromolecular Bioscience, 2019. **19**(11).
- 227. Peters, M.D.J., et al., *Updated methodological guidance for the conduct of scoping reviews*. JBI Evid Synth, 2020. **18**(10): p. 2119-2126.
- 228. Zheng, Y., et al., Exosomes Derived from Adipose Tissue-Derived Mesenchymal Stromal Cells Prevent Medication-Related Osteonecrosis of the Jaw through IL-1RA. International Journal of Molecular Sciences, 2023. **24**(10).
- 229. Thavornyutikarn, B., et al., *Biodegradable Dual-Function Nanocomposite Hydrogels for Prevention of Bisphosphonate-Related Osteonecrosis of the Jaw.* Acs Applied Bio Materials, 2023. **6**(4): p. 1658-1675.
- 230. Sungkhaphan, P., et al., *Dual-Functional Drug Delivery System for Bisphosphonate-Related Osteonecrosis*Prevention and Its Bioinspired Releasing Model and In Vitro Assessment. Acs Omega, 2023. **8**(29): p. 26561-26576.

- 231. Du, Q.Z., et al., A multifunctional composite hydrogel promotes treatment of bisphosphonate-related osteonecrosis of the jaws. Applied Materials Today, 2023. **32**.
- 232. Dong, X., et al., *Adipose-Derived Stem Cells Promote Bone Coupling in Bisphosphonate-Related Osteonecrosis of the Jaw by TGF-81.* Frontiers in Cell and Developmental Biology, 2021. **9**.
- 233. Doppelt, O., et al., *Endothelial progenitors increase vascularization and improve fibroblasts function that prevent medication-related osteonecrosis of the jaw.* Oral Diseases, 2020. **26**(7): p. 1523-1531.
- 234. Wang, Q.Z., et al., Epidermal Growth Factor Reverses the Inhibitory Effects of the Bisphosphonate, Zoledronic Acid, on Human Oral Keratinocytes and Human Vascular Endothelial Cells <i>In Vitro</i> via the Epidermal Growth Factor Receptor (EGFR)/Akt/Phosphoinositide 3-Kinase (PI3K) Signaling Pathway. Medical Science Monitor, 2019. 25: p. 700-710.
- 235. Paulo, S., et al., Synthetic Calcium Phosphate Ceramics as a Potential Treatment for Bisphosphonate-Related Osteonecrosis of the Jaw. Materials, 2019. **12**(11).
- 236. Borsani, E., et al., Beneficial Effects of Concentrated Growth Factors and Resveratrol on Human Osteoblasts <i>In Vitro</i> Treated with Bisphosphonates. Biomed Research International, 2018. 2018.
- 237. Yuan, H., et al., *Revival of nitrogen-containing bisphosphonate-induced inhibition of osteoclastogenesis and osteoclast function by water-soluble microfibrous borate glass.* Acta Biomaterialia, 2016. **31**: p. 312-325.
- 238. Anitua, E., et al., *PRGF exerts a cytoprotective role in zoledronic acid-treated oral cells*. Clinical Oral Investigations, 2016. **20**(3): p. 513-521.
- 239. Kwon, T.K., et al., *Effect of recombinant human bone morphogenetic protein-2 on bisphosphonate-treated osteoblasts*. Journal of the Korean Association of Oral and Maxillofacial Surgeons, 2014. **40**(6): p. 291-296.
- 240. Kaibuchi, N., et al., *Allogeneic multipotent mesenchymal stromal cell sheet transplantation promotes healthy healing of wounds caused by zoledronate and dexamethasone in canine mandibular bones.*Regenerative Therapy, 2019. **10**: p. 77-83.
- 241. Kaibuchi, N., et al., *Multipotent mesenchymal stromal cell sheet therapy for bisphosphonate-related osteonecrosis of the jaw in a rat model.* Acta Biomaterialia, 2016. **42**: p. 400-410.
- Ogata, K., et al., Evaluation of the therapeutic effects of conditioned media from mesenchymal stem cells in a rat bisphosphonate-related osteonecrosis of the jaw-like model. Bone, 2015. **74**: p. 95-105.
- Zang, X., et al., Adipose-derived stem cells prevent the onset of bisphosphonate-related osteonecrosis of the jaw through transforming growth factor β-1-mediated gingival wound healing. Stem Cell Res Ther, 2019. **10**(1): p. 169.
- 244. Park, J.H., J.W. Kim, and S.J. Kim, *Does the Addition of Bone Morphogenetic Protein 2 to Platelet-Rich Fibrin Improve Healing After Treatment for Medication-Related Osteonecrosis of the Jaw?* Journal of Oral and Maxillofacial Surgery, 2017. **75**(6): p. 1176-1184.
- 245. Giudice, A., et al., *Can platelet-rich fibrin improve healing after surgical treatment of medication-related osteonecrosis of the jaw? A pilot study.* Oral Surgery Oral Medicine Oral Pathology Oral Radiology, 2018. **126**(5): p. 390-403.
- 246. Tatullo, M., et al., *Tissue Engineering and Regenerative Medicine in Oral and Maxillofacial Surgery: The Most Important Clinical Applications of Mesenchymal Stem Cells*. Regenerative Medicine and Plastic Surgery: Elements, Research Concepts and Emerging Technologies, ed. D. Duscher and M.A. Shiffman. 2019. 337-348.
- 247. Oh, H., et al., Reconstruction of mandibular defects in osteoradionecrosis and medication-related osteonecrosis of the jaw using fibula free flap and management of postoperative wound infections.

- Maxillofacial Plastic and Reconstructive Surgery, 2022. 44(1).
- 248. Kaoutzanis, C., et al., *Mandibular Reconstruction with Free Fibula Flap for Medication-related Osteonecrosis of the Jaw in Patients with Multiple Myeloma*. Plast Reconstr Surg Glob Open, 2020. **8**(10): p. e3186.
- 249. Bouland, C., et al., *Case reports of medication-related osteonecrosis of the jaw (MRONJ) treated with uncultured stromal vascular fraction and L-PRF.* Journal of Stomatology Oral and Maxillofacial Surgery, 2021. **122**(2): p. 212-218.
- 250. Cella, L., et al., *Autologous bone marrow stem cell intralesional transplantation repairing bisphosphonate related osteonecrosis of the jaw.* Head Face Med, 2011. **7**: p. 16.
- 251. De Santis, G.C., et al., *Mesenchymal stromal cells administration for osteonecrosis of the jaw caused by bisphosphonate: report of two cases.* Acta Oncologica, 2020. **59**(7): p. 789-792.
- 252. Takeuchi, H., et al., Surface pre-reacted glass-ionomer eluate protects gingival epithelium from penetration by lipopolysaccharides and peptidoglycans via transcription factor EB pathway. Plos One, 2022. **17**(7).
- 253. Shan, Z.J., et al., *?Gingival Soft Tissue Integrative? Lithium Disilicate Glass-Ceramics with High Mechanical Properties and Sustained-Release Lithium Ions*. Acs Applied Materials & Interfaces, 2022. **14**(49): p. 54572-54586.
- Wong, P.Y., et al., *A Novel Antimicrobial Hydrogel for the Management of Periodontal Diseases.* International Dental Journal, 2023. **73**(3): p. 354-361.
- 255. Alsharif, S.B., et al., *Strontium-loaded hydrogel scaffolds to promote gingival fibroblast function.* Journal of Biomedical Materials Research Part A, 2023. **111**(1): p. 6-14.
- 256. Hench, L.L., *The story of Bioglass (R).* Journal of Materials Science-Materials in Medicine, 2006. **17**(11): p. 967-978.
- 257. Hench, L.L., Bioceramics. Journal of the American Ceramic Society, 1998. 81(7): p. 1705-1728.
- 258. Naseri, S., W.C. Lepry, and S.N. Nazhat, *Bioactive glasses in wound healing: hope or hype?* Journal of Materials Chemistry B, 2017. **5**(31): p. 6167-6174.
- 259. Rahaman, M.N., et al., *Bioactive glass in tissue engineering*. Acta biomaterialia, 2011. **7**(6): p. 2355-2373.
- 260. Oliver, J.-a.N., et al., *Bioactive glass coatings on metallic implants for biomedical applications*. Bioactive Materials, 2019. **4**: p. 261-270.
- 261. Kaur, G., et al., *Mechanical properties of bioactive glasses, ceramics, glass-ceramics and composites:*State-of-the-art review and future challenges. Materials Science and Engineering: C, 2019. **104**: p. 109895.
- Hench, L.L. and J.R. Jones, *Bioactive Glasses: Frontiers and Challenges*. Frontiers in Bioengineering and Biotechnology, 2015. **3**.
- 263. Stein, F., et al., *Vascularization in Oral and Maxillofacial Tissue Engineering*. Tissue Engineering in Oral and Maxillofacial Surgery, 2019: p. 97-122.
- 264. Jones, J.R., Review of bioactive glass: from Hench to hybrids. Acta Biomater, 2013. 9(1): p. 4457-86.
- 265. Hench, L.L., et al., *Bonding mechanisms at the interface of ceramic prosthetic materials.* Journal of Biomedical Materials Research, 1971. **5**(6): p. 117-141.
- 266. Hench, L.L., *BIOCERAMICS FROM CONCEPT TO CLINIC*. Journal of the American Ceramic Society, 1991. **74**(7): p. 1487-1510.
- 267. Brauer, D.S., *Bioactive Glasses-Structure and Properties*. Angewandte Chemie-International Edition, 2015. **54**(14): p. 4160-4181.
- 268. Jones, J.R., 12 Bioactive glass, in Bioceramics and their Clinical Applications, T. Kokubo, Editor. 2008,

- Woodhead Publishing. p. 266-283.
- 269. Shearer, A., et al., *Trends and perspectives on the commercialization of bioactive glasses*. Acta Biomaterialia, 2023. **160**: p. 14-31.
- 270. Aitasalo, K.M., et al., *Craniofacial bone reconstruction with bioactive fiber -reinforced composite implant.* Head & Neck, 2014. **36**(5): p. 722-728.
- 271. Stanley, H.R., et al., *Using 45S5 bioglass cones as endosseous ridge maintenance implants to prevent alveolar ridge resorption: a 5-year evaluation.* Int J Oral Maxillofac Implants, 1997. **12**(1): p. 95-105.
- 272. Weinstein, A.M., J.J. Klawitter, and S.D. Cook, *Implant-bone interface characteristics of bioglass dental implants*. Journal of Biomedical Materials Research, 1980. **14**(1): p. 23-29.
- 273. Wilson, J. and S.B. Low, *Bioactive ceramics for periodontal treatment: comparative studies in the Patus monkey.* Journal of Applied Biomaterials, 1992. **3**(2): p. 123-129.
- 274. Schepers, E.J., et al., *Bioactive glass particles of narrow size range: a new material for the repair of bone defects.* Implant dentistry, 1993. **2**(3): p. 151-157.
- 275. Ilharreborde, B., et al., *Bioactive glass as a bone substitute for spinal fusion in adolescent idiopathic scoliosis: a comparative study with iliac crest autograft.* Journal of Pediatric Orthopaedics, 2008. **28**(3): p. 347-351.
- 276. Williams, C., *Arglaes controlled release dressing in the control of bacteria*. British Journal of Nursing, 1997. **6**(2): p. 114-115.
- 277. Madeo, M., et al., A randomized trial comparing Arglaes (a transparent dressing containing silver ions) to Tegaderm (a transparent polyurethane dressing) for dressing peripheral arterial catheters and central vascular catheters. Intensive and Critical Care Nursing, 1998. **14**(4): p. 187-191.
- 278. Gabr, A., et al., Liver transplantation following Yttrium -90 radioembolization: 15 -year experience in 207 -patient cohort. Hepatology, 2021. **73**(3): p. 998-1010.
- 279. Griffon, D., et al., Early dissolution of a morsellised impacted silicate -free bioactive glass in metaphyseal defects. Journal of Biomedical Materials Research: An Official Journal of The Society for Biomaterials, The Japanese Society for Biomaterials, and The Australian Society for Biomaterials and the Korean Society for Biomaterials, 2001. **58**(6): p. 638-644.
- 280. Low, S.B., C.J. King, and J. Krieger, *An evaluation of bioactive ceramic in the treatment of periodontal osseous defects*. International Journal of Periodontics & Restorative Dentistry, 1997. **17**(4).
- 281. Lindfors, N. and A. Aho, *Tissue response to bioactive glass and autogenous bone in the rabbit spine*. European Spine Journal, 2000. **9**: p. 30-35.
- 282. Kargozar, S., et al., *Multiple and promising applications of strontium (Sr)-containing bioactive glasses in bone tissue engineering*. Frontiers in bioengineering and biotechnology, 2019. **7**: p. 161.
- 283. Reddy, G.V., et al., *Comparative assessment of effectiveness of Biomin, NovaMin, herbal, and potassium nitrate desensitizing agents in the treatment of hypersensitive teeth: A clinical study.* J NTR Univ Health Sci. 2019; 8: 24-8. doi: 10.4103/JDRNTRUHS. JDRNTRUHS_110_18, 2019.
- 284. Cenzi, R., et al., *Clinical outcome of 285 Medpor grafts used for craniofacial reconstruction.* Journal of Craniofacial Surgery, 2005. **16**(4): p. 526-530.
- 285. Naik, M.N., R.K. Murthy, and S.G. Honavar, *Comparison of vascularization of Medpor and Medpor-Plus orbital implants: a prospective, randomized study.* Ophthalmic Plastic & Reconstructive Surgery, 2007. **23**(6): p. 463-467.
- 286. Jones, J.R., *Review of bioactive glass: from Hench to hybrids*. Acta biomaterialia, 2013. **9**(1): p. 4457-4486.
- 287. Vollenweider, M., et al., Remineralization of human dentin using ultrafine bioactive glass particles. Acta

- biomaterialia, 2007. 3(6): p. 936-943.
- 288. Barrey, C. and T. Broussolle, *Clinical and radiographic evaluation of bioactive glass in posterior cervical and lumbar spinal fusion*. European Journal of Orthopaedic Surgery & Traumatology, 2019. **29**: p. 1623-1629.
- 289. Palussière, J., et al., *Clinical results of an open prospective study of a bis-GMA composite in percutaneous vertebral augmentation.* European Spine Journal, 2005. **14**: p. 982-991.
- 290. Bae, H., et al., A prospective randomized FDA-IDE trial comparing Cortoss with PMMA for vertebroplasty: a comparative effectiveness research study with 24-month follow-up. 2012, LWW.
- 291. Westhauser, F., et al., Osteogenic differentiation of mesenchymal stem cells is enhanced in a 45S5-supplemented β-TCP composite scaffold: An in-vitro comparison of Vitoss and Vitoss BA. PloS one, 2019. **14**(2): p. e0212799.
- 292. Westhauser, F., et al., Supplementation with 45S5 bioactive glass reduces in vivo resorption of the 6-tricalcium-phosphate-based bone substitute material vitoss. International Journal of Molecular Sciences, 2019. **20**(17): p. 4253.
- 293. Shearer, A., et al., *Trends and perspectives on the commercialization of bioactive glasses*. Acta Biomaterialia, 2023.
- 294. Kirk, J.F., et al., *Osteoconductivity and osteoinductivity of NanoFUSE® DBM.* Cell and tissue banking, 2013. **14**: p. 33-44.
- 295. Kunert, M. and M. Lukomska-Szymanska, *Bio-inductive materials in direct and indirect pulp capping—a review article.* Materials, 2020. **13**(5): p. 1204.
- 296. Ferreira, S.A., et al., *Bioglass/carbonate apatite/collagen composite scaffold dissolution products promote human osteoblast differentiation*. Materials Science and Engineering: C, 2021. **118**: p. 111393.
- 297. Fredericks, D., et al., *Comparison of two synthetic bone graft products in a rabbit posterolateral fusion model.* The lowa Orthopaedic Journal, 2016. **36**: p. 167.
- 298. Su, Z., et al., Borate bioactive glass prevents zoledronate-induced osteonecrosis of the jaw by restoring osteogenesis and angiogenesis. Oral Dis, 2020. **26**(8): p. 1706-1717.
- 299. Wu, Y.L., et al., *Calcium-based biomaterials: Unveiling features and expanding applications in osteosarcoma treatment.* Bioactive Materials, 2024. **32**: p. 385-399.
- 300. Gu, J.F., et al., *Multifunctional bioactive glasses with spontaneous degradation for simultaneous osteosarcoma therapy and bone regeneration.* Biomaterials Advances, 2023. **154**.
- 301. Raitio, A., et al., *Biodegradable biomaterials in orthopedic surgery: A narrative review of the current evidence.* Scandinavian Journal of Surgery, 2023.
- 302. Dutta, S.D., et al., Unraveling the potential of 3D bioprinted immunomodulatory materials for regulating macrophage polarization: State-of-the-art in bone and associated tissue regeneration. Bioactive Materials, 2023. **28**: p. 284-310.
- 303. Fernandes, J.S., et al., *Multifunctional bioactive glass and glass-ceramic biomaterials with antibacterial properties for repair and regeneration of bone tissue.* Acta Biomaterialia, 2017. **59**: p. 2-11.
- 304. Waltimo, T., et al., *Antimicrobial effect of nanometric bioactive glass 45S5.* Journal of Dental Research, 2007. **86**(8): p. 754-757.
- 305. Bigham, A., et al., *Oxygen-Deficient Bioceramics: Combination of Diagnosis, Therapy, and Regeneration.*Advanced Materials, 2023. **35**(41).
- 306. Decker, S., et al., *In vitro and in ovo impact of the ionic dissolution products of boron-doped bioactive silicate glasses on cell viability, osteogenesis and angiogenesis.* Scientific Reports, 2022. **12**(1): p. 8510.
- 307. Xynos, I.D., et al., Gene-expression profiling of human osteoblasts following treatment with the ionic

- products of Bioglass® 45S5 dissolution. Journal of Biomedical Materials Research: An Official Journal of The Society for Biomaterials, The Japanese Society for Biomaterials, and The Australian Society for Biomaterials and the Korean Society for Biomaterials, 2001. **55**(2): p. 151-157.
- 308. Clupper, D., et al., *In vitro bioactivity of S520 glass fibers and initial assessment of osteoblast attachment.*Journal of Biomedical Materials Research Part A: An Official Journal of The Society for Biomaterials, The Japanese Society for Biomaterials, and The Australian Society for Biomaterials and the Korean Society for Biomaterials, 2003. **67**(1): p. 285-294.
- 309. Xynos, I.D., et al., *Ionic products of bioactive glass dissolution increase proliferation of human osteoblasts and induce insulin-like growth factor II mRNA expression and protein synthesis.* Biochem Biophys Res Commun, 2000. **276**(2): p. 461-5.
- 310. Que, Y., et al., *Ion cocktail therapy for myocardial infarction by synergistic regulation of both structural and electrical remodeling.* Exploration. **n/a**(n/a): p. 20230067.
- 311. Turner, J., et al., *The effect of Si species released from bioactive glasses on cell behaviour: A quantitative review.* Acta Biomater, 2023. **170**: p. 39-52.
- 312. Ratcliffe, S., et al., *Identification of a mammalian silicon transporter*. American Journal of Physiology-Cell Physiology, 2017. **312**(5): p. C550-C561.
- 313. Garneau, A.P., et al., *Aquaporins mediate silicon transport in humans*. PLoS One, 2015. **10**(8): p. e0136149.
- 314. Nielsen, F.H., *Update on the possible nutritional importance of silicon.* Journal of trace elements in medicine and biology, 2014. **28**(4): p. 379-382.
- 315. Sripanyakorn, S., et al., Dietary silicon and bone health. Nutrition Bulletin, 2005. 30(3): p. 222-230.
- Barel, A., et al., *Effect of oral intake of choline-stabilized orthosilicic acid on skin, nails and hair in women with photodamaged skin.* Archives of dermatological research, 2005. **297**: p. 147-153.
- 317. Macdonald, H.M., et al., *Dietary silicon interacts with oestrogen to influence bone health: evidence from the Aberdeen Prospective Osteoporosis Screening Study.* Bone, 2012. **50**(3): p. 681-7.
- 318. Jugdaohsingh, R., et al., *Dietary silicon intake is positively associated with bone mineral density in men and premenopausal women of the Framingham Offspring cohort.* J Bone Miner Res, 2004. **19**(2): p. 297-307.
- 319. Gillette-Guyonnet, S., S. Andrieu, and B. Vellas, *The potential influence of silica present in drinking water on Alzheimer's disease and associated disorders.* The Journal of nutrition, health & aging, 2007. **11**(2): p. 119.
- 320. Prescha, A., et al., Silicon intake and plasma level and their relationships with systemic redox and inflammatory markers in rheumatoid arthritis patients. Advances in Clinical & Experimental Medicine, 2019. **28**(11).
- 321. Hing, K.A., et al., *Effect of silicon level on rate, quality and progression of bone healing within silicate-substituted porous hydroxyapatite scaffolds.* Biomaterials, 2006. **27**(29): p. 5014-26.
- Jones, J.R., et al., *Bioactive glass scaffolds for bone regeneration and their hierarchical characterisation.*Proc Inst Mech Eng H, 2010. **224**(12): p. 1373-87.
- 323. Gough, J.E., J.R. Jones, and L.L. Hench, *Nodule formation and mineralisation of human primary osteoblasts cultured on a porous bioactive glass scaffold.* Biomaterials, 2004. **25**(11): p. 2039-46.
- Hoppe, A., N.S. Güldal, and A.R. Boccaccini, *A review of the biological response to ionic dissolution products from bioactive glasses and glass-ceramics*. Biomaterials, 2011. **32 11**: p. 2757-74.
- Oonishi, H., et al., *Quantitative comparison of bone growth behavior in granules of Bioglass, A-W glass-ceramic, and hydroxyapatite.* J Biomed Mater Res, 2000. **51**(1): p. 37-46.

- 326. Xynos, I.D., et al., *Gene-expression profiling of human osteoblasts following treatment with the ionic products of Bioglass® 45S5 dissolution.* Journal of Biomedical Materials Research, 2001. **55**(2): p. 151-157.
- 327. Shie, M.Y., S.J. Ding, and H.C. Chang, *The role of silicon in osteoblast-like cell proliferation and apoptosis.*Acta Biomater, 2011. **7**(6): p. 2604-14.
- 328. Zhang, D., et al., *Comparison of antibacterial effect of three bioactive glasses*. Key engineering materials, 2006. **309**: p. 345-348.
- 329. Zhang, D., M. Hupa, and L. Hupa, *In situ pH within particle beds of bioactive glasses*. Acta Biomater, 2008. **4**(5): p. 1498-505.
- 330. Zhang, D., et al., *Antibacterial effects and dissolution behavior of six bioactive glasses*. J Biomed Mater Res A, 2010. **93**(2): p. 475-83.
- 331. Li, H. and J. Chang, *Stimulation of proangiogenesis by calcium silicate bioactive ceramic*. Acta Biomaterialia, 2013. **9**(2): p. 5379-5389.
- 332. Dashnyam, K., et al., A mini review focused on the proangiogenic role of silicate ions released from silicon-containing biomaterials. J Tissue Eng, 2017. 8: p. 2041731417707339.
- 333. Salarkia, E., et al., *Exploring mesoporous silica nanoparticles as oral insulin carriers: In-silico and in vivo evaluation*. Heliyon, 2023. **9**(10): p. e20430.
- 334. Jiao, B., et al., *IRF4 Participates in Pulmonary Fibrosis Induced by Silica Particles through Regulating Macrophage Polarization and Fibroblast Activation*. Inflammation, 2023.
- 335. Lv, F., et al., *A conducive bioceramic/polymer composite biomaterial for diabetic wound healing.* Acta Biomaterialia, 2017. **60**: p. 128-143.
- 336. Dong, X.X., et al., Inhibition of the negative effect of high glucose on osteogenic differentiation of bone marrow stromal cells by silicon ions from calcium silicate bioceramics. Regenerative Biomaterials, 2020. **7**(1): p. 9-18.
- 337. Meng, L.S., et al., *The impact of leuprolide acetate-loaded calcium phosphate silicate cement to bone regeneration under osteoporotic conditions.* Biomedical Materials, 2021. **16**(4).
- 338. Kang, C.M., et al., Effects of Three Calcium Silicate Cements on Inflammatory Response and Mineralization-Inducing Potentials in a Dog Pulpotomy Model. Materials, 2018. **11**(6).
- 339. Naseri, S., W.C. Lepry, and S.N. Nazhat, *Bioactive glasses in wound healing: hope or hype?* J Mater Chem B, 2017. **5**(31): p. 6167-6174.
- da Costa, R.R., et al., *Antimicrobial and bone repair effects of boric acid in a rat model of dry socket* (alveolar osteitis) following dental extraction. Journal of Trace Elements in Medicine and Biology, 2023. **76**.
- 341. Tepedelen, B.E., E. Soya, and M. Korkmaz, *Boric Acid Reduces the Formation of DNA Double Strand Breaks and Accelerates Wound Healing Process.* Biol Trace Elem Res, 2016. **174**(2): p. 309-318.
- 342. Mogoşanu, G.D., et al., *Calcium Fructoborate for Bone and Cardiovascular Health*. Biological Trace Element Research, 2016. **172**(2): p. 277-281.
- 343. CHAPIN, R.E., et al., *The Effects of Dietary Boron on Bone Strength in Rats.* Toxicological Sciences, 1997. **35**(2): p. 205-215.
- 344. Turkez, H., et al., *Promising potential of boron compounds against Glioblastoma: In Vitro antioxidant, anti-inflammatory and anticancer studies.* Neurochem Int, 2021. **149**: p. 105137.
- 345. Shafaghi, R., et al., *In vitro evaluation of novel titania-containing borate bioactive glass scaffolds.* J Biomed Mater Res A, 2021. **109**(2): p. 146-158.
- 346. Tian, Y.M., et al., Differential sensitivity of hypoxia inducible factor hydroxylation sites to hypoxia and

- hydroxylase inhibitors. J Biol Chem, 2011. 286(15): p. 13041-51.
- 347. Quinlan, E., et al., *Hypoxia-mimicking bioactive glass/collagen glycosaminoglycan composite scaffolds to enhance angiogenesis and bone repair.* Biomaterials, 2015. **52**: p. 358-66.
- 348. Wu, C., et al., *Hypoxia-mimicking mesoporous bioactive glass scaffolds with controllable cobalt ion release for bone tissue engineering.* Biomaterials, 2012. **33**(7): p. 2076-85.
- 349. Solanki, A.K., et al., *Bioactive glasses and electrospun composites that release cobalt to stimulate the HIF pathway for wound healing applications.* Biomater Res, 2021. **25**(1): p. 1.
- 350. Fan, W., R. Crawford, and Y. Xiao, *Enhancing in vivo vascularized bone formation by cobalt chloride-treated bone marrow stromal cells in a tissue engineered periosteum model.* Biomaterials, 2010. **31**(13): p. 3580-9.
- 351. Rezaei, A., et al., *Hypoxia mimetics restore bone biomineralisation in hyperglycaemic environments.* Scientific Reports, 2022. **12**(1).
- 352. Zhang, M.H., et al., *Cobalt-containing borate bioactive glass fibers for treatment of diabetic wound.*Journal of Materials Science-Materials in Medicine, 2023. **34**(8).
- 353. Solanki, A.K., et al., *Cobalt containing glass fibres and their synergistic effect on the HIF-1 pathway for wound healing applications.* Frontiers in Bioengineering and Biotechnology, 2023. **11**.
- 354. Vinayak, M.N., et al., Accelerating full-thickness skin wound healing using Zinc and Cobalt doped-bioactive glass-coated eggshell membrane. Journal of Drug Delivery Science and Technology, 2023. **81**.
- 355. Wren, A.W., N.M. Cummins, and M.R. Towler, *Comparison of antibacterial properties of commercial bone cements and fillers with a zinc-based glass polyalkenoate cement.* Journal of Materials Science, 2010. **45**(19): p. 5244-5251.
- 356. Yoshizawa, S., et al., *Magnesium ion stimulation of bone marrow stromal cells enhances osteogenic activity, simulating the effect of magnesium alloy degradation.* Acta Biomaterialia, 2014. **10**(6): p. 2834-2842.
- 357. Seitz, J.M., et al., Application of a Bioactive Coating on Resorbable, Neodymium Containing Magnesium Alloys, and Analyses of their Effects on the In Vitro Degradation Behavior in a Simulated Body Fluid. Advanced Engineering Materials, 2012. **14**(6): p. B311-B321.
- 358. Zhang, X., et al., Enhancement of osteoporotic bone regeneration by strontium-substituted 45S5 bioglass via time-dependent modulation of autophagy and the Akt/mTOR signaling pathway. J Mater Chem B, 2021. **9**(16): p. 3489-3501.
- 359. Fiume, E., et al., Biological Evaluation of a New Sodium-Potassium Silico-Phosphate Glass for Bone Regeneration: In Vitro and In Vivo Studies. Materials, 2021. **14**(16).
- 360. Guimaraes, R.P., et al., Koh group influence on titanium surfaces and pure sol-gel silica for enhanced osteogenic activity. Journal of Biomaterials Applications, 2020. **35**(3): p. 405-421.
- 361. Wetzel, R., O. Bartzok, and D.S. Brauer, *Influence of low amounts of zinc or magnesium substitution on ion release and apatite formation of Bioglass 45S5.* Journal of Materials Science-Materials in Medicine, 2020. **31**(10).
- 362. Houaoui, A., et al., New Generation of Hybrid Materials Based on Gelatin and Bioactive Glass Particles for Bone Tissue Regeneration. Biomolecules, 2021. **11**(3).
- 363. Houaoui, A., et al., New Generation of Hybrid Materials Based on Gelatin and Bioactive Glass Particles for Bone Tissue Regeneration. Biomolecules, 2021. **11**(3): p. 444.
- 364. Serio, F., et al., *Electrospun Filaments Embedding Bioactive Glass Particles with Ion Release and Enhanced Mineralization*. Nanomaterials (Basel), 2019. **9**(2).
- 365. Liverani, L., et al., Nanocomposite electrospun fibers of poly(ε -caprolactone)/bioactive glass with shape

- memory properties. Bioactive Materials, 2022. 11: p. 230-239.
- 366. Qing, Y., et al., *Chemotactic ion-releasing hydrogel for synergistic antibacterial and bone regeneration.*Materials Today Chemistry, 2022. **24**: p. 100894.
- 367. Liu, X.Z., et al., Strontium doped mesoporous silica nanoparticles accelerate osteogenesis and angiogenesis in distraction osteogenesis by activation of Wnt pathway. Nanomedicine-Nanotechnology Biology and Medicine, 2022. **41**.
- Lee, S., Development of glass-related biomaterials for enhanced bone regeneration via stimulation of cell function. Journal of the Ceramic Society of Japan, 2020. **128**(7): p. 349-356.
- 369. Kim, S., et al., Identification of Potentially Pathogenic Variants Associated with Recurrence in Medication-Related Osteonecrosis of the Jaw (MRONJ) Patients Using Whole-Exome Sequencing. J Clin Med, 2022. **11**(8).
- 370. Yang, G., et al., *Genome-wide Association Study Identified Chromosome 8 Locus Associated with Medication-Related Osteonecrosis of the Jaw.* Clin Pharmacol Ther, 2021. **110**(6): p. 1558-1569.
- 371. Lee, K.H., et al., *Identifying genetic variants underlying medication-induced osteonecrosis of the jaw in cancer and osteoporosis: a case control study.* J Transl Med, 2019. **17**(1): p. 381.
- 372. Kastritis, E., et al., *Genetic factors related with early onset of osteonecrosis of the jaw in patients with multiple myeloma under zoledronic acid therapy.* Leukemia & Lymphoma, 2017. **58**(10): p. 2304-2309.
- 373. Yahara, H., et al., Shotgun metagenome sequencing identification of a set of genes encoded by Actinomyces associated with medication-related osteonecrosis of the jaw. PLoS One, 2020. **15**(11): p. e0241676.
- 374. Zirk, M., et al., *Microbial diversity in infections of patients with medication-related osteonecrosis of the jaw.* Clin Oral Investig, 2019. **23**(5): p. 2143-2151.
- 375. English, B.C., et al., A SNP in CYP2C8 is not associated with the development of bisphosphonate-related osteonecrosis of the jaw in men with castrate-resistant prostate cancer. Ther Clin Risk Manag, 2010. **6**: p. 579-83.
- 376. Kim, S. and A. Misra, *SNP genotyping: technologies and biomedical applications*. Annu Rev Biomed Eng, 2007. **9**: p. 289-320.
- 377. Raje, N., et al., *Clinical, radiographic, and biochemical characterization of multiple myeloma patients with osteonecrosis of the jaw.* Clin Cancer Res, 2008. **14**(8): p. 2387-95.
- 378. Wehrhan, F., et al., Expression of Msx-1 is suppressed in bisphosphonate associated osteonecrosis related jaw tissue-etiopathology considerations respecting jaw developmental biology-related unique features. J Transl Med, 2010. **8**: p. 96.
- 379. Majewski, J., et al., *What can exome sequencing do for you?* Journal of Medical Genetics, 2011. **48**(9): p. 580-589.
- 380. Piskol, R., G. Ramaswami, and J.B. Li, *Reliable Identification of Genomic Variants from RNA-Seq Data*.

 American Journal of Human Genetics, 2013. **93**(4): p. 641-651.
- 381. Tam, V., et al., *Benefits and limitations of genome-wide association studies*. Nature Reviews Genetics, 2019. **20**(8): p. 467-484.
- 382. Korte, A. and A. Farlow, *The advantages and limitations of trait analysis with GWAS: a review.* Plant Methods, 2013. **9**.
- 383. Brookes, A.J., *The essence of SNPs.* Gene, 1999. **234**(2): p. 177-86.
- 384. Nicoletti, P., et al., *Genomewide Pharmacogenetics of Bisphosphonate-Induced Osteonecrosis of the Jaw: The Role of RBMS3.* Oncologist, 2012. **17**(2): p. 279-287.
- 385. Choi, H., et al., Genetic association between VEGF polymorphisms and BRONJ in the Korean population.

- Oral Dis, 2015. **21**(7): p. 866-71.
- 386. Yang, G., et al., SIRT1/HERC4 Locus Associated With Bisphosphonate-Induced Osteonecrosis of the Jaw: An Exome-Wide Association Analysis. J Bone Miner Res, 2018. **33**(1): p. 91-98.
- 387. Such, E., et al., *CYP2C8 gene polymorphism and bisphosphonate-related osteonecrosis of the jaw in patients with multiple myeloma*. Haematologica, 2011. **96**(10): p. 1557-9.
- 388. Vangsted, A., T.W. Klausen, and U. Vogel, *Genetic variations in multiple myeloma II: association with effect of treatment.* European Journal of Haematology, 2012. **88**(2): p. 93-117.
- 389. Kosa, J.P., et al., EXAMINATION OF CYP2C8 rs1934951 POLYMORPHISM IN HUNGARIAN PATIENTS SUFFERING FROM BISPHOSPHONATE-INDUCED OSTEONECROSIS OF THE JAW. Osteoporosis International, 2012. 23: p. S373-S373.
- 390. Balla, B., et al., New approach to analyze genetic and clinical data in bisphosphonate-induced osteonecrosis of the jaw. Oral Diseases, 2012. **18**(6): p. 580-585.
- 391. Kluetz, P.G., et al., Evaluation of variants of the rs1934951 locus of CYP2C8 and bisphosphonate-related osteonecrosis of the jaw in castrate-resistant prostate cancer (CRPC) patients. Journal of Clinical Oncology, 2010. **28**(15).
- 392. Li, Q., et al., Porphyromonas, Treponema, and Mogibacterium promote IL8/IFNgamma/TNFalpha-based pro-inflammation in patients with medication-related osteonecrosis of the jaw. J Oral Microbiol, 2020. **13**(1): p. 1851112.
- 393. Hallmer, F., et al., *Bacterial diversity in medication-related osteonecrosis of the jaw.* Oral Surg Oral Med Oral Pathol Oral Radiol, 2017. **123**(4): p. 436-444.
- 394. Fleming, I., *Epoxyeicosatrienoic acids, cell signaling and angiogenesis*. Prostaglandins Other Lipid Mediat, 2007. **82**(1-4): p. 60-7.
- 395. Capdevila, J.H., J.R. Falck, and R.C. Harris, *Cytochrome P450 and arachidonic acid bioactivation. Molecular and functional properties of the arachidonate monooxygenase.* J Lipid Res, 2000. **41**(2): p. 163-81.
- 396. Tontonoz, P., et al., *PPARgamma promotes monocyte/macrophage differentiation and uptake of oxidized LDL*. Cell, 1998. **93**(2): p. 241-52.
- 397. Hoeben, A., et al., *Vascular endothelial growth factor and angiogenesis*. Pharmacol Rev, 2004. **56**(4): p. 549-80.
- 398. Hamid, R., et al., *Comparison of alamar blue and MTT assays for high through-put screening*. Toxicology in Vitro, 2004. **18**(5): p. 703-710.
- 399. MacDonald, C., *Development of new cell lines for animal cell biotechnology.* Crit Rev Biotechnol, 1990. **10**(2): p. 155-78.
- 400. Schurr, M.J., et al., *Phase I/II clinical evaluation of StrataGraft: a consistent, pathogen-free human skin substitute.* J Trauma, 2009. **66**(3): p. 866-73; discussion 873-4.
- 401. Soice, E. and J. Johnston, *Immortalizing Cells for Human Consumption*. International Journal of Molecular Sciences, 2021. **22**(21).
- 402. Pan, C.P., et al., Comparative Proteomic Phenotyping of Cell Lines and Primary Cells to Assess Preservation of Cell Type-specific Functions. Molecular & Cellular Proteomics, 2009. **8**(3): p. 443-450.
- 403. Czekanska, E.M., et al., *A phenotypic comparison of osteoblast cell lines versus human primary osteoblasts for biomaterials testing.* Journal of Biomedical Materials Research Part A, 2014. **102**(8): p. 2636-2643.
- 404. Scuteri, A., et al., *Mesengenic differentiation: comparison of human and rat bone marrow mesenchymal stem cells.* Int J Stem Cells, 2014. **7**(2): p. 127-34.

- 405. Roullet, J.B., et al., *Mevalonate availability affects human and rat resistance vessel function.* J Clin Invest, 1995. **96**(1): p. 239-44.
- 406. Olsson, J.M., et al., *Enzymes of the mevalonate pathway in rat liver nodules induced by 2-acetylaminofluorene treatment*. Carcinogenesis, 1995. **16**(3): p. 599-605.
- 407. Otto, M., et al., Geranyl-geraniol addition affects potency of bisphosphonates-a comparison in vitro promising a therapeutic approach for bisphosphonate-associated osteonecrosis of the jaw and oral wound healing. Oral and Maxillofacial Surgery-Heidelberg, 2022. **26**(2): p. 321-332.
- 408. Yamachika, E., et al., *The influence of zoledronate and teriparatide on gamma delta T cells in mice.* Journal of Dental Sciences, 2017. **12**(4): p. 333-339.
- 409. Lang, M., et al., *Influence of zoledronic acid on proliferation, migration, and apoptosis of vascular endothelial cells.* British Journal of Oral & Maxillofacial Surgery, 2016. **54**(8): p. 889-893.
- 410. Walter, C., A.M. Pabst, and T. Ziebart, Effects of a low-level diode laser on oral keratinocytes, oral fibroblasts, endothelial cells and osteoblasts incubated with bisphosphonates: An in vitro study. Biomedical Reports, 2015. **3**(1): p. 14-18.
- 411. Hagelauer, N., et al., *Bisphosphonates inhibit cell functions of HUVECs, fibroblasts and osteogenic cells via inhibition of protein geranylgeranylation.* Clinical Oral Investigations, 2015. **19**(5): p. 1079-1091.
- 412. Elsayed, R., et al., Role of dendritic cell-mediated immune response in oral homeostasis: A new mechanism of osteonecrosis of the jaw. Faseb Journal, 2020. **34**(2): p. 2595-2608.
- 413. Manzano-Moreno, F.J., et al., *Effect of Clodronate on Antigenic Profile, Growth, and Differentiation of Osteoblast-Like Cells*. Journal of Oral and Maxillofacial Surgery, 2016. **74**(9): p. 1765-1770.
- 414. Boyle, W.J., W.S. Simonet, and D.L. Lacey, *Osteoclast differentiation and activation*. Nature, 2003. **423**(6937): p. 337-342.
- 415. Stessuk, T., et al., *Osteogenic differentiation driven by osteoclasts and macrophages*. Journal of Immunology and Regenerative Medicine, 2021. **12**: p. 100044.
- 416. Huang, X.L., et al., *Zoledronic acid inhibits osteoclastogenesis and bone resorptive function by suppressing RANKL-mediated NF-kappa B and JNK and their downstream signalling pathways.*Molecular Medicine Reports, 2022. **25**(2).
- 417. Abe, K., et al., *Effects of bisphosphonates on osteoclastogenesis in RAW264.7 cells.* International Journal of Molecular Medicine, 2012. **29**(6): p. 1007-1015.
- 418. Zhao, D., et al., *Tetrahedral Framework Nucleic Acid Promotes the Treatment of Bisphosphonate-Related Osteonecrosis of the Jaws by Promoting Angiogenesis and M2 Polarization*. Acs Applied Materials & Interfaces, 2020. **12**(40): p. 44508-44522.
- 419. Tamaki, S., et al., Dynamic polarization shifting from M1 to M2 macrophages in reduced osteonecrosis of the jaw-like lesions by cessation of anti-RANKL antibody in mice. Bone, 2020. **141**.
- 420. Maki Nagasaki1) , K.N., 3), Lipopolysaccharide and High Concentrations of Glucose Enhances Zoledronate. 2021.
- 421. Gong, X., et al., Skeletal Site-specific Effects of Zoledronate on in vivo Bone Remodeling and in vitro BMSCs Osteogenic Activity. Scientific Reports, 2017. **7**.
- 422. Ohe, J.Y., Y.D. Kwon, and H.W. Lee, *Bisphosphonates modulate the expression of OPG and M-CSF in hMSC-derived osteoblasts.* Clinical Oral Investigations, 2012. **16**(4): p. 1153-1159.
- 423. Borsani, E., et al., Beneficial Effects of Concentrated Growth Factors and Resveratrol on Human Osteoblasts In Vitro Treated with Bisphosphonates. Biomed Research International, 2018. 2018.
- 424. Manzano-Moreno, F.J., et al., *Impact of bisphosphonates on the proliferation and gene expression of human fibroblasts*. International Journal of Medical Sciences, 2019. **16**(12): p. 1534-1540.

- 425. Huang, X., et al., *Dose-dependent inhibitory effects of zoledronic acid on osteoblast viability and function in vitro.* Molecular Medicine Reports, 2016. **13**(1): p. 613-622.
- 426. Bayram, H., et al., Effect of low level laser therapy and zoledronate on the viability and ALP activity of Saos-2 cells. International Journal of Oral and Maxillofacial Surgery, 2013. **42**(1): p. 140-146.
- 427. Basso, F.G., et al., *Zoledronic Acid Inhibits Human Osteoblast Activities*. Gerontology, 2013. **59**(6): p. 534-541.
- 428. Patntirapong, S., et al., *Zoledronic acid suppresses mineralization through direct cytotoxicity and osteoblast differentiation inhibition.* Journal of Oral Pathology & Medicine, 2012. **41**(9): p. 713-720.
- 429. Gao, F., et al., *Zoledronic acid regulates osteoblast differentiation via the mTORC1 signaling pathway.*International Journal of Clinical and Experimental Medicine, 2018. **11**(5): p. 4585-4594.
- 430. Suzuki, K., et al., Structure-Dependent Effects of Bisphosphonates on Inflammatory Responses in Cultured Neonatal Mouse Calvaria. Antioxidants (Basel), 2020. **9**(6).
- 431. Nagasaki, M., et al., *Lipopolysaccharide and High Concentrations of Glucose Enhances Zoledronate-induced Increase in RANKL/OPG Ratio by Upregulating PGE(2) Production in Osteoblasts*. Journal of Hard Tissue Biology, 2021. **30**(1): p. 37-43.
- 432. Koch, F.P., et al., *The influence of bisphosphonates on human osteoblast migration and integrin aVb3/tenascin C gene expression in vitro.* Head & Face Medicine, 2011. **7**.
- 433. Liu, X.H., et al., Interactive effect of interleukin-6 and prostaglandin E2 on osteoclastogenesis via the OPG/RANKL/RANK system. Ann N Y Acad Sci, 2006. **1068**: p. 225-33.
- 434. Li, M., et al., The Outcome of Bisphosphonate-Related Osteonecrosis of the Jaw Patients' Gingiva-Derived Mesenchymal Stem Cells on Wound Healing in a Mice Excisional Skin Model. 2021.
- 435. Yusa, K., et al., Influences of Compressive Force and Zoledronic Acid on Osteoblast Proliferation and Differentiation: An In Vitro Study. Applied Sciences-Basel, 2021. **11**(23).
- 436. Ishtiaq, S., et al., *The effect of nitrogen containing bisphosphonates, zoledronate and alendronate, on the production of pro-angiogenic factors by osteoblastic cells.* Cytokine, 2015. **71**(2): p. 154-160.
- 437. Acil, Y., et al., *Cytotoxic and inflammatory effects of alendronate and zolendronate on human osteoblasts, gingival fibroblasts and osteosarcoma cells.* Journal of Cranio-Maxillofacial Surgery, 2018. **46**(4): p. 538-546.
- 438. Kruger, T.B., et al., *Alendronate and omeprazole in combination reduce angiogenic and growth signals from osteoblasts.* Bone Reports, 2021. **14**.
- 439. Kaneko, J., et al., *Zoledronic acid exacerbates inflammation through M1 macrophage polarization.* Inflammation and Regeneration, 2018. **38**.
- 440. Zago, P.M.W., et al., Standardized Arrabidaea chica Extract Shows Cytoprotective Effects in Zoledronic Acid-Treated Fibroblasts and Osteoblasts. Clinical Cosmetic and Investigational Dentistry, 2020. 12: p. 327-333.
- Sung, C.M., et al., *In vitro effects of alendronate on fibroblasts of the human rotator cuff tendon.* Bmc Musculoskeletal Disorders, 2020. **21**(1).
- 442. Di Vito, A., et al., *Dose-Dependent Effects of Zoledronic Acid on Human Periodontal Ligament Stem Cells: An In Vitro Pilot Study.* Cell Transplantation, 2020. **29**.
- 443. Manzano-Moreno, F.J., et al., *High doses of bisphosphonates reduce osteoblast-like cell proliferation by arresting the cell cycle and inducing apoptosis.* Journal of Cranio-Maxillofacial Surgery, 2015. **43**(3): p. 396-401.
- 444. Ohnuki, H., et al., *Zoledronic acid induces S-phase arrest via a DNA damage response in normal human oral keratinocytes*. Archives of Oral Biology, 2012. **57**(7): p. 906-917.

- Orriss, I.R., et al., *Optimisation of the differing conditions required for bone formation in vitro by primary osteoblasts from mice and rats.* International Journal of Molecular Medicine, 2014. **34**(5): p. 1201-1208.
- Taciak, B., et al., Evaluation of phenotypic and functional stability of RAW 264.7 cell line through serial passages. Plos One, 2018. **13**(6).
- 447. Cuetara, B.L.V., et al., *Cloning and characterization of osteoclast precursors from the RAW264.7 cell line.*In Vitro Cellular & Developmental Biology-Animal, 2006. **42**(7): p. 182-188.
- 448. Li, A.Y., Understanding the role of orthopaedic implant dissolution ions in bone remodelling. 2019, University College London.
- 449. Marx, R.E., *Pamidronate (Aredia) and zoledronate (Zometa) induced avascular necrosis of the jaws: a growing epidemic.* J Oral Maxillofac Surg, 2003. **61**(9): p. 1115-7.
- 450. Tao, M.H., et al., *Oral bisphosphonate use and lung cancer incidence among postmenopausal women.*Annals of Oncology, 2018. **29**(6): p. 1476-1485.
- 451. Ruggiero, S.L., et al., American Association of Oral and Maxillofacial Surgeons position paper on bisphosphonate-related osteonecrosis of the jaws--2009 update. J Oral Maxillofac Surg, 2009. **67**(5 Suppl): p. 2-12.
- 452. Orriss, I.R., et al., *Inhibition of Osteoblast Function In Vitro by Aminobisphosphonates*. Journal of Cellular Biochemistry, 2009. **106**(1): p. 109-118.
- 453. Fliefel, R.M., et al., *Geranylgeraniol (GGOH) as a Mevalonate Pathway Activator in the Rescue of Bone Cells Treated with Zoledronic Acid: An In Vitro Study.* Stem Cells International, 2019. **2019**.
- 454. Manzano-Moreno, F.J., et al., *High doses of bisphosphonates reduce osteoblast-like cell proliferation by arresting the cell cycle and inducing apoptosis.* Journal of Cranio-Maxillofacial Surgery, 2015. **43**(3): p. 396-401.
- 455. Chen, X., et al., Geranylgeraniol Restores Zoledronic Acid-Induced Efferocytosis Inhibition in Bisphosphonate-Related Osteonecrosis of the Jaw. Frontiers in Cell and Developmental Biology, 2021. 9.
- 456. Taniguchi, N., et al., *Bisphosphonate-induced reactive oxygen species inhibit proliferation and migration of oral fibroblast: A pathogenesis of bisphosphonate-related osteonecrosis of the jaw.* Journal of Periodontology, 2020. **91**(7): p. 947-955.
- 457. Feng Gao, Y.L., Mingfa Liu, and L. Zhu, *Zoledronic acid regulates osteoblast differentiation via the mTORC1 signaling pathway.* Int J Clin Exp Med, 2018. **11(5):4585-4594**.
- 458. Bills, C.E., H. Eisenberg, and S.L. Pallante, *COMPLEXES OF ORGANIC ACIDS WITH CALCIUM PHOSPHATE VON KOSSA STAIN AS A CLUE TO COMPOSITION OF BONE MINERAL*. Johns Hopkins Medical Journal,
 1971. **128**(4): p. 194-+.
- 459. <On the history and mechanism of alizarin and alizarin red S stains for calcium.pdf>. 1969.
- 460. Bertazzo, S. and E. Gentleman, *Aortic valve calcification: a bone of contention*. European Heart Journal, 2017. **38**(16): p. 1189-+.
- 461. Kapustin, A.N., et al., *Vascular Smooth Muscle Cell Calcification Is Mediated by Regulated Exosome Secretion*. Circulation Research, 2015. **116**(8): p. 1312-1323.
- 462. Zafar, S., et al., *Zoledronic acid and geranylgeraniol regulate cellular behaviour and angiogenic gene expression in human gingival fibroblasts.* Journal of Oral Pathology & Medicine, 2014. **43**(9): p. 711-721.
- 463. Scheper, M.A., et al., *A novel bioassay model to determine clinically significant bisphosphonate levels.* Support Care Cancer, 2009. **17**(12): p. 1553-7.
- 464. Lo Faro, A.F., et al., Development and validation of a method using ultra performance liquid chromatography coupled to tandem mass spectrometry for determination of zoledronic acid concentration in human bone. Journal of Pharmaceutical and Biomedical Analysis, 2019. **162**: p. 286-

290.

- 465. Pourgonabadi, S., et al., *In vitro assessment of alendronate toxic and apoptotic effects on human dental pulp stem cells.* Iranian Journal of Basic Medical Sciences, 2018. **21**(9): p. 905-910.
- 466. Anagnostis, P. and J.C. Stevenson, *Bisphosphonate drug holidays--when, why and for how long?* Climacteric, 2015. **18 Suppl 2**: p. 32-8.
- 467. De Colli, M., et al., *Nitric oxide-mediated cytotoxic effect induced by zoledronic acid treatment on human gingival fibroblasts.* Clinical Oral Investigations, 2015. **19**(6): p. 1269-1277.
- 468. Vermeer, J., et al., *Jaw Bone Marrow-Derived Osteoclast Precursors Internalize More Bisphosphonate than Long-Bone Marrow Precursors*. Journal of Bone and Mineral Research, 2013. **28**.
- 469. Knighton, D.R., et al., *Oxygen tension regulates the expression of angiogenesis factor by macrophages.* Science, 1983. **221**(4617): p. 1283-5.
- 470. Yazici, T., et al., *Zoledronic Acid, Bevacizumab and Dexamethasone-Induced Apoptosis, Mitochondrial Oxidative Stress, and Calcium Signaling Are Decreased in Human Osteoblast-Like Cell Line by Selenium Treatment.* Biological Trace Element Research, 2018. **184**(2): p. 358-368.
- 471. Chua, C.C., R.C. Hamdy, and B.H. Chua, *Upregulation of vascular endothelial growth factor by H2O2 in rat heart endothelial cells.* Free Radical Biology and Medicine, 1998. **25**(8): p. 891-897.
- 472. Fay, J., et al., Reactive oxygen species induce expression of vascular endothelial growth factor in chondrocytes and human articular cartilage explants. Arthritis Research & Therapy, 2006. **8**(6): p. R189.
- 473. Israeli, R.S., et al., *The Effect of Zoledronic Acid on Bone Mineral Density in Patients Undergoing Androgen Deprivation Therapy.* Clinical Genitourinary Cancer, 2007. **5**(4): p. 271-277.
- 474. Everts-Graber, J., et al., *Effects of zoledronate on bone mineral density and bone turnover after long-term denosumab therapy: Observations in a real-world setting.* Bone, 2022. **163**: p. 116498.
- Wedemeyer, C., et al., *Stimulation of bone formation by zoledronic acid in particle-induced osteolysis.*Biomaterials, 2005. **26**(17): p. 3719-3725.
- 476. Pan, B., et al., *The nitrogen-containing bisphosphonate, zoledronic acid, increases mineralisation of human bone-derived cells in vitro.* Bone, 2004. **34**(1): p. 112-123.
- 477. Abdik, H., et al., *The effects of bisphosphonates on osteonecrosis of jaw bone: a stem cell perspective.*Molecular Biology Reports, 2019. **46**(1): p. 763-776.
- 478. Koch, F.P., et al., *Zoledronate, ibandronate and clodronate enhance osteoblast differentiation in a dose dependent manner A quantitative in vitro gene expression analysis of Dlx5, Runx2, OCN, MSX1 and MSX2.* Journal of Cranio-Maxillofacial Surgery, 2011. **39**(8): p. 562-569.
- 479. Wang, L., et al., Alendronate promotes the gene expression of extracellular matrix mediated by SP-1/SOX-9. Human & Experimental Toxicology, 2021. **40**(7): p. 1173-1182.
- 480. Koch, F.P., et al., *The impact of bisphosphonates on the osteoblast proliferation and Collagen gene expression in vitro*. Head & Face Medicine, 2010. **6**.
- 481. Kubatzky, K.F., F. Uhle, and T. Eigenbrod, *From macrophage to osteoclast How metabolism determines function and activity.* Cytokine, 2018. **112**: p. 102-115.
- 482. Väänänen, H.K. and T. Laitala-Leinonen, *Osteoclast lineage and function*. Arch Biochem Biophys, 2008. **473**(2): p. 132-8.
- 483. Ibáñez, L., et al., Osteostatin Inhibits M-CSF+RANKL-Induced Human Osteoclast Differentiation by Modulating NFATc1. Int J Mol Sci, 2022. **23**(15).
- 484. Song, C., et al., Evaluation of efficacy on RANKL induced osteoclast from RAW264.7 cells. J Cell Physiol, 2019. **234**(7): p. 11969-11975.
- 485. Matsuo, K. and N. Irie, [Transcription factors in osteoclast differentiation]. Nihon Rinsho, 2005. 63(9): p.

- 1541-6.
- 486. Lorenzo, J., *The many ways of osteoclast activation*. J Clin Invest, 2017. **127**(7): p. 2530-2532.
- 487. Kim, J.M., et al., Osteoblast-Osteoclast Communication and Bone Homeostasis. Cells, 2020. 9(9).
- 488. Frith, J.C., et al., The molecular mechanism of action of the antiresorptive and antiinflammatory drug clodronate: evidence for the formation in vivo of a metabolite that inhibits bone resorption and causes osteoclast and macrophage apoptosis. Arthritis Rheum, 2001. **44**(9): p. 2201-10.
- 489. Kong, L., W. Smith, and D. Hao, *Overview of RAW264.7 for osteoclastogensis study: Phenotype and stimuli.* J Cell Mol Med, 2019. **23**(5): p. 3077-3087.
- 490. Lampiasi, N., et al., Osteoclasts Differentiation from Murine RAW 264.7 Cells Stimulated by RANKL: Timing and Behavior. Biology (Basel), 2021. **10**(2).
- 491. Mira-Pascual, L., et al., A Sub-Clone of RAW264.7-Cells Form Osteoclast-Like Cells Capable of Bone Resorption Faster than Parental RAW264.7 through Increased De Novo Expression and Nuclear Translocation of NFATc1. Int J Mol Sci, 2020. 21(2).
- 492. Vincent, C., et al., *The generation of osteoclasts from RAW 264.7 precursors in defined, serum-free conditions.* J Bone Miner Metab, 2009. **27**(1): p. 114-9.
- 493. Nguyen, J. and A. Nohe, *Factors that Affect the Osteoclastogenesis of RAW264.7 Cells.* J Biochem Anal Stud, 2017. **2**(1).
- 494. Xie, D.N., et al., Sensory denervation increases potential of bisphosphonates to induce osteonecrosis via disproportionate expression of calcitonin gene-related peptide and substance P. Annals of the New York Academy of Sciences, 2021. **1487**(1): p. 56-73.
- 495. Anoop, M., et al., *Zoledronic acid conjugated calcium phosphate nanoparticles for applications in cancer immunotherapy.* Materials Today Communications, 2022. **30**.
- 496. Zhao, W., et al., *Inhibition Effect of Zoledronate on the Osteoclast Differentiation of RAW264.7 Induced by Titanium Particles*. Biomed Res Int, 2021. **2021**: p. 5578088.
- 497. Surface, L.E., et al., *ATRAID regulates the action of nitrogen-containing bisphosphonates on bone.* Science Translational Medicine, 2020. **12**(544).
- 498. Elsayed, R., et al., *Removal of matrix-bound zoledronate prevents post-extraction osteonecrosis of the jaw by rescuing osteoclast function.* Bone, 2018. **110**: p. 141-149.
- 499. Gu, M.H., et al., SPHK Inhibitors and Zoledronic Acid Suppress Osteoclastogenesis and Wear Particle-Induced Osteolysis. Frontiers in Pharmacology, 2022. **12**.
- 500. Desai, S., et al., RANKL-dependent osteoclast differentiation and gene expression in bone marrow-derived cells from adult mice is sexually dimorphic. Bone Rep, 2023. **19**: p. 101697.
- 501. Vuoti, E., et al., *Osteoclastogenesis of human peripheral blood, bone marrow, and cord blood monocytes.*Scientific Reports, 2023. **13**(1): p. 3763.
- 502. Huang, X.L., et al., *Zoledronic acid inhibits osteoclast differentiation and function through the regulation of NF-κB and JNK signalling pathways.* Int J Mol Med, 2019. **44**(2): p. 582-592.
- 503. Dong, W., et al., *Zoledronate and high glucose levels influence osteoclast differentiation and bone absorption via the AMPK pathway.* Biochemical and Biophysical Research Communications, 2018. **505**(4): p. 1195-1202.
- 504. McLeod, N.M.H., et al., *In Vitro Effect of Bisphosphonates on Oral Keratinocytes and Fibroblasts*. Journal of Oral and Maxillofacial Surgery, 2014. **72**(3): p. 503-509.
- 505. Hodgins, N.O., et al., In vitro potency, in vitro and in vivo efficacy of liposomal alendronate in combination with $\gamma\delta$ T cell immunotherapy in mice. J Control Release, 2016. **241**: p. 229-241.
- 506. Gangoiti, M.V., et al., Opposing effects of bisphosphonates and advanced glycation end-products on

- osteoblastic cells. European Journal of Pharmacology, 2008. 600(1-3): p. 140-147.
- 507. Ge, X.Y., et al., Reactive Oxygen Species and Autophagy Associated Apoptosis and Limitation of Clonogenic Survival Induced by Zoledronic Acid in Salivary Adenoid Cystic Carcinoma Cell Line SACC-83. Plos One, 2014. **9**(6).
- Tai, T.W., et al., Reactive oxygen species are required for zoledronic acid-induced apoptosis in osteoclast precursors and mature osteoclast-like cells. Sci Rep, 2017. **7**: p. 44245.
- 509. Piper, K., A. Boyde, and S.J. Jones, *The relationship between the number of nuclei of an osteoclast and its resorptive capability in vitro*. Anat Embryol (Berl), 1992. **186**(4): p. 291-9.
- 510. Orihuela, R., C.A. McPherson, and G.J. Harry, *Microglial M1/M2 polarization and metabolic states*. Br J Pharmacol, 2016. **173**(4): p. 649-65.
- 511. Cuetara, B.L., et al., *Cloning and characterization of osteoclast precursors from the RAW264.7 cell line.*In Vitro Cell Dev Biol Anim, 2006. **42**(7): p. 182-8.
- 512. Ng, A.Y., et al., Comparative Characterization of Osteoclasts Derived From Murine Bone Marrow Macrophages and RAW 264.7 Cells Using Quantitative Proteomics. JBMR Plus, 2018. **2**(6): p. 328-340.
- 513. Zhu, W.Y., et al., *Biodegradable magnesium implant enhances angiogenesis and alleviates medication*related osteonecrosis of the jaw in rats. Journal of Orthopaedic Translation, 2022. **33**: p. 153-161.
- 514. Paulo, S., et al., *Calcium Phosphate Ceramics Can Prevent Bisphosphonate-Related Osteonecrosis of the Jaw.* Materials, 2020. **13**(8).
- Pramanik, C., et al., A mechanistic study of the interaction of water-soluble borate glass with apatite-bound heterocyclic nitrogen-containing bisphosphonates. Acta Biomaterialia, 2016. **31**: p. 339-347.
- 516. Pramanik, C., et al., *Microfibrous borate bioactive glass dressing sequesters bone-bound bisphosphonate in the presence of simulated body fluid.* Journal of Materials Chemistry B, 2015. **3**(6): p. 959-963.
- 517. Al-Harbi, N., et al., Silica-Based Bioactive Glasses and Their Applications in Hard Tissue Regeneration: A Review. Pharmaceuticals, 2021. **14**(2).
- 518. Hoppe, A., N.S. Güldal, and A.R. Boccaccini, *A review of the biological response to ionic dissolution products from bioactive glasses and glass-ceramics*. Biomaterials, 2011. **32**(11): p. 2757-74.
- 519. Crovace, M.C., et al., *Biosilicate (R) A multipurpose, highly bioactive glass-ceramic. In vitro, in vivo and clinical trials.* Journal of Non-Crystalline Solids, 2016. **432**: p. 90-110.
- 520. Han, P.P., C.T. Wu, and Y. Xiao, *The effect of silicate ions on proliferation, osteogenic differentiation and cell signalling pathways (WNT and SHH) of bone marrow stromal cells.* Biomaterials Science, 2013. **1**(4): p. 379-392.
- 521. Liang, W., et al., *Bioactive comparison of a borate, phosphate and silicate glass*. Journal of Materials Research, 2006. **21**(1): p. 125-131.
- 522. Xiao, L., et al., Sustained Release of Melatonin from GelMA Liposomes Reduced Osteoblast Apoptosis and Improved Implant Osseointegration in Osteoporosis. Oxid Med Cell Longev, 2020. **2020**: p. 6797154.
- 523. Turner, J., *Joel's Si review.* 2023.
- 524. Uribe, P., et al., Soluble silica stimulates osteogenic differentiation and gap junction communication in human dental follicle cells. Scientific Reports, 2020. **10**(1).
- 525. Jugdaohsingh, R., Silicon and bone health. Journal of Nutrition Health & Aging, 2007. 11(2): p. 99-110.
- 526. Valerio, P., et al., *The effect of ionic products from bioactive glass dissolution on osteoblast proliferation and collagen production.* Biomaterials, 2004. **25**(15): p. 2941-2948.
- 527. Reffitt, D.M., et al., Orthosilicic acid stimulates collagen type 1 synthesis and osteoblastic differentiation in human osteoblast-like cells in vitro. Bone, 2003. **32**(2): p. 127-135.

- 528. Calomme, M.R. and D.A. VandenBerghe, Supplementation of calves with stabilized orthosilicic acid Effect on the Si, Ca, Mg, and P concentrations in serum and the collagen concentration in skin and cartilage. Biological Trace Element Research, 1997. **56**(2): p. 153-165.
- Ferraris, S., et al., *Antioxidant Activity of Silica-Based Bioactive Glasses*. ACS Biomater Sci Eng, 2021. **7**(6): p. 2309-2316.
- 530. Day, R.M., *Bioactive glass stimulates the secretion of angiogenic growth factors and angiogenesis in vitro*. Tissue Engineering, 2005. **11**(5-6): p. 768-777.
- 531. Day, R.M., et al., Assessment of polyglycolic acid mesh and bioactive glass for soft-tissue engineering scaffolds. Biomaterials, 2004. **25**(27): p. 5857-5866.
- 532. Wang, Y., et al., *The hypoxia-inducible factor a pathway couples angiogenesis to osteogenesis during skeletal development.* Journal of Clinical Investigation, 2007. **117**(6): p. 1616-1626.
- 533. Ke, Q.D. and M. Costa, *Hypoxia-inducible factor-1 (HIF-1)*. Molecular Pharmacology, 2006. **70**(5): p. 1469-1480.
- 534. Salceda, S. and J. Caro, *Hypoxia-inducible factor 1 alpha (HIF-1 alpha) protein is rapidly degraded by the ubiquitin-proteasome system under normoxic conditions Its stabilization by hypoxia depends on redox-induced changes.* Journal of Biological Chemistry, 1997. **272**(36): p. 22642-22647.
- 535. Kaelin, W.G. and P.J. Ratcliffe, *Oxygen sensing by metazoans: The central role of the HIF hydroxylase pathway.* Molecular Cell, 2008. **30**(4): p. 393-402.
- 536. Harris, A.L., *Hypoxia A key regulatory factor in tumour growth.* Nature Reviews Cancer, 2002. **2**(1): p. 38-47.
- 537. Epstein, A.C.R., et al., *C-elegans EGL-9 and mammalian homologs define a family of dioxygenases that regulate HIF by prolyl hydroxylation*. Cell, 2001. **107**(1): p. 43-54.
- 538. Carmeliet, P., et al., *Role of HIF-1 alpha or in hypoxia-mediated apoptosis, cell proliferation and tumour angiogenesis.* Nature, 1998. **394**(6692): p. 485-490.
- 539. Koh, M.Y. and G. Powis, *Passing the baton: the HIF switch.* Trends in Biochemical Sciences, 2012. **37**(9): p. 364-372.
- 540. Wang, G.L., et al., HYPOXIA-INDUCIBLE FACTOR-1 IS A BASIC-HELIX-LOOP-HELIX-PAS HETERODIMER REGULATED BY CELLULAR O-2 TENSION. Proceedings of the National Academy of Sciences of the United States of America, 1995. **92**(12): p. 5510-5514.
- Yuan, Y., et al., *Cobalt inhibits the interaction between hypoxia-inducible factor-alpha and von Hippel-Lindau protein by direct binding to hypoxia-inducible factor-alpha.* Journal of Biological Chemistry, 2003. **278**(18): p. 15911-15916.
- 542. Lu, C., et al., *Tibial fracture decreases oxygen levels at the site of injury.* lowa Orthop J, 2008. **28**: p. 14-21
- 543. Chen, W., et al., HIF-1 α Regulates Bone Homeostasis and Angiogenesis, Participating in the Occurrence of Bone Metabolic Diseases. Cells, 2022. **11**(22).
- 244. Zhang, Y., et al., Exosomes from human umbilical cord mesenchymal stem cells enhance fracture healing through HIF-1 α -mediated promotion of angiogenesis in a rat model of stabilized fracture. Cell Prolif, 2019. **52**(2): p. e12570.
- 545. Bai, H., et al., HIF signaling: A new propellant in bone regeneration. Biomater Adv, 2022. 138: p. 212874.
- Taguchi, K., et al., *The role of bone marrow-derived cells in bone fracture repair in a green fluorescent protein chimeric mouse model.* Biochem Biophys Res Commun, 2005. **331**(1): p. 31-6.
- 547. Rochefort, G.Y., et al., *Multipotential mesenchymal stem cells are mobilized into peripheral blood by hypoxia*. Stem Cells, 2006. **24**(10): p. 2202-8.

- 548. Lakkisto, P., et al., Heme oxygenase-1 and carbon monoxide promote neovascularization after myocardial infarction by modulating the expression of HIF-1alpha, SDF-1alpha and VEGF-B. Eur J Pharmacol, 2010. **635**(1-3): p. 156-64.
- 549. Azevedo, M.M., et al., *Hypoxia inducible factor-stabilizing bioactive glasses for directing mesenchymal stem cell behavior.* Tissue Eng Part A, 2015. **21**(1-2): p. 382-9.
- 550. Qi, X., et al., $HIF-1\alpha$ regulates osteoclastogenesis and alveolar bone resorption in periodontitis via *ANGPTL4*. Arch Oral Biol, 2023. **153**: p. 105736.
- Tao, J., et al., Spatiotemporal correlation between HIF-1 α and bone regeneration. Faseb j, 2022. **36**(10): p. e22520.
- 552. Knowles, H.J., Distinct roles for the hypoxia-inducible transcription factors HIF-1 α and HIF-2 α in human osteoclast formation and function. Sci Rep, 2020. **10**(1): p. 21072.
- Tang, Y., et al., HIF-1 α Mediates Osteoclast-Induced Mandibular Condyle Growth via AMPK Signaling. J Dent Res, 2020. **99**(12): p. 1377-1386.
- 554. Yu, X.J., et al., Effect of hypoxia on the expression of RANKL/OPG in human periodontal ligament cells in vitro. Int J Clin Exp Pathol, 2015. **8**(10): p. 12929-35.
- Tian, Y.-M., et al., *Differential Sensitivity of Hypoxia Inducible Factor Hydroxylation Sites to Hypoxia and Hydroxylase Inhibitors* *. Journal of Biological Chemistry, 2011. **286**(15): p. 13041-13051.
- 556. Wang, G.L. and G.L. Semenza, *Desferrioxamine induces erythropoietin gene expression and hypoxia-inducible factor 1 DNA-binding activity: implications for models of hypoxia signal transduction.* Blood, 1993. **82**(12): p. 3610-5.
- 557. Nguyen, L.K., et al., *A dynamic model of the hypoxia-inducible factor 1a (HIF-1a) network.* J Cell Sci, 2015. **128**(2): p. 422.
- 558. Semenza, G.L., *Targeting hypoxia-inducible factor 1 to stimulate tissue vascularization*. J Investig Med, 2016. **64**(2): p. 361-3.
- 559. Utting, J.C., et al., *Hypoxia inhibits the growth, differentiation and bone-forming capacity of rat osteoblasts.* Experimental cell research, 2006. **312**(10): p. 1693-1702.
- 560. Knowles, H.J., *Hypoxic regulation of osteoclast differentiation and bone resorption activity.* Hypoxia, 2015. **3**: p. 73-82.
- 561. Knowles, H.J., et al., *Hypoxia-inducible factor regulates osteoclast-mediated bone resorption: role of angiopoietin-like 4.* Faseb Journal, 2010. **24**(12): p. 4648-4659.
- 562. Agidigbi, T.S. and C. Kim, Reactive Oxygen Species in Osteoclast Differentiation and Possible Pharmaceutical Targets of ROS-Mediated Osteoclast Diseases. International Journal of Molecular Sciences, 2019. **20**(14).
- 563. Wang, D., et al., *Hypoxia-inducible factor* 1α *enhances RANKL-induced osteoclast differentiation by upregulating the MAPK pathway.* Ann Transl Med, 2022. **10**(22): p. 1227.
- 564. Malkov, M.I., C.T. Lee, and C.T. Taylor, *Regulation of the Hypoxia-Inducible Factor (HIF) by Pro-Inflammatory Cytokines*. Cells, 2021. **10**(9).
- 565. Luo, G., et al., *TNF-alpha and RANKL promote osteoclastogenesis by upregulating RANK via the NF-kappa B pathway.* Molecular Medicine Reports, 2018. **17**(5): p. 6605-6611.
- Yao, Z.Q., S.J. Getting, and I.C. Locke, *Regulation of TNF-Induced Osteoclast Differentiation*. Cells, 2022. **11**(1).
- 567. Ni, S., et al., *Hypoxia inhibits RANKL-induced ferritinophagy and protects osteoclasts from ferroptosis.* Free Radic Biol Med, 2021. **169**: p. 271-282.
- 568. Greijer, A.E., et al., Up-regulation of gene expression by hypoxia is mediated predominantly by hypoxia-

- inducible factor 1 (HIF-1). J Pathol, 2005. 206(3): p. 291-304.
- 569. Semenza, G.L., Angiogenesis in ischemic and neoplastic disorders. Annu Rev Med, 2003. 54: p. 17-28.
- 570. Quintero-Fabián, S., et al., *Role of Matrix Metalloproteinases in Angiogenesis and Cancer.* Front Oncol, 2019. **9**: p. 1370.
- 571. Petcu, E.B., et al., *Bisphosphonate-related osteonecrosis of jaw (BRONJ): an anti-angiogenic side-effect?*Diagn Pathol, 2012. **7**: p. 78.
- 572. Kun-Darbois, J.D., et al., Bone mineralization and vascularization in bisphosphonate-related osteonecrosis of the jaw: an experimental study in the rat. Clinical Oral Investigations, 2018. **22**(9): p. 2997-3006.
- 573. Giraudo, E., M. Inoue, and D. Hanahan, *An amino-bisphosphonate targets MMP-9-expressing macrophages and angiogenesis to impair cervical carcinogenesis.* Journal of Clinical Investigation, 2004. **114**(5): p. 623-633.
- 574. Wood, J., et al., *Novel antiangiogenic effects of the bisphosphonate compound zoledronic acid.* Journal of Pharmacology and Experimental Therapeutics, 2002. **302**(3): p. 1055-1061.
- 575. Tang, X., et al., Bisphosphonates suppress insulin-like growth factor 1-induced angiogenesis via the HIF-1alpha/VEGF signaling pathways in human breast cancer cells. Int J Cancer, 2010. **126**(1): p. 90-103.
- 576. Jia, X.Q., et al., *Zoledronic acid sensitizes breast cancer cells to fulvestrant via ERK/HIF-1 pathway inhibition in vivo*. Molecular Medicine Reports, 2018. **17**(4): p. 5470-5476.
- 577. Yang, Q., et al., VEGF enhancement of osteoclast survival and bone resorption involves VEGF receptor-2 signaling and 63-integrin. Matrix Biology, 2008. **27**(7): p. 589-599.
- 578. Kim, H.R., et al., *The effect of vascular endothelial growth factor on osteoclastogenesis in rheumatoid arthritis.* PLoS One, 2015. **10**(4): p. e0124909.
- 579. Fielding, J., *DIFFERENTIAL FERRIOXAMINE TEST FOR MEASURING CHELATABLE IRON*. Journal of Clinical Pathology, 1965. **18**(1): p. 88-+.
- 580. Zhu, H., et al., *Protective effects of Zn2+ against cobalt nanoparticles and cobalt chloride-induced cytotoxicity of RAW 264.7cells via ROS pathway.* Biochemical and Biophysical Research Communications, 2017. **486**(2): p. 357-363.
- 581. Chamaon, K., et al., *Ionic cobalt but not metal particles induces ROS generation in immune cells in vitro.*Journal of Biomedical Materials Research Part B-Applied Biomaterials, 2019. **107**(4): p. 1246-1253.
- Zou, W.G., et al., Cobalt chloride induces PC12 cells apoptosis through reactive oxygen species and accompanied by AP-1 activation. Journal of Neuroscience Research, 2001. **64**(6): p. 646-653.
- 583. Huang, B.K., et al., Modulating Electronic Structure Engineering of Atomically Dispersed Cobalt Catalyst in Fenton-like Reaction for Efficient Degradation of Organic Pollutants. Environmental Science & Technology, 2023. 57(37): p. 14071-14081.
- 584. Chen, J.R., et al., *Cobalt nanoparticles induce mitochondrial damage and ?-amyloid toxicity via the generation of reactive oxygen species.* Neurotoxicology, 2023. **95**: p. 155-163.
- 585. Gao, J., et al., *Leptin attenuates hypoxia-induced apoptosis in human periodontal ligament cells via the reactive oxygen species-hypoxia-inducible factor-1α pathway.* Experimental Physiology, 2021. **106**(8): p. 1752-1761.
- 586. Jin, W.S., et al., Radioprotective effect on HepG2 cells of low concentrations of cobalt chloride: induction of hypoxia-inducible factor-1 alpha and clearance of reactive oxygen species. Journal of Radiation Research, 2013. **54**(2): p. 203-209.
- 587. Triantafyllou, A., et al., Cobalt induces hypoxia-inducible factor- 1α (HIF- 1α) in HeLa cells by an iron-independent, but ROS-, PI-3K- and MAPK-dependent mechanism. Free Radical Research, 2006. **40**(8): p.

- 847-856.
- 588. Patntirapong, S., P. Habibovic, and P.V. Hauschka, *Cobalt incorporation into calcium phosphate layers* stimulates osteoclast differentiation and activation via hypoxia inducible factor pathway. Journal of Bone and Mineral Research, 2007. **22**: p. S381-S381.
- 589. Patntirapong, S., P. Habibovic, and P.V. Hauschka, *Effects of soluble cobalt and cobalt incorporated into calcium phosphate layers on osteoclast differentiation and activation*. Biomaterials, 2009. **30**(4): p. 548-555.
- 590. Habermann, B., et al., *Tartrate-resistant acid phosphatase 5b (TRAP 5b) as a marker of osteoclast activity in the early phase after cementless total hip replacement.* Acta Orthopaedica, 2007. **78**(2): p. 221-225.
- 591. Halleen, J.M., et al., *Tartrate-resistant acid phosphatase 5b: A novel serum marker of bone resorption.*Journal of Bone and Mineral Research, 2000. **15**(7): p. 1337-1345.
- 592. Redza-Dutordoir, M. and D.A. Averill-Bates, *Activation of apoptosis signalling pathways by reactive oxygen species*. Biochim Biophys Acta, 2016. **1863**(12): p. 2977-2992.
- 593. Liu, X.J., et al., Cobalt Protoporphyrin Induces HO-1 Expression Mediated Partially by FOXO1 and Reduces Mitochondria-Derived Reactive Oxygen Species Production. Plos One, 2013. **8**(11).
- 594. Liu, L., et al., *Lycium barbarum polysaccharides protects retinal ganglion cells against oxidative stress injury.* Neural Regeneration Research, 2020. **15**(8): p. 1526-1531.
- 595. Gaba, S., et al., *Comprehensive Genome Analysis of Halolamina pelagica CDK2: Insights into Abiotic Stress Tolerance Genes.* Journal of Pure and Applied Microbiology, 2022. **16**(1): p. 460-470.
- 596. Tsuyuki, R., et al., Enhancement of Trichothecene Production in Fusarium graminearum by Cobalt Chloride. Journal of Agricultural and Food Chemistry, 2011. **59**(5): p. 1760-1766.
- 597. Chen, C.L., S.C. Wang, and P. Liu, *Deferoxamine Enhanced Mitochondrial Iron Accumulation and Promoted Cell Migration in Triple-Negative MDA-MB-231 Breast Cancer Cells Via a ROS-Dependent Mechanism.* International Journal of Molecular Sciences, 2019. **20**(19).
- 598. Orriss, I.R., S.E. Taylor, and T.R. Arnett, Rat osteoblast cultures. Methods Mol Biol, 2012. 816: p. 31-41.
- 599. Volpato, V. and C. Webber, *Addressing variability in iPSC-derived models of human disease: guidelines to promote reproducibility.* Dis Model Mech, 2020. **13**(1).
- Taylor, S.E., M. Shah, and I.R. Orriss, *Generation of rodent and human osteoblasts*. Bonekey Rep, 2014. **3**: p. 585.
- 601. Kushner, I.K., et al., *Individual Variability of Protein Expression in Human Tissues*. J Proteome Res, 2018. **17**(11): p. 3914-3922.
- 602. Spiller, K.L., et al., *Differential gene expression in human, murine, and cell line-derived macrophages upon polarization*. Experimental cell research, 2016. **347**(1): p. 1-13.
- 603. Teitelbaum, S.L., Bone Resorption by Osteoclasts. Science, 2000. 289(5484): p. 1504-1508.
- Thang, Y., et al., *Species-independent stimulation of osteogenic differentiation induced by osteoclasts.*Biochemical and Biophysical Research Communications, 2022. **606**: p. 149-155.
- 605. Idrisova, K.F., H.U. Simon, and M.O. Gomzikova, *Role of Patient-Derived Models of Cancer in Translational Oncology.* Cancers (Basel), 2022. **15**(1).
- Russ, H.A., et al., Epithelial-mesenchymal transition in cells expanded in vitro from lineage-traced adult human pancreatic beta cells. PLoS One, 2009. **4**(7): p. e6417.
- 607. Stroncek, D.F. and L. England, *Protecting the Health and Safety of Cell and Tissue Donors.* ISBT Sci Ser, 2015. **10**(Suppl 1): p. 108-114.
- 608. Hume, D.A., et al., *The mononuclear phagocyte system revisited.* J Leukoc Biol, 2002. **72**(4): p. 621-7.
- 609. Yuan, Y. and Y. Chai, Regulatory mechanisms of jaw bone and tooth development. Curr Top Dev Biol,

- 2019. 133: p. 91-118.
- 610. Matsuura, T., et al., *Distinct Characteristics of Mandibular Bone Collagen Relative to Long Bone Collagen:*Relevance to Clinical Dentistry. BioMed Research International, 2014. **2014**: p. 769414.
- 611. Aghaloo, T.L., et al., *Osteogenic potential of mandibular vs. long-bone marrow stromal cells.* J Dent Res, 2010. **89**(11): p. 1293-8.
- de Molon, R.S., et al., *Rheumatoid Arthritis Exacerbates the Severity of Osteonecrosis of the Jaws (ONJ)* in Mice. A Randomized, Prospective, Controlled Animal Study. J Bone Miner Res, 2016. **31**(8): p. 1596-607.
- 613. Soma, T., et al., *Tooth extraction in mice administered zoledronate increases inflammatory cytokine levels and promotes osteonecrosis of the jaw.* J Bone Miner Metab, 2021. **39**(3): p. 372-384.
- Reissis, Y., et al., *The effect of temperature on the viability of human mesenchymal stem cells*. Stem Cell Res Ther, 2013. **4**(6): p. 139.
- 615. Wang, Z., et al., Effects of sintering temperature on surface morphology/microstructure, in vitro degradability, mineralization and osteoblast response to magnesium phosphate as biomedical material. Scientific Reports, 2017. **7**(1): p. 823.
- 616. Payr, S., et al., *Direct comparison of 3D and 2D cultivation reveals higher osteogenic capacity of elderly osteoblasts in 3D.* Journal of Orthopaedic Surgery and Research, 2021. **16**(1).
- 617. Buttery, L., et al., Osteogenic Differentiation of Embryonic Stem Cells in 2D and 3D Culture, in 3d Cell Culture: Methods and Protocols, J.W. Haycock, Editor. 2011. p. 281-308.
- 618. Kleinhans, C., et al., Comparison of osteoclastogenesis and resorption activity of human osteoclasts on tissue culture polystyrene and on natural extracellular bone matrix in 2D and 3D. Journal of Biotechnology, 2015. **205**: p. 101-110.
- 619. Borciani, G., et al., *Co–culture systems of osteoblasts and osteoclasts: Simulating in vitro bone remodeling in regenerative approaches.* Acta Biomaterialia, 2020. **108**: p. 22-45.
- 620. Remmers, S.J.A., et al., *Osteoblast-osteoclast co-cultures: A systematic review and map of available literature.* PLoS One, 2021. **16**(11): p. e0257724.
- 621. Zhu, S., et al., From the Clinical Problem to the Basic Research—Co-Culture Models of Osteoblasts and Osteoclasts. International Journal of Molecular Sciences, 2018. **19**(8): p. 2284.
- 622. Shah, F.A., *Towards refining Raman spectroscopy-based assessment of bone composition.* Scientific Reports, 2020. **10**(1): p. 16662.
- 623. Taylor, E.A. and E. Donnelly, *Raman and Fourier transform infrared imaging for characterization of bone material properties.* Bone, 2020. **139**: p. 115490.
- 624. Cadena, E.A., In situ SEM/EDS compositional characterization of osteocytes and blood vessels in fossil and extant turtles on untreated bone surfaces; different preservational pathways microns away. PeerJ, 2020. **8**: p. e9833.
- 625. Holtmann, H., et al., *Pathogenesis of medication-related osteonecrosis of the jaw: a comparative study of in vivo and in vitro trials.* J Int Med Res, 2018. **46**(10): p. 4277-4296.
- 626. Vahtsevanos, K., et al., Longitudinal cohort study of risk factors in cancer patients of bisphosphonate-related osteonecrosis of the jaw. J Clin Oncol, 2009. **27**(32): p. 5356-62.
- 627. Fehm, T., et al., *Bisphosphonate-induced osteonecrosis of the jaw (ONJ): Incidence and risk factors in patients with breast cancer and gynecological malignancies.* Gynecol Oncol, 2009. **112**(3): p. 605-9.
- 628. Pautke, C., et al., *Bisphosphonate related osteonecrosis of the jaw: A minipig large animal model.* Bone, 2012. **51**(3): p. 592-9.
- 629. Mitsimponas, K.T., et al., Search for a reliable model for bisphosphonate-related osteonecrosis of the

- *jaw: establishment of a model in pigs and description of its histomorphometric characteristics.* British Journal of Oral and Maxillofacial Surgery, 2016. **54**(8): p. 883-888.
- 630. Li, Y., et al., Allogeneic mesenchymal stem cell therapy for bisphosphonate-related jaw osteonecrosis in Swine. Stem Cells Dev, 2013. **22**(14): p. 2047-56.
- 631. Aguirre, J.I., E.J. Castillo, and D.B. Kimmel, *Preclinical models of medication-related osteonecrosis of the jaw (MRONJ)*. Bone, 2021. **153**.
- 632. Nalla, R.K., J.H. Kinney, and R.O. Ritchie, *Mechanistic fracture criteria for the failure of human cortical bone.* Nature Materials, 2003. **2**(3): p. 164-168.
- 633. Bailey, S. and D. Vashishth, *Mechanical Characterization of Bone: State of the Art in Experimental Approaches-What Types of Experiments Do People Do and How Does One Interpret the Results?* Curr Osteoporos Rep, 2018. **16**(4): p. 423-433.
- 634. Zhao, S., et al., *Standardizing compression testing for measuring the stiffness of human bone*. Bone Joint Res, 2018. **7**(8): p. 524-538.
- 635. Attia, T. and T.L. Willett, *Chapter 11 Tension and Compression Testing of Cortical Bone*, in *Experimental Methods in Orthopaedic Biomechanics*, R. Zdero, Editor. 2017, Academic Press. p. 167-183.
- 636. Agidigbi, T.S. and C. Kim, Reactive Oxygen Species in Osteoclast Differentiation and Possible Pharmaceutical Targets of ROS-Mediated Osteoclast Diseases. International Journal of Molecular Sciences, 2019. **20**(14): p. 3576.
- 637. Kakabadse, G. and J.W. Dewsnap, *The Sodium Silicate Hydrogen Peroxide System.* Nature, 1960. **185**(4715): p. 761-761.
- 638. Pignatello, J.J., E. Oliveros, and A. MacKay, *Advanced Oxidation Processes for Organic Contaminant Destruction Based on the Fenton Reaction and Related Chemistry.* Critical Reviews in Environmental Science and Technology, 2006. **36**(1): p. 1-84.
- 639. Al-Huqail, A.A., et al., Silicon supplementation modulates antioxidant system and osmolyte accumulation to balance salt stress in Acacia gerrardii Benth. Saudi J Biol Sci, 2019. **26**(7): p. 1856-1864.
- 640. Triantafyllou, A., et al., Cobalt induces hypoxia-inducible factor-1alpha (HIF-1alpha) in HeLa cells by an iron-independent, but ROS-, PI-3K- and MAPK-dependent mechanism. Free Radic Res, 2006. **40**(8): p. 847-56.
- 641. Li, L., et al., Desferrioxamine regulates HIF-1 alpha expression in neonatal rat brain after hypoxia-ischemia. Am J Transl Res, 2014. **6**(4): p. 377-83.
- 642. Ge, C., et al., *Zoledronic Acid Inhibits Angiogenesis Through Promoting HIF-1 alpha Protein Degradation in Human Umbilical Vein Endothelial Cells.* Journal of Biomaterials and Tissue Engineering, 2016. **6**(9): p. 745-753.
- 643. Li, K., et al., *Pretreatment-Etidronate Alleviates CoCl2 Induced-SH-SY5Y Cell Apoptosis via Decreased HIF-*1 and TRPC5 Channel Proteins. Neurochemical Research, 2019. **44**(2): p. 428-440.
- Tsubaki, M., et al., Nitrogen-containing bisphosphonates inhibit RANKL- and M-CSF-induced osteoclast formation through the inhibition of ERK1/2 and Akt activation. Journal of Biomedical Science, 2014. **21**(1): p. 10.
- 645. Siekkinen, M., et al., *Dissolution of Bioactive Glass S53P4 in Continuous Flows of Tris Buffer and Lactic Acid.* Biomedical Materials & Devices, 2024. **2**(2): p. 1089-1101.
- 646. Hoppe, A., et al., *In vitro cell response to Co-containing 1393 bioactive glass.* Materials Science and Engineering: C, 2015. **57**: p. 157-163.
- 647. Zhang, M., et al., *Cobalt-containing borate bioactive glass fibers for treatment of diabetic wound.* J Mater Sci Mater Med, 2023. **34**(8): p. 42.

- 648. Cannio, M., et al., *Bioactive Glass Applications: A Literature Review of Human Clinical Trials.* Materials (Basel), 2021. **14**(18).
- 649. Müller, P., et al., *Calcium phosphate surfaces promote osteogenic differentiation of mesenchymal stem cells.* Journal of cellular and molecular medicine, 2008. **12**(1): p. 281-291.
- 650. Shih, Y.-R.V., et al., *Calcium phosphate-bearing matrices induce osteogenic differentiation of stem cells through adenosine signaling*. Proceedings of the National Academy of Sciences, 2014. **111**(3): p. 990-995.
- Obata, A., et al., Osteoblast-like cell responses to silicate ions released from 45S5-type bioactive glass and siloxane-doped vaterite. Journal of Materials Science, 2017. **52**(15): p. 8942-8956.
- 652. Ryu, J.I., H.Y. Kim, and Y.D. Kwon, *Is implant surgery a risk factor for osteonecrosis of the jaw in older adult patients with osteoporosis? A national cohort propensity score-matched study.* Clin Oral Implants Res, 2021. **32**(4): p. 437-447.
- 653. Sarkarat, F., et al., Efficacy of hyaluronic acid, absorbable collagen sponge, and their combination in minimizing bisphosphonate-related osteonecrosis of the jaws (BRONJ) after dental extraction: a preliminary animal histomorphometric study. Maxillofacial Plastic and Reconstructive Surgery, 2022. 44(1).
- 654. Sadat-Ali, M., et al., *Treatment of bisphosphonate induced osteonecrosis of jaw in rats using an angiogenesis factor (A-Heal) and ABMDO (Autologous Bone Marrow Derived Osteoblasts).* Saudi Dental Journal, 2022. **34**(2): p. 100-106.
- 655. Jamalpour, M.R., et al., Complementarity of surgical therapy, photobiomodulation, A-PRF and L-PRF for management of medication-related osteonecrosis of the jaw (MRONJ): an animal study. Bmc Oral Health, 2022. **22**(1).
- 656. Hadad, H., et al., *Beta tricalcium phosphate, either alone or in combination with antimicrobial photodynamic therapy or doxycycline, prevents medication-related osteonecrosis of the jaw.* Scientific Reports, 2022. **12**(1).
- 657. Tanaka, Y., et al., Suppression of Bone Necrosis around Tooth Extraction Socket in a MRONJ-like Mouse Model by E-rhBMP-2 Containing Artificial Bone Graft Administration. International Journal of Molecular Sciences, 2021. 22(23).
- Razmara, F., et al., Application of a collagen scaffold saturated with platelet-rich plasma in prevention of bisphosphonate-related osteonecrosis of the jaw in the rat animal model. Heliyon, 2021. **7**(5).
- 659. Kushiro, H., H. Takahashi, and A. Tanaka, *Effects of the prevention of medication-related osteonecrosis* of the jaw by local administration of a dental pulp stem cell-conditioned medium to the rat tooth extraction socket. Odontology, 2021. **109**(4): p. 836-844.
- 660. Huang, J., L. Wang, and W.D. Tian, *Small Extracellular Vesicles Derived from Adipose Tissue Prevent Bisphosphonate-Related Osteonecrosis of the Jaw by Promoting Angiogenesis*. International Journal of Nanomedicine, 2021. **16**: p. 3161-3172.
- 661. Gao, S.Y., et al., *PDGF-BB exhibited therapeutic effects on rat model of bisphosphonate-related osteonecrosis of the jaw by enhancing angiogenesis and osteogenesis.* Bone, 2021. **144**.
- Sharma, D., et al., Local delivery of hydrogel encapsulated vascular endothelial growth factor for the prevention of medication-related osteonecrosis of the jaw. Sci Rep, 2021. **11**(1): p. 23371.
- 663. Rodríguez-Lozano, F.J., et al., *Allogeneic Bone Marrow Mesenchymal Stem Cell Transplantation in Tooth Extractions Sites Ameliorates the Incidence of Osteonecrotic Jaw-Like Lesions in Zoledronic Acid-Treated Rats.* Journal of Clinical Medicine, 2020. **9**(6).
- 664. Mikai, A., et al., BMP-2/8-TCP Local Delivery for Bone Regeneration in MRONJ-Like Mouse Model.

- International Journal of Molecular Sciences, 2020. 21(19).
- 665. Ning, H.R., et al., *Microfiber-Reinforced Composite Hydrogels Loaded with Rat Adipose-Derived Stem Cells and BMP-2 for the Treatment of Medication-Related Osteonecrosis of the Jaw in a Rat Model.* Acs Biomaterials Science & Engineering, 2019. **5**(5): p. 2430-2443.
- Zang, X.L., et al., Adipose-derived stem cells prevent the onset of bisphosphonate-related osteonecrosis of the jaw through transforming growth factor-1-mediated gingival wound healing. Stem Cell Research & Therapy, 2019. 10.
- 667. Toro, L.F., et al., Application of Autologous Platelet-Rich Plasma on Tooth Extraction Site Prevents Occurence of Medication-Related Osteonecrosis of the Jaws in Rats. Scientific Reports, 2019. **9**.
- 668. Taysi, A.E., et al., *The efficacy of sustained-release chitosan microspheres containing recombinant human parathyroid hormone on MRONJ.* Brazilian Oral Research, 2019. **33**.
- 669. Imada, M., et al., Prevention of tooth extraction-triggered bisphosphonate-related osteonecrosis of the jaws with basic fibroblast growth factor: An experimental study in rats. Plos One, 2019. **14**(2).
- 670. Ogata, K., et al., *Cytokine Mixtures Mimicking Secretomes From Mesenchymal Stem Cells Improve Medication-Related Osteonecrosis of the Jaw in a Rat Model.* Jbmr Plus, 2018. **2**(2): p. 69-80.
- 671. Kuroshima, S., et al., *Transplantation of Noncultured Stromal Vascular Fraction Cells of Adipose Tissue Ameliorates Osteonecrosis of the Jaw-Like Lesions in Mice*. Journal of Bone and Mineral Research, 2018. **33**(1): p. 154-166.
- 672. Oh, J.S. and S.G. Kim, *Collagen sponge and rhBMP-2 improve socket healing in rats treated with zoledronic acid.* Brazilian Oral Research, 2017. **31**.
- 673. Barba-Recreo, P., et al., *Adipose-derived stem cells and platelet-rich plasma for preventive treatment of bisphosphonate-related osteonecrosis of the jaw in a murine model.* Journal of Cranio-Maxillofacial Surgery, 2015. **43**(7): p. 1161-1168.
- 674. Li, Y.S., et al., *Allogeneic Mesenchymal Stem Cell Therapy for Bisphosphonate-Related Jaw Osteonecrosis in Swine.* Stem Cells and Development, 2013. **22**(14): p. 2047-2056.
- 675. Kikuiri, T., et al., *Cell-Based Immunotherapy With Mesenchymal Stem Cells Cures Bisphosphonate-Related Osteonecrosis of the Jaw-like Disease in Mice.* Journal of Bone and Mineral Research, 2010. **25**(7): p. 1668-1679.